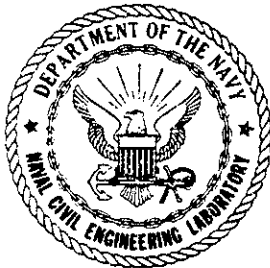


**REVIEW OF SEMISUBMERSIBLE AND TENSION LEG PLATFORM  
ANALYSIS TECHNIQUES**

**VOLUME I – LITERATURE SURVEY**

F. Rajabi, S. Ghosh, C. Oran  
Brown & Root Development, Inc.

D. R. Shields  
Naval Civil Engineering Laboratory



Prepared for:

Naval Civil Engineering Laboratory  
Ocean Structures Division  
Port Hueneme, California 93043



and

Minerals Management Service  
Technology Assessment and Research Branch  
Reston, Virginia 22091

Sponsors:

Naval Facilities Engineering Command  
Minerals Management Service

Program Nos: YF60.534.091.01.A351  
44-065



## FOREWARD

This report constitutes Task I of the contract No. N62474-83-C6716 entitled "Engineering Services for Conceptual Formulation and Design, Feasibility Studies, Detail Design, and Development of Plans for Fixed and Moored Ocean Structures". It was performed under Brown and Root Development, Inc. (BARDI), Job No. XF-0030.

Task I included two parallel activities - (1) a literature review of state-of-the-art techniques and theory involved in motion and structural analysis of semisubmersibles and tension leg platforms; and (2) a worldwide survey of the software capabilities for design and analysis of such structures.

Motion and structural analysis capabilities of semisubmersible and tension leg platforms are dependent on techniques developed in the disciplines of: meteorology; physical, geological and biological oceanography; mathematics and statistics; physics and mechanics; computer sciences; naval architecture; coastal, geotechnical, materials, ocean and structural engineering. There are literally tens of thousands of publications in each of these disciplines ranging from the basic to those that are specialized and highly technical in nature. Clearly it is not possible to provide an in-depth discussion of each discipline and topic without producing a voluminous amount of text. Volume I provides an integrated basic multi-disciplinary introduction to the topic for graduate civil and mechanical engineers with limited knowledge or training in this area. It could easily serve as an introductory text to the subject for first year graduate students.

The literature review in Volume I covers many topics which provide the reader with an introduction to selected fundamentals involved in the determination of hydrodynamic loading, motions and responses, structural analysis, and mooring analysis for semisubmersibles and tension leg platforms. Consistent with the spirit of the charter for the report, the nomenclature adopted in the various chapters of this review reflects that widely used by researchers, industry and regulatory agencies. To assist the reader, a summary of significant nomencla-

ture terms, broken down by chapter, is presented on page xvi just prior to the formal introduction to this review.

As previously discussed, an in-depth discussion of each topic is not possible within this report. A bibliography compiled by me lists 34 easily obtainable "classic" text and design level books which will provide the reader with a more in-depth understanding of those topics in which he has this desire. An extensive list of over 350 references are cited in this review which should enable the reader to achieve a more detailed understanding of specific phenomena and recent developments in related areas when so required.

To conduct the worldwide software survey, more than 40 organizations in eight different countries were contacted. These organizations are engaged in a variety of activities and included research centers, academic institutions, engineering consultants and contractors. Since standard universally accepted definitions are not in use for most of the parameters included in the motion and structural analysis of semisubmersibles and tension leg platforms, a questionnaire was prepared for requesting uniform information from various organization. Summary tables reflecting responses received from participants in the survey are included in Volume II of this report. Responses received by August 6, 1984 were included. A synopsis of each response is also included in Volume II. Questionnaires completed by various organizations are compiled in Appendix 1.

BARDI was directed to make no attempt to evaluate the programs nor compare one program against another. There is no endorsement of any program or any program over another and none should be inferred. Therefore, the software survey should be regarded simply as a compilation of worldwide software capabilities for motion and structural analysis in a uniform and easy to understand format. Programs are continually in a state of development and maintenance. Therefore a user should generally find programs with similar general capabilities and then confirm the present capabilities with the developers of the programs before making a final selection of the program best suited to the problem he wishes to analyze.

The programs listed in the survey accommodate a range of problem complexities from performing linearized frequency domain analysis for concept investigations to nonlinear time domain analysis required in the final detailed design phase. The programs covered range from those that may be regarded as quite user friendly, even to the extent of being menu driven, to those which should be regarded as principally research tools with which only a few individuals are knowledgeable enough to code and perform analyses. The principal programs which are actively being used for design and analysis of semisubmersibles and tension leg platforms are felt to be adequately represented in this report.

A set of blank forms are provided at the end of Appendix I which may be reproduced and used to document new programs or update programs which are included in the present report. If new programs are documented or present ones updated it is requested that this information be provided to NCEL directed to the attention of the Ocean Structures Division Director. Copies of this updated information will be forwarded to other parties on the original distribution list. Because of the nature of the material in Volume II and Appendix I it is not for public distribution.

Dr. Farhad Rajabi is gratefully acknowledged for his outstanding contribution to the success of the preparation of these reports both as the BARDI project manager and principal author. Without his dedication to excellence the report could have been much less than the superior results obtained. Dr. Cenap Oran, BARDI, is gratefully acknowledged as a contributing author. Mr. Susobhan Ghosh, BARDI, is gratefully acknowledged for his diligence in assisting in the preparation of the software matrices and compiling their results.

The principal reviewers for the draft version of the report were Mr. Robert F. Zueck, Civil Engineer, NCEL, Dr. Robert Hudspeth, Professor Civil and Ocean Engineering, Oregon State University, who was serving in an NCEL staff consulting position and myself. Mr. Andrew R. Del Collo and Ms. Terri Regan, Civil Engineers, of the Naval Facilities Engineering Command's Ocean Engineering and Construction Project Office also reviewed the draft report and provided constructive input. Dr. William J. Nordell, Director, Ocean Structures Division, and LCDR Arnold E. Bertsche, Assistant Program Manager Offshore Facilities, NCEL, were instrumental in the establishment of this effort and are so acknow-

ledged. This work was originally sponsored by the Naval Facilities Engineering Command under its 6.2 program. Mr. Robert Peloquin was the NAVFAC Program Director.

The Minerals Management Service (MMS) joined in the sponsorship of this work in its early phase. Without this additional sponsorship the scope, detail and completeness provided in this report would have been considerably less. Mr. Charles E. Smith, Assistance Research Program Manager, Technology Assessment and Research Program, MMS, was instrumental in their participation leading to the success of this effort.

Finally a note of appreciation is extended to the many firms and individuals who supplied information on their programs which contributed to the success and usefulness of the software matrix.

David Shields  
Civil Engineer  
Ocean Structures Division  
Naval Civil Engineering Laboratory  
Port Hueneme, California

## TABLE OF CONTENTS

	<u>PAGE NO.</u>
LIST OF TABLES	viii
LIST OF FIGURES	ix
ABBREVIATIONS	xiv
NOMENCLATURE	xvi
1.0 INTRODUCTION	1
2.0 GUYED TOWER PLATFORMS (GTP's)	5
3.0 FLOATING MOORED STRUCTURES	9
3.1 Introduction	9
3.2 Semisubmersibles	11
3.2.1 Evolution of Semisubmersibles	11
3.2.2 Design Considerations for Semisubmersibles	18
3.3 Tension Leg Platforms (TLP's)	22
3.3.1 Evolution of TLP's	23
3.3.2 Design Considerations for TLP's	25
3.4 Major Dynamic Response Differences between Semisubmersibles and TLP's	33
4.0 EQUATIONS OF MOTION AND DYNAMIC RESPONSE ANALYSIS	59
4.1 Philosophy of and Need for Dynamic Response Analysis	59
4.2 Equations of Motion	62
4.2.1 General	62
4.2.2 Coordinate System	67
4.2.3 Equations of Motion (F.D.)	68
4.2.4 Solution of Frequency Domain Equations	71
4.3 Time Domain Analysis	76
4.3.1 Equations of Motion (T.D.)	77
4.3.1.1 Force Ramp Function	80
4.3.1.2 Time Domain Solution Process	81

TABLE OF CONTENTS (Continued)

	<u>PAGE NO.</u>
4.3.2 Regular Wave Versus Irregular Wave Analysis	82
4.3.3 Output of Time Domain Analysis	82
4.4 Frequency Domain Versus Time Domain Analysis	83
5.0 WAVE MODELS	92
5.1 Principal Factors in Analysis and Design	92
5.2 Ocean Waves	94
5.2.1 Introduction	94
5.2.2 Classification of Waves	95
5.2.3 Real Versus Perfect Fluids	98
5.2.4 Rotational and Irrotational Flow	99
5.2.5 Velocity Potential Stream Function and Bernoulli Equation	100
5.2.6 Wave Theories	103
5.2.7 Airy Waves	107
5.2.8 Empirical Modification of the Airy Wave Theory	111
5.2.9 Higher Order Wave Theories	113
5.2.10 Stokes Waves	114
5.2.11 Cnoidal Waves	116
5.2.12 Other Wave Theories	117
5.2.13 Numerical Wave Theories	118
5.2.14 Range of Validity and Selection of Wave Theory	120
5.2.15 Comparison with Experiment	122
5.2.15.1 Laboratory Waves	122
5.2.15.2 Sea Waves	123
5.3 Random Waves	124
5.3.1 Wave Height Distribution	126
5.3.2 Ocean Wave Energy Spectra	128
5.3.3 Proposed Wave Spectra	130
5.3.3.1 Darbyshire Spectrum (1952)	131
5.3.3.2 Neumann Spectrum (1953)	132



TABLE OF CONTENTS (Continued)

	<u>PAGE NO.</u>
5.3.3.3 Pierson-Moskowitz Spectrum (1964)	132
5.3.3.4 Bretschneider Spectrum (1959)	133
5.3.3.5 JONSWAP Spectrum, Hasselmann (1973)	133
5.3.3.6 ISSC Spectrum (International Ship Structures Congress, 1964)	135
5.3.3.7 Ochi-Hubble Spectrum (1976)	136
5.3.3.8 Scott Spectrum (1965)	136
5.4 Short-Crested Waves	137
6.0 FLUID-STRUCTURE INTERACTION	154
6.1 Effects of Viscosity	154
6.2 Wave Force Regimes	155
6.3 Morison Equation	157
6.4 Diffraction Method	160
7.0 WAVE FORCES ON SMALL BODIES	163
7.1 Application of the Morison Equation	163
7.2 Extension of the Morison Equation	164
7.3 Force Coefficients	168
7.3.1 Vertical Cylinders with Laboratory Waves	169
7.3.2 Ocean Tests	170
7.3.3 Laboratory Tests	172
7.4 Sources of Uncertainty	173
7.4.1 Fluid Particle Kinematics	174
7.4.2 Experimental Methods	174
7.4.3 Experimental Error	175
7.4.4 Inexact Description of Complex Flow	175
7.4.5 Incomplete Parameterization of the Force Coefficients	176
7.5 Suggested Values for Force Coefficients	178

TABLE OF CONTENTS (Continued)

	<u>PAGE NO.</u>	
7.6	Effects of Orbital Motion, Current, Orientation, Marine Growth, and Interference	180
7.6.1	Effect of Wave Orbital Motion	180
7.6.2	Effect of Current	180
7.6.3	Effect of Member Orientation	181
7.6.4	Effect of Marine Growth	182
7.6.5	Interference and Shielding Effect	184
7.7	Linearization of the Morison Equation	185
7.8	Vortex Shedding on Flexible Cylinders	188
7.8.1	Theoretical Background	190
7.8.2	Forcing Functions Model	195
8.0	WAVE FORCES ON LARGE BODIES	216
8.1	Introduction	216
8.2	Wave Diffraction Theory	217
8.3	Linear Wave Diffraction Theory	218
8.4	Hydrodynamic Solutions	223
8.4.1	Analytic	224
8.4.2	Strip Theory	225
8.4.2.1	Conformal Mapping	225
8.4.2.2	Frank Close-Fit Method	226
8.4.2.3	Schwartz-Christoffel Method	226
8.4.3	Three-Dimensional Problem: Vertical Wall Boundaries	227
8.4.4	Three-Dimensional Problem: Axisymmetric Bodies	227
8.4.5	General Three-Dimensional Problem	227
8.4.5.1	Boundary Element Method (BEM)	228
8.4.5.2	Finite Element Method (FEM)	229
8.4.5.3	Finite Difference Method (FDM)	231
8.4.6	Computational Considerations on FEM and BEM	231
8.4.7	General Comments on Various Numerical Methods	232

TABLE OF CONTENTS (Continued)

	<u>PAGE NO.</u>
8.5 Applications and Experimental Validation	233
8.6 Nonlinear Wave Effects	236
9.0 WAVE DRIFT FORCES	246
9.1 Viscous Drift Forces	247
9.1.1 Wave Drag Drift	247
9.1.2 Current-Wave Drift	248
9.2 Potential Flow Drift Forces	249
9.2.1 Wave Elevation Drift	250
9.2.2 Velocity Head Drift	250
9.2.3 Body Translation Drift	250
9.2.4 Body Rotation Drift	251
9.2.5 Slowly Varying Wave Drift Forces	251
9.2.6 Effect of Second Order Potential	252
9.2.7 Relative Significance of Wave Drift Forces	252
10.0 WIND LOADS	256
10.1 Description of Wind	256
10.1.1 Wind Speed	256
10.1.2 Wind Spectra	257
10.2 Wind Force Calculation	261
10.3 Discussion of Wind Force Calculation Methods	264
11.0 CURRENT LOADS	270
11.1 Current Profile	270
11.2 Drag Coefficients	271
11.3 Current Force Calculation	272
12.0 STABILITY ANALYSIS	278
12.1 Stability Requirements	280
12.1.1 Intact Stability	280

TABLE OF CONTENTS (Continued)

	<u>PAGE NO.</u>
12.1.2 Damaged Stability	281
12.1.3 Additional Intact Stability Criteria	282
12.2 Comparisons of Existing Stability Criteria	283
12.3 Discussion of Stability Analysis	284
13.0 MOORING SYSTEM ANALYSIS	292
13.1 Design Methodology for Catenary Mooring Systems	293
13.2 Design Criteria	295
13.3 Preliminary Analysis	296
13.3.1 Mooring Pattern Selection	296
13.3.2 Frequency Domain Analysis	297
13.3.3 System Stiffness Study	299
13.4 Mooring Line Design	300
13.4.1 Mooring System Force Balance	300
13.4.2 Mooring Line Force-Deflection Characteristics	301
13.4.3 Time Domain Analysis	301
13.5 TLP Tendons	302
13.5.1 Description of Tendon System	302
13.5.2 Catenary Versus Vertical Pretensioned Mooring Systems	303
13.5.3 Methods of Analysis	304
13.5.4 Design Considerations	305
13.6 Mathieu Instabilities	305
14.0 STRUCTURAL DESIGN AND ANALYSIS	326
14.1 Introduction	326
14.2 Catalog of Loading and Weight Estimates	327
14.3 Hydrodynamic Loads Generation	329
14.4 Integrated Motion-Structural Analysis Method	332
14.5 Platform Structure Design	333
14.5.1 General	333

TABLE OF CONTENTS (Continued)

	<u>PAGE NO.</u>
14.5.2 Platform Structure Preliminary Design Procedure	335
14.5.2.1 Deck Design	336
14.5.2.2 Column Design	337
14.5.2.3 Pontoon Design	338
14.6 Structural Analysis	338
14.6.1 General	338
14.6.2 Space Frame Model	339
14.6.3 Static Stress Analysis	340
14.6.4 Dynamic Stress Analysis	342
14.6.5 Platform Stress Analysis During Floatout of TLP's	342
14.6.6 Platform Stress Analysis During Installation of TLP's	343
14.6.7 Platform Stress Analysis During Operational and Survival Conditions for TLP's	343
14.6.8 Detailed Stress Analysis	344
14.6.9 Local Stress Analysis and Design Modification	344
14.6.10 Fatigue Analysis	345
14.7 Detailed Design	345
14.8 Platform Structure Weight Summary	345
14.9 Final Structural Configuration	346
14.10 Concluding Remarks	347
15.0 REFERENCES	369
16.0 BIBLIOGRAPHY	408



## LIST OF TABLES

<u>TABLE NO.</u>	<u>SUBJECT</u>	<u>PAGE NO.</u>
3.1	Comparison of Various Types of Mobile Drilling Units	36
3.2	Mobile Drilling Unit Construction Cost	36
3.3	Semisubmersible and TLP Dynamic Characteristics	37
5.1	Classification of Wave Theories	97
5.2	Results of Linear Wave Theory	139
5.3	Shallow and Deep Water Approximations to Linear Wave Theory	140
7.1	BSRA Tabulated Field and Laboratory Studies on Drag and Inertia Coefficients	199
8.1	Some Comparisons Between Linear Wave Diffraction Theory and Experiment	238
8.2	Application of Diffraction Theory and the Morison Equation to Semisubmersibles and TLP's	240
10.1	Height Coefficients for Wind Speed Profile	266
10.2	Values of the Factor "K"	267
10.3	Shape Factors $C_s$	267
11.1	Drag Coefficients	273
12.1	Comparison of Stability Criteria for Semisubmersible Barge	286





## LIST OF FIGURES

<u>FIGURE NO.</u>	<u>SUBJECT</u>	<u>PAGE NO.</u>
1.1	Wave-Structure Dynamic Interaction	4
2.1	Pile Founded Guyed Tower	7
2.2	Lena Guyed Tower	8
3.1	Definition Sketch of the Six Components of Motion of a Floating Body	38
3.2	Sketches of Key Semisubmersible Rigs	39
3.3	Various Types of Semisubmersible Drilling Units	40
3.4	Castoro Sei Semisubmersible Pipelay Vessel	41
3.5	Nomad Semisubmersible Derrick Barge	42
3.6	J. Ray McDermott's DB 100 Semisubmersible Crane Vessel	42
3.7	Sedco/Oxy MSV	43
3.8	Heerema Semisubmersible Crane Vessel	43
3.9	The Air Force ACMI Semisubmersible	44
3.10	Cluff-Copson's Semi-Flex Floating Production Facility	45
3.11	ODECO's New Semisubmersible Ocean Odyssey	46
3.12	Norsk Hydro Climatized Semisubmersible	47
3.13	German RS 35 Semisubmersible Concept	48
3.14	Optimization Cycle for Pipelay/Derrick Semisubmersible Design	49
3.15	Hutton Field Tension Leg Platform	50
3.16	Typical TLP Designs	51
3.17	Typical TLP Designs	52
3.18	Tecnomare TLP Design	53
3.19	Network Activities for TLP Design	54
3.20	TLP Stability Assessment Check Conditions	55
3.21	Dynamic Stability Criteria Curve	55
3.22	Multiple Piece Anchor Template Lowering to Seabed	56
3.23	Single Piece Subsea Anchor Template Installation Using a D/P Vessel	56
3.24	Semisubmersible and TLP Natural Frequencies Comparison	57

LIST OF FIGURES (Continued)

<u>FIGURE NO.</u>	<u>SUBJECT</u>	<u>PAGE NO.</u>
3.25	TLP Tether Weights vs. Platform Weights	58
3.26	TLP Tether and Riser Periods vs. Water Depth and Pretension	58
4.1	Overview of Solution Techniques Associated with Floating Objects Subject to Wave Excitation	86
4.2	Steps Involved in Transferring the Sea State Information into Structural Response Data	87
4.3	Analytical Tools of Seaway and Floating Platforms Motion Analysis and Prediction	88
4.4	Schematic of Coordinate System	89
4.5	Platform Equations of Motion Using Diffraction Theory	90
4.6	Platform Equations of Motion Using the Morison Equation	91
5.1	Definition Sketch for Progressive Waves	141
5.2	Classification of Ocean Waves According to Wave Period	141
5.3	Angular Deformation Without Rotation of Fluid Element	142
5.4	Relation Between $\psi$ and Velocity Components $u$ and $v$	142
5.5	Particle Orbits and Variation of Particle Velocity Amplitudes with Depth	143
5.6	Extended and Stretch Methods for Modification of Airy Wave Theory	144
5.7	The Cnoidal Wave Profile with its Limiting Forms	145
5.8	Ranges of Wave Theories Giving the Best Fit to the Free Surface Boundary Condition	146
5.9	Ranges of Suitability for Various Wave Theories	147
5.10	Regions of Validity for Various Wave Theories	148
5.11	Horizontal Particle Velocity Under Wave Crest for Deep Water	149
5.12	Horizontal Particle Velocity Under Wave Crest for Shallow Water	149
5.13	Comparison Between Stokes Fifth-Order and Maximum Velocities in Sea Waves During Tropical Storm 'Delia'	150
5.14	Profile of Ocean Waves	151

LIST OF FIGURES (Continued)

<u>FIGURE NO.</u>	<u>SUBJECT</u>	<u>PAGE NO.</u>
5.15	Rayleigh Distribution Curve	151
5.16	Excess Probability Curve for Rayleigh Distribution	151
5.17	Dimensionless Form of Bretschneider and Pierson-Moskowitz Spectra	152
5.18	Comparison of the JONSWAP and Pierson-Moskowitz Spectra	152
5.19	Illustration of a Directional Wave Spectrum	153
6.1	Regions of Validity for Wave Interaction with a Pile	162
6.2	Wave Force Regimes	162
7.1	Ocean Test Structure Results	207
7.2	Variation of Drag Coefficient with Reynolds Number	208
7.3	Marine Roughness Definition	209
7.4	Typical Distribution of Marine Growth	209
7.5	Post-Critical Drag Coefficient for Cylinders	210
7.6	Alternating Vortex Shedding and Resulting Lift and In-Line Forces	211
7.7	Initiation of Vortex Shedding	212
7.8	Alternate Shedding of Vortices and Its Relation to the Lift Force	213
7.9	Strouhal Number Versus Reynolds Number	214
7.10	Free Transverse Oscillations of Circular Cylinders in Harmonic Flow	214
7.11	Lift Amplification Correlation	215
7.12	Schematic of Local Axis System for Flexible Cylinders	215
8.1	Wave Diffraction Theory Example of Facet Model for a Floating Production Platform	242
8.2	Illustration of Finite Element Meshes for Vertical and Horizontal Plane Problems	243
8.3	Wave Forces on a Gravity Structure: Theory and Experiment	244

LIST OF FIGURES (Continued)

<u>FIGURE NO.</u>	<u>SUBJECT</u>	<u>PAGE NO.</u>
8.4	Comparison Between Theory and Experiment for a Tethered Buoyant Platform in Surge Amplitude and Mooring Cable Tension	245
10.1	Wind Exposed Areas	268
10.2	Variation of Wind Forces with Trim	269
10.3	Wind Heeling Levers Obtained from Wind Tunnel Test and from ABS Wind Force Calculations	269
11.1	Current Velocity Profile	274
11.2	Drag Coefficient Variation	275
11.3	Drag Coefficient Values	276
11.4	Effect of Roughness	276
11.5	Drag Coefficient of Circular Cylinders	277
12.1	Definition Sketch for Center of Buoyancy and Metacenter	289
12.2	Dynamic Stability Curve	290
12.3	Stability Curve	291
13.1	Hybrid Mooring System, Slack Profile	312
13.2	Hybrid Mooring System, Pretension Profile	313
13.3	Hybrid Mooring System Details	314
13.4	Design Methodology for Catenary Mooring Systems	315
13.5	Current Forces Versus Heading Angle	316
13.6	Environmental Loading Directions Used in Mooring System Design	317
13.7	Horizontal Line Tensions Due to Current with 55 Degree Mooring Pattern	318
13.8	Forces and Moments as a Function of Wind Heading	319
13.9	Horizontal Line Tensions Due to Wind with 55 Degree Mooring Pattern	320
13.10	Sway Motion Due to Waves as a Function of Horizontal Stiffness	321

LIST OF FIGURES (Continued)

<u>FIGURE NO.</u>	<u>SUBJECT</u>	<u>PAGE NO.</u>
13.11	Horizontal Line Tension Due to Waves as a Function of Horizontal Stiffness	322
13.12	Mathieu Instability Regions (System with Linear Damping)	323
13.13	Mathieu Instability Regions (Undamped System)	324
13.14	Periods of Secondary Lateral Modes	325
14.1	Space Frame Structural Model	348
14.2	Computer Generated Source-Sink Model for a TLP	349
14.3	Integrated Motion - Structural Analysis Procedure for a TLP	350
14.4	Integrated Motion - Structural Analysis Procedure for a TLP	351
14.5	A Method for Overall Design of a Semisubmersible or TLP	352
14.6	Semisubmersible or TLP Preliminary Design Process	353
14.7	Deck Support Structure	354
14.8	Deck Design Procedure	355
14.9	Hydrodynamic Pressure on a Column	356
14.10	TLP Column Structural Components Shown in Cutaway View	357
14.11	TLP Column Structural Arrangement	358
14.12	Overall Column Design Procedure	359
14.13	View of Pontoon Framing	360
14.14	Overall Pontoon Design Procedure	361
14.15	TLP Configuration at Maximum Offset	362
14.16	Intact and Damaged TLP Floatout	363
14.17	In-Place Structural Analysis of TLP for Damaged Condition	364
14.18	Method of Semisubmersible Structural Analysis	365
14.19	Column to Pontoon Node Finite Element Analysis	366
14.20	Fatigue Analysis Procedure for a Semisubmersible/TLP	367
14.21	Analytical Procedure for Hutton TLP Analysis	368



## ABBREVIATIONS

<u>Abbreviation</u>	<u>Definition</u>
2-D	Two-Dimensional
3-D	Three-Dimensional
ABS	American Bureau of Shipping
ACMI	Air Combat Maneuvering Instrumentation
AIAA	American Institute of Aeronautics and Astronautics
AISC	American Institute of Steel Construction
API	American Petroleum Institute
ASCE	American Society of Civil Engineers
ASME	American Society of Mechanical Engineers
BEM	Boundary Element Method
BOSS	Behavior of Offshore Structures
BSRA	British Ship Research Association
c.g.	Center of Gravity
CIRIA	Construction Industry Research and Information Association
D.A.F.	Dynamic Amplification Factor
DnV	Det norske Veritas
DOE	Department of Energy
DOF	Degrees of Freedom
D/P	Dynamically Positioned
D.T.M.B.	David W. Taylor Model Basin
EPR	Exxon Production Research Company
erf	Error Function
ETCE	Energy Technology Conference and Exhibition
EXVP	Extended Velocity Profile
F.D.	Frequency Domain
FDM	Finite Difference Method
FEM	Finite Element Method
GTP	Guyed Tower Platform
HEM	Hybrid Element Method
ISSC	International Ship Structures Congress
JONSWAP	Joint North Sea Wave Project

## ABBREVIATIONS

<u>Abbreviation</u>	<u>Definition</u>
MD	Maritime Directorate (Norway)
MWL	Mean Water Level
NMI	National Maritime Institute
N.S.M.B.	Netherlands Ship Model Basin
NSRDC	Naval Ship Research and Development Center
NSTL	National Space Technology Laboratories
ONR	Office of Naval Research
OTC	Offshore Technology Conference
OTEC	Ocean Thermal Energy Conversion
OTS	Ocean Test Structure
P-M	Pierson-Moskowitz
RINA	Royal Institution of Naval Architects
R.M.S.	Root Mean Square
SCF	Stress Concentration Factor
S.F.	Safety Factor
S.I.	Standing Instruction
SNAME	Society of Naval Architects and Marine Engineers
SSDU	Semisubmersible Drilling Unit
STAR	Scientific and Technical Aerospace Reports
SWATH	Small Water Plane Area Twin Hull
SWL	Still Water Level
TBP	Tethered Buoyant Platform
T.D.	Time Domain
TLP	Tension Leg Platform
TPP	Tethered Production Platform
UK	United Kingdom
UK DTI	United Kingdom Department of Trade and Industry
U.S.	United States
USCG	U.S. Coast Guard
USGS	U.S. Geological Survey
VMP	Vertically Moored Platform



## NOMENCLATURE

### CHAPTER 1

- $T_n$  = natural period  
 $T_p$  = spectral peak period

### CHAPTER 3

- $^{\circ}\text{F}$  = degrees Fahrenheit

### CHAPTER 4

- $A$  = projected area per unit length perpendicular to flow direction or area of cross section  
 $A_{jk}$  = added mass matrix  
 $B$  = linear damping coefficient  
 $(B_R)_{jk}$  = radiation damping matrix  
 $B_S$  = structural damping coefficient  
 $(B_V)_{jk}$  = viscous damping matrix  
 $B_{jk}$  = hydrodynamic damping matrix  
 $C$  = stiffness coefficient  
 $C_d$  = drag coefficient  
 $C_{d1}$  = linearized drag coefficient  
 $C_{jk}$  = stiffness matrix (hydroelastic restoring plus mooring)  
 $C_m$  = inertia coefficient  
 $(C_H)_{jk}$  = hydrostatic stiffness matrix  
 $E$  = modulus of elasticity  
 $F_D$  = drag force  
 $F_I$  = inertia force

## CHAPTER 4 (Cont'd)

$F_j(t)$	=	forcing functions = time varying exciting forces
$f$	=	generic resultant force acting on body
$g$	=	gravitational acceleration
$H$	=	wave height
$H(\omega)$	=	complex frequency response function
$ H(\omega) $	=	gain factor = response amplification operator (RAO)
$I_{jj}$	=	mass moment of inertia
$I_{jk}$	=	product of inertia
$j, k$	=	subscripts for modes 1 to 6 (surge, sway, heave, roll, pitch, and yaw)
$K_{jk}(t)$	=	retardation function
$k$	=	wave number
$(L_M)_{jk}$	=	mooring stiffness matrix
$L_j(t)$	=	nonlinear mooring restoring forces
$M$	=	structural mass
$m_a$	=	generic added mass
$m_{jk}$	=	frequency-independent impulsive added mass matrix
$M_{jk}$	=	structural mass matrix
$S_{\eta\eta}(\omega)$	=	wave spectrum
$S_{xx}$	=	response spectrum
$t$	=	time
$u$	=	water particle velocity
$V$	=	volume per unit length of slender member
$X$	=	structural displacement
$\dot{X}$	=	structural velocity

#### CHAPTER 4 (Cont'd)

$X$	=	structural acceleration
$X_1$	=	surge (positive forward) displacement
$X_2$	=	sway (positive to port) displacement
$X_3$	=	heave (positive upward) displacement
$X_4$	=	roll (positive, deck down to starboard) displacement
$X_5$	=	pitch (positive, bow downward) displacement
$X_6$	=	yaw (positive, bow to port) displacement
$X_i$	=	( $i = 1$ to $6$ ) displacement components of platform c.g.
$X_0$	=	amplitude of response
$X, Y, Z$	=	coordinating system attached to platform c.g.
$X, Y, Z$	=	fixed coordinate system
$(X)_{rms}$	=	root mean square of random variable $X$
$f_0$	=	amplitude of forcing function
$\beta$	=	wave heading measured from the $X$ -axis
$\Delta t$	=	small time interval
$\rho$	=	water mass density
$\phi(\omega)$	=	phase factor
$\omega$	=	wave circular frequency
$(\alpha, \beta, \theta)$	=	Euler angles

#### CHAPTER 5

$A$	=	amplitude of wave
$C$	=	speed of wave propagation (phase speed, phase velocity, celerity, = $L/T = \omega/k$ ) = wave celerity
$C(n)$	=	normalizing function

CHAPTER 5 (Cont'd)

d	=	distance from MWL to bottom = water depth
E	=	area under energy spectrum
f	=	wave frequency (= 1/T)
G( $\theta$ )	=	wave spreading function
H	=	wave height (= 2A for small amplitude wave theory)
(H, T)	=	mean wave height and period
( $H_{1/10}$ , $T_{1/10}$ )	=	average one-tenth highest wave height and period
( $H_{1/3}$ , $T_{1/3}$ )	=	significant wave height and period
( $H_{\max}$ , $T_{\max}$ )	=	maximum wave height and period
k	=	wave number (= $2\pi/L$ )
L	=	wave length
$\bar{L}$	=	average apparent wave length
$M_n$	=	nth moment of energy spectrum
$M_0$	=	area under energy spectrum = E
N	=	number of waves
p	=	pressure
q	=	magnitude of velocity vector = $(u^2 + v^2 + w^2)^{1/2}$
q (u,v,w)	=	fluid particle velocity vector = grad $\phi$
S	=	spectrum
S(f, $\theta$ )	=	wave directional spectrum = S(f) G( $\theta$ )
T	=	wave period
U	=	UrSELL number (= $HL^2/d^3$ )
u	=	wave velocity component in X-direction
v	=	wave velocity component in Y-direction
w	=	wave velocity component in Z-direction

## CHAPTER 5 (Cont'd)

$\overline{X}, \overline{Y}, \overline{Z}$	=	coordinate system attached to platform c.g.
$X, Y, Z$	=	fixed coordinate system
$\phi(x,y,z,t)$	=	velocity potential
$\eta(x,t)$	=	instantaneous vertical displacement of sea surface above MWL
$\theta$	=	angle showing direction of waves
$\overline{\theta}$	=	direction about which wave spectrum is centered
$\sigma^2$	=	mean square value of a wave record
	=	area E under energy spectrum = $M_0$
	=	1/2 area under amplitude spectrum
$\Omega$	=	rotation vector
$\Omega_x$	=	component of rotation vector about x-axis
$\Omega_y$	=	component of rotation vector about y-axis
$\Omega_z$	=	component of rotation vector about z-axis
$\omega$	=	wave angular frequency (= $2\pi/T = 2\pi f$ )
$\omega_p$	=	wave spectrum peak frequency

## CHAPTER 6

$C_a$	=	$C_m - 1$ = added mass coefficient
$C_d$	=	drag coefficient
$C_m$	=	inertia coefficient
$D$	=	diameter
$F$	=	the Morison force per unit length of cylinder
$F_D$	=	drag force
$F_I$	=	inertia force

## CHAPTER 6 (Cont'd)

KC	=	Keulegan-Carpenter number = $uT/D$
Re	=	Reynolds number = $uD/\nu$
u	=	horizontal water particle velocity
$\dot{u}$	=	horizontal water particle acceleration
$V_c$	=	current velocity
W	=	orbit width of the water particle
$\nu$	=	kinematic viscosity
$\rho$	=	water mass density

## CHAPTER 7

A	=	projected area per unit length
$C_L$	=	lift coefficient
$C_L/C_L^0$	=	lift amplification parameter
$C_L^0$	=	lift coefficient of stationary cylinder in hydrodynamically similar flow
$C_a$	=	$C_m - 1$ = added mass coefficient
$C_d$	=	drag coefficient
$C_{da}$	=	drag coefficient for cylinder undergoing hydroelastic oscillations
$C_m$	=	inertia coefficient
D	=	diameter
F	=	the Morison force per unit length
$F_L$	=	lift force
$f_n$	=	natural frequency of the body
$F_r$	=	resisting force

## CHAPTER 7 (Cont'd)

$F_{trans}$	=	transverse force per unit length = $F_L - F_r$
$f_n$	=	natural period of cylinder
$f_v$	=	vortex shedding frequency
$f_v/f_w$	=	ratio of dominant shedding (lift) frequency to wave frequency
$H$	=	wave height
$KC$	=	Keulegan-Carpenter number = $uT/D$
$KC^*$	=	$KC$ at perfect synchronization
$kd$	=	water depth parameter = wave number x depth
$k_r$	=	roughness height
$k_r/D$	=	relative roughness
$L$	=	wave length
$m$	=	effective mass of the cylinder
$Re$	=	Reynolds number = $uD/\nu$
$R_p$	=	response parameter
$r$	=	increase in cylinder diameter due to marine growth buildup
$St$	=	Strouhal number = $f_v D/u$
$T$	=	wave period
$u$	=	horizontal fluid particle velocity
$\dot{u}$	=	horizontal water particle acceleration
$V$	=	volume per unit length
$V_c$	=	current velocity
$V_r^*$	=	reduced velocity at location on cylinder where shedding frequency chosen to be dominant

## CHAPTER 7 (Cont'd)

$V_r$	=	reduced velocity = $u/f_n D$
$X$	=	structural velocity
$\dot{X}$	=	structural acceleration
$y$	=	cylinder displacement in the in-line direction
$z$	=	cylinder displacement in the transverse direction
$\nu$	=	kinematic viscosity
$\rho$	=	water mass density
$\omega_p$	=	spectral peak frequency
$\omega_v$	=	predominant (or dominant) circular lift frequency

## CHAPTER 8

$A_{jk}$	=	added mass matrix
$B_{jk}$	=	damping matrix
$C_{jk}$	=	stiffness matrix
$D$	=	diameter
$F^e$	=	exciting force on the body
$F_j^{(e)}$	=	total wave force or "exciting force", harmonic in time
$f(p)$	=	unknown source strength distribution
$F_j^{(w)}$	=	Froude-Krylov force
$G(X,p)$	=	Green's function of a point wave source of unit strength at point $p$
$L$	=	wave length
$M_{jk}$	=	structural mass matrix
$N$	=	number of sources to describe body contour in wave source method



## CHAPTER 8 (Cont'd)

$n$	=	normal to surface of body
$n_j$	=	components of generalized normal vector
$n_x, n_y, n_z$	=	direction cosines of normal to body surface
$(r, \theta)$	=	cylindrical polar coordinates
$S$	=	body surface
$V_n$	=	velocity of body in direction of the normal
$X_k$	=	structural response
$\phi_b$	=	body wave potential
$\phi_d$	=	diffracted wave potential
$\phi_e$	=	excitation potential = $\phi_w + \phi_d$
$\phi_k(x,y,z,t)$	=	body potential associated with mode $X_k$
$\phi_w$	=	incident wave potential

## CHAPTER 9

$C_d$	=	drag coefficient
$C_{mds}$	=	dimensional constant
$D$	=	diameter
$F_D$	=	drag force
$F_{mds}$	=	mean drift force acting on semisubmersible hull
$F_{wc}$	=	wave-current drift force
$H_s$	=	significant wave height
$L$	=	wave length
$p$	=	pressure
$q$	=	water velocity at body surface due to first order velocity potential = $(u^2 + v^2 + w^2)^{1/2}$

## CHAPTER 9 (Cont'd)

$T$	=	wave period
$T_s$	=	significant wave period
$u_{wm}$	=	maximum horizontal orbital velocity at a particular point
$V_c$	=	current velocity
$h$	=	length of wetted part of column below mean water level
$h+\eta$	=	length of wetted part of column in the presence of waves ("instantaneous wetted length")
$\epsilon$	=	a small parameter ( $\epsilon \ll 1$ )
$\phi$	=	velocity potential
$\phi^{(1)}$	=	first order velocity potential
$\phi^{(2)}$	=	second order velocity potential

## CHAPTER 10

$A_c$	=	projected area against current
$A_i$	=	area of $i$ th windage
$A_{wind}$	=	wind exposed area of windage
$C_d$	=	drag coefficient
$C_h$	=	height coefficient for wind velocity profile
$C_s$	=	shape factor
$(C_s)_i$	=	shape factor for $i$ th object
$(C_{sh})_i$	=	shielding factor for $i$ th object
$d$	=	distance from water surface to mudline
$d_{lw}$	=	width (or diameter) of the leeward member
$d_{ww}$	=	width (or diameter) of the windward member

## CHAPTER 10 (Cont'd)

$F_w$	=	wind force on platform with "N" number of items exposed to wind
$f_m$	=	non-dimensional frequency
$f_s$	=	non-dimensional frequency
$K_w$	=	wind surface stress coefficient
$k_v$	=	von Karman constant ( $\approx 0.40$ )
$L$	=	length scale dimension
	=	5900 feet for Harris spectrum
	=	4000 feet for Davenport spectrum
$L_u$	=	integral scale of longitudinal wind velocity fluctuations (in direction of mean wind speed)
$N$	=	number of items exposed to wind
$n$	=	fluctuation frequency
$Re$	=	Reynolds number
$S_v(n)$	=	wind spectrum
$V_i$	=	wind velocity at centroid of $A_i$
$V_{wind}$	=	wind velocity at the center of wind exposed area
$V_z$	=	wind speed at height $z$ feet above SWL
$V_{30(10)}$	=	wind speed at a reference height of 30 feet (10 meters) above SWL
$v$	=	longitudinal wind velocity
$\frac{v}{v_{ref}}$	=	mean velocity of wind at reference elevation
$v'$	=	longitudinal wind velocity fluctuation
$v^*$	=	friction velocity
$x$	=	distance above mudline

## CHAPTER 10 (Cont'd)

$Z$	=	any elevation
$Z_o$	=	roughness length = sea drag coefficient $K$
$Z_{ref}$	=	reference elevation
'	=	(prime) denotes fluctuating part
—	=	(bar over letter) denotes mean value
$1/n$	=	exponent between 1/13 and 1/7 for wind speed determination
$\beta$	=	coefficient defining mean square value of turbulent fluctuation in terms of friction velocity $v_*$
$\nu$	=	kinematic viscosity of water
$\rho_{air}$	=	air mass density
$\rho_{water}$	=	water mass density

## CHAPTER 11

$A_c$	=	projected area in direction of current
$C_d$	=	drag coefficient
$d$	=	distance from water surface to mudline = water depth
$F_{current}$	=	current force
$Re$	=	Reynolds number
$(V_c)_s$	=	current velocity at water surface
$(V_c)_x$	=	current velocity at distance $x$ above mudline
$x$	=	distance above mudline
$\rho_{water}$	=	water mass density

## CHAPTER 12

FSC	=	free surface correction
GM	=	metacentric height
$(I_T)_i$	=	moment of inertia of liquid plane in the $i$ th tank about the tank heeling or trimming axis
KB	=	distance of center of buoyancy above keel
KG	=	distance of center of gravity above keel
N	=	number of tanks
$\delta_{\text{liquid}}$	=	specific volume of the liquid in the tank
$\Delta$	=	displacement of the vessel

## CHAPTER 13

B	=	linear damping coefficient
$F(t)$	=	horizontal wave force acting on the platform
$F_0$	=	amplitude of wave force
$f_0$	=	peak spectrum frequency
k	=	wave number
L	=	length of tendons
M	=	structural mass
$m_a$	=	added mass
T	=	total tensile force in tendon system
T/L	=	stiffness coefficient (spring constant) of fictitious horizontal and linearly elastic spring
$T_0$	=	constant tensile force
$T_w$	=	wave period
$T_x$	=	period of TLP in simple surge motion

CHAPTER 13 (Cont'd)

- $T(t)$  = total tendon force
- $\mu$  = excitation parameter
- $\omega_x$  = undamped circular frequency of TLP

INTRODUCTION

Over the past thirty years pile founded steel jacket-type platforms (commonly referred to as fixed platforms) have represented the most common structural solution for offshore structures and in particular the offshore oil and gas industry's drilling and production facilities. The need to move into deeper waters, technological advancements, ever-growing expertise, more sophisticated analytical techniques and faster and larger computers have pushed the state-of-the-art further and further. Today the tallest steel jacket, Shell's Cognac platform, stands in 1050 feet of water in the Gulf of Mexico. There are various indications that with the present technology, water depths much beyond 1000 feet may require an altogether different approach.

One of the main problems to be faced by the designer of deep water platforms is the dynamic interaction between waves and structure. Figure 1.1, shows a set of design conditions typical of the Gulf of Mexico. The main diagram shows three wave spectra, labeled as operating weather, winter storm, and design storm. The curve in the frame describes how the dynamic amplification factor (D.A.F.) varies with the ratio of the structural period to the dominant wave period. It should be noted that the curve shown is valid for systems with a single degree of freedom, while an offshore structure is obviously a multi-degree of freedom system. For a qualitative discussion, however, the simplification is acceptable.

The shallow water (300 feet) steel jacket has a natural sway period ( $T_n$ ) of about 2 seconds; this period is much lower than the peak period of a sea state ( $T_p$ ), of the various sea states. Accordingly, the ratio of the periods is less than one ( $T_n/T_p \ll 1$ ), and the point representing this ratio on the dynamic amplification factor (D.A.F.) curve is on the left side of the resonance peak. As long as the period ratio ( $T_n/T_p$ ) is small enough, the D.A.F. is very close to 1 and the structural response is essentially static.

As the water depth increases, the structure's natural sway period increases and approaches the spectral peak period of a sea state while the D.A.F. becomes larger than 1 and moves closer to the resonance peak. For a 1000-foot water depth steel jacket, the structure's natural sway period (4-6 seconds) is such that the interaction with the design storm is limited; but the energy associated with the operating sea states is amplified significantly. As a consequence, fatigue becomes a critical aspect of the design; modifications may be needed to stiffen the structure. This results in a dramatic increase in steel tonnage, in additional costs, and in fabrication and installation difficulties.

The logical question to be asked is whether or not the problem could be solved by resorting to a different approach. Rather than trying to minimize the dynamic wave-structure interaction by reducing the structural period, could the same effect be obtained by making the structural period higher than the wave period? The answer is provided by the so-called compliant structures such as the guyed tower platform, the tension leg platform, the buoyant tower, etc. The common characteristic of these structural concepts is that the ratio of the surge and sway periods to the wave period is greater than 1; accordingly, the D.A.F. becomes less than 1, thereby reducing the dynamic loads.

Semisubmersibles are also compliant structures and have very large surge, sway, and yaw natural periods (about 100 seconds). The new generation, large displacement semisubmersibles have roll and pitch natural periods of about 25 seconds and are designed to have heave periods in the 20 second range. For large displacement semisubmersibles the natural periods for all rigid body motions are greater than the dominant sea wave period. This ensures workable response characteristics and prevents a resonant condition with most sea states encountered worldwide. However, studies have shown that lighter semisubmersibles (about 250 short ton displacement) have the surge, sway, and yaw natural periods of the same order of magnitude



as the larger concepts, but their roll and pitch natural periods are in the 18 second range and their heave period may be around 12 seconds. Therefore, special consideration should be given to the design of these small displacement semisubmersibles because these important response characteristics fall in the range of dominant wave periods.

Mooring system characteristics have a significant effect on the natural periods of the structures under consideration. The influence of the mooring system will be more pronounced in the case of small displacement semisubmersibles than in the case of larger platforms.

This review is mainly concerned with loadings and responses of floating moored structures. In particular, attention will be focused on semisubmersibles and tension leg platforms. While a detailed description of the guyed tower platforms is outside the scope of this review, a few basic items will be discussed for the sake of completeness and in order to understand the difficulties relative to the design and analysis of this structural concept.

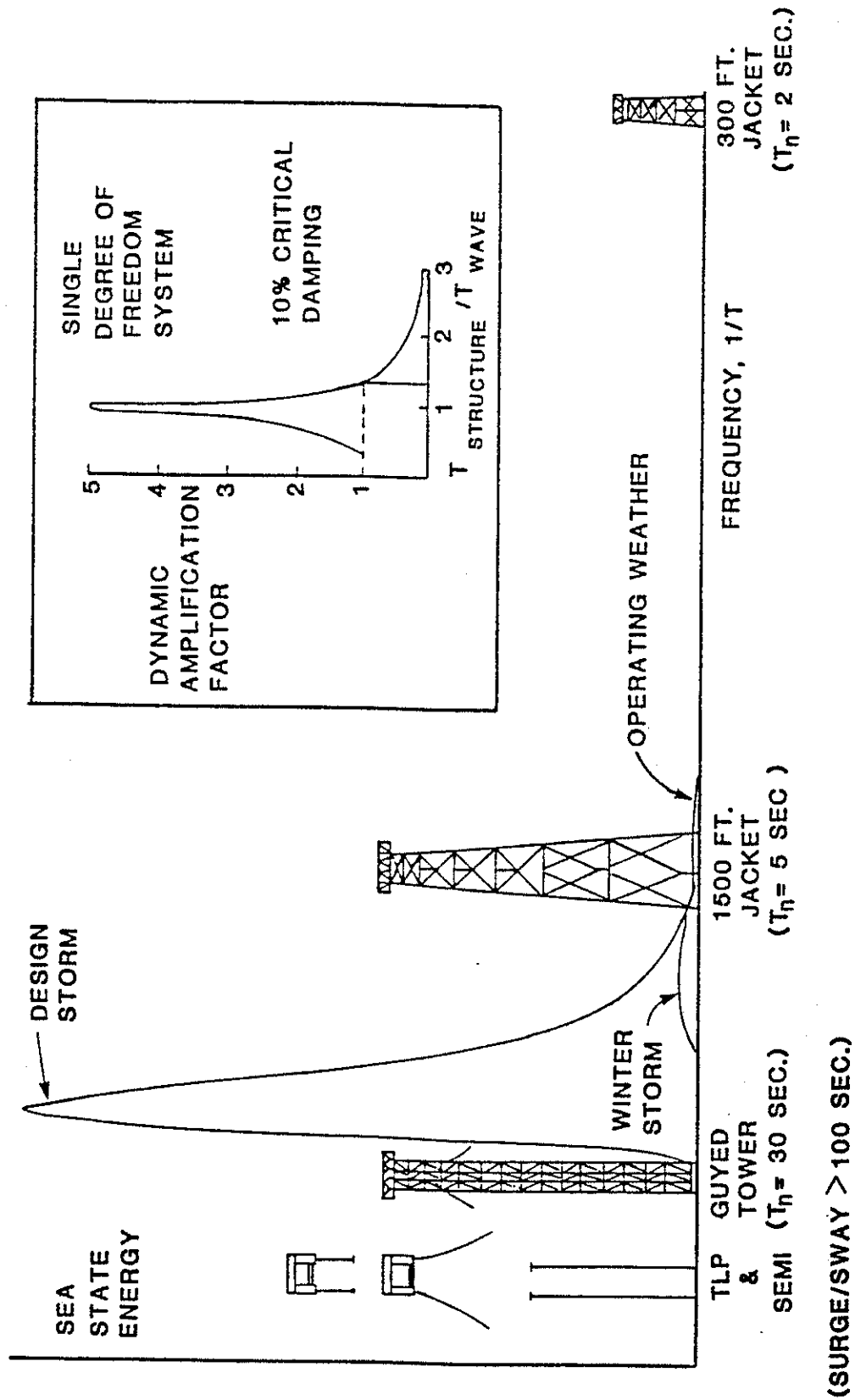


FIGURE 1.1 WAVE - STRUCTURE DYNAMIC INTERACTION

GUYED TOWER PLATFORMS (GTP's)

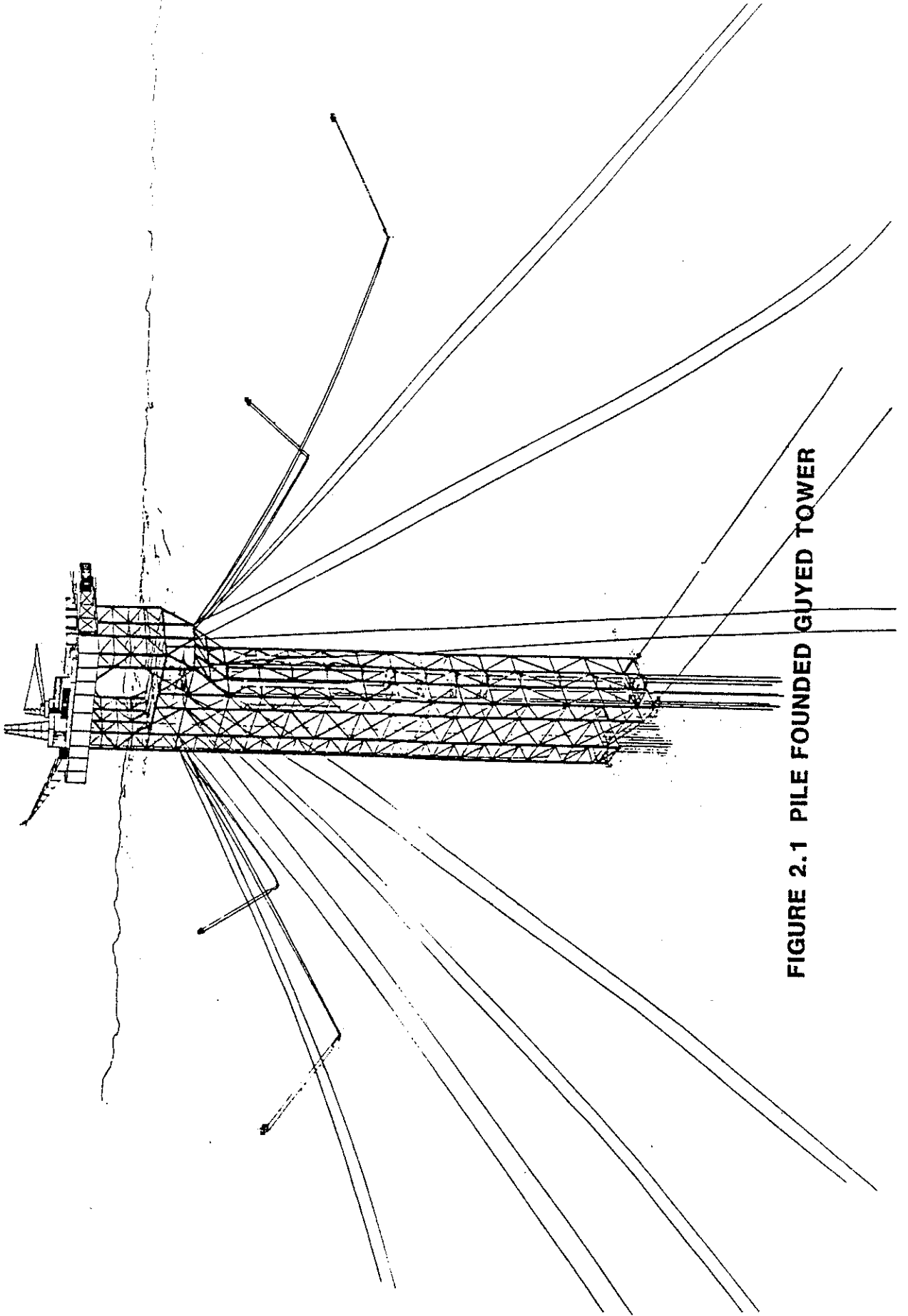
The guyed tower platform (GTP) concept has been described in various papers by Finn (1976), Finn and Young (1978), Finn et al. (1979), Mangiavacchi et al. (1980), and Glasscock and Finn (1984). The GTP is a trussed structure that rests on the ocean floor and extends upward to a deck supported above the waves. The tower is laterally supported by an array of mooring lines.

Each mooring line (or guyline) consists of a lead (or catenary) line, a clump weight, and a trailing (or anchor) line. The presence of the clump weight limits the maximum tension in a single line. As the tension exceeds a preset limit, the clump weight lifts, the trailing line becomes active, and the mooring system's stiffness decreases. This phenomenon will increase both the surge and sway natural periods of the structure, reducing the likelihood of wave-structure interaction.

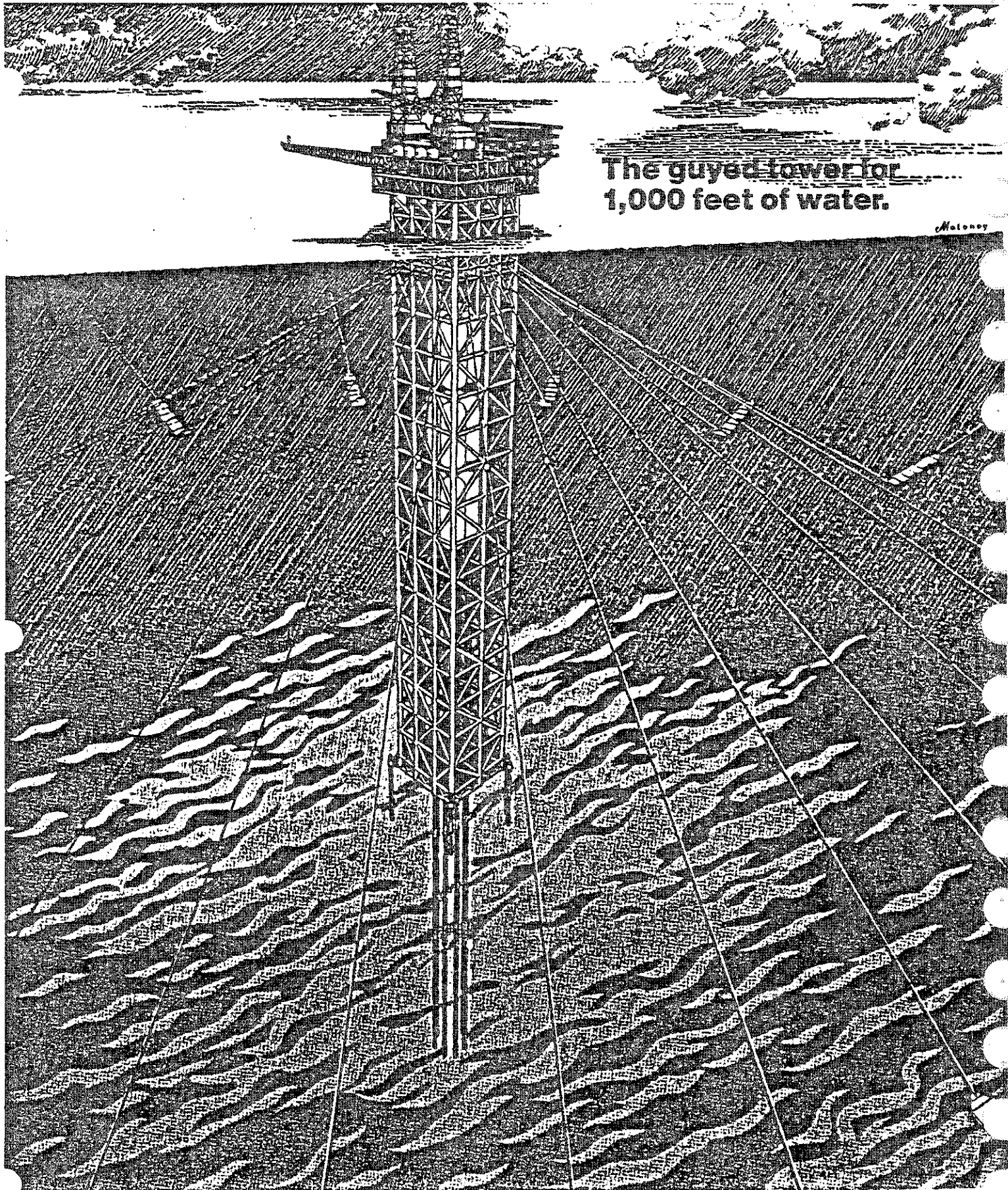
Because of the lateral support provided by the mooring lines, the tower is not expected to resist the total overturning moment like a conventional jacket. Hence, a uniform tower cross section can be used with 12 or 16 main jacket legs extending from the mudline to the top of the jacket. This reduces the total required steel compared to a fixed jacket for the same water depth. It should be noted that most of the members in the tower are buoyant, and the gravity load supported by the foundation is therefore reduced. Should the gravity load be too heavy for the foundation, permanent buoyancy tanks may be utilized to offset the excess weight. The main problem to be solved is how to obtain sufficient compliancy to enable the structure to oscillate with the waves without overstressing the foundation. Finn (1976), Finn and Young (1978), Finn et al. (1979) and Audibert et al. (1979) presented concepts based on the adoption of the spud can as the foundation solution, while Mangiavacchi et al. (1980) introduced an original development in which the foundation consisted of conventional piles. Figure 2.1 shows a sketch of a pile founded guyed tower designed for the North Sea.

The analysis of the GTP presents formidable challenges because of various nonlinearities involved. The presence of the clump weights obviously introduces a nonlinearity in the system. Wave-structure interaction is another nonlinearity that has to be accounted for. Compared to fixed jackets, the structural motions of GTP's in surge and sway are relatively large (GTP's are designed to have the total offset less than a couple of degrees from vertical). Consequently, the hydrodynamic drag forces due to wave and current must be written in terms of relative velocity between the fluid and structure in the Morison equation. Additional overturning moment due to the large offset and heavy deck weight contributes to the geometric nonlinearity. Finally, the high nonlinear soil behavior affects the foundation stiffness of GTP's. An efficient method for the nonlinear dynamic analysis of GTP's is presented by Hanna et al. (1981).

The GTP is a technological reality today. The first commercial GTP (Lena) was installed by Exxon in the summer of 1983 in a water depth of 1000 feet in the Gulf of Mexico, see LeBlanc (1983), Figure 2.2. Research work is underway to simplify the GTP and make it more economical and cost effective for production of smaller reservoirs.



**FIGURE 2.1 PILE FOUNDED GUYED TOWER**



The guyed tower for  
1,000 feet of water.

Maloney

FIGURE 2.2 LENA GUYED TOWER

## 3.0 FLOATING MOORED STRUCTURES

### 3.1 Introduction

The concept of an ocean platform as a stable floating unit capable of remaining on station with limited motion characteristics was introduced in the early 1920's as indicated by St. Denis and Almendinger (1971). These platforms today are designed to accomplish a number of missions, including mineral recovery, oil drilling, pipe laying and support, and research work.

Five basic types of floating platforms can generally be identified, viz., submersibles, semisubmersibles, jackups, ship-shaped vessels, and tension leg platforms (TLP's). The reasons for a clear distinction between semisubmersibles and TLP's are presented in Section 3.4.

These platforms are either connected to the bottom by legs (often called tendons or tethers for TLP's) or mooring lines, or are free and kept on location by means of propulsion devices. According to Van Sluijs and Minckenberg (1977), there are three important considerations in the design of the floating ocean platforms:

1. Stability and survival. The platform should be operable under adverse weather conditions and should be able to survive in high seas, wind gusts, and overridden moorings (See Numata and Michel, 1974).
2. Strength. The platform should remain intact under survival conditions. Under these circumstances it is necessary for semisubmersible platforms, TLP's and jackups to maintain a proper clearance (referred to as air gap) between the upper deck and the water surface to avoid hydrodynamic impacts.

3. Mobility. The hydrodynamic resistance in transit condition has to be as low as practical (see Macy 1966).

Most applications of floating ocean platforms require that they be designed for minimum motion characteristics. Therefore the platforms should have long natural motion periods to avoid or minimize resonance with dominant waves. The most effective platforms have natural surge and sway periods greater than 20 seconds, and natural periods of pitch and roll greater than 30 seconds (see Bell 1974). In order to avoid resonance in heave motions, the ocean platforms are usually designed to have heave natural periods larger than the dominant wave periods. However for TLP's the tendency is to keep heave natural periods below 5 seconds to prevent fatigue in the tendons. Since the subject of rigid body motions of a floating platform will be encountered repeatedly during the course of this review, a brief description of these motions is considered appropriate here.

A rigid floating body may have a motion with six degrees of freedom: three translational and three rotational. In the terminology of naval architecture, the translational motions in X, Y, and Z directions are referred to respectively as surge, sway and heave; and the rotational motions about the X, Y, and Z directions respectively as roll, pitch and yaw. In Figures 3.1a and 3.1b the X coordinate is taken to lie along the longitudinal axis of the body and Z is the vertical direction. However, for symmetrical platforms of equilateral triangle, square, or circular shape which do not have a preferred longitudinal axis, the coordinate system may be arbitrarily placed along one of the axes of symmetry of the structure. An example of this case is shown in Figure 3.1c. A more detailed description of the coordinate system and rigid body motion associated with floating bodies is given in Chapter 4.0.

A review of the studies on all ocean platform motions is beyond the scope of the survey. A synopsis of the subject may be found in a



paper by Van Sluijs and Minkenberg (1977). This study will be focused on loadings and responses of semisubmersibles and tension leg platforms.

### 3.2 Semisubmersibles

Semisubmersible platforms consist of submerged bodies connected to the working decks above the water by means of columns or slender walls. Some derrick barges, pipelaying barges, storage platforms, production platforms, and drilling platforms are built in this way, since experience has shown that the motions of this type of vessel are smaller for a given sea state than the motions of ship-type vessels or barges. Semisubmersibles were introduced starting from the idea that their wave-induced motions are decreased by lowering a large part of the buoyancy to a region of reduced wave excitation. Motora and Koyama (1959) indicated that semisubmersibles undergo smaller motions than ship-shaped vessels.

Only column-stabilized semisubmersibles can meet the small motion requirement, as their water plane area is small in relation to the displacement. Column-stabilized implies that heave static stability is obtained from the water plane area and that pitch and roll static stability are obtained from the water plane moment of inertia of the surface piercing vertical columns. More elaborate descriptions of this concept are given by Paulling (1970).

The mooring system of a semisubmersible is usually a conventional catenary system, which offers restoring forces predominantly in the horizontal plane and very little in the vertical plane. For this reason semisubmersibles have larger heave motions than TLP's.

#### 3.2.1 Evolution of Semisubmersibles

Construction and deployment of semisubmersibles have gone through a dramatic evolution since they were first introduced.

Macy (1969) describes and illustrates several oil-drilling platforms of this type. One of them, BLUE WATER II, consists of a square base configuration approximately 200 feet by side, made up of cylindrical members 14.5 feet in diameter, with four vertical corner columns 24.7 feet in diameter supporting the main deck. This platform normally operated at a draft of about 40 feet. A second platform, the SEDCO 135, 16,000 short tons displacement, consists of three main vertical columns located approximately at the vertices of an equilateral triangle, several diagonal tubular truss members, and, at the bottom of the main columns, elongated pontoons of oval shape (see Figures 3.2 and 3.3).

Howe (1967) reviewed some developments of offshore drilling and production technology up to 1967. Figure 3.2 shows some of key semisubmersible rigs which he reviewed.

McClure (1965) described a platform designed for the MOHOLE deep sea drilling project. This platform was to consist of two submerged main horizontal pontoons 35 feet in diameter, and 390 feet long, with a centerline separation of 215 feet. Three vertical columns 31 feet in diameter extended from each horizontal pontoon through the free water surface to support the main working deck. This platform had a displacement of 25,000 short tons and was intended to operate in a water depth of 14,000 feet. It was to be dynamically positioned by means of trainable propulsion units controlled through a central computer system.

Since 1970, the need for exploration in deeper waters has given a noticeable momentum to the design and fabrication of heavy construction, drilling and production semisubmersibles.

Rodnight (1983) has reviewed a new generation of semisubmersibles for offshore drilling operation. He points out that the semisubmersible drilling units (SSDU's) are considered the most suited for drilling in harsh environments due to their excellent motion characteristics

(see Table 3.1). A comparison between various drilling platforms is presented in Table 3.1. The cost comparison among various drilling platforms is given in Table 3.2.

Throughout the development of the drilling semisubmersible there has been a general trend to simplify the structural design. Some of the early semisubmersibles were extremely complicated structures when compared with the most recent units (see Figure 3.3). The structural design of today's semisubmersibles has been simplified by:

- o Reduction in number of displacement hulls or pontoons
- o Fewer brace members and nodal joints.
- o Simpler brace connections.
- o Modular deck structures.

Two longitudinal pontoons with four, six, or eight columns supporting the main deck structure has become the universal design for semisubmersibles built over the last 10 years.

Some semisubmersible designs have deleted the horizontal braces tying the pontoons together at the column base level to reduce the drag at transit draught and wave slamming forces on the horizontal braces. This particular design feature has not received widespread approval because of excessive sagging forces occurring at deck structure level.

Construction and pipelay barges have also gone through dramatic changes. Their evolution in the seventies and early eighties shows their suitability for performing operations that some years ago seemed impossible. The following is a brief list of the most notable construction and pipelay semisubmersibles put into service during the 1970's and early 1980's. A more detailed description of these vessels may be found in Ocean Industry, July 1978 and Offshore, August 1978.

- o Castoro Sei -  
Castoro Sei is the newest and largest pipelaying semisubmersible in existence today (Figure 3.4). This vessel was completed in 1978 and its first job was the Trans-mediterranean gas pipeline from Algeria to Sicily.

Castoro Sei has the following specifications:

Length	595 feet
Beam	231 feet
Depth	97 feet
Draft	21 to 50 feet
Displacement	30,000 short tons (minimum)
Operating Depth	2000 feet

The Castoro Sei's two 187-short ton cranes permit the unit to undertake light platform installation work and pipeline tie-in; however, the vessel was designed primarily for pipelaying. A total of 74 vessels worldwide are or can be equipped to lay pipe.

- o Nomad -  
The horseshoe shape of the semisubmersible derrick barge Nomad (Figure 3.5), now in the final design stages, is a result of efforts to provide more points of access to stationary structures by the revolving crane aboard. The hull concept is owned jointly by Nippon Kokan, the owner, and Baker Marine Corporation.

A revolving crane with a fixed lift capacity of 2,000 tons and rotary capacity of 1500 short tons is situated at the top of the horseshoe hull. The semisubmersible has five stabilizing columns. The deck load capacity is 6600 short tons, one of the largest in the industry. Accommodations for 300 workmen will be provided.

The Nomad will be self-propelled with four azimuthing thrusters for limited dynamic positioning and a conventional eight-point mooring system for stationkeeping.

o DB 100 -

J. Ray McDermott's 406 foot long semisubmersible, DB 100 (Figure 3.6), is unique in that it has 13 columns atop a centerline and two outboard hulls. Two of the columns are directly beneath the single-derrick crane. The DB 100's crane has a lift capacity of 2000 short tons fixed and 1600 short tons revolving.

The DB 100 has the following specifications:

Length	406 feet
Beam	275 feet
Depth	130 feet
Draft	27 to 70 feet
Operating Depth	1000 feet

The DB 100 is also capable of moving away from a platform work position to a distance of 500 feet and maintaining a standby mooring position through Sea State Eight. It can maintain station at maximum buoyancy in waves up to 98 feet.

o Sedco/Oxy MSV -

The Sedco/Oxy MSV (Figure 3.7) is of a design similar to the Sedco/Phillips SS with a multitude of firefighting facilities aboard. The unit is being constructed by Mitsubishi Heavy Industries in Japan.

Sedco/Oxy MSV has the following specifications:

Length	300 feet
Beam	249 feet
Depth	114 feet
Draft	22 to 80 feet

Its primary functions are platform diving inspection, maintenance, package lift, pipeline inspection and repair, and construction support. A 100-foot boom supported gangway allows for personnel movement during construction support and firefighting.

The twin-hulled unit has eight support columns, is self-propelled and has a dynamic positioning capability. Remote control firefighting monitors are mounted atop the 350-short ton crane at the center aft of the vessel.

All of the diving equipment aboard the Sedco/Oxy MSV is located below deck and the diving bell enters the hull below the wave zone. This unique feature allows the bell to operate at higher sea states than normally possible.

o NOC Units -

The two large semisubmersible derrick vessels built for Heerema Engineering are unique in that each has two heavy-lift rated cranes aboard instead of one. One is rated for 3000 short tons and the other at 2000 short tons. Only one other vessel in the industry, Heerema's derrick ship Odin, has a 3000-ton lift crane (see Figure 3.8).

The workability expectations of the two Heerema semisubmersibles are 320-340 days per year, comparable to or slightly more than the 475-foot Narwhal's performance in the North Sea. Ship-shape derrick vessels now working in the North Sea have a work expectation of 109 days per year, which make installation time and scheduling difficult and often delays field development.

Ship-shape derrick units were used widely in the southern areas of the North Sea but the latitudes further to the North are subjected to heavier swells. Semisubmersibles are considered to be the most stable hull structures for work in heavy seas. With the use of

computer directed movement of ballast water, in amounts up to 5000 short tons in 20 seconds, the semisubmersible shape can accommodate much heavier lifts than have been previously undertaken.

The evolution of semisubmersibles will continue in future decades since these vessels promise a reliable, feasible, and economical concept for diverse purposes. The degree of versatility of semisubmersibles may be noted in a semisubmersible buoy designed for data collection and telemetry for the United States Air Force Air Combat Maneuvering Instrumentation (ACMI) range in the Philippine Sea (see Figure 3.9). This range will employ five semisubmersibles of this type. These semisubmersible platforms have 250 short tons of displacement and will be trimoored in water depths of 3000 feet to 11,000 feet. McClure and Kirshner (1983) give a more detailed description of this platform. Garzke et al. (1978), Shields et al. (1983) and Shields and Zueck (1984) have also performed studies which have looked at semisubmersibles with displacements of less than 5000 long tons. In each case the small semisubmersible was determined to have superior motion characteristics when compared to discus and spar buoys. The one-third scale Deep Oil Technology TLP "X-1", Horton (1975), was also used as a catenary moored semisubmersible in 1000 feet of water for OTEC cold water pipe testing, Donnelly et al. (1979) and Johns Hopkins University (1980).

The objective of making the semisubmersible as transparent as possible to the passage of waves and while providing a larger waterplane area has produced several conceptual designs for future semisubmersibles. Figure 3.10 shows Cluff-Copson's semi-flex floating production facility which combines vertical columns on universal joints to provide wave transparency, fewer stress points and a larger waterplane.

A new generation of completely winterized (climatized) semisubmersibles will be deployed in the arctic regions. Ocean Drilling and Exploration Company's Ocean Odyssey is an example of this new

generation platform. It is a super-class arctic semisubmersible drilling rig (Figure 3.11). Odyssey is extremely winterized, and all equipment and systems are designed for service temperatures down to -31°F. The derrick is fully enclosed with steel to 115 feet above the heated drill floor, permitting all-weather operation. A comprehensive description of this platform is given in the Mobile Rig Construction section of Offshore magazine (January 1983).

Another winterized semisubmersible presently in the design stage is the Norsk Hydro rig (Figure 3.12), which will be the first completely enclosed and climatized semisubmersible to operate year round at 72° north latitude on the Tromsflaket, on the Norwegian continental shelf. A comprehensive description of this platform is given in the Mobile Rig Construction section of Offshore magazine (January 1983).

Another semisubmersible concept on the drawing board is the German RS 35 Concept (Figure 3.13), as related by the Mobile Rig Construction section of Offshore (January 1983). This semisubmersible is designed to operate in the hostile environment north of the 62nd parallel in the North Sea and to offer a careful balance between economics and safety. The fundamental concept of the RS 35 generation is a uniform and well balanced submerged ring hull of tubular sections, with the deck and superstructure carried on four vertical columns. The columns are ice-strengthened for operations in arctic waters.

### 3.2.2 Design Considerations for Semisubmersibles

The principal considerations for the design of semisubmersibles are in general the same as for any other floating vessel, as listed below:

- o Owner's Requirement
- o General Arrangement
- o Principal Dimensions
- o Stability
- o Motion Response Characteristics



- o Structural Design
- o Mooring System Design

The Owner's requirement will in general include the functional purpose of the vessel, the environmental conditions for the operating site, the performance criteria for operational requirements and any other personal preference. Environmental conditions should specify the design wave height, wave statistics, wind velocity and the current profile. The performance criteria depend on the functional purpose of the vessel, and are often described by the limiting motion prior to shutdown of operation. For example, the limiting condition for a floating production platform is given by the vertical and horizontal excursion, whereas for a derrick barge it may be the motion of the crane boom tip.

The space allocation, facilities layout and general arrangement for any floating vessel are guided by operational objectives, desired capability, needed equipment, particular construction goals and individual preference. Thus for semisubmersibles designed to lay pipe, the general arrangement will be greatly influenced by the flow of pipe segments from the conveyor to the welding station to the pontoon or stinger and onto the ocean bottom, whereas for a drilling platform, the layout objective is to facilitate the drilling operation. For a semisubmersible buoy designed to collect and telemeter data as for the U.S. Air Force ACMI range, the utmost concern may be for the motions at the antenna tip.

The principal dimensions of a semisubmersible vessel include the deck size, number, size, and height of columns, and the size and length of the pontoons. These dimensions should be chosen to satisfy the requirements due to general arrangement, displacement, stability and other performance related criteria. The vessel should provide enough buoyancy to support the structural steel weight, ballast, mooring equipment, and all other weight items including machinery, HVAC, piping, electrical, any special equipment, etc. Usually the

principal dimensions are chosen on a trial basis at an early stage of the design and are then changed during many iterative steps during design process to provide adequate stability and meet the other performance requirements.

The requirement of stability for any floating vessel is a fundamental one. Motion response characteristics of a floating vessel more often give an idea of the vessel performance. The method of evaluating and the considerations for stability and motion response are provided in detail in Chapters 12.0 and 13.0 respectively.

Structural design will require identification of all the loadings before carrying out the analysis. A vessel is usually subjected to static loads such as dead load, live load and current load, and dynamic loads due to waves and wind. The wave induced loading will produce significant inertial loads on the structure. The wind loading is often assumed to be static, which may be acceptable for structural design. Wind dynamics may, however, cause larger horizontal excursion. The wind and current loadings are described in detail in Chapters 10.0 and 11.0 respectively.

Another important element in the design of semisubmersible vessels is the mooring system. A proper mooring system design will specify the number, size, material and the pattern of mooring lines which will keep the vessel on station in the design sea state.

The most common mooring system is a spread (catenary) mooring consisting of wire rope, chain, or a chain-wire combination. The system will be subjected to loadings due to current, wind and waves which should be described in the environmental conditions. During 1982, more than 90 percent of the semisubmersible drilling units working in North European waters were equipped with chain mooring systems.

A chain-wire combination mooring system is designed to further improve water depth capability by employing wire at the semisubmersible end to increase the mooring length. This feature minimizes weight increases, but requires complex drive and spooling units.

The design water depth capability of moored semisubmersible drilling units working in the North Sea has increased from 600 feet in the early 1970s to approximately 1500 feet for the latest units. Several of the semisubmersible drilling units built in the mid-1970's were upgraded from 600 feet to 1000 feet. This was achieved by increasing the chain lengths from approximately 3500 to 4500 feet and modifying the chain lockers.

While it is possible to design larger and better mooring systems, the practical aspects of running and retrieving moorings in deep waters and harsh environments should not be understated. Operations in such conditions take longer periods of time and require larger workboats and reliable windlass braking systems.

Many of the early semisubmersibles were equipped with wire mooring systems, but chain is strongly favored because:

- o The chain system is considered more robust and durable.
- o The chain catenary shape enables chain to embed into the sea bottom and improve overall anchor holding capability.

A wire mooring system, however, offers reduced weight, reduced cost, and better mooring characteristics in shallower waters.

Some of the latest semisubmersibles equipped with wire or the wire-chain mooring systems have located the wire storage reels in the pontoons or lower columns.

Many problems were experienced with mooring systems during the last decade of semisubmersible operations. These included chain and

anchor failures, broken dog clutches and bull gears, fairleader foundation welding problems, and incorrect design of fairleader and gypsy pockets. Recent improvements include the use of hydraulic power, torque converters, better braking systems, and removal of wildcats. The new regulations, design features, and manufacturing techniques are obviously aimed at improving the reliability of mooring systems.

Mooring systems can be improved by specifying a higher quality chain. During the last few years, chain manufacturing techniques have progressed from the normal oil rig quality or similar Grade 3, to provide either an arctic or Grade 4. The arctic grade provides Charpy impact test results at  $-60^{\circ}\text{C}$ , while Grade 4 provides approximately 35 percent improvement in tensile yield values.

Finally, due consideration should be given to optimizing the hull configuration, design parameters such as ratio of column displacement to pontoon displacement, column spacing, etc. A detailed description of optimization procedures is given by Ghosh et al. (1979) for designing a pipelay/derrick semisubmersible barge. The same philosophy can be applied to the design of other semisubmersible vessels with very little change in the logic. Figure 3.14, adopted from a paper by Ghosh et al. (1979), shows optimization cycles for a pipelay/derrick semisubmersible.

### 3.3 Tension Leg Platforms (TLP's)

Mercier et al. (1982) describe the tension leg platform (TLP) as a floating structure connected to anchors fixed in the seabed by vertical mooring lines (tension legs) at each corner of the platform (Figure 3.15). These vertical mooring lines virtually eliminate the vertical plane motions of heave, pitch and roll, while the lateral movements in surge, sway, and yaw are compliantly restrained. Buoyancy is provided by the vertical columns and the horizontal pontoons connecting the bottoms of these columns. An excess of

buoyancy greater than the platform weight keeps the mooring lines in tension for all weather and all loading conditions. Column height is sufficient to support the deck above the wave crest elevations for all tide and wave conditions when the TLP is fixed to the seabed foundations by the tension legs.

### 3.3.1 Evolution of TLP's

In the early days of the TLP conceptual development most drillers and oil and gas production engineers considered the TLP as a logical extension of semisubmersible rigs. Accordingly, conceptual systems were developed on the basis of the existing semisubmersible design technology. However, while a TLP is indeed highly compliant in the surge, sway, and yaw directions (periods over 100 seconds), it is virtually fixed against pitch, roll and heave motions (periods less than 5 seconds). These motion restrictions result in fundamental differences between a TLP and a semisubmersible platform.

An example of the TLP was shown by Macy (1969) as early as 1969 and described by Paulling and Horton (1970) in 1970.

Also in the early 1970's, a team of CONOCO, Inc. engineers analyzed subsea production system for deep water. As a result, they recommended that designs be developed to provide above-water platform space to accommodate drilling and production facilities in deep water. The TLP was recognized as a potential system with a cost that should be relatively insensitive to water depth. An intensive study concluded that this concept was feasible and could be designed to be reliable.

As a consequence of these studies, another in-depth design study was carried out in 1977 on the application of a TLP for development of the Hutton Field in the British North Sea. In addition, the application of a semisubmersible early production system was investigated. Following a comprehensive investigation of alternative

development methods, including a steel jacket structure, the team recommended the use of a TLP to develop Hutton (see Figure 3.15).

The tension leg platform family encompasses several different designs, e.g. vertically moored platform (VMP), tethered production platform (TPP), and tethered buoyant platform (TBP), etc. Various designs include numerous alternative solutions. For example, the TLP could be anchored by a gravity base, driven piles, or drilled and grouted piles. However, all TLP designs have been developed on the basis of a vertical mooring system under pretension due to excess buoyancy. The term TLP is used in this review in a general sense without reference to any specific design.

Figures 3.16 and 3.17 from Angelides et al. (1982) show some of the most common designs for tension leg platforms. Four of the five designs have two axes of symmetry, while one is axisymmetric. The buoyancy in two of them is provided mainly by the vertical bottle shaped members, while in the other three configurations, a significant amount of the total buoyancy is provided by horizontal members as well.

Another TLP design that deserves some attention is a TLP concept developed by Tecnomare. Paruzzolo (1981) describes this TLP as having a gravity type foundation mainly to facilitate installation. Figure 3.18 shows the Tecnomare TLP design in construction, towing, and installation configurations. The tendons for this design are welded pipes.

Today the TLP concept is a technological reality and appears to be one of the most promising platform configurations for deeper waters.

Currently, the design, analysis, fabrication, and installation of the first tension leg platform for CONOCO, Inc., Hutton Field, British North Sea, in 490 feet of water are complete. The hull, deck, and other components were fabricated in Scotland. Installation was

completed in the summer of 1984.

### 3.3.2 Design Considerations for TLP's

Among the proposed deepwater compliant concepts, the TLP represents a unique challenge to a wide spectrum of engineering disciplines. Capanoglu (1979) and Karsan and Mangiavacchi (1982), emphasize the fact that a close interaction among naval architects, hydrodynamicists, structural and mechanical engineers, foundation and soil engineers, and fabrication and installation specialists is necessary for a successful and cost-effective TLP design. The roles of project managers, schedulers and weight control engineers should also be integral in the design process.

The high interaction between many disciplines and specialists in all the phases of a TLP system design and construction demands stronger project and schedule control than is usually required for a standard fixed platform. Minor changes in the equipment weights and center of gravity, tendons, risers or foundation configurations may result in major changes in other TLP components, thereby greatly affecting the cost and schedule.

Ghosh et al. (1980), review the design considerations of a TLP. They divide the design activities into the following areas:

- o Platform geometry
- o Platform structure
- o Mooring systems
- o Equipments
- o Hardware

They further list the major tasks for a TLP design to be as follows:

- o Owner's specifications
- o Design criteria

- o Deck arrangement
- o Platform characteristics
- o Stability analysis
- o Motion analysis
- o Riser and tether system
- o Transportation study
- o Installation method
- o Structural analysis and design
- o Foundation structure design

An example of a TLP design activity network is shown in Figure 3.19. For a TLP design, the owner will in general specify the production rate based on the geological survey and exploratory drilling, location and the water depth. Other owners such as the Navy require specifications which may be motion or cost related. The owner often provides information related to the environmental data and might also impose some constraints such as fabrication site requirements and the transportation method and route. The environmental data should include statistical data related to wave, wind and current criteria.

The TLP concept is relatively new and there are no well defined design criteria for each task. The regulatory agencies who are involved in classifying the various types of offshore platforms generally consider the TLP as a special case. A collection of recommended practices for the design of TLP's is being prepared by the American Petroleum Institute (API). Until these are published, various design criteria developed for semisubmersible design may be used for a TLP. For example, during transportation and various stages of installation, a TLP is no different from a semisubmersible. Therefore the existing criteria for intact and damaged stability evaluation for a semisubmersible can be used for a free floating TLP. These criteria are described in detail in Chapter 12.0. The other criteria for semisubmersible type vessels related to accommodations, safety equipments and requirements such as column height above mean water line, miscellaneous outfittings, etc., are,



in general, applicable to TLP's.

Another important concern, for drilling and production TLP's, is represented by the horizontal excursion and the response behavior of the platform, which directly influence the tendon response and its fatigue life. The horizontal excursion will be governed directly or indirectly by tendon response and the allowable riser angle at base; the latter being dependent on the bottom ball joint design. The tendons are subjected to cyclic loading, which makes it necessary to satisfy these criteria: fatigue (which depends on the desired structural life of the platform), maximum tension (which should not induce tendon stresses higher than the allowable), and minimum tension (no tendon should go slack). Unlike semisubmersibles, the TLP system has a natural period around 2-4 seconds in the vertical plane. The low natural period of the system makes fatigue consideration very important. The tendon connectors are not designed to take any compressive load, so the criterion that the tendon not go slack should be satisfied in the design.

Wind, currents, and waves acting on the TLP cause steady and oscillatory lateral movements and variations in the loads in the tension legs. The motions and loads must be determined and accounted for in the design of TLP systems, such as foundations, tension legs, risers, equipment supports, and the structure.

The dynamic behavior of the TLP may be compared to an inverted pendulum, with the excess buoyancy playing the role of gravity. While vertical motions (heave, pitch, roll) are effectively restrained, it is free to surge, sway, and yaw. The tension legs are, in effect, parallel motion linkages. The natural periods of oscillation of the TLP depend on tension leg length, among other factors.

The tension of the tension legs serves two functions: (1) it prevents "snap" loads in case an extreme wave produces an excess downward

force, causing the anchor legs to go slack and (2) the horizontal component of the tension in the inclined anchor line balances the time-average horizontal forces due to wind, current, and waves. Anchor line tension variations are kept to a minimum by careful design of the proportions between columns and horizontal bracing, in a manner similar, but not quite identical, to the design of semisubmersible vessels. In the case of the semisubmersible, the prime objective is to minimize heave motions, while the TLP's members are sized to reduce variations in the vertical anchor line forces.

Since the tension legs act as parallel motion linkages, a horizontal displacement of the platform will produce a vertical setdown. This affects the required air gap (clearance between deck and mean water level to accommodate the highest wave and tide combination). Further displacement due to wave-induced oscillations would cause additional setdown, but the effect on the required air gap is not substantial since wave crest and platform motions are approximately 90° out of phase (see Mercier et al. 1982).

Intact and damaged stability needed for a safe and stable TLP configuration requires special attention. Because of its relatively small water plane areas, a TLP configuration possesses a much smaller metacentric height than a ship hull section. This makes the system quite sensitive to variations of deck equipment weight and center of gravity (c.g.). As a consequence, any change in deck equipment, weight and c.g. during the design phase may result in major modifications to the TLP hull configuration. Lack of proper weight and ballast control procedures during the installation and operation phases may result in serious safety problems. Figure 3.20 from a paper by Karsan and Mangiavacchi (1982) shows various conditions which need to be checked for overall stability assessment of a TLP system. The current industry practice is to check the stability conditions against the dynamic stability criteria recommended by the American Bureau of Shipping (ABS) (Figure 3.21). While this empirical method introduces current and wave effects through a

suitable safety factor, the effects of other parameters such as spectral shape and dynamic characteristics of the vessel are not directly considered. More advanced methods (such as modifying the heeling moment line accounting for current and wave effects) need to be developed. This may require extensive model testing and analytical work.

The TLP hull is generally composed of columns and pontoons, which are essentially stiffened thin shells. A question not yet completely answered is whether a configuration with a circular cross section would be preferable to one with a rectangular cross section. The fabrication of the latter might be easier, but the connection design might be much more difficult. Also, with particular reference to the pontoons, the hydrodynamic behavior might show some undesirable characteristics.

Two different structural concepts have been considered for the deck. One consists of a plate girder construction, very similar to the approach used in the shipbuilding industry. The other concept is based on the use of a tubular truss as the main deck structure, to be covered by steel plate floors and walls. The latter solution may present the advantage of an increased flexibility of design and operation, since minor modifications needed to accommodate equipment, wiring and piping will not affect the main load-carrying members.

Like other areas of a TLP design, the main difficulty lies in the highly interactive nature of the problem. To achieve a satisfactory configuration in terms of minimum weight, sufficient strength and adequate stability, several passes through the design loop may be necessary. Variations to the platform geometry, to the hull component sizes and weight, and to the production and drilling equipment weight and location may result in substantial changes in the TLP motion characteristics and in the tendon response. As a consequence, an integrated TLP analysis package requires an efficient interface between naval architecture software (motion analysis) and

structural engineering software (stress analysis). Liu et al. (1980) and Tein et al. (1981) discuss such an integrated structural and hydrodynamic analysis method. Capanoglu (1979) emphasizes the need for close interaction between the naval architecture and structural analysis of TLP's.

Tendons are one of the most critical elements of the TLP system. Various types of tendons such as steel wire bridge strand, Kevlar, high strength drill pipe and specially forged threaded high strength pipe joints have been proposed by early TLP investigators. Kevlar is not favored because of the lack of satisfactory material information and field experience. Possible fatigue and corrosion problems discourage the use of the steel bridge strand. In their Hutton Field TLP, CONOCO has used specially forged, high strength, conically threaded tendons similar to oilfield drill strings.

The tendon termination points at the TLP hull and at the seabed anchor template undergo large rotations; fixed connections at these points would be subject to very high stresses. The means for providing gimbal action at the termination points have been studied by various researchers. These efforts resulted in the development of elastomeric compression connectors. Field experience with the underwater long term behavior of elastomeric rubber materials subjected to cyclic shear and compression loadings is generally lacking. More field data and tests on these connectors are required to establish their long term reliability.

A proper method for anchoring the TLP to the seabed is another challenging task to consider.

In the early days of TLP development efforts, two schools of thought for restraining the heave motions existed. One considered the possibility of providing gravity anchors; the other favored an anchor template(s) fastened to the seabed by piles. The piles, in turn, could be either driven, drilled and grouted, or perhaps jacked in.

Large weight and installation difficulties discouraged the use of gravity anchors. Advancements in the template lowering and underwater pile driving equipment and its inherent light weight added impetus to the use of steel frame anchor templates. Berman and Blenkarn (1978) proposed a single-piece anchor template for their Vertically Moored Platform (VMP) concept where risers were employed as vertical mooring elements. Drilling and production risers were located inside the drilled and grouted tension piles. Since then, the idea of using the risers as structural tension members has been temporarily shelved, mostly because of safety considerations.

Currently, the use of either multiple anchor templates or single anchor templates is equally favored. Some favor the use of individual lightweight anchor templates (300 to 600 short tons per unit) which can be lowered to the seabed using a common floating drilling rig (Figure 3.22). Others favor the use of a single anchor template because of the reduced risk of misalignment in the positions of the individual anchor pile clusters. This scheme has the added advantage of offering the possibility of installing tethers and anchors in a single operation and of providing space for an ample number of piles (Figure 3.23) (see Karsan and Mangiavacchi, 1982).

Fabrication and installation of TLP's are two areas that deserve particular attention. Two strategies prevail today based on the ongoing state of technology and the capabilities of fabrication yards. In single-piece fabrication the entire structure is fabricated in one fabrication yard by first assembling the deck and the facilities and progressively jacking it up to assemble it on the hull. This may create serious fabrication, scheduling and tow out difficulties. This is especially true for a drilling and production TLP where the size and the weight of the deck and hull are very large. This method may be very successful and economical for a lightweight TLP with moderate geometrical dimensions where a high tow out draft may not be required.

Currently the favored approach is to fabricate the hull and deck with its assembled facilities as two separate pieces in two fabrication yards and then tow and mate the two pieces in a protected deep water location near shore. In this method the deck and the facilities are fabricated and hooked-up in a graving dock, near a quay wall or over a dry dock and then towed out in a manner similar to the Maureen Field HIDECK or multiple outrigger barge(s). Similarly, the hull is either built in a graving dock or on launch skids and then floated out to the deep water mating site. The deck and the hull are then mated by ballasting the deck transport barge(s) down while the hull structure is deballasted. The hull-deck assembly is then towed to the offshore location for connection to the subsea anchor template(s).

Installation of multiple anchor template(s), similar to those used for the CONOCO Hutton TLP, requires very close tolerances. From a static standpoint, the TLP with more than three tether clusters is an indeterminate structure, and any deviations from the originally designed template positions will result in large variations in the design tendon forces. These tolerance problems are reduced as the water depth increases. Another installation operation that requires particular attention is the connection of the tendons to the anchor template.

During the connection of the tendons to the anchor template(s), the TLP characteristics vary from an unrestrained configuration with a heave period in excess of 10 seconds to a restrained configuration with a heave period of 4 seconds or less. During this operation, the system might be highly vulnerable to the dominant sea states, which exhibit significant energy at these frequencies. Today's philosophy is to achieve the heave restraint as rapidly as possible by lowering one tendon from each corner of the TLP hull simultaneously and achieving rapid reductions in the heave period in a short, predictable time span, such as 24 hours or less.

### Major Dynamic Response Differences Between Semisubmersibles and TLP's

A TLP resembles a semisubmersible platform except for the mooring systems and foundation structure. The mooring system of a semisubmersible is the conventional catenary system which offers restoring forces predominantly in the horizontal plane and very little in the vertical plane. For a TLP, the mooring lines may be vertical or inclined. These mooring lines or tendons are pretensioned in the in-place condition by excess buoyancy provided by the hull. The tendons provide very large stiffness in the vertical plane and little restraint in the horizontal plane. Thus, while a TLP is indeed highly compliant in the surge, sway, and yaw directions with periods over 100 seconds, it is virtually fixed against pitch, roll and heave motions with periods less than five seconds. These motion restrictions result in fundamental differences between a TLP and a semisubmersible platform. Figure 3.24 shows the natural periods for a TLP and a semisubmersible in connection with sea spectra for 10-foot and 20-foot significant wave heights. It is interesting to note that all natural periods of a semisubmersible fall on one side of the spectra, while the natural periods of a TLP are split on the two sides of the spectra. This will have a direct impact on the considerations concerning fatigue life of the mooring lines. In the case of semisubmersibles the fatigue considerations for mooring lines are mainly based on a high stress range and low frequency phenomenon while in a TLP fatigue occurs under a low stress range and high frequency conditions.

Another major difference between a TLP and a semisubmersible is the payload capacity of these platforms. Conceptually a TLP can carry more payload than a similar semisubmersible. This is the direct result of the in-place stability considerations. For a semisubmersible a positive metacentric height is a must while a TLP may accommodate also a negative metacentric height when it is installed in place.

Table 3.3 the shows the major dynamic characteristics of semisubmersibles and TLP's.

As far as major differences in dynamic analysis methods are concerned, the TLP design exhibits a strong interaction between the geometry, the motions and the loads acting on its hull and tendons.

For TLP motion analysis purposes, the tendons are simulated as weightless springs. This simulation is quite satisfactory for shallow water depths, where the total mass of the tendons is a small fraction of the total platform weight. In deeper waters, the approximation of tendons as massless springs is questionable and may lead to significant errors in predicting the motion response of the TLP system. In fact, in order to limit the heave and roll periods below 5 seconds, the tendon to platform weight ratio will rapidly increase with water depth (Figure 3.25). The natural bending periods of tendons and risers also increase as a linear function of the water depth and above 2000 feet, strong interaction with waves may be expected (Figure 3.26). Consequently, a coupled dynamic motion analysis of the TLP may be required.

During an individual maximum wave loading cycle, the axial force on a tendon varies with time (anywhere from 10 percent to 80 percent of its yield strength) indicating that the spring constants are not really constant but they are dependent on loads and frequency. Additionally, complex dynamic phenomena within the tendon itself, such as resonant lateral vibrations, may further reduce the axial tendon stiffness. Research work and parametric studies are currently in progress for better understanding of the behavior of tendons in deeper waters.

Albeit, in the case of a drilling semisubmersible the usual assumption is that the dynamics of the mooring lines do not affect the motions of the semisubmersible and this assumption has proven to be valid based on experimental investigations (see Hooft, 1971).



However, in the case of rather small semisubmersibles such as those discussed in Section 3.2.1 this assumption may be somewhat questionable.

TABLE 3.1 COMPARISON OF VARIOUS TYPES OF MOBILE DRILLING UNITS

	Jackup	Drillship	Semisubmersible
Construction cost	Low to medium	Medium to expensive	Expensive
Water depth capability	Shallow to medium water	Medium to very deep water	Medium to deep water
Transit variable deck load	Fair	Very good	Fair
Operational VDL	Fair	Very good	Good
Motion characteristics	n/a	Poor	Good
Mobilization	Fair	Very good	Good
Setting up on location	Difficult	Fair	Fair

TABLE 3.2 MOBILE DRILLING UNIT CONSTRUCTION COSTS (IN \$1,000,000)

Year	Jackup		Semisubmersible		Drillship	
	Shallow	Deepwater	Moored	Dynamically positioned	Moored	Dynamically positioned
1972	\$7-8	\$9.5-10.5	\$20-25		\$10-12	\$20-22
1973	\$8-11	\$11-13	\$33.3		\$14-20	\$25-27
1974	\$10-16	\$15-16	\$34		\$16-22	\$35-40
1975	\$18-22	\$20-25	\$30-42		\$25-30	\$40-55
1976	\$16-20	\$22-28	\$50-51	\$62	\$25-30	\$45-60
1977	\$17-21	\$22-30	\$57			
1978	\$16-22	\$25-35			\$59	\$80-85
1979	\$17-21	\$28-44	\$60-70		\$60-68	\$75-85
1980	\$20-25	\$35-45	\$73-75	\$120	\$90	
1981	\$21-30	\$51-63	\$115-\$130	\$156	\$50-100	
1982	\$27-30	\$68-75	\$100-130	\$180	\$75-130	\$160-180

TABLE 3.3

**SEMISUBMERSIBLE & TLP DYNAMIC CHARACTERISTICS**

<b>● MOTIONS:</b>	<b><u>SEMISUBMERSIBLE</u></b>	<b><u>TLP</u></b>
<b>HORIZONTAL</b>	<b>MODERATE</b>	<b>MODERATE</b>
<b>VERTICAL &amp; ANGULAR</b>	<b>LARGE</b>	<b>SMALL</b>
<b>MOORING LINE PRETENSION</b>	<b>LOW</b>	<b>HIGH</b>
<b>TENSION VARIATION</b>	<b>HIGH</b>	<b>LOW</b>
<b>STABILITY (IN-PLACE)</b>	<b>IMPORTANT</b>	<b>NOT SIGNIFICANT</b>

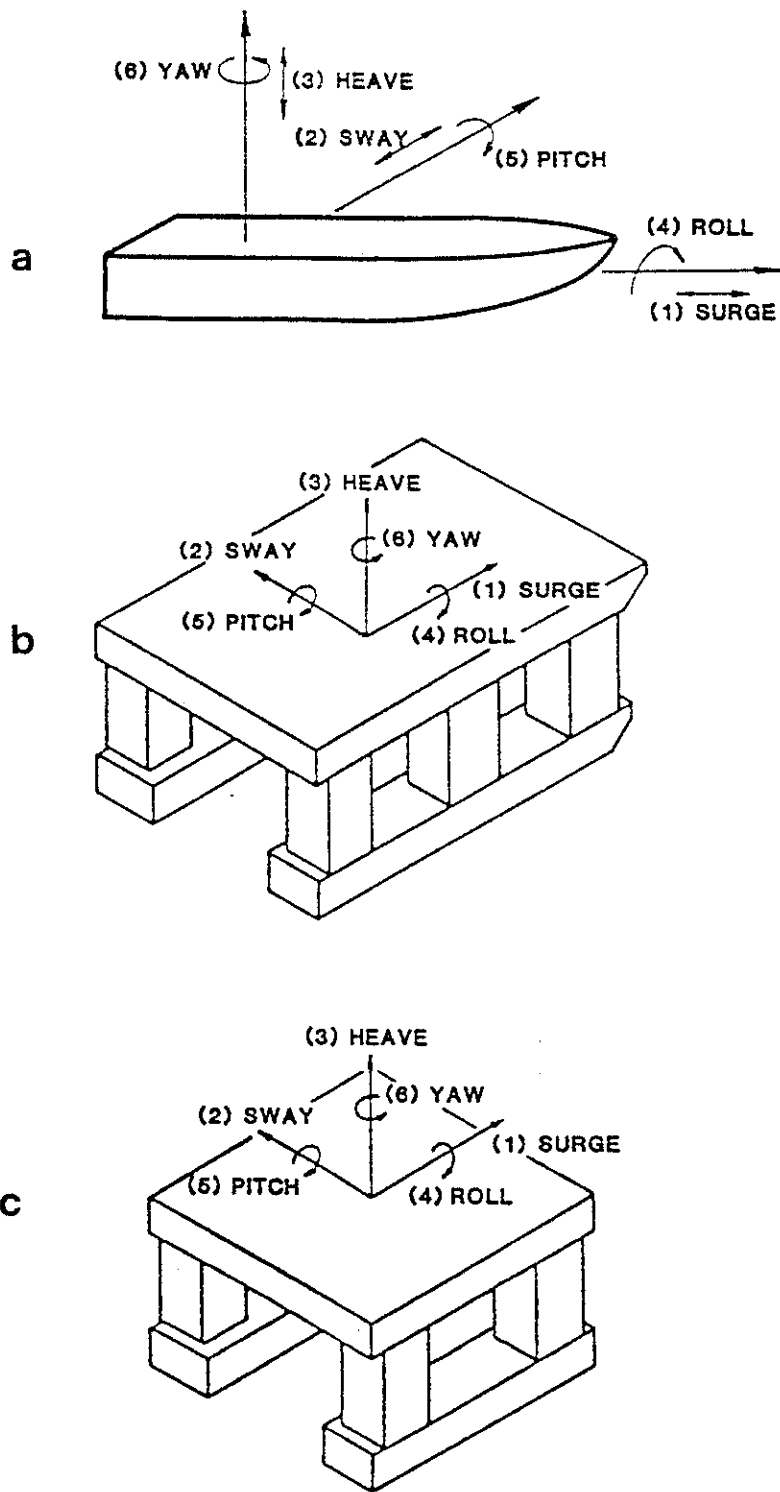


FIGURE 3.1 DEFINITION SKETCH OF THE SIX COMPONENTS OF MOTION OF A FLOATING BODY

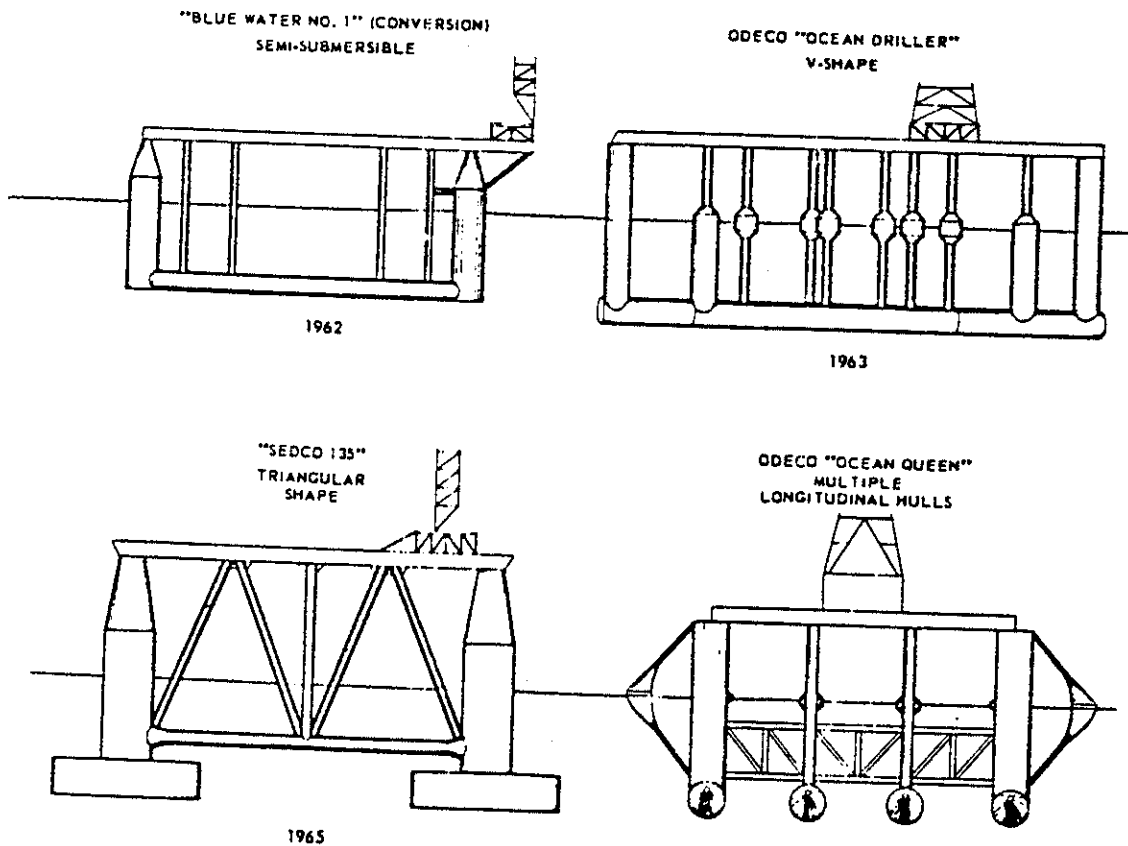


FIGURE 3.2 SKETCHES OF KEY SEMISUBMERSIBLE RIGS  
(Howe, 1967)

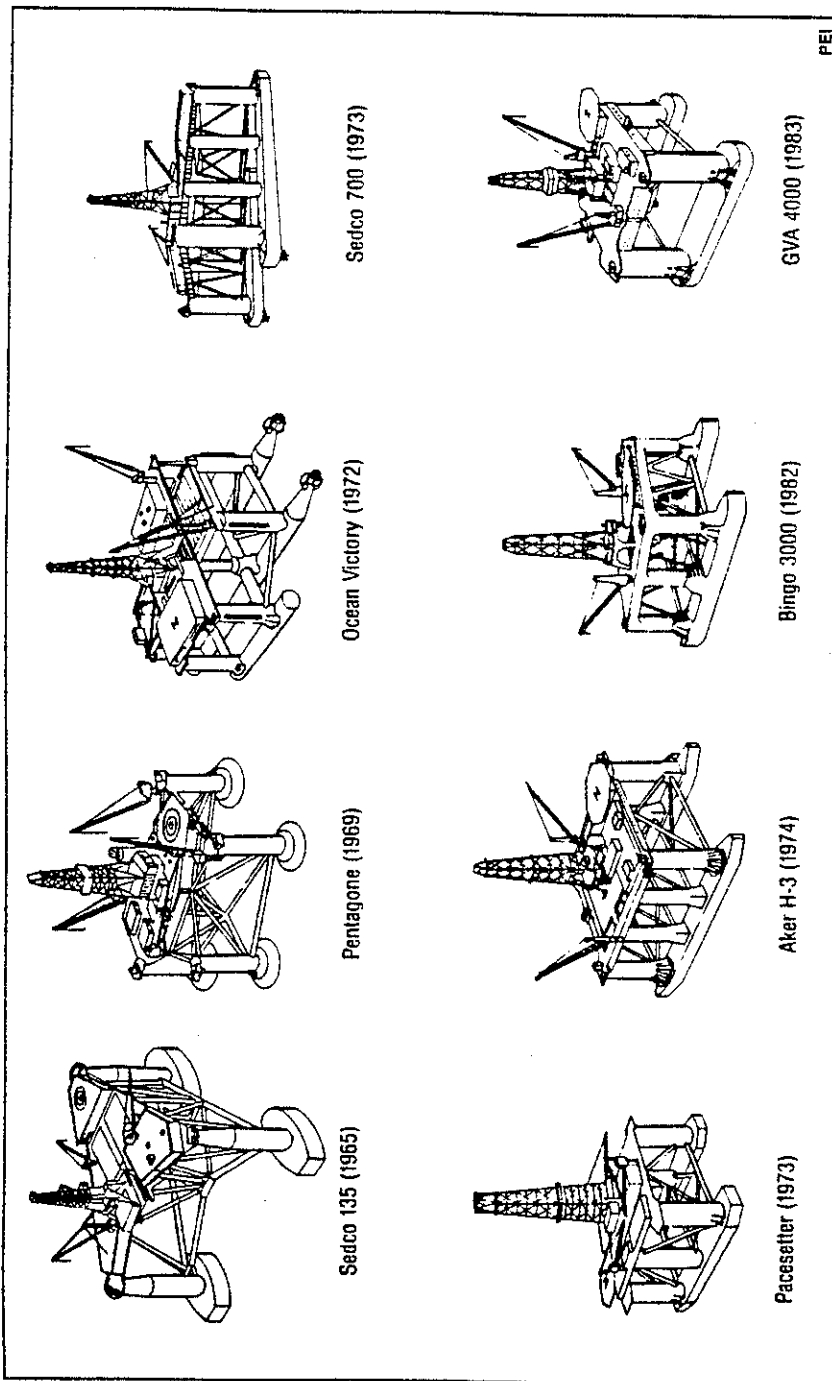


FIGURE 3.3 VARIOUS TYPES OF SEMISUBMERSIBLE DRILLING UNITS (1965-1983) (RODKNIGHT, 1983)

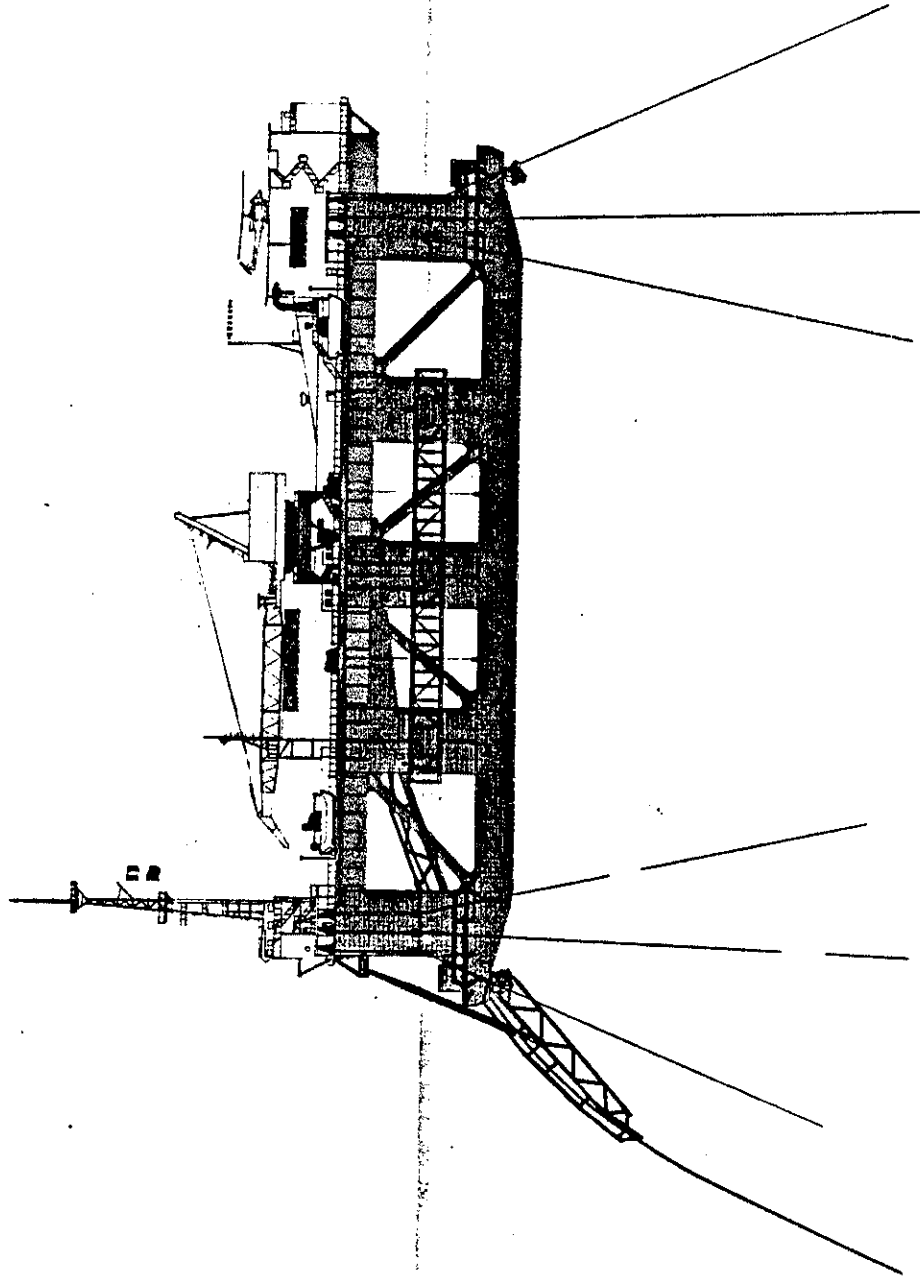


FIGURE 3.4 CASTORO SEI (OCEAN INDUSTRY, JULY 1978)

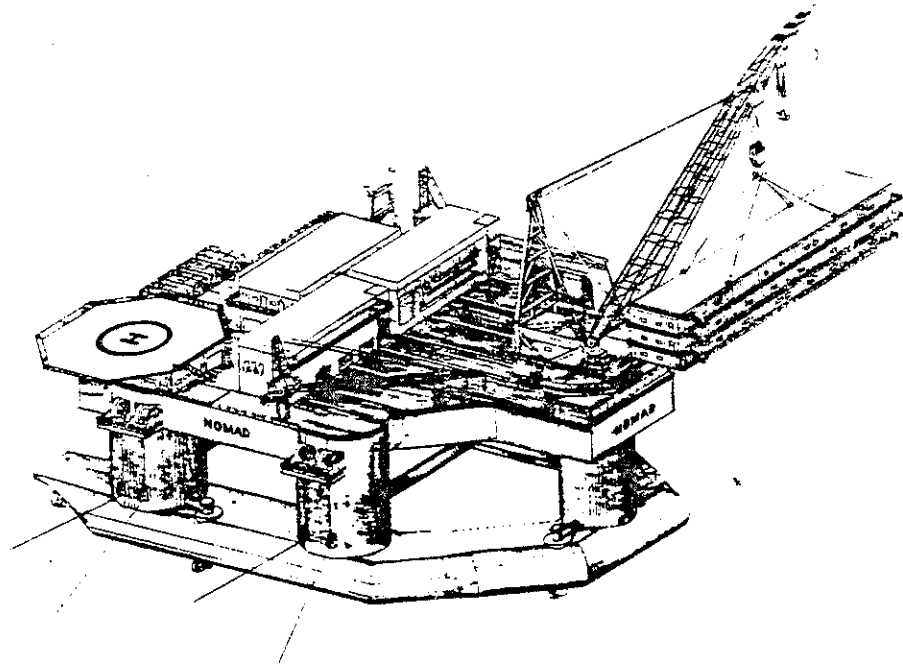


FIGURE 3.5 THE NOMAD HAS A RATED ROTARY CRANE LIFTING CAPACITY OF 1,600 TONS (OFFSHORE, AUGUST 1978)

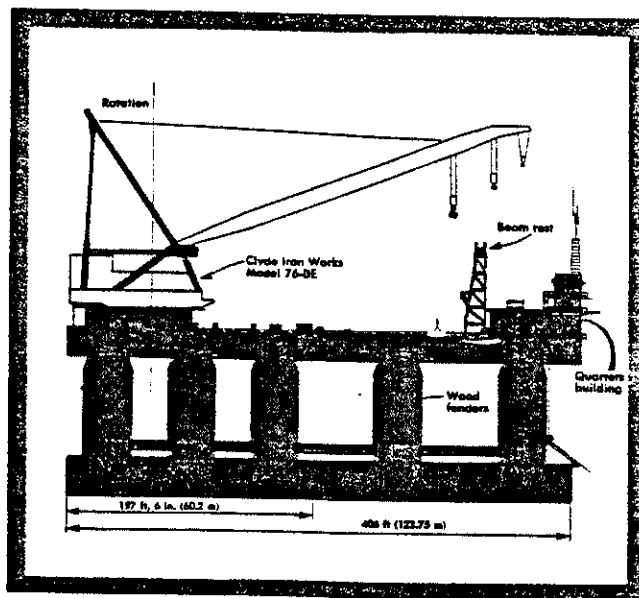


FIGURE 3.6 J. RAY McDERMOTT'S DB 100 IS THE FIRST SEMISUBMERSIBLE IN ITS FLEET AND THE LARGEST (OFFSHORE, AUGUST 1978)



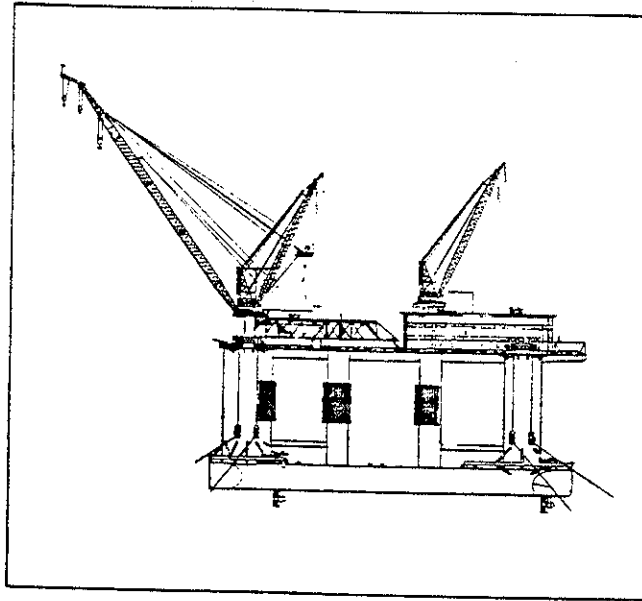


FIGURE 3.7 THE SEDCO/OXY MSV IS THE FIRST OF SECOND-GENERATION PLATFORM SUPPORT-STANDBY VESSELS IN NORTH SEA (OFFSHORE, AUGUST 1978)

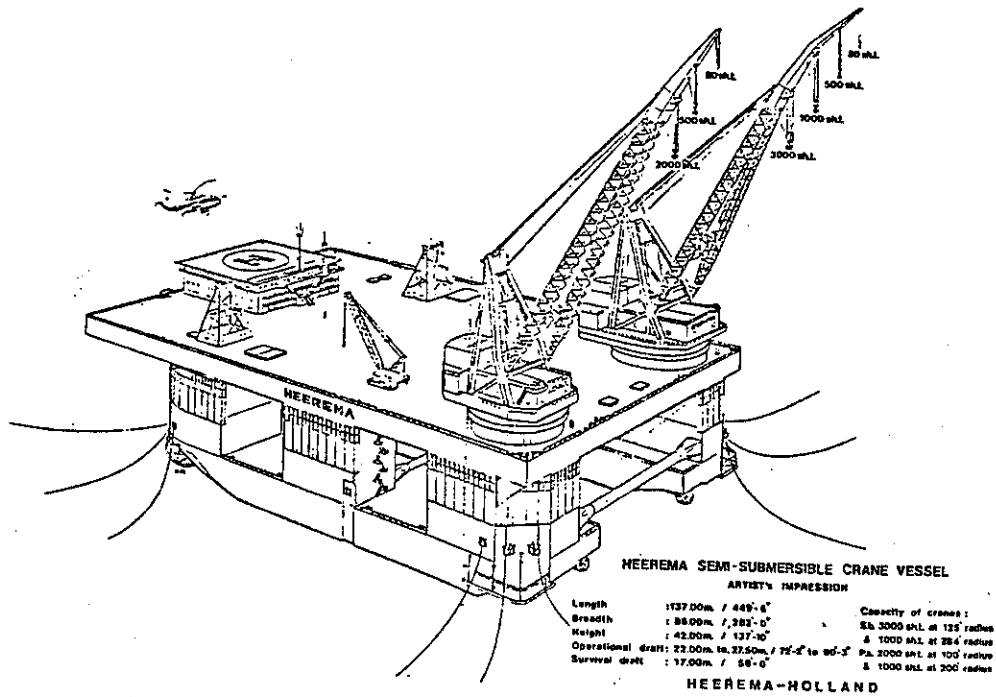


FIGURE 3.8 HEEREMA SEMI-SUBMERSIBLE CRANE VESSEL

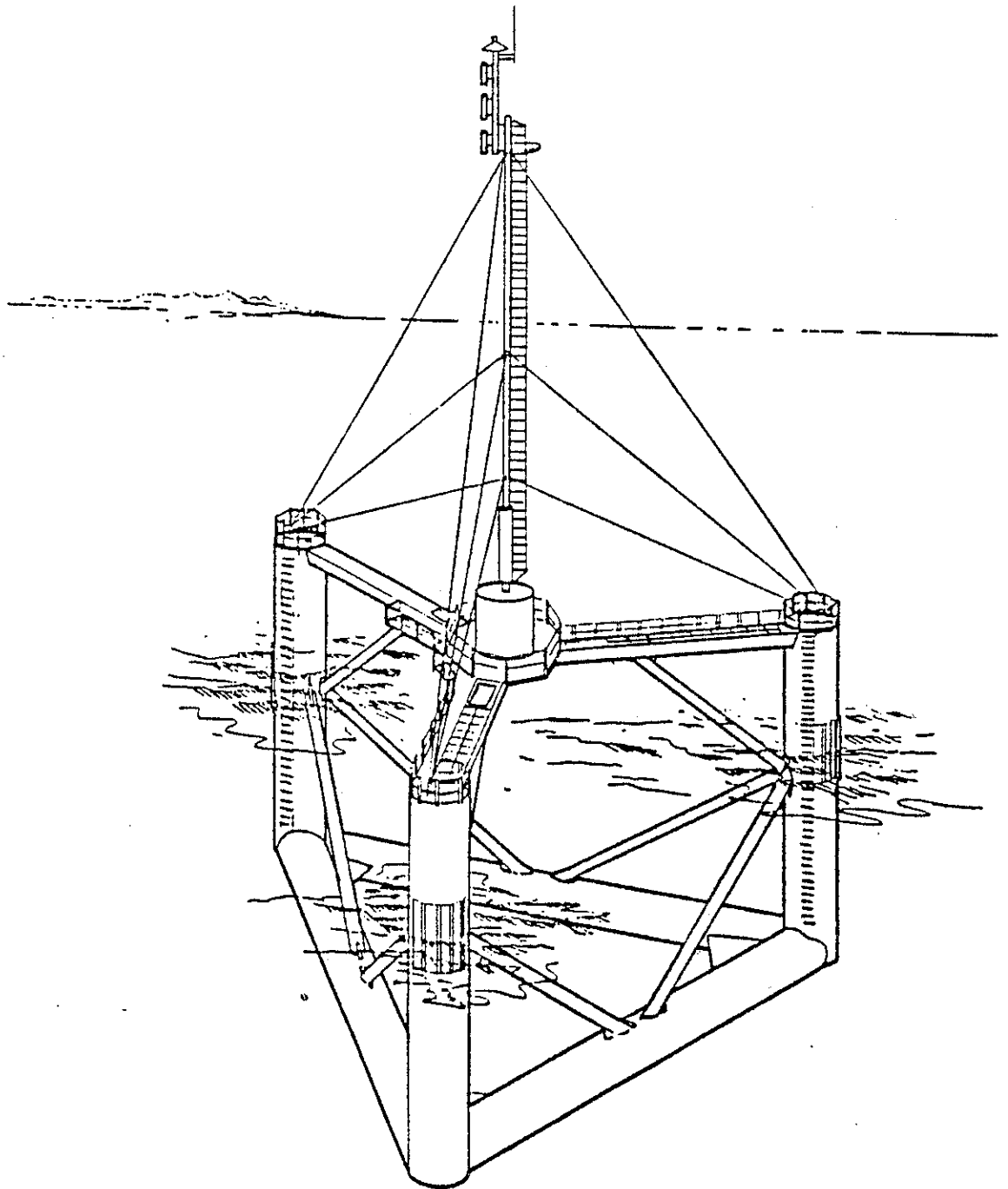


FIGURE 3.9 THE AIR FORCE SEMISUBMERSIBLE (McCLURE AND KIRSCHNER, 1983)

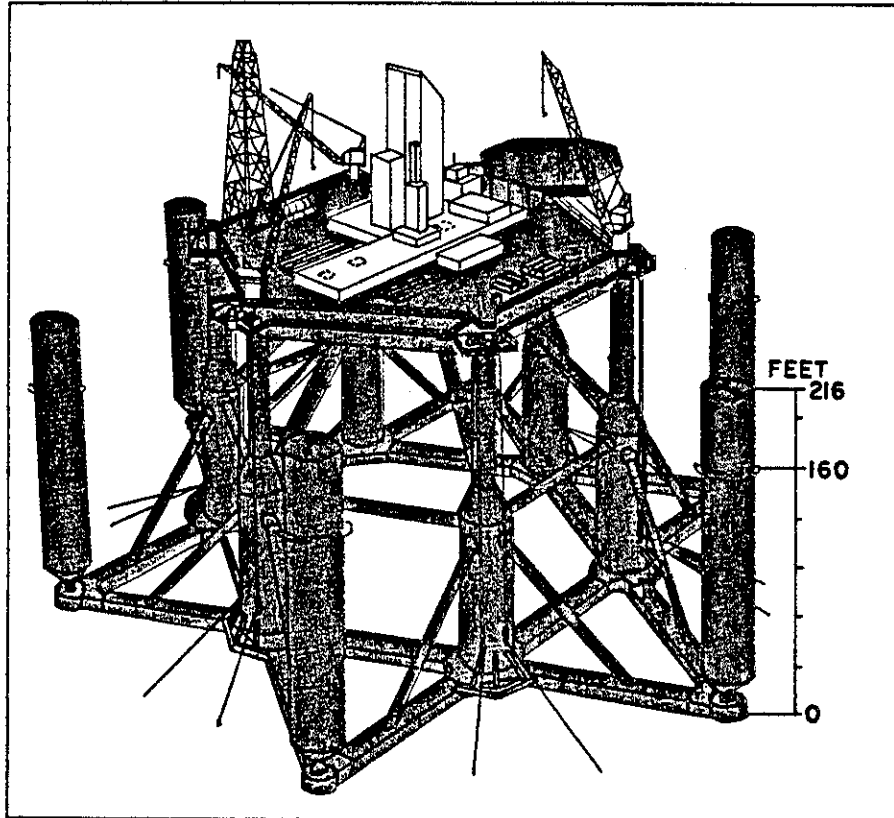


FIGURE 3.10 CLUFF-COPSON'S SEMI-FLEX FLOATING PRODUCTION FACILITY COMBINES VERTICAL COLUMNS ON UNIVERSAL JOINTS TO PROVIDE WAVE TRANSPARENCY, FEWER STRESS POINTS AND A LARGER WATERPLANE. (OFFSHORE, JANUARY 1983)

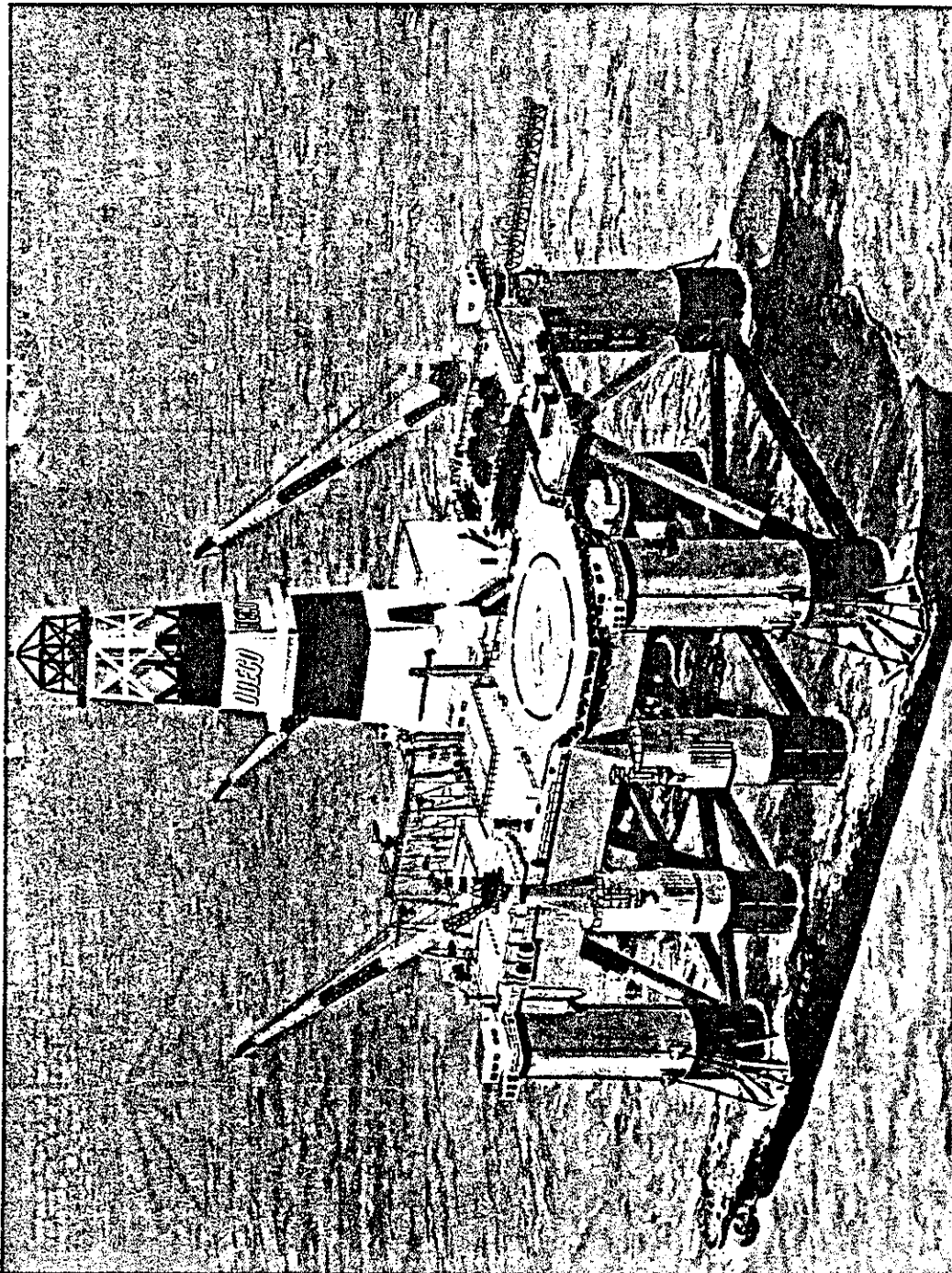


FIGURE 3.11 ODECO'S NEW SEMISUBMERSIBLE OCEAN ODYSSEY  
(OFFSHORE, JANUARY 1983)

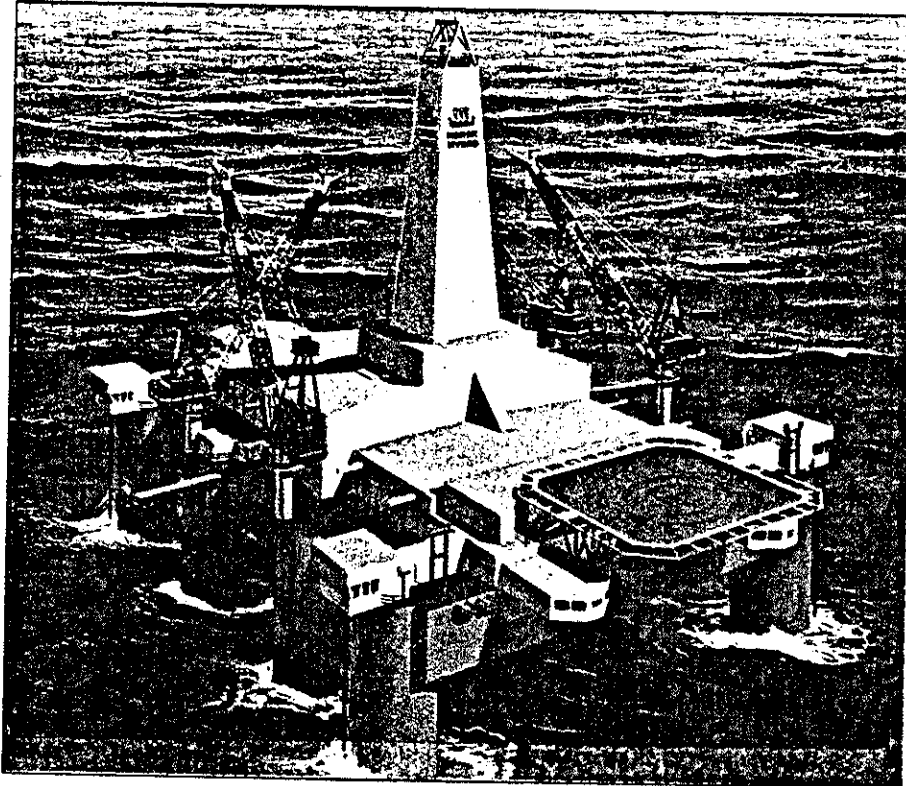


FIGURE 3.12 THE NORSK HYDRO RIG, WHICH IS NOW BEING DESIGNED BY SONAT OFFSHORE AND WILH. WILHELMSSEN, WILL BE A DRILLING PIONEER WORKING OFF THE NORTHERN COAST OF NORWAY. (OFFSHORE, JANUARY, 1983)

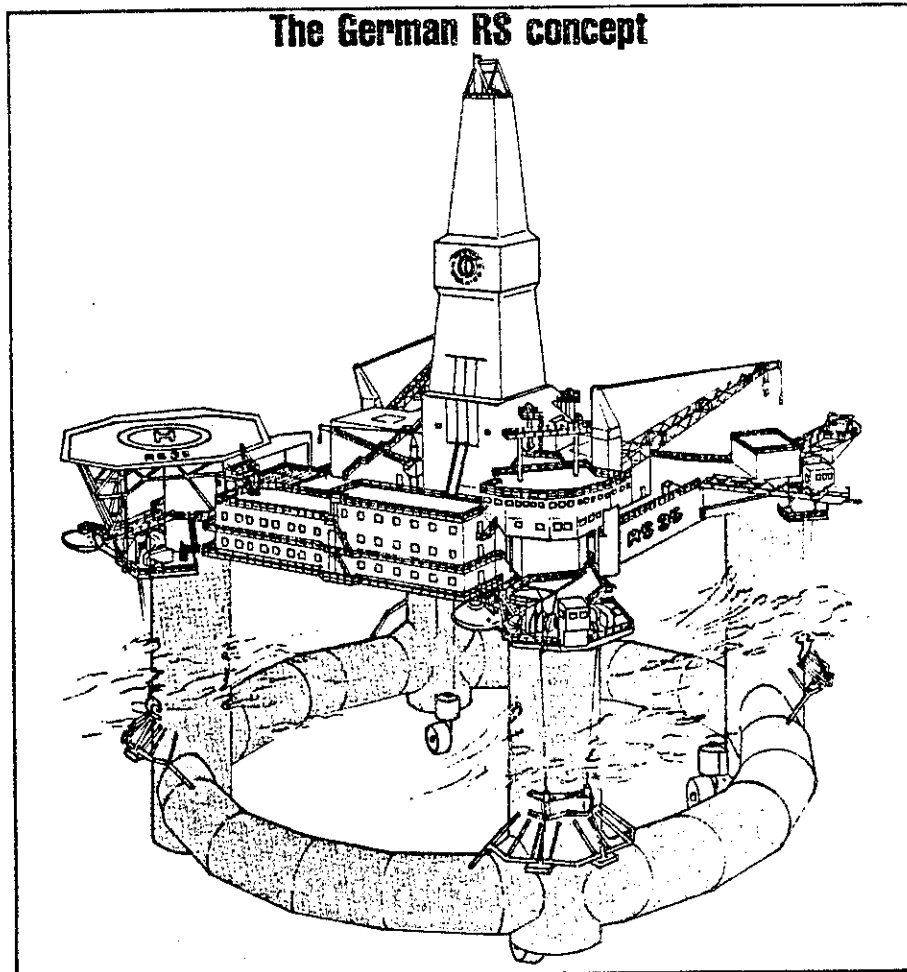


FIGURE 3.13 NEW RS 35 SEMIS DESIGNED FOR NORTH SEA  
(OFFSHORE, JANUARY 1983)

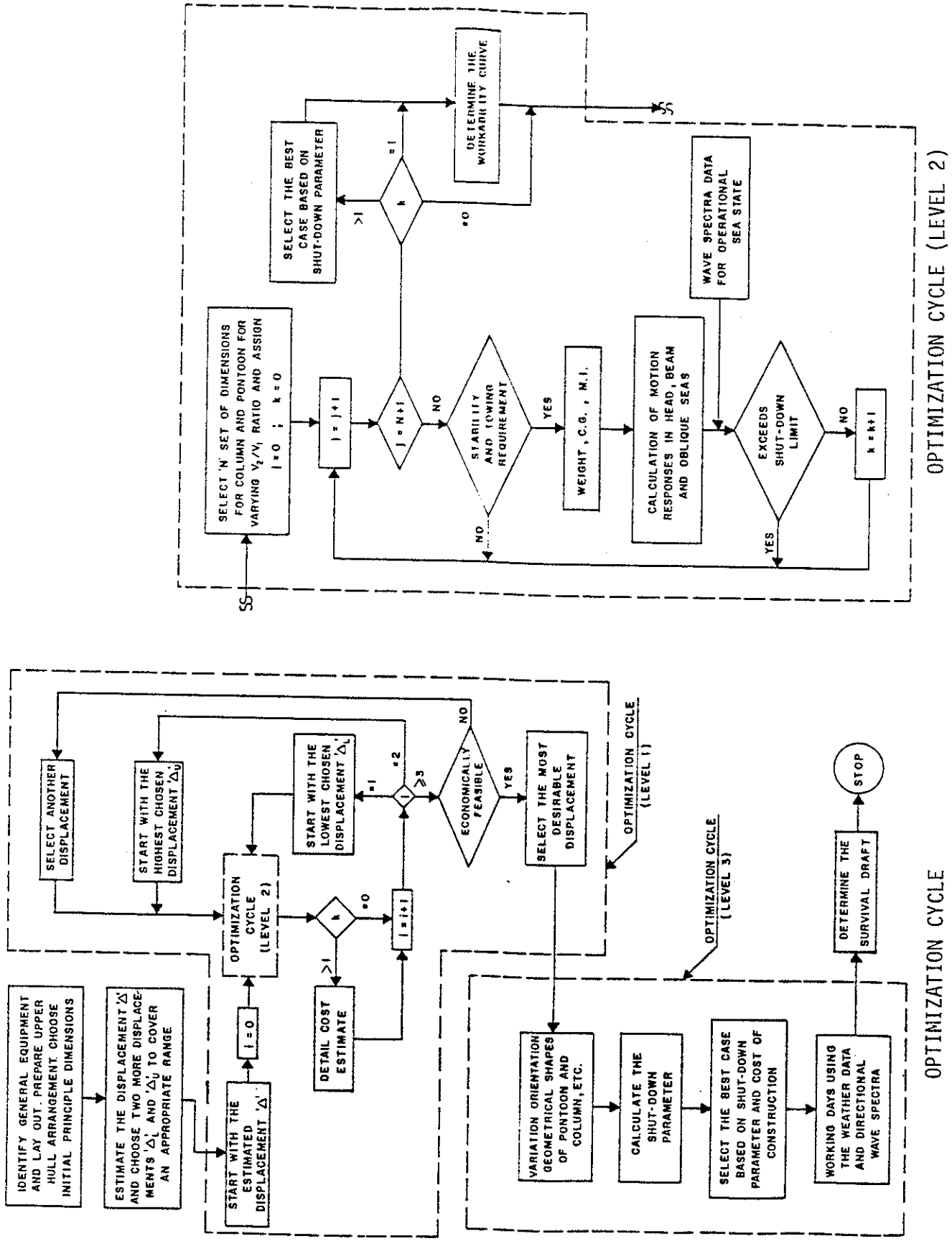
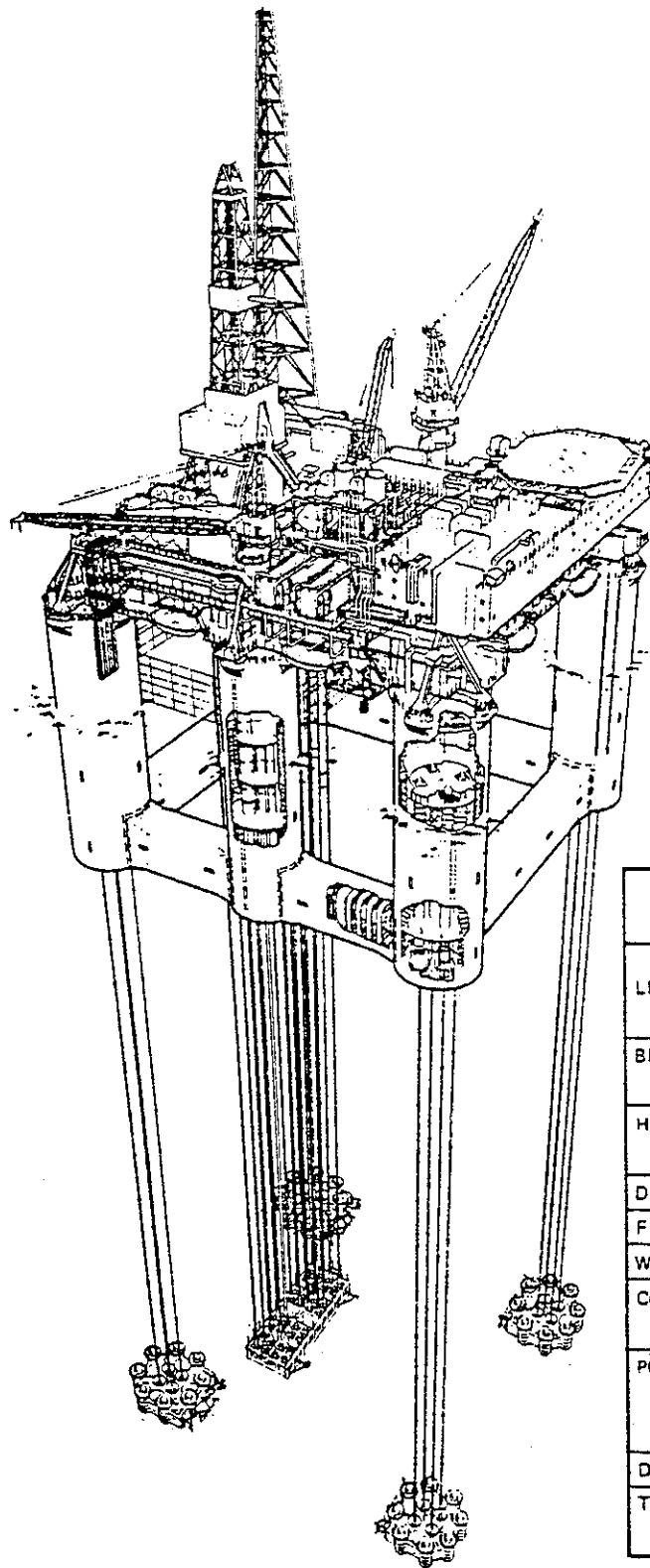


FIGURE 3.14 OPTIMIZATION CYCLE FOR PIPELAY/DERRICK SEMISUBMERSIBLE (GHOSH ET AL. 1979)



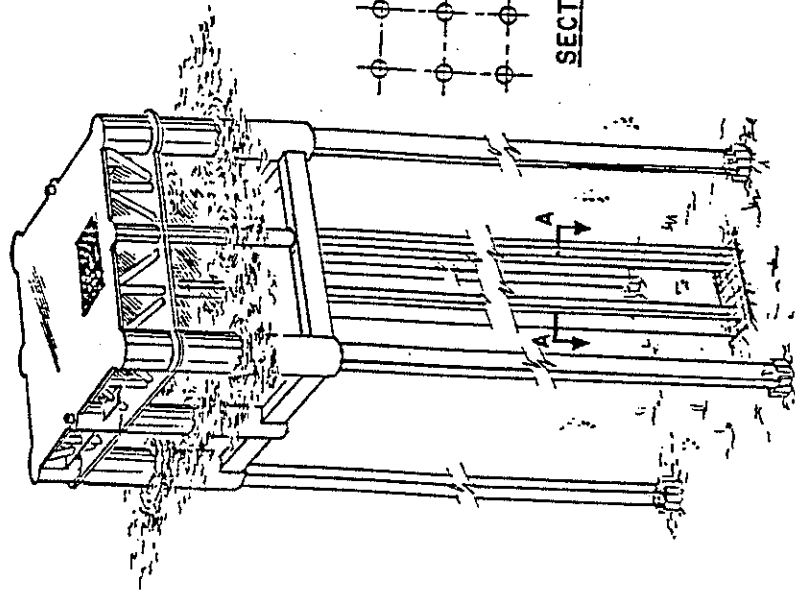
## HUTTON FIELD TENSION LEG PLATFORM

GEOMETRY		
(All dimension to moulded lines)		
LENGTH	- Between column centres	78.00 M
	- Overall	95.70 M
BREADTH	- Between column centres	74.00 M
	- Overall	91.70 M
HEIGHT	- Keel to main deck	57.70 M
	- Main deck to weather deck	11.25 M
DRAUGHT	- Operating	32.00 M at L.A.T.
FREEBOARD	- To underside of main deck	24.50 M at L.A.T.
WATER PLANE	- Area	1324.00 M <sup>2</sup>
COLUMNS	- 4 Corners	17.70 M Dia.
	- 2 Centre	14.50 M Dia.
PONTOONS	- Height	10.80 M
	- Width	8.00 M
	- Corner radius	1.50 M
DISPLACEMENT	- Approx.	61500 Tonnes
TOTAL WEIGHT	- Including riser tension (Approx)	48500 Tonnes

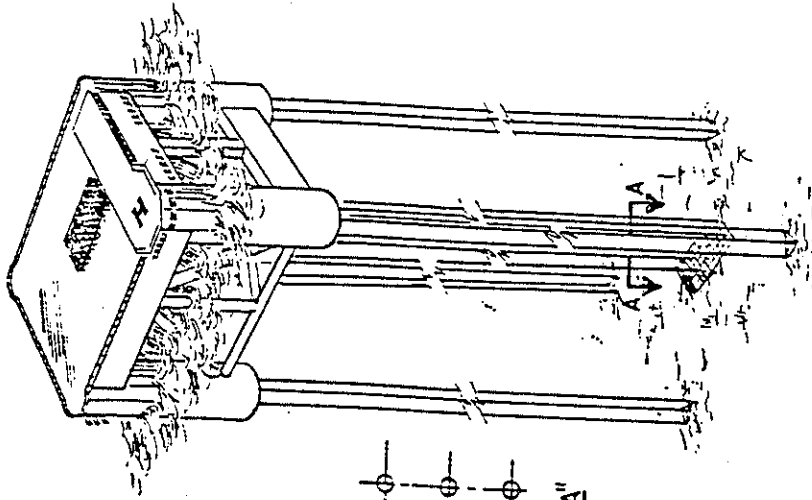
FIGURE 3.15 OVERALL VIEW OF HUTTON KEY DIMENSIONS  
(ELLIS ET AL, 1982)



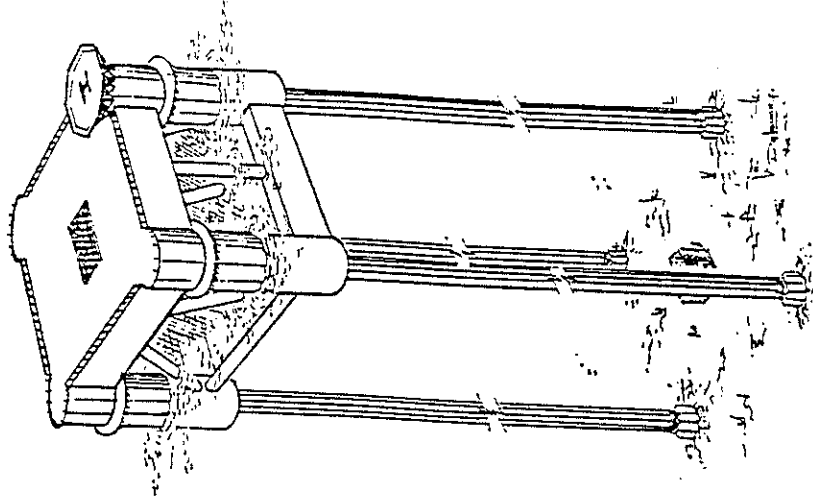
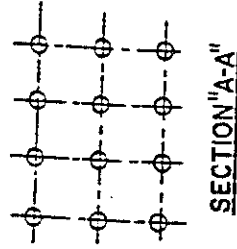
TYPICAL TLP DESIGNS



Mercier et al. (1982)  
HUTTON TLP



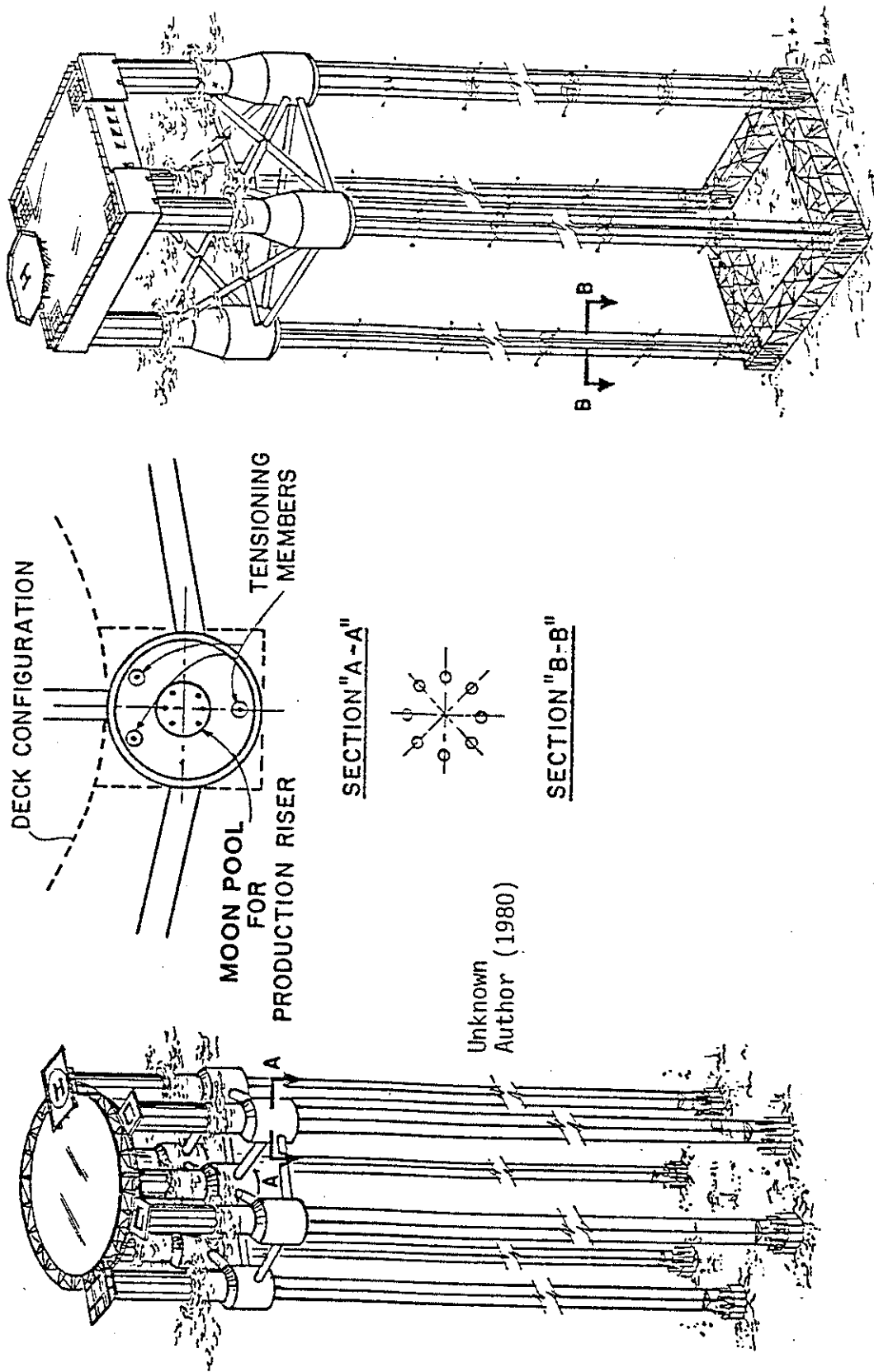
Natvig and Pendered (1979)  
TPP



Perrett and Webb (1980)  
TBP

FIGURE 3.16 TYPICAL TLP DESIGNS (ANGELIDES ET AL, 1982)

TYPICAL TLP DESIGNS



VMP  
 Berman and Blenkarn (1978)  
 Beynet et al. (1978)

FIGURE 3.17 TYPICAL TLP DESIGNS (ANGELIDES ET AL, 1982)

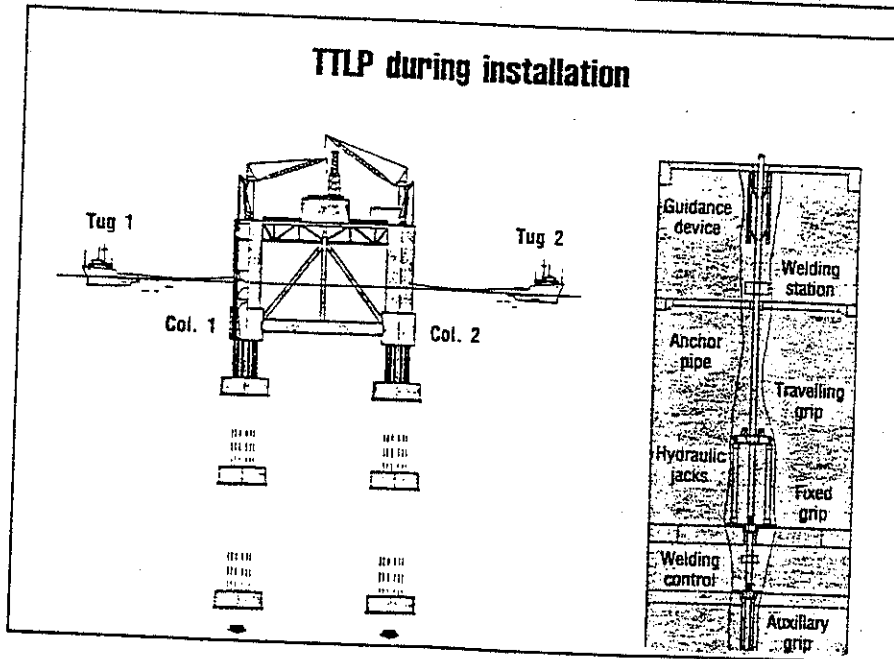
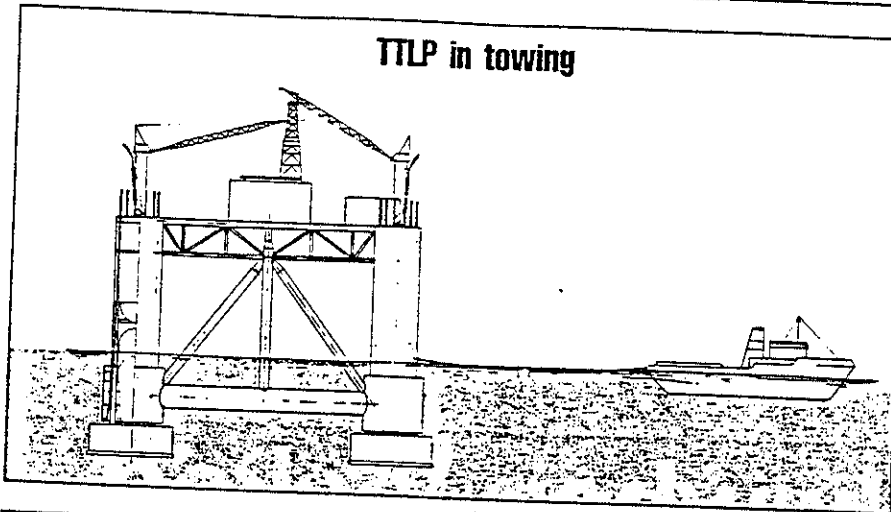
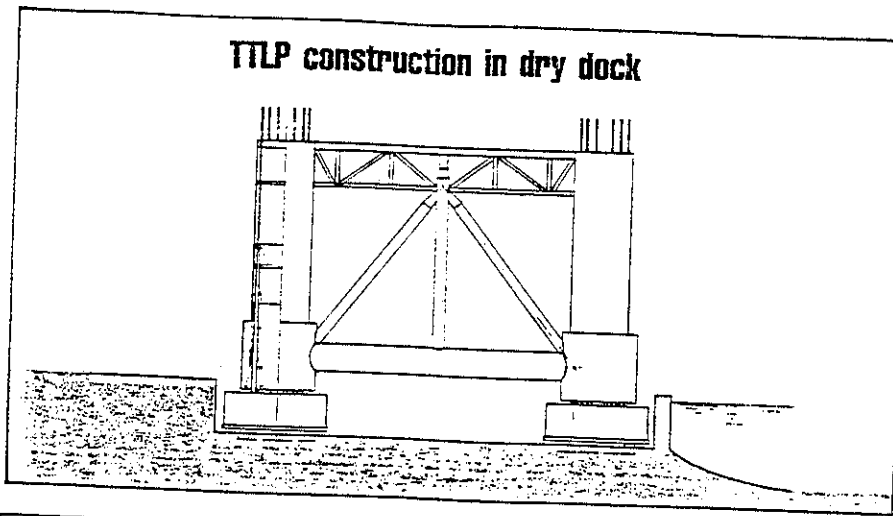


FIGURE 3.18 TECNOMARE TLP (PARUZZOLO, 1981)

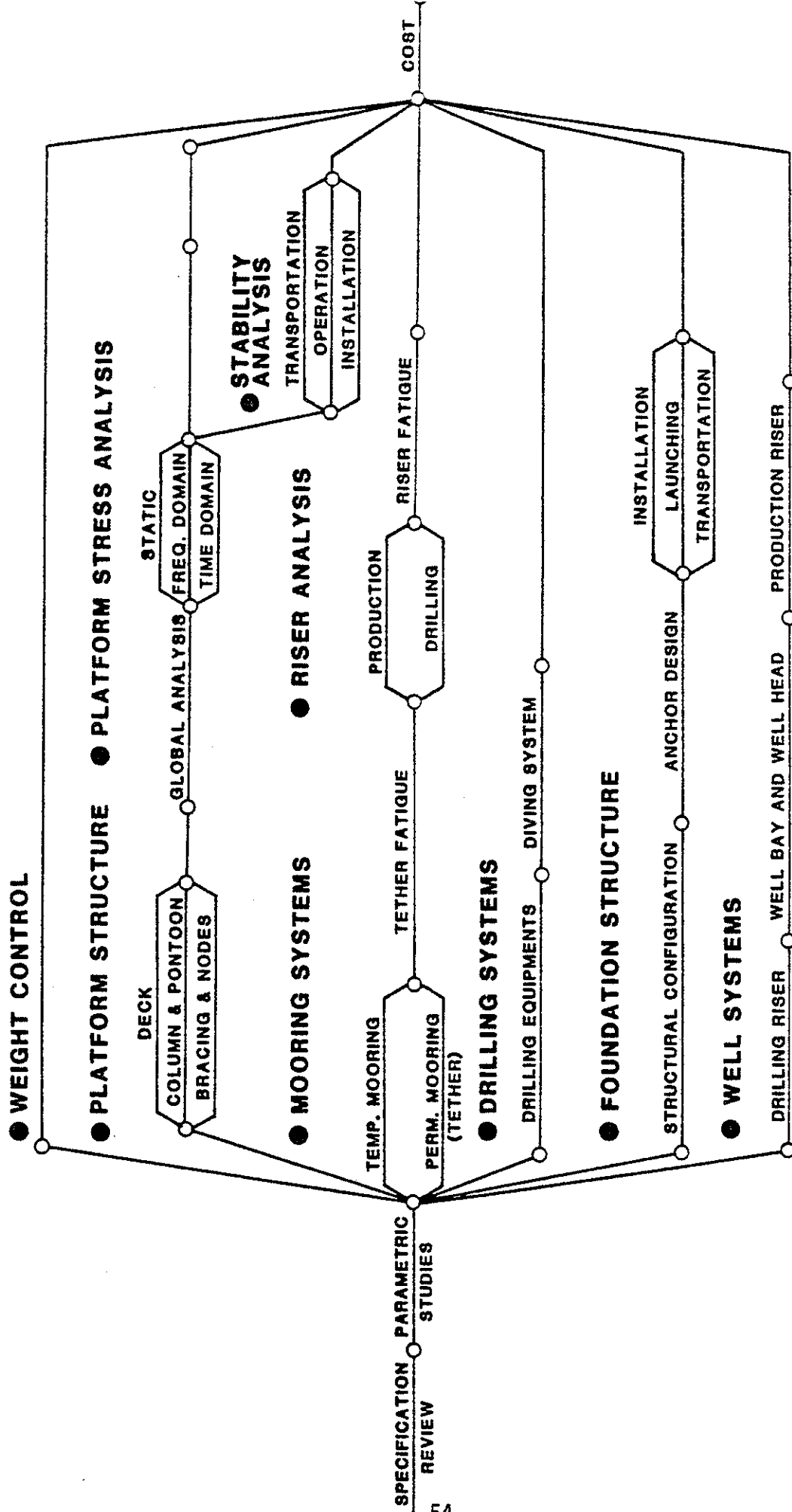


FIGURE 3.19 NETWORK ACTIVITIES FOR TLP (GHOSH ET AL, 1980)

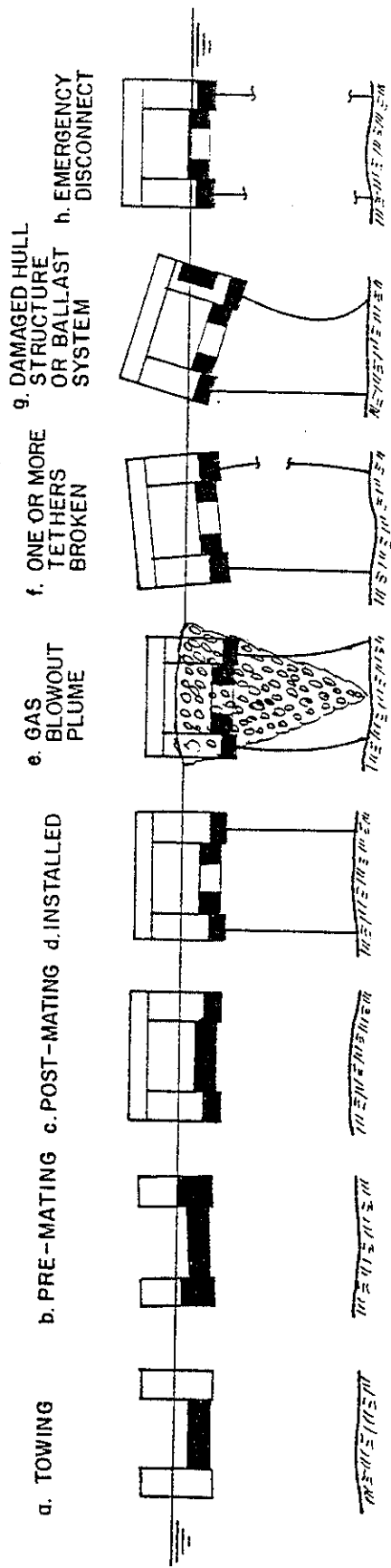


FIGURE 3.20 STABILITY CHECK CONDITIONS (KARSAN AND MANGIACACCHI, 1982)

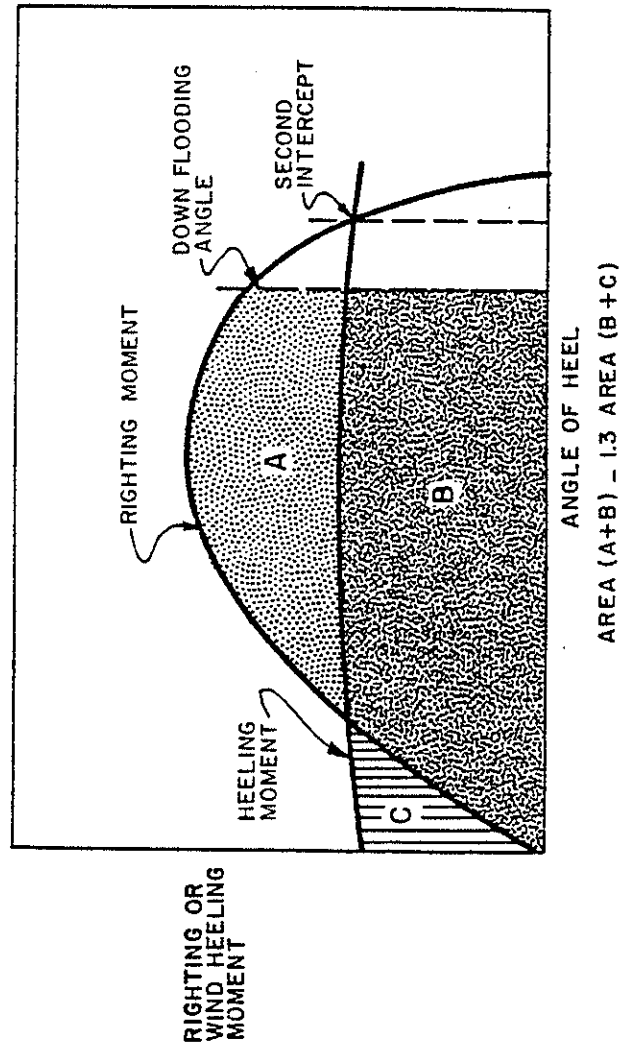


FIGURE 3.21 DYNAMIC STABILITY CURVE (KARSAN AND MANGIACACCHI, 1982)

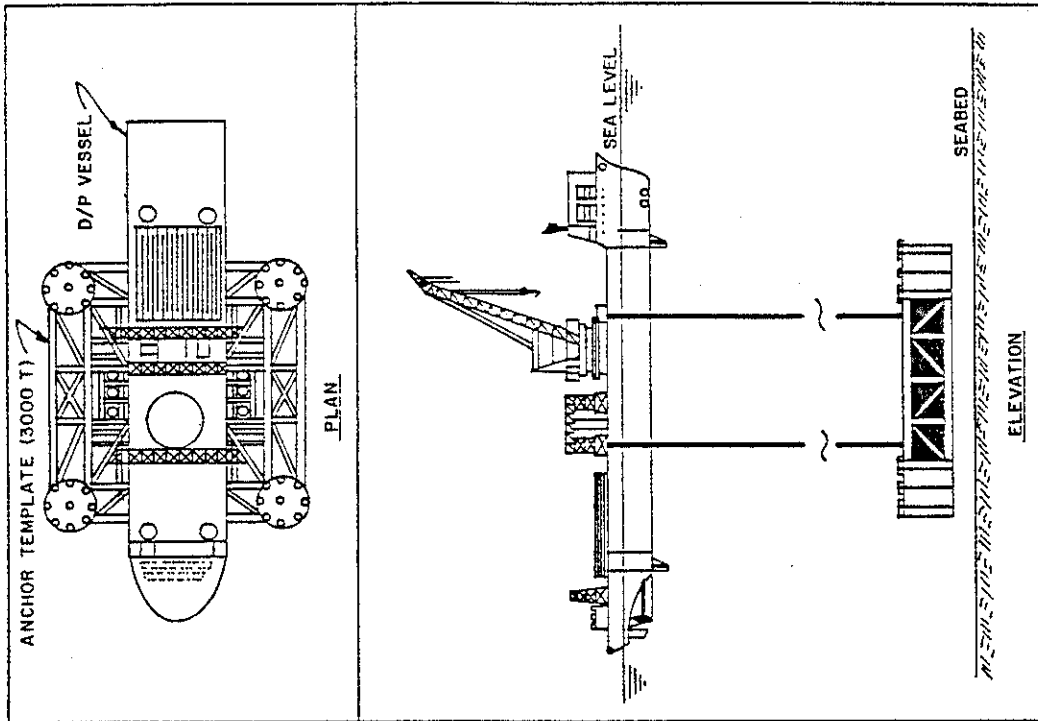


FIGURE 3.23 SINGLE PIECE SUBSEA ANCHOR TEMPLATE INSTALLATION USING A DYNAMICALLY POSITIONED (D/P) VESSEL

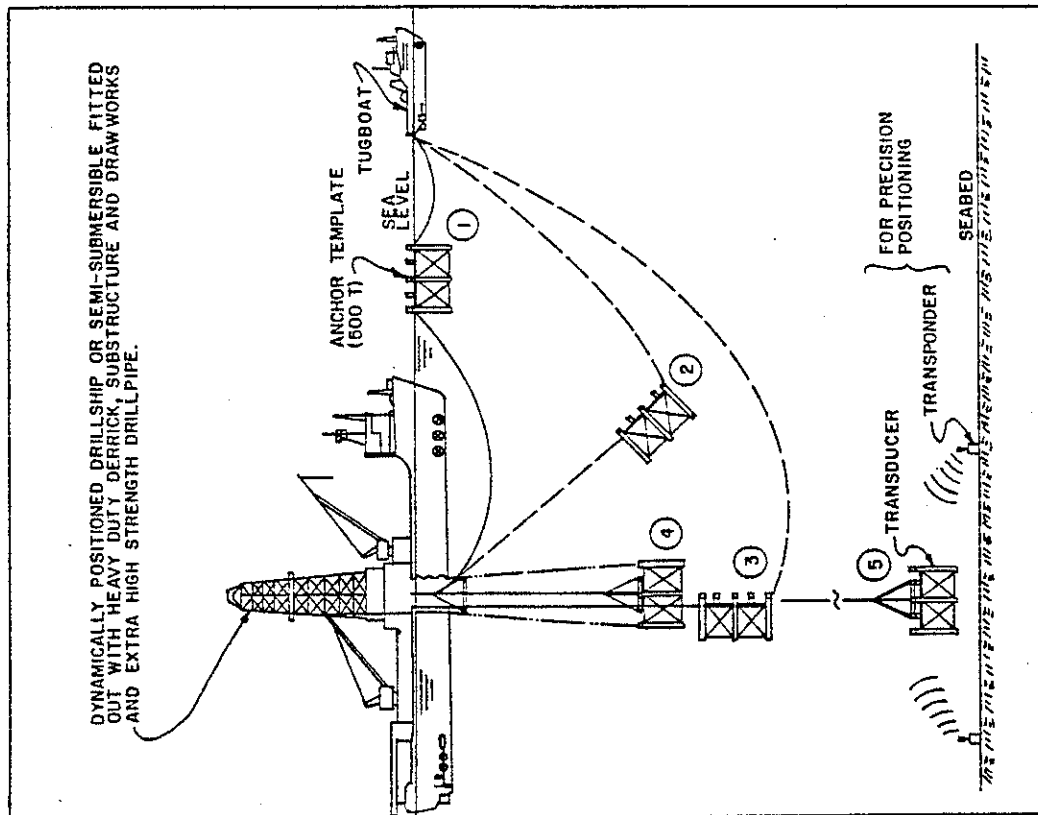


FIGURE 3.22 MULTIPLE PIECE ANCHOR TEMPLATE LOWERING TO SEABED

(KARSAN AND MANGIAVACCHI, 1982)

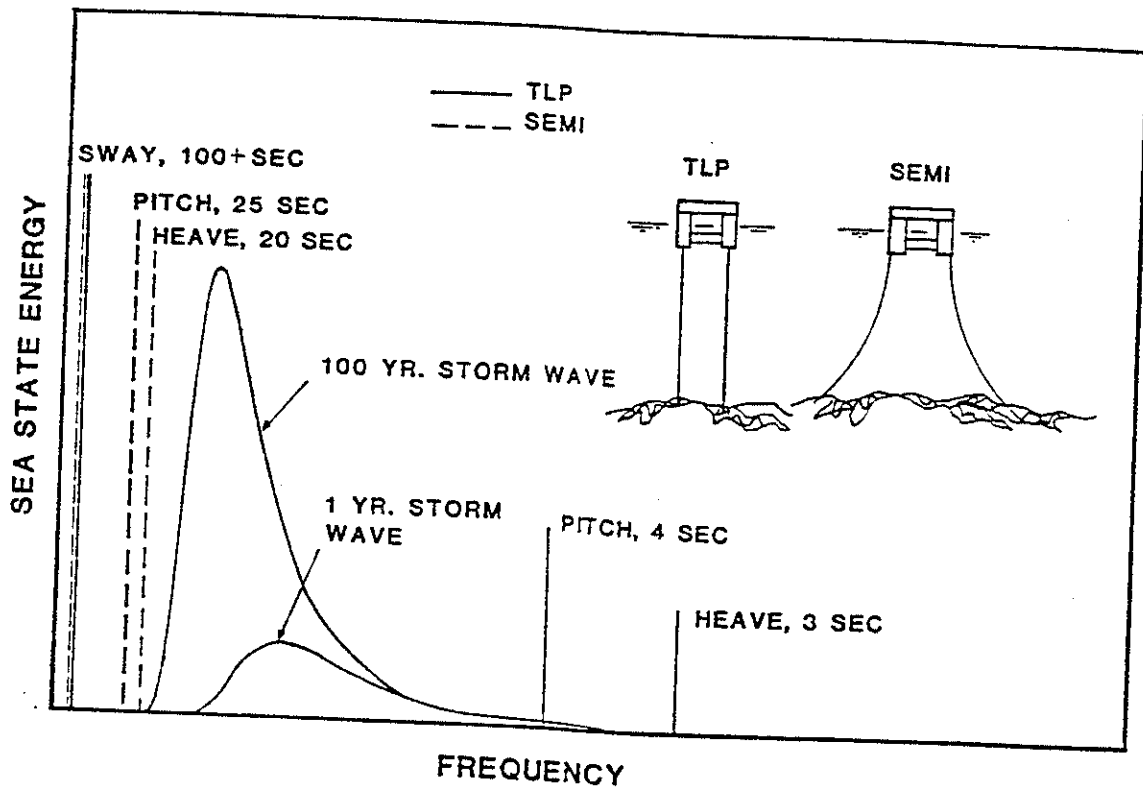


FIGURE 3.24 SEMISUBMERSIBLE & TLP NATURAL FREQUENCIES COMPARISION

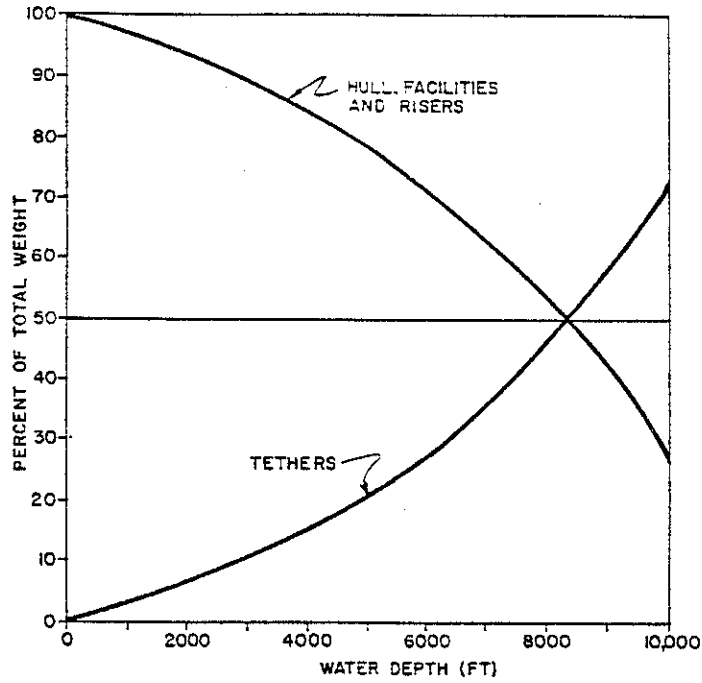


FIGURE 3.25 TETHER VS. PLATFORM WEIGHTS (IN HOUSE STUDY, NO TETHER DYNAMICS CONSIDERED) (KARSAN AND MANGIAVACCHI, 1982)

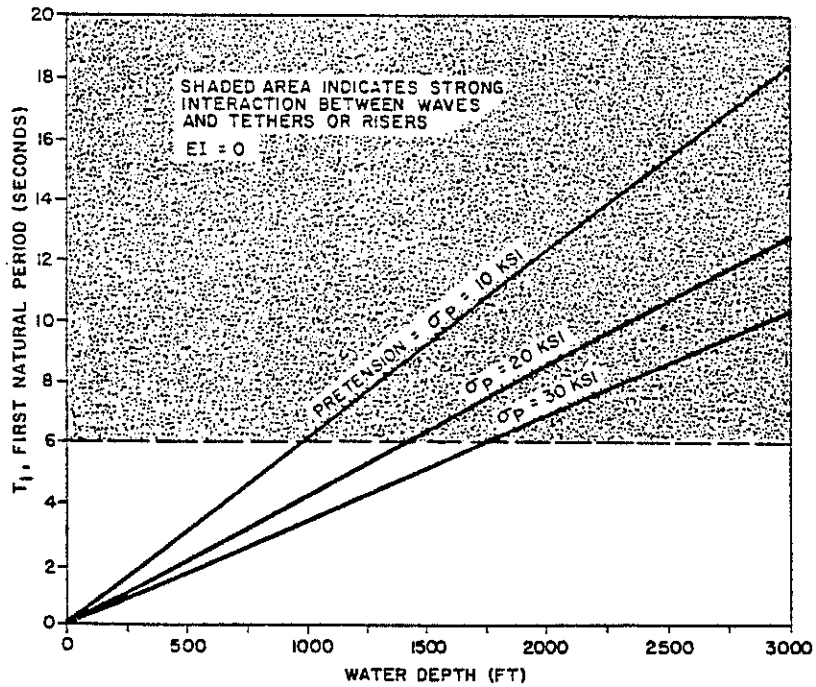


FIGURE 3.26 TETHER AND RISER PERIODS VS. WATER DEPTH AND PRETENSION (KARSAN AND MANGIAVACCHI, 1982)



#### 4.0

### EQUATIONS OF MOTION AND DYNAMIC RESPONSE ANALYSIS

In this chapter a simple derivation of the equations of motion for floating platforms is presented. Particular emphasis is placed on moored platforms since semisubmersibles and tension leg platforms belong to this group of ocean structures. In addition a brief description of various dynamic response analysis techniques for floating platforms along with the philosophy and the need for these analyses is discussed.

#### 4.1

### Philosophy Of And Need For Dynamic Response Analysis

It is important to distinguish between dynamic loading and dynamic response. The CIRIA Report (1980) and Hallam et al. (1978) define dynamic loading as a parameter that varies with time in magnitude and/or direction. The dynamic response which results from this loading depends on the stiffness (as in the case of static loads) and, additionally, on the mass and damping of the structure. The important distinction between static and dynamic problems is that in the latter the forces required to accelerate (and decelerate) the masses of the structure are important and must be taken into account when considering the "equilibrium" of the structure.

Accurate evaluation of the platform motions is essential for a reliable assessment of the loads, stresses and fatigue life of the entire system.

St. Denis (1975) states that the prediction of the oscillations that a platform undergoes in a generic seaway is a problem in dynamics and kinetics. Dynamics in this context stands for the determination of the forces imposed by the seaway on the platform and kinetics is the determination of the motions resulting from the forces imposed by the seaway. However, it is not always feasible to separate the two aspects from each other since the hydrodynamical loading on a platform is affected by its motions.

The casual relationship between a seaway and the oscillations that a platform experiences usually develops in four steps.

Seaway >	Fluid Kinematics >	Environmental >	Platform >	Structural
	and Fluid	Loads	Motions	Design
	Pressures			and Analysis
	(Step 1)	(Step 2)	(Step 3)	(Step 4)

In the first step the fluid kinematics and pressure distribution on the submerged portion of the platform are evaluated.

In the second step the forces acting on the platform are derived; these include

- o the seaway induced excitation forces corresponding to each degree of freedom
- o the platform's reactions corresponding to (as yet unknown) platform motions; namely the dynamical coefficients of the equations of motion.

The third step (kinetics) consists of the solution to the equations of motion which will yield the platform responses.

Finally, the knowledge of the environmental loads and platform response allows structural design and analysis to be performed in the fourth step.

Motions can be characterized either as steady or as transient. Steady motions only are usually taken into consideration for floating structures. They are defined as processes where statistical characteristics are time invariant. Obviously, platform motions, like seaways that excite them, are steady only over a short period of time.

The waves at sea manifest a random nature whose descriptive parameters tend themselves to vary with time. This randomness, which is a basic characteristic of the seaway, can be properly described only by statistical models. The random character of the seaway in turn reflects itself in the platform motions it stimulates, so that the solution to a prediction of platform motions also has statistical expressions.

The dynamic analysis can proceed along two paths: in time domain or in frequency domain. One can work in the frequency domain, in which case transient effects are neglected and one concentrates on steady-state solutions. The method assumes a linear system and the work is considerably less burdensome and requires less computer work. The other possibility is to analyze the system in the time domain by some technique, in which case transient effects may be considered as well as nonlinearities. Figure 4.1 adopted from a paper by Migliore and Palo (1979) shows an overview of the solution techniques associated with floating objects subject to wave excitation. In this figure also a distinction is made between large and small objects, the diffraction theory applicable to large objects and the Morison equation for small objects. Theoretical definitions of the concepts are given in Chapters 6.0, 7.0 and 8.0.

There are also two alternative approaches to translate sea state conditions into hydrodynamic loading and response of offshore structures: deterministic (in design wave approach) and stochastic (in spectral or probabilistic approach). The traditional design wave method, for analyzing fixed platforms, is being improved or replaced by the use of spectral or probabilistic techniques, which are more appropriate when dynamic response and fatigue are important.

The design wave approach is concerned with survival in the largest wave which the structure is likely to encounter during its lifetime.

The spectral and probabilistic approaches are largely complementary, describing different features of an irregular sea. The spectral approach is in terms of its frequency content, and demonstrates clearly the effects of natural frequency response. The probabilistic approach is concerned with the number of times given stress or response levels are exceeded. Figure 4.2 adopted from a paper by Tickell (1979) shows schematically the steps involved in the transformation of sea state information to the structural response data.

The assumptions inherent in the stochastic approach (spectral and probabilistic) require that the surface elevation, wave force, and the response be related linearly. Therefore, this approach is applicable to the frequency domain technique. Some statistical information is also obtained from results of the time domain analysis. The time history of platform response in the time domain can be transformed into a response spectrum from which statistical information similar to that in the frequency domain analysis may be obtained.

Figure 4.3, inspired from a paper by Hutchison and Bringloe (1978), shows the analytical tools of seaway and floating platform motion analysis and prediction.

## 4.2 Equations of Motion

### 4.2.1 General

This section describes the equations of motion governing the response of a semisubmersible or TLP under the action of wind, current and wave loads. Before undertaking a detailed examination of this subject, it appears desirable to briefly discuss a few relevant concepts and review the associated terminology.

From a structural viewpoint, a semisubmersible or TLP consists of two distinct parts, namely, a platform (i.e. hull-deck structure) and a set of mooring lines. The platform itself is made up of a number of vertical and horizontal (and, occasionally, inclined) cylindrical members usually referred to as columns and pontoons (and braces), respectively. For motion analysis purposes, the platform is usually idealized as a rigid body with six degrees of freedom. In relatively shallow water, the mass of the mooring system is much smaller than that of the platform/equipment combination, thus implying that the mooring system may be idealized as a set of weightless springs, at least in preliminary motion analysis. In deeper water, however, the mass of the mooring system would have to be accounted for somehow, at least in the final design stage.

In "coupled analysis", the platform/mooring system combination is analyzed as a "whole" by first discretizing each mooring line by a standard numerical technique such as finite differences or finite elements. This approach, while being capable of predicting the dynamic response of the system with high accuracy, usually requires the utilization of a very large number of degrees of freedom and, consequently, is computationally highly expensive. In "uncoupled analysis", a motion analysis is first performed for the platform by idealizing the mooring system as a set of weightless springs. The dynamic response of each individual mooring line is then analyzed separately by using the results of the preceding platform motion analysis as input for the top end of the mooring line. This approach, which is computationally less expensive, is also less accurate.

In undertaking a platform motion analysis, first a decision has to be made as to what specific approach will be used in the calculation of the hydrodynamic loads, i.e. whether the platform will be treated as a "large body" or an assemblage of "small bodies". As discussed in greater detail in Chapters 6.0, 7.0 and 8.0, potential flow theory (as represented by incident, diffraction and radiation wave theories)

is more suitable for large bodies whereas the Morison equation, which aims at accounting for viscous drag effects, is more widely used in connection with small bodies. Also needed at this point is a choice between the frequency and time domain approaches. The frequency domain approach, which is substantially more economical and consequently more popular, requires that the formulation of the problem be completely linearized. Potential flow theory, which is inherently linear, is ideally suited to frequency domain analysis. The Morison equation, on the other hand, involves a nonlinear drag term which must somehow be linearized before the frequency domain approach can be applied. Various linearization techniques that have been suggested in the literature are reviewed in Section 7.7.

Assuming, for simplicity, that there is no current, let the drag force be expressed as

$$F_D = 1/2 \rho C_d A |u - \dot{X}| (u - \dot{X}) \quad (4.1)$$

in which  $u$  and  $\dot{X}$  denote water particle and structural velocities, respectively,  $\rho$  is the water mass density,  $C_d$  is the drag coefficient, and  $A$  is the projected area per unit length perpendicular to the flow direction. According to Malhotra and Penzien (1970), Equation (4.1) can be linearized as

$$F_D \cong 1/2 \rho C_{d1} A (u - \dot{X}) \quad (4.2)$$

in which, as will be shown later in Section 7.7,

$$C_{d1} = C_d \sqrt{\frac{8}{\pi}} (u - \dot{X})_{rms} \quad (4.3)$$

While  $u$  is known ahead of time,  $\dot{X}$  is not. The process of linearization thus involves an iterative scheme whereby an assumption is first made for the motion amplitude,  $C_{d1}$  is calculated from Equation (4.3), and a motion analysis is carried out. This solution

is then used to obtain an improved value for  $C_{d1}$  and the motion analysis is repeated. While this iterative process may conceivably continue until the assumed and calculated values of  $C_{d1}$  agree with each other within a prescribed tolerance, Burke (1969) expresses the view that various other approximations already inherent in the analysis would not warrant more than two iterations. Note that, from a computational viewpoint, the term  $(1/2 \rho C_{d1} A)\dot{X}$  in Equation (4.2) would go to the left hand side of an equation of motion and represent hydrodynamic damping whereas  $(1/2 \rho C_{d1} A)u$  would stay on the right hand side and serve as a forcing function.

The Morison equation also involves an inertia term which may be expressed as

$$F_I = \rho V [C_m \dot{u} - (C_m - 1) \ddot{X}] \quad (4.4)$$

in which  $C_m$  is the inertia coefficient for the particular member under consideration and  $V$  is the volume per unit length. Numerical values of  $C_m$  corresponding to various geometric shapes (which may have been obtained from experiments and/or from analysis based on potential flow theory) may be found in standard texts such as that by Sarpkaya and Isaacson (1981). The product  $\rho V(C_m - 1)\ddot{X}$ , when passed to the left hand side of an equation of motion, would represent the "added mass" whereas  $\rho V C_m \dot{u}$  would stay on the right hand side and serve as a forcing function.

In the time domain approach, the presence of a nonlinear drag term (i.e. the use of the Morison equation) poses no conceptual difficulty. From a computational viewpoint, however, the situation deserves some attention. Depending on the particular step-by-step numerical integration technique used, it sometimes becomes necessary to rewrite the equations of motion in an incremental form, i.e. linearize these equations over a small time interval  $\Delta t$ . As part of this process the drag term in Equation (4.1) must also be written in

an incremental form. After some mathematical manipulation (the details of which will not be given here), one arrives at an equation of the type

$$\Delta F_D = F_D(t + \Delta t) - F_D(t) \cong A - B \Delta \dot{X} \quad (4.5)$$

in which A and B are functions of  $X(t)$  and  $u(t + \Delta t)$ , i.e., they both are known quantities at time t. The product  $B \Delta \dot{X}$ , when passed to the left hand side of an equation of motion, represents a contribution to hydrodynamic damping.

It is important to emphasize at this point that the analysis of the motion of a floating body is essentially a study in fluid-solid interaction. Using Newton's second law, the equation of motion of the body in a certain coordinate direction may be written symbolically as

$$M\ddot{X} = f \quad (4.6)$$

in which M and  $\ddot{X}$  denote mass and acceleration, respectively, and f represents the resultant force acting on the body in the particular direction under consideration. Normally, f would be a function of t, X and  $\dot{X}$  so that Equation (4.6) would be written as

$$M\ddot{X} = f(t, X, \dot{X}) \quad (4.7)$$

In a fluid-solid interaction problem of the type considered here, however, f also contains inertia effects stemming from accelerations of surrounding water particles, i.e. it is a function of  $\ddot{X}$  as well, thus suggesting that Equation (4.7) be rewritten as

$$M\ddot{X} = f(t, X, \dot{X}, \ddot{X}) \quad (4.8)$$



The contribution of  $\ddot{X}$  to  $f(t, X, \dot{X}, \ddot{X})$  can generally be isolated from the rest and passed to the left hand side of the equation thus transforming Equation (4.8) into

$$(M + m_a) \ddot{X} = g(t, X, \dot{X}) \quad (4.9)$$

in which  $m_a$  is the so-called "added mass" and  $g(t, X, \dot{X})$  represents the sum of all exciting, restoring and damping forces acting on the body. The evaluation of these individual forces depends on the particular hydrodynamic approach used, i.e. on whether the body is treated as a "large" or "small" body as discussed in detail in Chapters 7.0 and 8.0. In the former case, the exciting forces would be determined from the incident and diffraction wave theories, and the damping and inertia effects from the radiation wave theory. In the latter case, all the hydrodynamic forces would be obtained from the Morison equation which, in turn, would have to be written in terms of "relative" velocities and accelerations.

Applications of these ideas to the motion analysis of semisubmersibles and TLP's will be examined in detail in subsequent sections.

#### 4.2.2 Coordinate System

In studying the motion of a rigid body in three-dimensional space, it is convenient to define two coordinate systems, namely, one fixed in space,  $(X, Y, Z)$ , and one attached to the body,  $(\bar{X}, \bar{Y}, \bar{Z})$ , as illustrated in Figure 4.4. The two coordinate systems are assumed to be parallel to each other when the body is at rest. The motion of the body can be described fully and conveniently in terms of three translational displacements (e.g. translations of the origin of  $(\bar{X}, \bar{Y}, \bar{Z})$  in the  $X, Y,$  and  $Z$  directions) and three rotation angles (such as the well known Euler angles  $\alpha, \beta$  and  $\theta$ ).

The mathematical formulation of the problem becomes simpler if the origin of the  $(\bar{X}, \bar{Y}, \bar{Z})$  coordinate system is chosen to coincide with the c.g. of the rigid body (i.e. the c.g. of the floating platform in the present review). Also, when the rotation angles are small (as assumed herein), it is more convenient to work with the three rotation components about the X, Y, Z axes than with the Euler angles. In line with the foregoing comments, the displacements of the platform will herein be described in terms of  $X_i$  ( $i = 1$  to 6) as illustrated in Figure 4.4. Note that  $X_i$  ( $i = 1$  to 3) denote translational displacements of the c.g. (with dimension of length) and  $X_i$  ( $i = 4$  to 6) denote rotations (with dimension of radians). Note also that  $X_3$  represents a vertical displacement whereas  $X_1$  and  $X_2$  represent horizontal displacements. In the usual terminology of naval architecture, all six displacement components can now be identified as follows:

- $X_1$  = surge (positive forward)
- $X_2$  = sway (positive to port)
- $X_3$  = heave (positive upward)
- $X_4$  = roll (positive, deck down to starboard)
- $X_5$  = pitch (positive, bow downward)
- $X_6$  = yaw (positive, bow to port)

This terminology is entirely consistent with that recommended by API (Draft 1984) for TLP motion analysis. While API suggests, for simplicity, that the  $(\bar{X}, \bar{Y}, \bar{Z})$  coordinate axes be coincident with the principal directions of the platform, the general theoretical development presented in this report is free of such a limitation.

#### 4.2.3 Equations of Motion (F.D.)

As emphasized in various other sections of this review, the frequency domain approach requires that the mathematical formulation of the problem be completely linearized. By modeling the mooring system as a set of weightless linear springs, the equations of motion of a

rigid floating platform can be written as

$$\sum_{k=1}^6 [(M_{jk} + A_{jk}) \ddot{X}_k + B_{jk} \dot{X}_k + C_{jk} X_k] = F_j \quad (4.10)$$

in which,

- $j, k$  = modes 1 to 6 (corresponding to surge, sway, heave, roll, pitch and yaw, respectively)
- $X_k$  = displacements (1 to 3 translations of platform c.g., 4 to 6 rotations)
- $M_{jk}$  = structural mass matrix
- $A_{jk}$  = added mass matrix
- $B_{jk}$  = hydrodynamic damping matrix
- $C_{jk}$  = stiffness matrix (hydrostatic restoring plus mooring)
- $F_j$  = forcing functions.

Assuming, as previously indicated, that the displacements of the platform are referred to the c.g. of the platform, the structural mass matrix has the form.

$$[M] = \begin{bmatrix} M & 0 & 0 & 0 & 0 & 0 \\ 0 & M & 0 & 0 & 0 & 0 \\ 0 & 0 & M & 0 & 0 & 0 \\ 0 & 0 & 0 & I_{44} & I_{45} & I_{46} \\ 0 & 0 & 0 & I_{54} & I_{55} & I_{56} \\ 0 & 0 & 0 & I_{64} & I_{65} & I_{66} \end{bmatrix} \quad (4.11)$$

in which  $M$  is the mass of the structure, and  $I_{jj}$  and  $I_{jk}$  denote mass moment of inertia and product of inertia, respectively. If the coordinate system used coincides with the principal directions of the platform, then  $I_{jk} = 0$  for  $i \neq j$ . The stiffness coefficient  $C_{jk}$  may be written as

$$C_{jk} = (C_H)_{jk} + (L_M)_{jk} \quad (4.12)$$

in which  $C_H$  and  $L_M$  refer to contributions of hydrostatic forces and mooring line forces, respectively. Inasmuch as there is no such thing as a horizontal buoyancy force,  $(C_H)_{jk} = 0$  when  $(j \text{ or } k) = 1, 2 \text{ or } 6$ . Depending on the symmetry properties of the mooring system,  $(L_M)_{jk}$  may also vanish for certain combinations of  $j \neq k$ .

The values of the added mass and hydrodynamic damping coefficients  $A_{jk}$  and  $B_{jk}$  depend on the general approach used in calculating hydrodynamic effects.  $B_{jk}$  can be written as

$$B_{jk} = (B_R + B_V)_{jk} \quad (4.13)$$

in which the subscripts R and V refer to radiation and viscous damping, respectively. When the platform is treated as a large body,  $A_{jk}$  and  $(B_R)_{jk}$  are determined simultaneously from radiation wave theory by using a suitable numerical technique as outlined in Chapter 8.0.  $(B_V)_{jk}$  would normally be estimated from model tests as pointed out by Chou, et al. (1983). When the platform is treated as an assemblage of small bodies,  $A_{jk}$  and  $(B_V)_{jk}$  are obtained from a linearized version of the Morison equation as discussed in some detail in Section 7.7. The forcing functions  $F_j$  are either calculated from incident and diffraction wave theories or from the linearized Morison equation depending on whether the platform is treated as a large or small body. The derivation of Equation (4.10) is summarized schematically in Figures 4.5 and 4.6.

It is important to note that, in determining  $F_j$ ,  $A_{jk}$  and  $(B_R)_{jk}$  from potential flow theory, a series of analyses must be carried out, each analysis corresponding to a single wave with a particular circular frequency  $\omega$ . This explains why the added mass and radiation damping coefficients, as well as the wave exciting forces, are frequency-dependent. (More specifically, these quantities depend on the direction of the waves as well as on their frequencies). This condition poses no difficulties in the frequency domain approach since then each wave frequency is analyzed separately

anyway. In the time domain approach, however, it becomes necessary to introduce certain modifications into the analysis as is discussed in Section 4.3, since then a large number of wave frequencies are generally present simultaneously. When the platform is treated as an assemblage of small bodies and the Morison equation is used in formulating the problem, the particular quantities under consideration, while they are not frequency-dependent, may be functions of Reynolds and/or Keulegan-Carpenter numbers.

Mooring forces are usually nonlinear functions of displacements. For the purpose of frequency domain analysis, however, these relationships are linearized by assuming that the displacements are small. In the case of a catenary mooring line, equivalent spring stiffnesses are obtained by considering unit displacements at the line top and calculating the associated changes in the forces. In the case of a pretensioned vertical mooring system, the problem is simpler in that equivalent spring constants in the vertical and horizontal directions are simply equal to  $EA/L$  and  $T/L$ , respectively, where  $E$  = modulus of elasticity,  $A$  = area of cross section,  $L$  = length and  $T$  = pretension.

This weightless spring idealization for the mooring system becomes less and less satisfactory as the water depth increases. It then becomes necessary to use a more elaborate mooring system model that is capable of accounting for both hydrodynamic and structural nonlinearities of the problem. Such a refined analysis can only be carried out in the time domain.

#### 4.2.4 Solution of Frequency Domain Equations

Before going into a detailed discussion of the frequency domain approach as applied to platform motion analysis, it may be useful to review the special case of a single-degree-of-freedom system.

The general equation of motion for a simple mass-spring-dashpot system can be written as

$$M\ddot{X} + B\dot{X} + CX = f \quad (4.14)$$

in which  $M$  = mass,  $B$  = damping coefficient,  $C$  = stiffness coefficient,  $X(t)$  = response (displacement) function and  $f(t)$  = forcing function. The problem here consists of determining the output  $X(t)$  corresponding to a prescribed input  $f(t)$ . The use of complex variables proves to be a particularly powerful tool in the analysis of this problem. Consider now the special case of

$$f(t) = f_0 \exp(-i\omega t) \quad (4.15)$$

Letting

$$X(t) = X_0 \exp(-i\omega t) \quad (4.16)$$

and substituting into Equation (4.14), one obtains

$$X_0 = H(\omega)f_0 \quad (4.17)$$

in which

$$H(\omega) = \frac{1}{[C - iB\omega - M\omega^2]} \quad (4.18)$$

is the "complex frequency response function". Note that  $X_0$  is, in general, a complex quantity even though  $f_0$  may be a real one. In complex polar notation,

$$H(\omega) = |H(\omega)| \exp[-i\phi(\omega)] \quad (4.19)$$

in which  $|H(\omega)|$  and  $\phi(\omega)$  are sometimes called gain factor and phase factor, respectively. Substituting this result into Equations (4.15) to (4.17), one obtains

$$X(t) = |H(\omega)| f_0 \exp[-i(\omega t + \phi)] \quad (4.20)$$

which, in turn, indicates that  $H(\omega)$  represents essentially a "response amplification operator", RAO, and  $\phi$  is a phase angle between input and output.

To extend these ideas to the motion analysis of a six degree of freedom (DOF) floating platform, consider a regular sea state with the sea surface elevation given by

$$\eta(X,Y,t) = \frac{H}{2} \exp[-i(\omega t + kX \cos \beta + kY \sin \beta)] \quad (4.21)$$

with  $H$  = wave height,  $\omega$  = wave frequency,  $k$  = wave number and  $\beta$  = wave heading (measured from the X-axis as shown in Figure 4.4). Let the wave exciting forces associated with a wave height  $H$  be expressed as

$$F_j = |F_j| \exp[-i(\omega t + \alpha_j)] = |F_j| \exp(-i\alpha_j) \exp(-i\omega t) \quad (4.22)$$

in which  $\alpha_j$  denote phase angles relative to the wave. In a multidegree of freedom system such as the platform under consideration, each response parameter  $X_k$  has its own complex frequency response function  $H_k(\omega)$ , i.e. its own RAO and phase angle. Letting, by analogy to Equation (4.22),

$$X_k = |X_k| \exp(-i\phi_k) \exp(-i\omega t) \quad (4.23)$$

one can identify  $|X_k|/H$  and  $\phi_k$  as RAO and phase angle, respectively, for  $X_k$ . Alternately, one can write

$$X_k = H_k(\omega) H \exp(-i\omega t) \quad (4.24)$$

Theoretically speaking,  $H_k(\omega)$  can be determined by substituting Equations (4.22) and (4.23) into Equation (4.10), dividing through by  $\exp(-i\omega t)$  and solving the resulting algebraic equations for  $H_k(\omega)$ . Symbolically, one can write

$$H_k(\omega) = \frac{\Delta_k}{H\Delta} \quad (4.25)$$

in which  $\Delta$  is a 6 x 6 determinant with elements

$$\Delta_{mn} = -\omega^2 (M_{mn} + A_{mn}) - i\omega B_{mn} + C_{mn} \quad (4.26)$$

and  $\Delta_k$  is obtained from  $\Delta$  by simply replacing the  $k$ th column by  $F_m \exp(-i\alpha_m)$ . This approach, while being an elegant one, is of little practical value because the resulting expressions are extremely complicated. In practice, the problem is generally solved by a numerical approach, i.e. by expressing all input and output parameters in terms of their real and imaginary parts and solving two sets of algebraic equations (corresponding to real and imaginary terms, respectively) for each specific value of  $\omega$  considered. Let the solution thus obtained be expressed as

$$H_k(\omega) = H_{kr} + iH_{ki} \quad (4.27)$$

in which the subscripts  $r$  and  $i$  denote real and imaginary parts, respectively. Then

$$(X_k)_{\text{RAO}} = \sqrt{H_{kr}^2 + H_{ki}^2} \quad (4.28)$$



$$\phi_k = \tan^{-1} \left( \frac{H_{ki}}{H_{kr}} \right) \quad (4.29)$$

The concept of complex frequency response function is particularly useful in the analysis of response spectra. For example, letting  $S_{nn}(\omega)$  denote the wave spectrum it is shown in standard texts such as Clough and Penzien (1975) that

$$S_{X_k X_k}(\omega) = |H_k(\omega)|^2 S_{nn}(\omega) \quad (4.30)$$

$$S_{n X_k}(\omega) = H_k(\omega) S_{nn}(\omega) \quad (4.31)$$

in which  $S_{X_k X_k}(\omega)$  is the response spectrum for  $X_k$  whereas  $S_{n X_k}(\omega)$  denotes cross spectrum for the pair  $X_k$  and  $n$ .

An important statistical parameter for any random variable  $X$  is the so-called "root mean square" defined by

$$(X)_{\text{rms}} = \sqrt{\int_0^{\infty} S_{XX}(\omega) d\omega} \quad (4.32)$$

Other statistical parameters, such as the average of the highest  $1/n$  peaks, are functions of  $(X)_{\text{rms}}$ . As discussed in detail by Sarpkaya and Isaacson (1981),

$$\frac{H_{1/n}}{H_{\text{rms}}} = [L_n(n)]^{1/2} + \frac{n\sqrt{\pi}}{2} \left\{ 1 - \text{erf} [(Ln(n))^{1/2}] \right\} \quad (4.33)$$

in which the error function erf is defined as

$$\text{erf}(x) = \frac{2}{\pi} \int_0^x \exp(-t^2) dt \quad (4.34)$$

The results corresponding to some selected value of  $n$  are given in the table below:

<u>n</u>	<u><math>\frac{H_{1/n}}{H_{rms}}</math></u>
3	1.416
10	1.800
100	2.359
1000	2.805

#### 4.3 Time Domain Analysis

In the time domain approach, the equations of motion of the system are solved by a step-by-step numerical integration technique over a sufficiently long time interval. The number of simultaneous equations involved in a given application depends on whether the analysis is "coupled" or "uncoupled". In the latter case, the problem reduces to that of a rigid body motion with six degrees of freedom. In the former case, however, the total number of degrees of freedom, which depends on the particular mathematical model used for the mooring lines, is usually considerably higher. Also, as previously pointed out, time domain equations of motion are usually highly nonlinear from both hydrodynamic and structural viewpoints.

A large number of step-by-step numerical integration methods are currently available as reviewed, for example, by Crandall (1956), Bathe and Wilson (1976) and Bathe (1982). It is useful to distinguish between the "explicit" and "implicit" methods. For

simplicity, consider the special case of a single degree of freedom system with an equation of motion of the type

$$G(t, X, \dot{X}, \ddot{X}) = 0 \quad (4.35)$$

in which  $t$  = time and  $X$ ,  $\dot{X}$  and  $\ddot{X}$  denote displacement, velocity and acceleration, respectively. From a computational viewpoint,  $X_t$ ,  $\dot{X}_t$  and  $\ddot{X}_t$  are known at time  $t$ , and  $X_{t+\Delta t}$ ,  $\dot{X}_{t+\Delta t}$  and  $\ddot{X}_{t+\Delta t}$  are to be determined at time  $t+\Delta t$ . Obviously, three equations are needed for that purpose. First, two equations are written to reflect the differential/integral nature of the relationships between the three unknown quantities. The specific form of these equations depends on the specific step-by-step integration technique used. The third equation is obtained by invoking the equation of motion either at  $t$  (explicit method) or at  $t+\Delta t$  (implicit method). For details of these two classes of methods the reader may wish to refer to Bathe (1982).

#### 4.3.1 Equations of Motion (T.D.)

As pointed out earlier in Section 4.2.3, one difficulty with the frequency domain approach is that the coefficients in the equations of motion turn out to be frequency-dependent when these coefficients are determined from diffraction/radiation wave theories. If, instead, the Morison equation is used, then the coefficients are frequency-independent but may depend on Reynolds and/or Keulegan-Carpenter numbers.

Inasmuch as the time domain approach is intended to be general enough to deal with irregular sea states, the coefficients in the corresponding equations of motion must somehow be made frequency-independent. To that end, Cummins (1962) developed a technique whereby an arbitrary motion is viewed as a succession of small impulsive displacements. Basically, it is assumed that, at any time, the total fluid force is the sum of the reactions to the

individual impulsive displacements, with each response being calculated with an appropriate time lag from the instant of the corresponding impulsive motion. The following technical discussion is based on the work of Van Oortmersen (1976b).

Assuming that the platform is treated as a "large" body (i.e. diffraction/radiation wave theories are used in formulating the problem) the time domain equations of motion of a rigid floating platform can be written as

$$\sum_{k=1}^6 [M_{jk} + m_{jk}] \ddot{X}_k + \int_{-\infty}^t K_{jk}(t-\tau) \dot{X}_k(\tau) d\tau + C_{jk} X_k = F_j(t) + L_j(x,t) \quad (4.36)$$

in which

- $M_{jk}$  = structural mass matrix (same as in F.D.)
- $m_{jk}$  = frequency-independent impulsive added mass matrix (related to  $A_{jk}(\omega)$  as shown below)
- $K_{jk}$  = retardation function (related to  $B_{jk}(\omega)$  as shown below)
- $C_{jk}$  = stiffness matrix (representing hydrostatic restoring forces only)
- $F_j(t)$  = time-varying exciting forces representing first order incident/diffraction wave loads, second order wave drift forces, current and wind loads and, possibly, forces stemming from viscous effects.
- $L_j(t)$  = nonlinear mooring restoring forces.

The retardation function is given by

$$K_{jk}(t) = \frac{2}{\pi} \int_0^{\infty} B_{jk}(\omega) \cos(\omega t) d\omega \quad (4.37)$$

in which  $B_{jk}(\omega)$  is the radiation damping matrix defined in Equation (4.10) in connection with the frequency domain approach. On the other hand,

$$m_{jk} = A_{jk}(\omega') + \frac{1}{\omega'} \int_0^{\infty} K_{jk}(t) \sin(\omega't) dt \quad (4.38)$$

in which  $\omega'$  is an arbitrarily chosen value of  $\omega$ . While this equation seems to suggest that  $m_{jk}$  would be a function of  $\omega'$ , it is in fact a frequency-independent quantity as indicated by Van Oortmerssen (1976b). In practice, the numerical value calculated for  $m_{jk}$  may vary somewhat with the particular value used for  $\omega'$ , these slight variations stemming mainly from the approximate character of the numerical integration technique used in calculating  $m_{jk}$ . One way of eliminating this difficulty would be to calculate  $m_{jk}$  for several different values of  $\omega'$  and then take the average.

As pointed out by Van Oortmerssen (1976b), the impulsive added mass can alternately be obtained as

$$m_{jk} = A_{jk}(\omega) \text{ for } \omega \gg \infty \quad (4.39)$$

The definite integrals in Equations (4.36) to (4.38) are calculated by applying a simple numerical integration technique such as the trapezoidal rule or Simpson's rule. Since the retardation function dies down rapidly with increasing  $t$ , Van Oortmerssen (1976b) points out that the upper limit in Equation (4.38) can be replaced by a finite value (e.g. 25 seconds) with no significant loss in accuracy.

It should be emphasized that the left hand side of Equation (4.36) above contains only radiation type damping as represented by the retardation function  $K_{jk}$ , all forces of viscous origin being thrown into the  $F_j(t)$  term on the right hand side. In the case of a "large" body as considered herein, the extent of possible viscous

damping would have to be estimated on the basis of model tests and/or previous experience as pointed out earlier in Section 4.2.3. Viscous damping forces, if linearized, may be passed to the left side of Equation (4.36) and combined with radiation damping forces.

If the platform is treated as a "small" body and the Morison equation is used to calculate all hydrodynamic loads, then the foregoing theoretical development will have to be modified as follows in light of the introductory remarks offered earlier in Section 4.2.1. The added mass matrix  $m_{jk}$  will now be obtained by simply passing the inertia term in the Morison equation to the left hand side of Equation (4.36). The radiation damping term will be eliminated. The principal force represented by  $F_j(t)$  will now be the quadratic drag term in the Morison equation which, in turn, will have to be written in terms of "relative" velocities. It is important to note that this drag term represents essentially a combination of excitation and damping effects, the relative significance of the two effects being a function of the relative magnitudes of the two velocities (water particle and structure) that enter the drag term.

In "coupled" analysis, the platform/mooring system combination is treated as a whole, thus considerably increasing the number of degrees of freedom of the system. The specific form and number of the resulting equations of motion depend on the particular modeling technique used in discretizing the mooring lines.

#### 4.3.1.1 Force Ramp Function

The wave exciting force, drifting force, and the constant external forces are customarily multiplied by a ramp function such as  $(1-\exp(-0.02t))$  to prevent a sudden loading at the start of the simulation. In this manner, the loads gradually increase from zero to over 98 percent of their value in a span of 200 seconds of simulation time.

#### 4.3.1.2 Time Domain Solution Process

A numerical technique for the solution of the six coupled second order equations of motion in the time domain is described in detail by Van Oortmerssen (1976b). A brief description of this procedure is given here for the sake of completeness.

Supposing that the simulation has been carried out to instant  $t$ , the equations of motion must now be solved for instant  $t+\Delta t$ , where  $\Delta t$  is the time step. The velocities at  $t+\Delta t$  and  $t+\Delta t/2$  are first estimated by extrapolating the obtained time histories by a Taylor series expansion:

$$\dot{X}_j(t+\Delta t) = \dot{X}_j(t) + \Delta t \ddot{X}_j(t) + \frac{\Delta t}{2} [\ddot{X}_j(t) - \ddot{X}_j(t-\Delta t)] \quad (4.40)$$

$$\dot{X}_j(t+\frac{\Delta t}{2}) = \dot{X}_j(t) + \frac{\Delta t}{2} \ddot{X}_j(t) + \frac{\Delta t}{4} [\ddot{X}_j(t) - \ddot{X}_j(t-\frac{\Delta t}{2})] \quad (4.41)$$

These values are then substituted into the well known Simpson's rule to determine  $X_j$  at  $t+\Delta t$ :

$$X_j(t+\Delta t) = \dot{X}_j(t) + \frac{\Delta t}{6} [X_j(t) + 4\dot{X}_j(t+\frac{\Delta t}{2}) + \dot{X}_j(t+\Delta t)] \quad (4.42)$$

The convolution integral involving the damping retardation function  $K_{jk}$  can now be computed since the time histories of all the velocities are now known up to time  $t+\Delta t$ . This is achieved by utilizing Simpson's rule with the same time step,  $\Delta t$ , as used previously. The mooring line forces and the hydrostatic restoring forces can also be determined and substituted back into the equations of motion (Equation (4.36)) along with the values of the convolution integrals. Solution of the six equations of motion yields the accelerations,  $\ddot{X}_j(t+\Delta t)$ , which can then be integrated and compared with the predicted velocities. If the agreement is good, the simulation can proceed to the next step, otherwise the time increment

must be reduced. Note that this method is an "implicit" one because the equations of motion are used at time  $t+\Delta t$ , not at time  $t$ .

#### 4.3.2 Regular Wave Versus Irregular Wave Analysis

Regular wave time domain analysis is a deterministic analysis. A discrete maximum design regular wave with one or several selected periods is used to predict the worst system response to this event. Note that the coefficients in the equations of motion, which have already been made frequency-independent, need not be recalculated for each specific frequency under consideration.

In the case of irregular waves, any specific wave train used in the analysis is deterministic, too.

A design wave spectrum is used to simulate the irregular wave condition. First order wave exciting forces and second order slowly varying wave drift forces are both represented in the form of random generated time histories. For details of this approach the reader may refer to Van Oortmerssen (1976b).

#### 4.3.3 Output of Time Domain Analysis

The output of a time domain analysis consists of time histories of responses. This can be used in a number of ways.

- o Regular wave simulations can be used to predict transfer functions by taking the ratio of the response amplitude to the input wave amplitude. (This approach is somewhat similar to the frequency domain approach except that nonlinear effects can now be included in the analysis).
- o The spectrum of the response can be calculated from the time domain analysis content, providing information similar to that of the frequency domain analysis. This can be used for



predicting extreme responses through a statistical procedure.

- o The extreme response can be estimated directly from the distribution of peaks of the response.

#### 4.4 Frequency Domain Versus Time Domain Analysis

Frequency domain techniques are useful tools in the design and analysis of semisubmersible and TLP's. In particular, they are used for preliminary design of the platform, for analysis in operational sea states and/or for fatigue life assessment. The frequency domain approach requires that the formulation of the problem be completely linearized. The solution leads to a set of linear transfer functions for the platform which represents a mathematical expression of the dynamic characteristics of that platform. These transfer functions (more frequently called Response Amplitude Operators, RAO's) can be used directly with wave spectra, thus resulting in response spectra from which various statistical information can be derived and fatigue life can be predicted.

Frequency domain solutions are generally more efficient and require less computer time than time domain solutions when random excitation of the system must be investigated.

The more direct and straight forward method is by direct integration of time domain equations. These methods lend themselves very well for determining responses of the platforms to extreme waves and/or design waves where nonlinear effects are important. They permit the inclusion of all nonlinearities. There is virtually no limitation on the nonlinear phenomena that may be included. The drawback is the cost. The solutions should be carried out over a relatively large number of iterations as each solution represents only one combination of the parameters.

A list of possible nonlinear effects which may contribute to semisubmersible or TLP responses and may be incorporated into the time domain analysis is given here for the sake of completeness.

- o Second-order, wave-induced mean and slowly-varying drift force.
- o Nonlinear tendon restoring forces and moments.
- o Slowly varying time-dependent wind forces.
- o Pendulum type effects, such as centrifugal force and TLP setdown, which are due to the vertical restraint of the tendons.
- o Nonlinear effects resulting from satisfying the hull boundary condition at the instantaneous wetted surface rather than the mean undisturbed wetted surface. (Note that some of these effects are included in the second order drift force computation.)
- o Effect of viscous drag force induced by large wave amplitude.
- o Nonlinearity of the hydrostatic restoring forces and moments as a consequence of the instantaneous position of the structure in the wave.
- o Nonlinear dynamic behavior of the tendons when their mass increases rapidly as the water depth increases.
- o Effect of coupling interactions between TLP hull and tendon/riser systems.
- o Effect of structure flexibility.
- o Nonlinear viscous drag forces.

o Current and wave interactions.

# OBJECTS SUBJECT TO WAVE EXCITATION

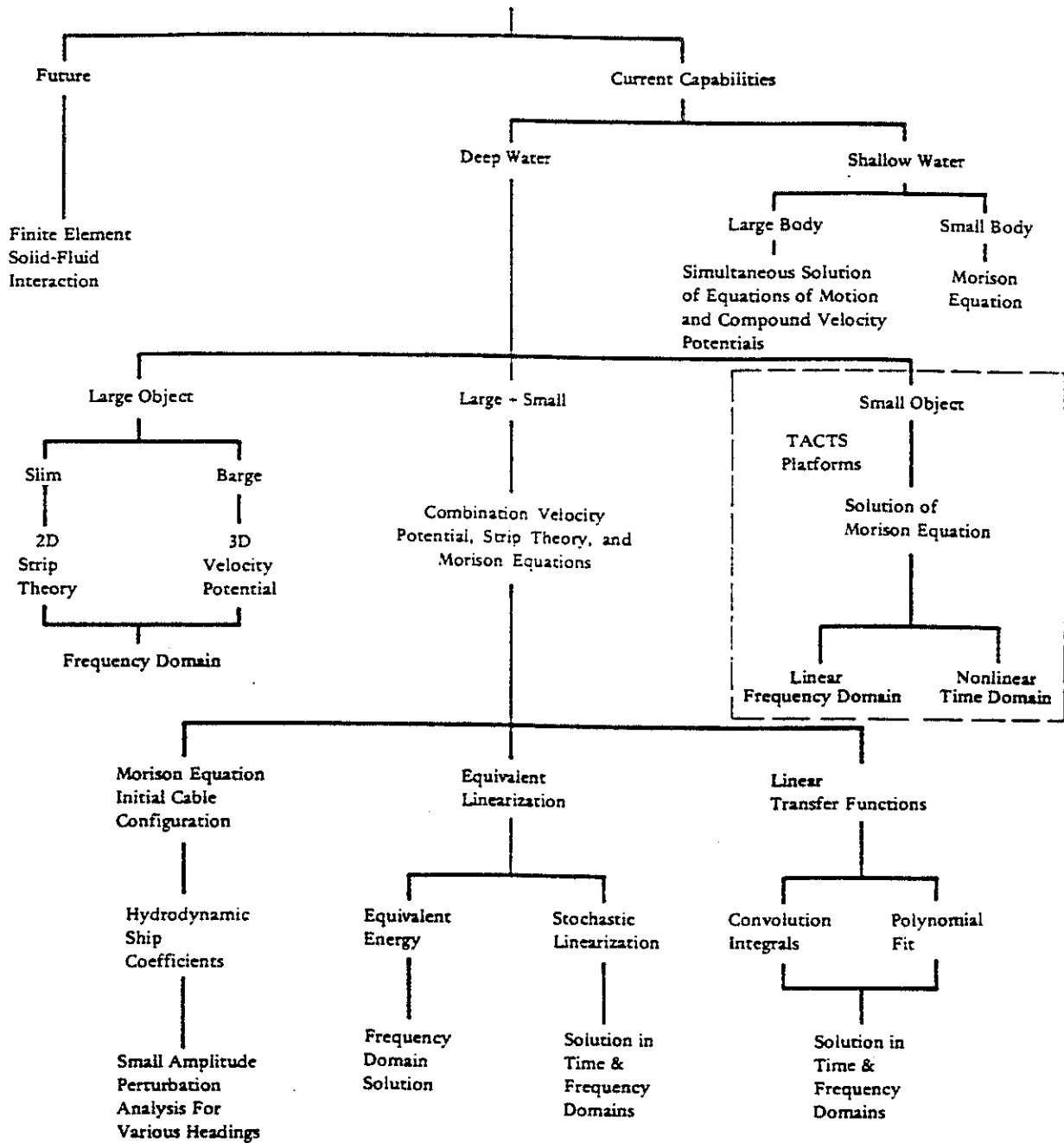


FIGURE 4.1 OVERVIEW OF SOLUTION TECHNIQUES ASSOCIATED WITH FLOATING OBJECTS SUBJECT TO WAVE EXCITATION. (ADAPTED FROM MIGLIORE AND PALO, 1979).

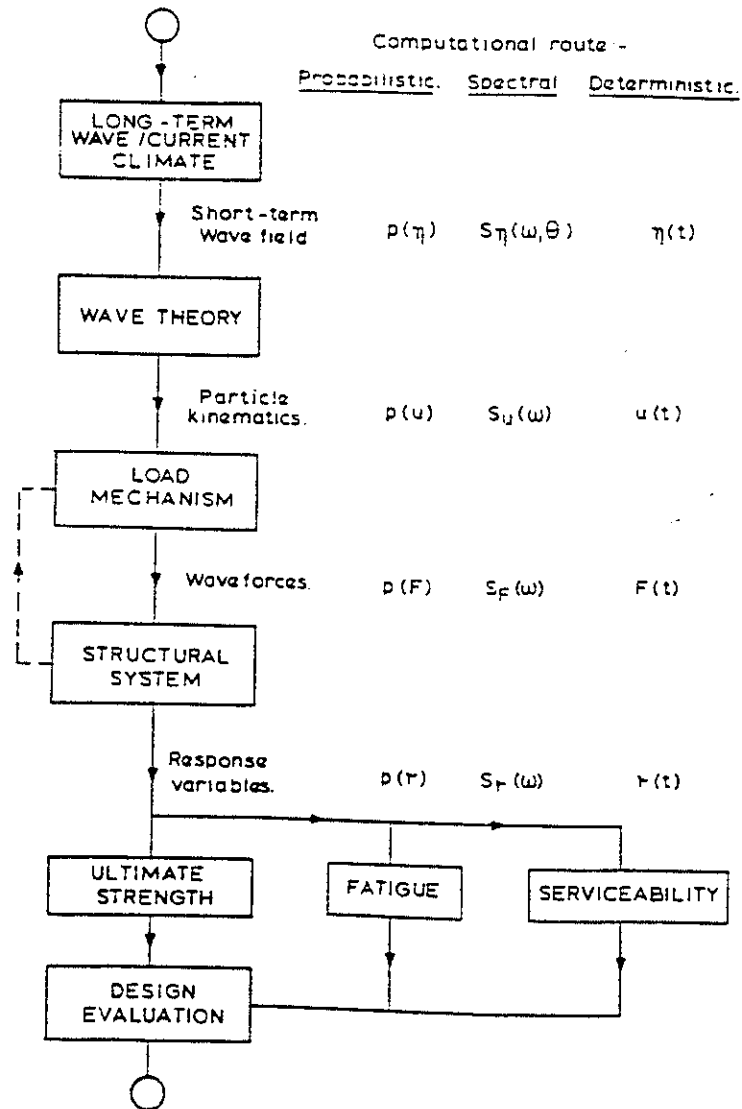


FIGURE 4.2 STEPS INVOLVED IN TRANSFERRING THE SEA STATE INFORMATION INTO STRUCTURAL RESPONSE DATA. (TICKELL, 1979)

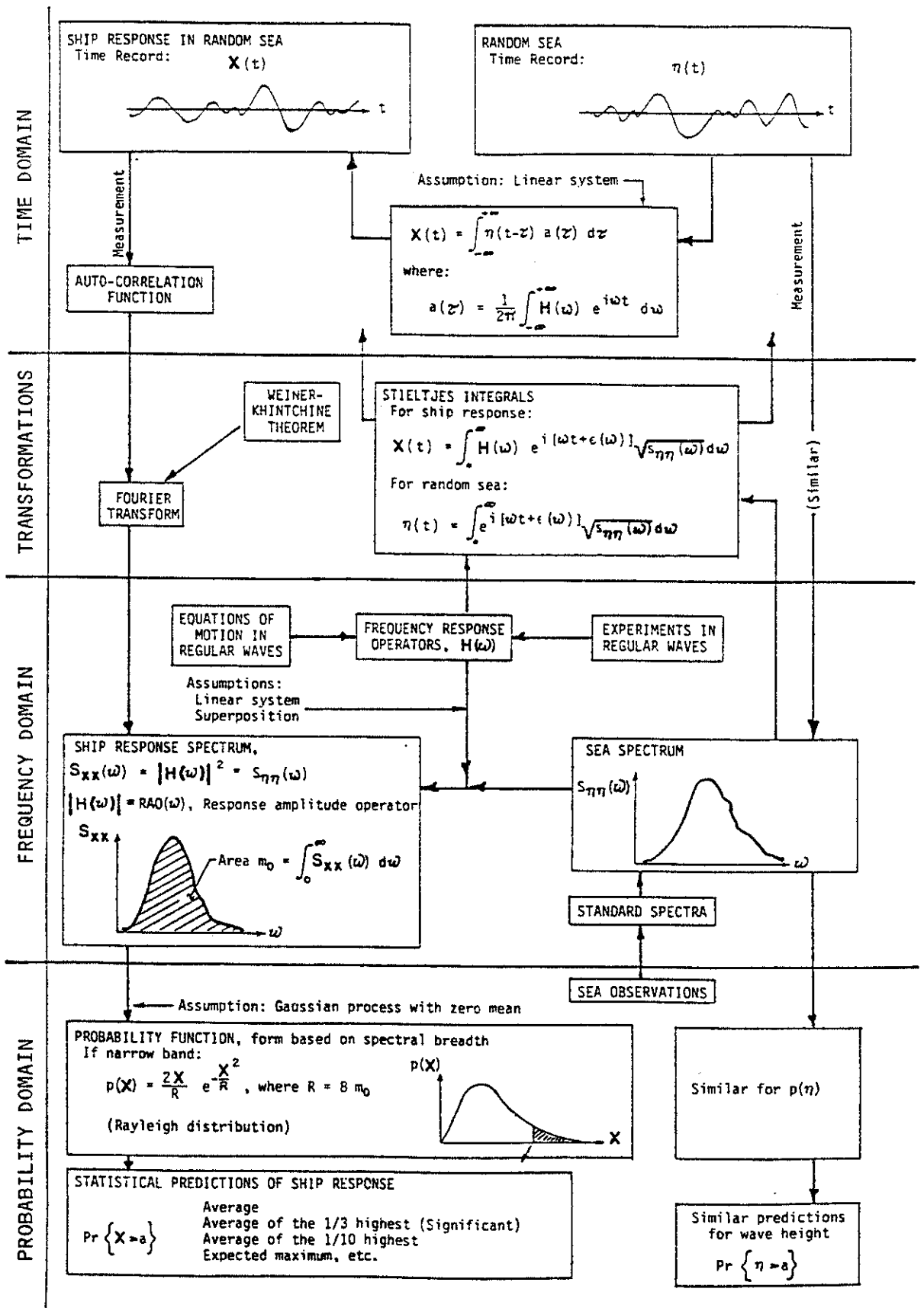
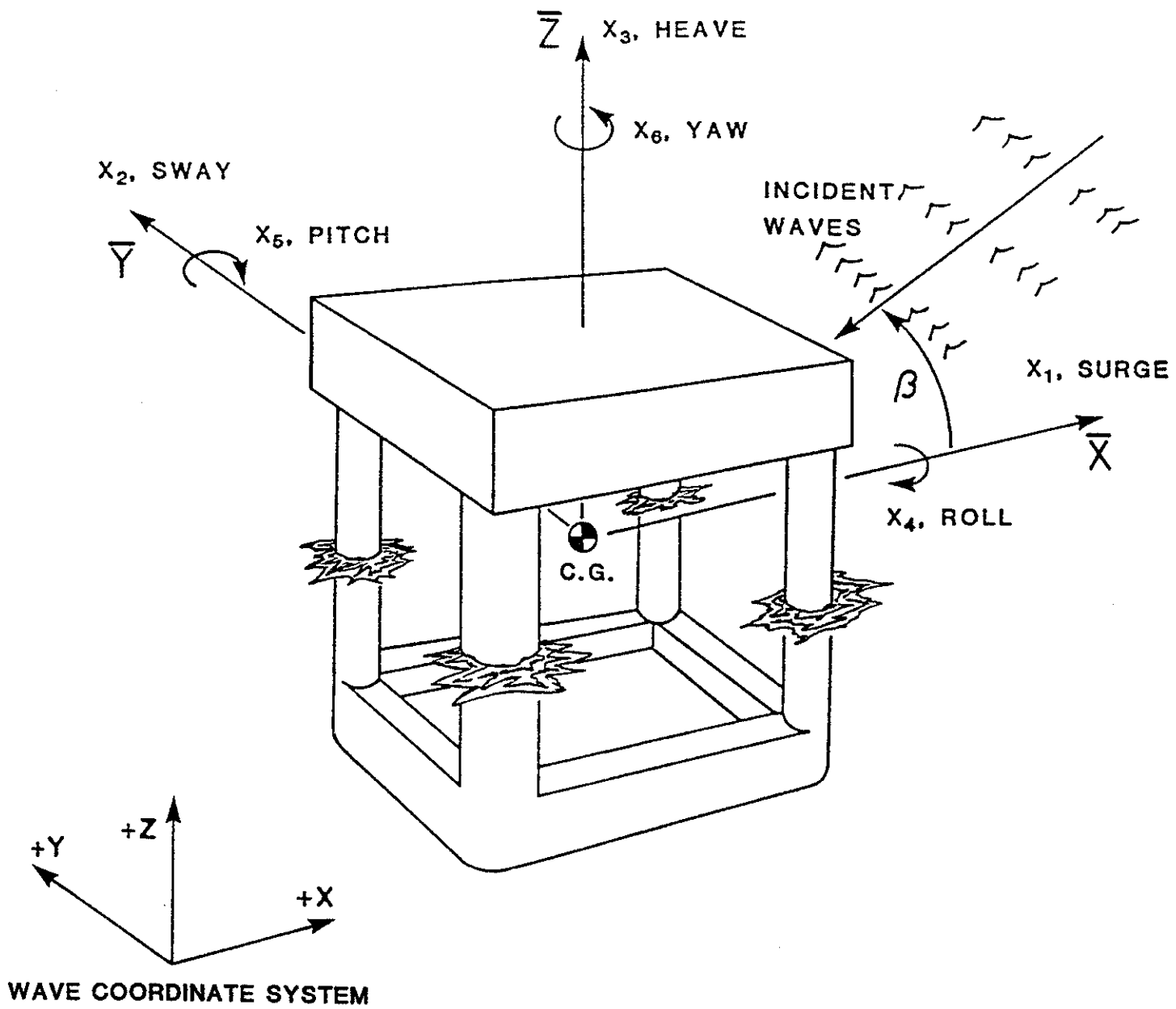
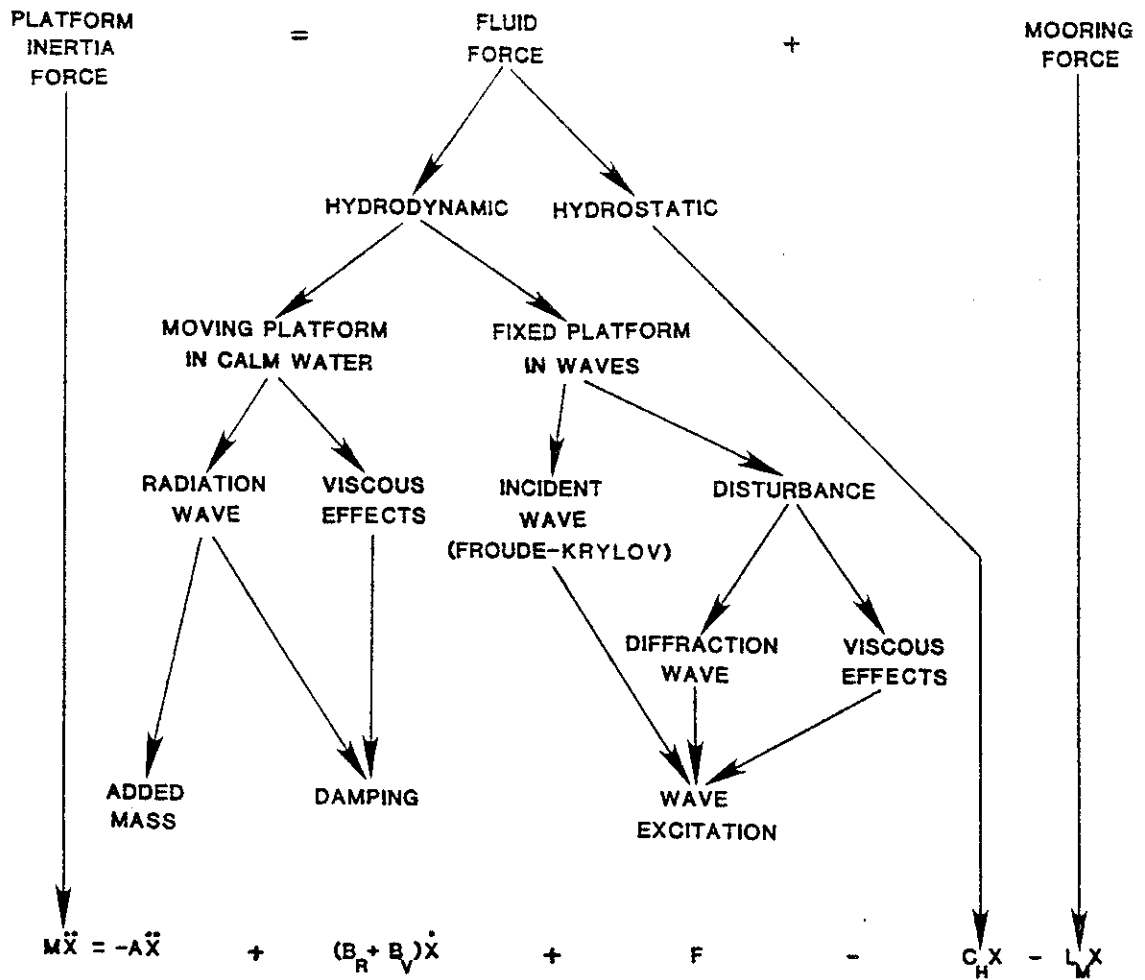


FIGURE 4.3 ANALYTICAL TOOLS OF SEAWAY AND FLOATING PLATFORMS MOTION ANALYSIS AND PREDICTION; INSPIRED BY A SIMILAR PRESENTATION BY HUTCHISON AND BRINGLOE (1978).



NOTE: A POSITIVE PHASE ANGLE INDICATES MOTION LEADS WITH RESPECT TO A WAVE CREST AT C.G.

FIGURE 4.4 SCHEMATIC OF COORDINATE SYSTEM



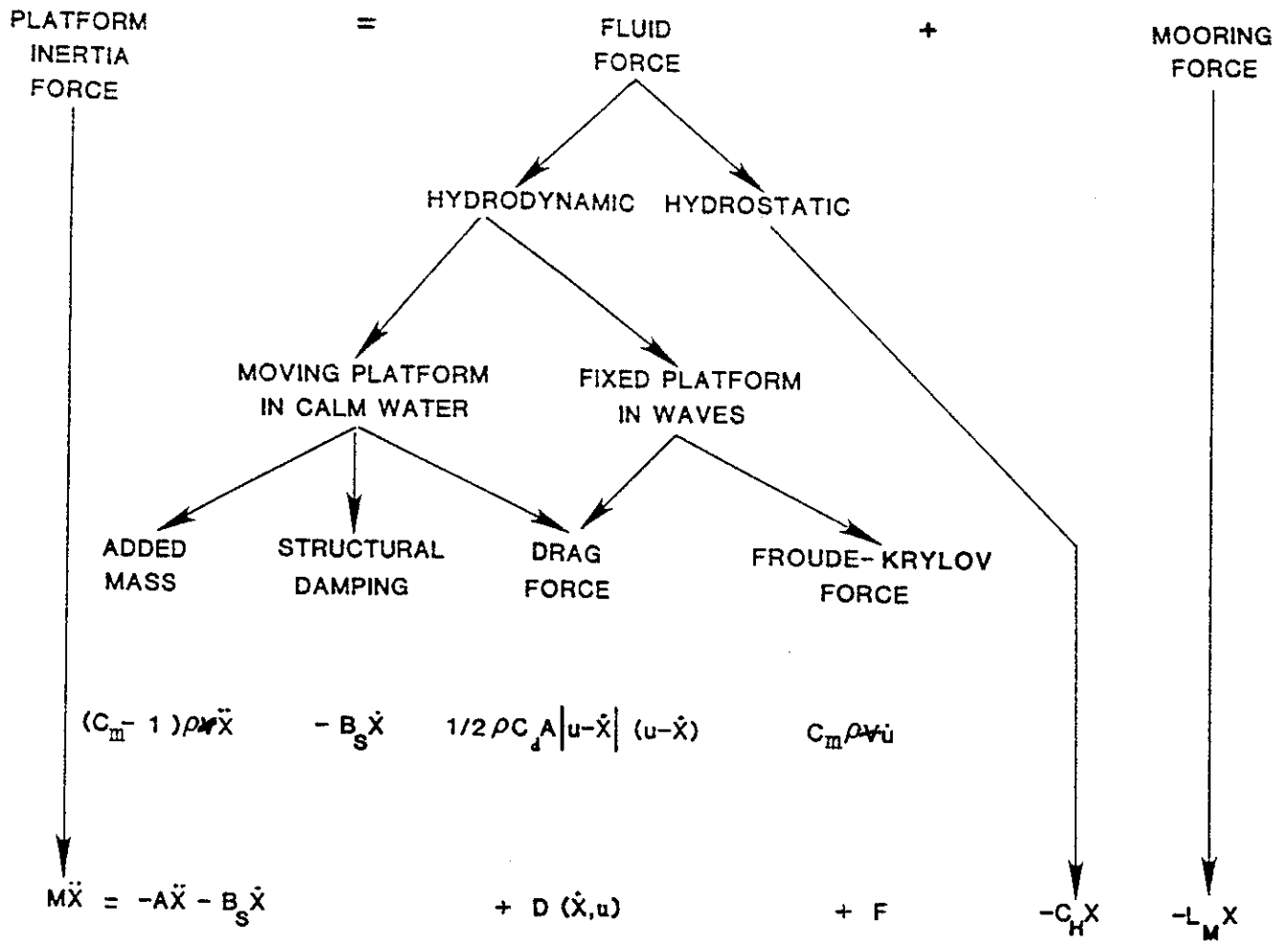
$$(M + A)\ddot{X} + (B_R + B_V)\dot{X} + (C_H + L_M)X = F$$

- M - STRUCTURAL MASS
- A - ADDED MASS
- B<sub>R</sub> - RADIATION DAMPING
- B<sub>V</sub> - VISCOUS DAMPING (STRUCTURAL AND OTHERS)

- F - EXCITATION FORCE
- C<sub>H</sub> - HYDROSTATIC STIFFNESS
- L<sub>M</sub> - MOORING STIFFNESS

FIGURE 4.5 PLATFORM EQUATIONS OF MOTION USING DIFFRACTION THEORY





$$(M+A)\ddot{X} + B_S \dot{X} + (C_H + L_M) X = D(\dot{X}, u) + F$$

M - STRUCTURAL MASS

A - ADDED MASS

B<sub>S</sub> - STRUCTURAL DAMPING

C<sub>H</sub> - HYDROSTATIC STIFFNESS

C<sub>m</sub> - INERTIA COEFFICIENT

L<sub>M</sub> - MOORING STIFFNESS

F - EXCITING FORCE

D - DRAG FORCE

u - WATER PARTICLE VELOCITY

FIGURE 4.6 PLATFORM EQUATIONS OF MOTION USING THE MORISON EQUATION



## 5.0 WAVE MODELS

### 5.1 Principal Factors in Analysis and Design

In dynamic analysis of floating structures there are two approaches to translate sea state conditions into hydrodynamic loading on a structure: deterministic (in design wave approach), and stochastic (in spectral or probabilistic approach) Bea and Lai (1978), Brebbia and Walker (1979), Standing (1981), and Sarpkaya and Isaacson (1981) describe these methods in some detail.

The "design wave" approach is concerned with survival in the largest wave which the structure is likely to encounter during its lifetime. With this approach, traditional in the design of static structures, the platform must survive the forces exerted by a train of regular waves. The height of this wave train is related to sea statistics at the structure's offshore location, and taken to be the height that is exceeded, on average, once in a 50 or 100 year period. The design wave method is straightforward to apply and understand, and usually makes no exceptional computational demands. There are always difficulties, however, in choosing an appropriate design wave period, and often a range of periods has to be considered. Draper (1965), and Arhan et al. (1979) describe the appropriate wave period range associated with the design wave. The design wave approach can be employed in both time and frequency domain analysis. However, since in extreme conditions nonlinearities manifest themselves, time domain analyses which are able to simulate or mimic these nonlinearities generally are required.

The "survival" condition for a dynamic structure is even more difficult to define, and indeed the problem is more often one of fatigue than failure in a single large wave. Long-period waves are often less critical than shorter smaller waves, because of

- o their lower rates of occurrence,

o the structure's compliance at lower frequencies.

As oil exploration and production have moved into deeper waters, structures have grown larger and (relatively) more compliant, and dynamic response and fatigue have become increasingly important factors in design. In these circumstances the design process has to take into account the whole range of sea conditions which will be encountered during the structure's lifetime, rather than a single severe wave.

For this reason the alternative spectral and probabilistic approaches to design are being more widely adopted. A brief description of these methods is given by Sarpkaya and Isaacson (1981). However, a more rigorous mathematical treatment of these concepts may be found in a paper by Price and Bishop (1974). They are largely complementary, describing different features of an irregular sea. The spectral approach is in terms of its frequency content, and demonstrates clearly the effects of natural frequency response. The probabilistic approach is concerned with the number of times given stress or response levels are exceeded, and is thus relevant to fatigue life.

Corresponding to the two alternative design philosophies, there are two different kinds of wave theory. The design wave approach requires a train of very large regular waves. Several nonlinear wave theories are suitable for this purpose: some analytic and others numerical. Spectral methods on the other hand, can model the frequency and directional content of sea waves. These models are usually based on linear (Airy) wave theory, and can represent irregular multidirectional seas by linear superposition. This method is obviously well suited for frequency domain analysis.

## 5.2 Ocean Waves

### 5.2.1 Introduction

Standing on the coast and looking at the sea surface, waves with a period of several seconds continuously arriving from offshore may be observed. Several hours later, standing again at the same place, it may be recognized that the shoreline has changed its position landward or seaward. This is caused by a variation of the mean sea level, which is mainly due to tidal motion. The waves first cited above are short period waves, while tidal waves are long period waves. Besides these waves, other waves with differing periods are generated in numerous ways in the sea.

In order to describe the size of these waves, the wave height  $H$  and wavelength  $L$  are usually employed as shown in Figure 5.1. Wave height is defined as the vertical distance between a crest and a trough of the wave train in question, while wave length is defined as the horizontal distance between successive wave crests or wave troughs. Another characteristic measure of waves is the wave period,  $T$ , which is defined as the time required for two successive wave crests to pass a fixed measuring point. Wave speed or wave celerity,  $C$ , is the speed at which a wave travels, so that the relationship  $C = L/T$  is obtained. The dimensionless ratio commonly used to express wave profile characteristics is the wave steepness, defined as  $H/L$ .

Ocean waves have a very wide range of periods. The energy of waves of fixed period is proportional to  $H^2$ . Figure 5.2 is a diagram originally drawn by Munk (1951) which displays the predominant types of waves in the ocean, the names of the various waves for each period range, and the agents generating these waves.

The wave with the shortest period is a capillary wave; it has a wave period of less than 0.07 seconds, wavelength of less than 2/3 inch, and a maximum height of 4/10 to 8/10 inch. Because surface tension

is the main restoring force of this wave motion, these waves are called capillary waves. The restoring force of waves with a period larger than that of capillary waves is gravity; thus such waves are called gravity waves.

As shown in Figure 5.2, waves of the greatest energy concentration are wind waves. Wind waves are generated and developed by wind action, and their wave period is normally less than 10 to 15 seconds, while heights of as much as 112 feet have been reported. Swells consist of wind-generated waves that have traveled out of their generating area. Swells are characterized by a rather more regular and longer period than that of wind waves.

Examples of some longer waves are surface oscillations in a harbor basin (secondary harbor oscillation); tsunamis, generated by either submarine earthquakes or the eruption of a submarine volcano (the period being several minutes to about one hour); storm surges, generated in a rather large-scale bay by such meteorological disturbances as typhoons, hurricanes, and so on; and astronomical tides. These long period waves play an important role in the preservation and exploitation of coastal zones, as well as in disaster prevention.

This section deals mainly with short period waves.

### 5.2.2 Classification of Waves

Muga and Wilson (1970) state that of all the forces induced by the ocean environment, those due to surface gravity waves are the most important and at the same time the most difficult to determine.

To the uninitiated, the large number of "wave theories" discussed in the literature, all arranged according to various classification schemes which overlap and merge into one another, would appear to be about as unordered as actual ocean waves are to the first-time

observer. As a matter of fact, there are several classification schemes of wave theories which serve various useful purposes but when applied indiscriminately can be misleading. The problem is simply the lack of a unified comprehensive classification scheme of water wave theories. To illustrate, we have rotational and irrotational, long-crested and short-crested, finite periodic wave theories. The latter presumably include the oscillatory and translatory wave classification scheme. In addition, we have a numerical wave theory which includes at least two evaluation procedures. We have seen a classification of waves by wave period in the previous section.

From a physical point of view, gravity water waves can be considered as being free (swell) or forced (sea). Swell waves are sea waves which have moved beyond the influence of the generating wind.

It is useful to classify waves as being either long-crested or short-crested. The essential distinction is that long-crested waves are waves whose crests extend infinitely far in the direction normal to the direction of wave propagation and that the crests coincide with a level surface. This permits the wave profile to be represented in a two-dimensional vertical plane in the direction of wave propagation, since any vertical plane is identical to any other parallel vertical plane. On the other hand, short-crested waves are waves whose crests do not coincide with a "level" surface. Thus, the crests may be considered to be of finite length.

Long-crested waves are sometimes called unidirectional waves to distinguish them from short-crested (directional) waves. Long-crested waves may be either deterministic (sometimes called regular) or non-deterministic (sometimes called random) while short-crested waves are basically random with a defined directional distribution. Muga and Wilson (1970) point out the salient features with the short-crested waves as follows:

- o In a sense all waves generated in the ocean are short-crested since crest lengths are finite.
- o As the short-crested waves propagate, they tend to become long-crested since there is a flow of energy along the crests (normal to the direction of wave advance).
- o The wave celerity,  $C$ , is greater for short-crested waves than for long-crested waves of the same wavelength  $L$  in the same water depth.

Waves may be further classified as being either periodic (oscillatory), aperiodic, or translatory, as shown in Table 5.1 below. Note that short-crested waves are considered as belonging to the class of periodic waves. All other wave types listed in the table are long-crested waves. In addition to the solitary wave, the most important translatory waves are those generated by the tides, floods and seismic effects.

The recently developed numerical wave theories describe surface disturbances which can belong to either class depending on the boundary conditions.

Table 5.1 Classification of Wave Theories

<u>Periodic</u>	<u>Numerical</u>	<u>Translatory</u>
(a) Short-Crested Waves	(a) Periodic Stream Function	(a) Solitary Waves
(b) Airy Linear Waves	Chappellear	(b) Various Long Waves including Tidal
(c) Gerstner-Rankine (Trochoidal) Waves	EXVP, etc.	Waves and Flood
(d) Stokes Finite Amplitude Waves	(b) Aperiodic	Waves
(e) Cnoidal Waves	Random	

Discussion of the various wave theories requires some theoretical background about irrotational flow and potential theory. A full



treatment of these subjects is beyond the scope of this report. However, since the subject of irrotational or potential flow will be encountered repeatedly in the following sections, a brief discussion of some of the basic concepts is presented.

### 5.2.3 Real Versus Perfect Fluids

The velocity of flow for most engineering problems in fluid dynamics is of primary concern. If application involves flow past structural members, a knowledge of the velocity allows pressures and subsequently forces acting on the structures to be calculated. The information is then used in the analysis and design of the structure. Therefore the velocity and pressure constitute the two fundamental unknowns of the fluid flow problem.

Most theoretical investigations in the field of fluid dynamics are based on the concept of a perfect, i.e. frictionless and incompressible fluid. In the motion of such a perfect fluid, two contacting layers experience no tangential forces (shearing stresses) but act on each other with normal forces (pressures) only. This is equivalent to stating that a perfect fluid offers no internal resistance to a change in shape. The theory describing the motion of a perfect fluid is mathematically very far developed and supplies in many cases a satisfactory description of real motions, such as e.g. the motion of surface waves. On the other hand the theory of perfect fluids fails completely to account for the viscous drag of a body in a fluid. In this connection it leads to the statement that a body which moves uniformly through a fluid which extends to infinity experiences no drag (d'Alembert's paradox).

This unacceptable result of the theory of a perfect fluid can be traced to the fact that the inner layers of a real fluid transmit tangential as well as normal stress, this being also the case near a solid wall wetted by a fluid. These tangential or friction forces in a real fluid are connected with a physical property of the fluid,

called viscosity.

The existence of tangential (shearing) stresses and the condition of no slip near solid walls constitute the essential differences between a perfect and a real fluid.

For a perfect fluid the density is usually taken to be invariant, while surface tension and other fluid properties are neglected.

In the absence of viscosity, vorticity does not appear, and the motion is irrotational (see Schlichting, 1968). Irrotationality is a property of the flow and it is a direct consequence of the absence of viscosity which is a fluid property (Batchelor, 1967).

#### 5.2.4 Rotational and Irrotational Flow

Whether or not a representative fluid element tends to rotate during translation from point to point serves as a distinction between two types of motion. If the velocity distribution is such that the angular rotation of a fluid particle about its mass center is zero, then the flow is said to be irrotational. This does not mean that the fluid element cannot deform during its motion, but only that it cannot rotate. Note that this is a direct consequence of the absence of the viscosity in the fluid.

Mathematically speaking, a rotation vector for fluid particle  $p$  can be described in a convenient system of coordinates (see Figure 5.3). The component of this rotation vector about the  $z$ -axis is defined as

$$\Omega_z = \frac{1}{2} \left( \frac{\partial v}{\partial x} - \frac{\partial u}{\partial y} \right) \quad (5.1)$$

The two other components of the rotation vector about x and y axis are defined by

$$\Omega_x = \frac{1}{2} \left( \frac{\partial w}{\partial y} - \frac{\partial v}{\partial z} \right) \quad (5.2)$$

$$\Omega_y = \frac{1}{2} \left( \frac{\partial u}{\partial z} - \frac{\partial w}{\partial x} \right) \quad (5.3)$$

Therefore, the irrotational flow may be defined as the absence of rotation at every point in the fluid. That is

$$\Omega_x = \Omega_y = \Omega_z = 0 \quad (5.4)$$

or

$$\frac{\partial w}{\partial y} = \frac{\partial v}{\partial z} \quad (5.5)$$

$$\frac{\partial u}{\partial z} = \frac{\partial w}{\partial x} \quad (5.6)$$

$$\frac{\partial v}{\partial x} = \frac{\partial u}{\partial y} \quad (5.7)$$

The above expressions are the Euler's conditions of irrotationality.

### 5.2.5 Velocity Potential, Stream Function and Bernoulli Equation

#### o Velocity Potential

Irrotational motion exists only when all components of the rotational vector are equal to zero. It is then possible to define a continuous, differentiable, scalar function  $\phi = \phi(x, y, z, t)$  such that its gradients satisfy the Euler's condition of irrotationality automatically. Therefore, it is possible to define components of the fluid particle velocity vector  $\bar{q}$  (u, v, w) as follows:

$$\bar{q} = \text{grad } \phi \quad (5.8)$$

or

$$u = \frac{\partial \phi}{\partial x} \quad (5.9)$$

$$v = \frac{\partial \phi}{\partial y} \quad (5.10)$$

$$w = \frac{\partial \phi}{\partial z} \quad (5.11)$$

Replacing the velocity by its potential may first seem an unnecessary complication, since we can envisage the velocity and measure it with suitable instruments in the laboratory, whereas the velocity potential is no more than a mathematical abstraction. However, the velocity is a vector quantity with three unknown scalar components, whereas the velocity potential is a single scalar unknown from which all three velocity components may be computed.

With the introduction of the velocity potential, the problem is reduced to finding the velocity potential  $\phi$  and pressure  $p$  in accordance with the momentum equations and the equation of continuity.

The principle of conservation of mass is mathematically stated as the equation of continuity. This equation for an incompressible flow has the form

$$\frac{\partial u}{\partial x} + \frac{\partial v}{\partial y} + \frac{\partial w}{\partial z} = 0 \quad (5.12)$$

Substituting Equations (5.9), (5.10), and (5.11) into Equation (5.12) one obtains

$$\nabla^2 \phi = \frac{\partial^2 \phi}{\partial x^2} + \frac{\partial^2 \phi}{\partial y^2} + \frac{\partial^2 \phi}{\partial z^2} = 0 \quad (5.13)$$

This is the Laplace equation from which the velocity potential is to be determined. The solution to this equation with appropriate boundary conditions defines completely the irrotational flow field. The solutions to the Laplace equation are known as harmonic functions. The direct determination of harmonic functions which satisfies all the given boundary conditions is often a difficult problem. Intuition, heuristic reasoning, experience, and numerous methods must be called upon not only to obtain a solution but also to ascertain that the solution based on the inviscid-fluid assumption is a reasonable approximation to the actual behavior of the fluid.

o Stream Function

Sarpakaya and Isaacson (1981) define Lagrange's stream function (first introduced by d'Alembert) as a scalar quantity which describes not only the geometry of a two-dimensional flow but also the components of the velocity vector at any point and the flow rate between any two streamlines. Thus for a flow from left to right (see Figure 5.4) the velocity components are defined as

$$u = \frac{\partial \psi}{\partial y} \quad (5.14)$$

$$v = - \frac{\partial \psi}{\partial x} \quad (5.15)$$

The definition of stream functions does not require that the motion be irrotational. In other words  $\psi$  exists irrespective of whether the flow is rotational or irrotational, as long as it is continuous. However, only for an irrotational flow the stream function satisfies the Laplace equation such that

$$\nabla^2 \psi = 0 \quad (5.16)$$

The stream functions for an irrotational two-dimensional flow are orthogonal to the potential functions.

The Bernoulli equation is a mathematical representation of the principle of conservation of momentum. The equation for an unsteady, irrotational flow has the form

$$\frac{q^2}{2} + \frac{p}{\rho} + gh + \frac{\partial \phi}{\partial t} = f(t) \quad (5.17)$$

where  $q = u^2 + v^2 + w^2$  is the velocity,  $p$  is the pressure,  $g$  is the gravitational acceleration,  $\rho$  is the fluid mass density,  $h$  is the elevation from a reference point, and  $f(t)$  is an arbitrary function of time. Frequently, the  $f(t)$  is absorbed into  $\phi$  since this does not affect the physical quantities of interest. The Bernoulli equation describes the relationship between the two principal unknowns of the flow field,  $q$  and  $p$ . Once the velocity is obtained from the equation of continuity (Laplace equation), the pressure can be found from the Bernoulli equation. The integration of this pressure over the submerged areas of the structure results in the forces needed for analysis and design of the structure under consideration.

This brief mathematical background was necessary in order to discuss various wave theories that will be presented in the following sections.

#### 5.2.6 Wave Theories

The full treatment of all wave theories is beyond the scope of this report. However, in the following sections a brief introductory description of some of the most important wave theories is given. Some texts which outline the development and results of wave theories

include those by Lamb (1945), Stoker (1957), Wehausen and Laitone (1960), Wiegel (1964), Kinsman (1965), Ippen (1966), Milne-Thompson (1968), Silvester (1974), Whitham (1974), LeMehaute (1976), Phillips (1977), Horikawa (1978), LeBlond and Myask (1978), Sorenson (1978), Sarpkaya and Isaacson (1981) and Dean and Dalrymple (1984).

It is necessary at this time to define the coordinate system and the terminology that will be used in the development of wave theories. Figure 5.1 shows the coordinate system (x, y, z) with x measured in the direction of wave propagation, z measured upwards from the still water level and y orthogonal to x and z. It is assumed that the waves are two-dimensional in the x-z plane, that they are progressive in the positive x direction and that they propagate over a smooth horizontal bed in water of constant undisturbed depth d. We further assume that the wave maintains a permanent form, that there is no underlying current and that the free surface is uncontaminated. The fluid (water) is taken to be incompressible and inviscid and the flow to be irrotational. Figure 5.1 also indicates the general form of a wave train conforming to these assumptions. Here the following definitions hold:

d	=	distance from MWL to bottom
$\eta(x,t)$	=	instantaneous vertical displacement of sea surface above MWL
A	=	amplitude of wave
H	=	height of wave (= 2A for small amplitude wave theory)
L	=	wave length
T	=	wave period
C	=	speed of wave propagation (phase speed, phase velocity, celerity, = $L/T = \omega/k$ )
k	=	wave number (= $2\pi/L$ )
$\omega$	=	wave angular frequency (= $2\pi/T = 2\pi f$ )
f	=	wave frequency (= $1/T$ )
MWL	=	mean water level

Any particular wave train is generally specified by the quantities H, L and d or by H, T and d, and the objective of any wave theory is to determine C (and therefore T or L as appropriate) and a description of the water particle motions throughout the flow. Dimensionless parameters are frequently used to characterize a wave train. The wave height is often expressed in terms of  $H/gT^2$ , the wave steepness H/L or the relative height H/d. The water depth is often expressed in terms of the depth parameters  $d/gT^2$  or kd or the relative depth d/L. For steeper waves in shallow water the Ursell number  $U = HL^2/d^3$  is often used. Thus a design wave specified by H, T and d may conveniently be characterized, for example, by the parameters  $H/gT^2$  and  $d/gT^2$ .

The velocity potential  $\phi$  pertaining to the fluid region needs to be determined. This satisfies the Laplace equation

$$\frac{\partial^2 \phi}{\partial x^2} + \frac{\partial^2 \phi}{\partial z^2} = 0 \quad (5.18)$$

and will be subject to the boundary conditions

$$\frac{\partial \phi}{\partial z} = 0 \quad \text{at } z = -d \quad (5.19)$$

$$\frac{\partial \eta}{\partial t} + \frac{\partial \phi}{\partial x} \frac{\partial \eta}{\partial x} - \frac{\partial \phi}{\partial z} = 0 \quad \text{at } z = \eta \quad (5.20)$$

$$\frac{\partial \phi}{\partial t} + \frac{1}{2} \left[ \left( \frac{\partial \phi}{\partial x} \right)^2 + \left( \frac{\partial \phi}{\partial z} \right)^2 \right] + g\eta = f(t) \quad \text{at } z = \eta \quad (5.21)$$

$$\phi(x, z, t) = \phi(x - Ct, z) \quad (5.22)$$

where  $\eta(x, t)$  is the free surface elevation measured above the still water level  $z = 0$ .

The existence of the velocity potential  $\phi$  and the validity of the Laplace equation follow from the assumptions of an irrotational flow



and an incompressible fluid. Equation (5.19) corresponds to the boundary condition at the seabed which imposes a zero vertical component on the fluid particle velocity at the seabed. Equations (5.20) and (5.21) represent the kinematic and dynamic free surface boundary conditions respectively. The former describes the condition that the fluid particle velocity normal to the free surface is equal to the velocity of the free surface itself in that direction, while the dynamic condition states that the pressure at the free surface, expressed in terms of the Bernoulli equation, is constant. This latter requirement follows from the assumptions that the atmospheric pressure (immediately above the fluid) is itself constant and that the free surface is uncontaminated (corresponding to a surface tension that may be taken as zero). Equation (5.22) describes the periodic nature of the wave train. In the absence of an underlying current the waves are progressive with a celerity  $C$  and are of permanent form: the dependence of variables of interest upon  $x$  and  $t$  may consequently be written in terms of dependence upon a single variable  $(x - Ct)$ .

Of course some of the assumptions made in order to establish Equations (5.18) through (5.22) are seldom justified. Perhaps the most severe are the assumptions that there is no underlying current, that the depth is constant and that the wave train is two-dimensional and of permanent form. On the other hand, the irrotationality assumption is generally found to be reasonable outside the (thin) boundary layers at the seabed and free surface. For the present, then, we continue to examine the formulation of wave theories on the basis of all the aforementioned assumptions.

In some cases, where it is convenient to specify that the incident wave direction makes an angle  $\alpha$  with the positive  $x$  axis, we have merely to replace  $x$  by  $(x \cos \alpha + y \sin \alpha)$  in any results that are obtained.

### 5.2.7 Airy Waves

Two serious difficulties arise in the attempt to obtain an exact solution for a two-dimensional wave train. The first is that the free-surface boundary conditions are nonlinear, and the second is that these conditions are prescribed at the free surface  $z = \eta$  which is initially unknown. The simplest and most fundamental approach is to seek a linear solution of the problem by taking the wave height  $H$  to be very much smaller than both the wave length  $L$  and the still water depth  $d$ : that is  $H \ll L, d$ . The wave theory which results from this additional assumption is referred to alternatively as small amplitude wave theory, linear wave theory, sinusoidal wave theory or as Airy theory. Because of the assumption that  $H \ll L, d$ , the nonlinear terms in Equations (5.20) and (5.21), which involve products of terms of order of the wave height (expressed in a suitably dimensionless form), are than negligible in comparison with the remaining linear terms which are themselves of the order of the wave height. Furthermore, the free-surface boundary conditions may now be applied directly at the still water level  $z = 0$ .

For small amplitude waves, the free-surface boundary conditions as expressed in Equations (5.20) and (5.21) reduce to

$$\frac{\partial \phi}{\partial z} - \frac{\partial \eta}{\partial t} = 0 \quad \text{at } z = 0 \quad (5.23)$$

$$\frac{\partial \phi}{\partial t} + g\eta = 0 \quad \text{at } z = 0 \quad (5.24)$$

which may be combined to give

$$\frac{\partial^2 \phi}{\partial t^2} + g \frac{\partial \phi}{\partial z} = 0 \quad \text{at } z = 0 \quad (5.25)$$

$$\eta = -\frac{1}{g} \left( \frac{\partial \phi}{\partial t} \right)_{z=0} \quad (5.26)$$

Bearing in mind the periodicity condition given by Equation (5.22), the solution to the problem may be obtained by a separation of variables technique.

With these boundary conditions the velocity potential will be obtained as

$$\phi = \frac{\pi H}{kT} \frac{\cosh(ks)}{\sinh(kd)} \sin \theta \quad (5.27)$$

where

$$\theta = k(x - Ct) = kx - \omega t \quad (5.28)$$

$$s = z + d \quad (5.29)$$

In the way to obtain velocity potential  $\phi$  another important equation is found in which the  $C$  or  $\omega$  is related to  $k$ . This is the linear dispersion relation defined as

$$\omega^2 = gk \tanh(kd) \quad (5.30)$$

or

$$C^2 = \frac{g}{k} \tanh(kd) \quad (5.31)$$

This equation describes how the wave speed increases with wave length. More generally, the dispersion relation for a finite amplitude wave train,  $C$  in terms of  $k$ , involves also the wave height  $H$  and may be developed according to any particular wave theory.

Once the velocity potential is obtained the two fundamental unknowns of the flow field, namely velocity and pressure along with other parameters of interest, may be evaluated.

The velocity components  $u$  and  $w$  can be found from

$$u = \frac{\partial \phi}{\partial x} \quad (5.32)$$

$$w = \frac{\partial \phi}{\partial z} \quad (5.33)$$

The pressure  $p$  is given by the linearized form of the unsteady Bernoulli equation, Equation (5.17), in which the nonlinear terms are omitted in accordance with the present linear approximation,

$$p = -\rho g z - \rho \frac{\partial \phi}{\partial t} \quad (5.34)$$

The results of linear wave theory, taken from Sarpkaya and Isaacson (1981), are presented in Table 5.2.

It is useful to note that depending upon the relative measure of water depth and wave length two extreme conditions of shallow and deep water can be described. The parameter  $kd$  specifies the ranges over which certain approximations are applicable.

The shallow and deep water ranges correspond to  $kd < \pi/10$  and  $kd > \pi$  respectively, and over these ranges approximate expressions may be substituted for the hyperbolic functions used to obtain flow field velocities.

$$\begin{aligned} \sinh(kd) &\approx \tanh(kd) \approx kd \\ \cosh(kd) &\approx 1 \end{aligned} \quad \text{for } kd < \pi/10$$

$$\begin{aligned} \sinh(kd) &\approx \cosh(kd) \approx \frac{1}{2} e^{kd} \\ \tanh(kd) &\approx 1 \end{aligned} \quad \text{for } kd > \pi$$

Substituting these into the results of Table 5.2, we obtain the simplified expressions that are summarized in Table 5.3. The complete range of water depths, then, is conveniently divided into

the shallow water, intermediate water and deep water ranges as follows:

shallow water waves:  $\frac{1}{20} > \frac{d}{L}; \quad 0.0025 > \frac{d}{gT^2};$

intermediate depth waves:  $\frac{1}{20} < \frac{d}{L} < \frac{1}{2}; \quad 0.0025 < \frac{d}{gT^2} < 0.08;$

deep water waves:  $\frac{d}{L} > \frac{1}{2}; \quad \frac{d}{gT^2} > 0.08.$

These limits in terms of  $d/gT^2$  are equivalent to those given in terms of  $d/L$  by the application of the dispersion relation.

Bearing these approximations in mind, we see that the expressions for the water particle displacements  $\xi$  and  $\zeta$  indicate that the particles travel in closed elliptic orbits as sketched in Figure 5.5. The amplitude of horizontal velocity (and displacement) decreases with depth according to  $\cosh(k(z+d))$ , while the amplitude of vertical velocity (and displacement) decreases according to  $\sinh(k(z+d))$ . Typical profiles relating to the shallow, intermediate and deep water ranges are sketched in Figure 5.5. Note that at intermediate depths the orbits diminish in amplitude with depth and also become flatter until the vertical component vanishes at the seabed in accordance with the seabed boundary condition; and also that the velocity and acceleration vectors at a given point and time are not collinear. In the shallow water range the elliptic orbits are relatively flat at all depths and diminish in amplitude only gradually with depth. In deep water the particle motions are circular, the amplitude of motion decreasing exponentially with depth, until at  $z=-L/2$  this amplitude is only 4 percent [i.e.  $\exp(-\pi)$ ] of its value at the still water level. Thus the wave-induced motion may conveniently be considered to penetrate up to a depth of half a wavelength below the free surface.

The linear wave theory (Airy) has been treated in some detail because of its importance in mathematical development of the potential flow theory and its application to the motion analysis of floating structures. Development of linear wave theory underlines the difficulties in dealing with the boundary conditions and assumptions required to overcome these difficulties.

The Airy waves cannot represent all the sea conditions that can occur in the real ocean.

According to Longuet-Higgins (1956), as quoted by Wiegel (1964), linear theory is valid if the Ursell number  $L^2H/d^3 \ll 100$  and the wave steepness  $H/L$  are small. Outside this range, however, linear theory may still be preferred because of its simplicity, because it behaves stably and describes physical processes quite well over a wide range of conditions, and because it can be readily extended to model irregular multidirectional seas and wave diffraction.

#### 5.2.8 Empirical Modification of the Airy Wave Theory

In Section 5.2.7 the Airy wave theory and inherent assumptions in its development were presented. One of the major simplifications introduced was the assumption of small amplitude of the wave with respect to the wave length and water depth. This assumption allowed the free surface boundary conditions to be satisfied at mean water level instead of being satisfied at the time varying and unknown wave free surface. Therefore, the water particle velocity and acceleration profiles needed for evaluation of wave forces are evaluated up to the mean water level only. However, in some applications where wave heights are considerable designers have modified the Airy wave theory to evaluate water particle velocity and acceleration up to the instantaneous wave surface elevation. Two approaches are widely used, namely "extended method" and "stretch method".

In the extended method the  $(s)$  appearing in the water particle velocity and acceleration (Table 5.2) is extended up to the instantaneous water surface elevation. The water particle velocity profile that results from application of this method is shown in Figure 5.6a. This approach was originally adopted by Ried (1958) in connection with his work on the correlation of water level variations with wave forces on a vertical pile.

In the stretch method the  $(s)$  in the water particle velocity and acceleration expressions is substituted by  $(sd)/(n+d)$ . This may be regarded as an effective height at which the force is to be evaluated. Thus effective height will always be less than mean water level. It bears the same ratio to mean water level that the actual height  $(s)$ , bears to the surface elevation above bottom at the time point for which calculations are being made. A velocity profile evaluated under the crest by application of this method is presented in Figure 5.6b. This method was adopted by Wheeler (1970) in his work on the method for calculating forces produced by irregular waves.

Both methods present some drawbacks. The extended method usually overestimates wave loads at the evaluations above mean water level. The stretch method is sensitive to the hydrodynamic model used in the response analysis. For example, in a lumped area and volume hydrodynamic model a negative mean displacement of the motion may be obtained in contrast to the experimental observation (Rajabi and Mangiavacchi, 1984).

A third method which is not in widespread use is the "hanging profile" or "floating profile" method. In this method the vertical coordinate is measured from the instantaneous free surface, directly above the point at which the kinematics are calculated. The result is a surface particle velocity at trough equal and opposite to that at the crest. The velocity and accelerations obtained by this method are very close to those obtained from the stretch method. The major difference between the stretch method and the floating profile method

lies in the fact that in the stretch method the velocity and acceleration profiles are stretched up under the crest and are compressed down under the trough, while in the floating profile method the velocity and acceleration profiles hang from the wave surface and the vertical coordinate is measured from the instantaneous free surface in their evaluation.

In summary, the present state of practice is to deploy the extended method for regular wave application and the stretch method in connection with the random wave simulation.

#### 5.2.9 Higher-Order Wave Theories

We have just seen that the waves derived from linearized equations on the assumption of the relative smallness of the parameters  $H/d$  and  $H/L$  compared to unity had the following properties:

- o The particle orbits were closed,
- o The shape of the surface profile was sinusoidal, and
- o There was no net displacement of the particle.

These facts were noted to be in disagreement with observations. If the amplitude of the surface disturbance is not required to be small relative to the length of wave or depth of water, then this category of waves is called finite amplitude waves. In what follows some of the most important finite amplitude theories of waves will be briefly described. The finite amplitude waves are nonlinear. For a horizontal bottom the source of the nonlinearity lies in the two free surface boundary conditions.

The results of Airy waves are valid for all ranges of the relative depth  $d/L$ . However, in finite amplitude wave theories both parameters  $H/d$  and  $H/L$  are important. Due to formidable mathematical difficulties, it has been found impossible to derive a comprehensive theory for all values of these parameters. The approach has been to



develop a theory valid for finite values of one of these parameters while regarding the other as small. In shallow water the important parameters turn out to be  $H/d$  and  $d$  while in deeper water they are  $H/L$  and  $L$ . For the shallow water case, cnoidal and solitary wave theories have been derived. For the intermediate water case the Stokes theory of various orders, the first order of which corresponds to the linear or Airy wave theory, has been developed. Cnoidal waves are considered to act as the separator between the other two. A comparison has been made between Cnoidal and Stokes waves by De (1955) in which he showed that the Stokes theory (to the fifth order) should not be used for  $d/L$  less than about 0.125, the minimum value depending upon the value of  $H/L$ , with greater values of  $H/L$  resulting in a greater value of  $d/L$  at which the theory of Stokes becomes unreliable.

In a broad sense the analytic nonlinear wave theories include two different types of series solution:

- o The Stokes series, in power of wave steepness  $H/L$ , which is valid in intermediate to deep water conditions (approximately  $L^2 H/d^3 < 26$ ),
- o The cnoidal series, in powers of  $H/d$  (the ratio of wave height to water depth), which is valid in shallow water conditions.

#### 5.2.10 Stokes Waves

The method used by Stokes (1847, 1880) and subsequently by many other investigators was to expand the velocity potential into a power series about the still water level. Thus a nonlinear surface condition for the potential on the plane of still water level is obtained. This consists of an infinite series containing partial derivatives of the potential. The solution is obtained by successive approximations. Stokes applied the perturbation method to the solution. By the perturbation method we mean that we can express the

solution in an expanded form where the unknowns are written in power series in a small parameter. In this case it is assumed that potential  $\phi$  and associated variables ( $\eta$ ,  $u$ ,  $w$ , ...) may be written in the form

$$\phi = \epsilon \phi^{(1)} + \epsilon^2 \phi^{(2)} + \epsilon^3 \phi^{(3)} + \dots \quad (5.35)$$

in which  $\epsilon$  is the perturbation parameter. By substituting Equation (5.35) into the governing equation (Laplace equation and boundary conditions presented in Section 5.2.6), it is possible to obtain successively higher order solutions, each expressed in terms of the preceding ones.

The number of terms contained in Equation (5.35) and associated variables also define the order of the wave theory. It is interesting to note that the governing equations of the first (linear) approximation are precisely those that were obtained previously in connection with the Airy wave theory. For example, when we refer to the fifth order Stokes waves that implies that terms up to  $\phi_5$  are included in deriving the solution. The solutions require a great amount of detailed calculations of coefficients. Stokes presented only the second order wave theory. However, the method has been carried in detail to higher orders. Skjelbreia (1958) obtained tables for third order Stokes waves. Skjelbreia and Hendrickson (1960) have presented the Stokes wave theory to the fifth order and their approach has found widespread usage in engineering practice. Bretschneider (1960) expanded the method, in principle, to any order.

According to Peregrine (1972), the Stokes wave expansion method is formally valid under the conditions  $H/d \ll (kd)^2$  for  $kd < 1$ , and  $H/L \ll 1$ . These conditions place a severe wave height restriction in shallow water and a separate shallow water wave expansion procedure may then be used.

According to Schwartz, (1974) the Stokes series becomes nonconvergent in very steep (near-breaking) waves, and diverges rapidly if  $HL^2/d^3$  is large (see Fenton, 1979). Therefore the Stokes waves should not be used to model steep shallow water waves. Cnoidal theory is largely complementary in its range of validity, but again diverges rapidly in steep intermediate to deep-water wave conditions.

#### 5.2.11 Cnoidal Waves

The lower order Stokes finite amplitude wave theories just described are generally inadequate in the shallow water range since many coefficients of the higher order terms then "blow up": that is they become excessive relative to the lowest order terms. Laitone (1961) has investigated the range of validity of Stokes third order wave theory on a theoretical basis, and suggests that it is most suitable for wave lengths less than about 8 times the depth ( $kd > 0.78$ ). For longer waves a different procedure is appropriate if the effects of finite wave height are to be investigated, and to this end nonlinear periodic wave theories suitable for shallow water have been developed since the last century.

The fundamental theory, termed the cnoidal wave theory, was first developed on an intuitive basis by Korteweg and De Vries (1895). According to this theory the wave characteristics are expressed in terms of the Jacobian elliptic function  $cn$  and hence the terminology "cnoidal wave theory" is used. A typical cnoidal wave profile is sketched in Figure 5.7a. One limiting case of this, in which the wavelength becomes infinite, corresponds to the solitary wave, whose profile is sketched in Figure 5.7b. Another limiting case corresponds to shallow water sinusoidal wave theory, with a wave profile as sketched in Figure 5.7c. Wiegel (1960, 1964) has given a summary of the first approximation that is directed towards engineering applications. Laitone (1961) and Chappellear (1962) have developed respectively second and third order approximations to cnoidal wave theory, the latter involving a numerical procedure

rather than explicit formulae. More recently, Fenton (1979) has presented a cnoidal wave theory which is capable of extension to any desired order, and which is readily suited to engineering applications. Details of the theory to the fifth order have been given by him.

The two nonlinear wave models described previously share a number of common features, which distinguish them from the linear solution. They can be described briefly as follows:

- o the nonlinear wave crests are peakier, and the troughs flatter. Particle velocities are greater at the crest than at the trough, and the maximum horizontal acceleration occurs nearer the crest;
- o the mean hydrodynamic pressure is nonzero. There may be an associated change in mean water level (set-down) as described by Longuet-Higgins and Stewart (1964), or mean uplift force on a bottom-mounted structure (see Lighthill, 1979);
- o fluid particle orbits are not closed, and there is a general drift of fluid in the direction of wave travel;
- o the nonlinear wave is longer, and travels faster, than a linear wave with the same period.

#### 5.2.12 Other Wave Theories

Additional wave theories that will be briefly described here include the Gerstner trochoidal theory, solitary wave theory, and long wave theory.

The trochoidal theory is largely of historic interest even though it has been applied to engineering problems to a limited extent. The trochoidal wave theory was introduced by Gerstner (1802) and has been adequately described by Milne-Thompson (1968). This theory differs

from most other finite amplitude wave theories in that it depends on a rotational fluid motion and also in that the solution is an exact one under the assumptions made.

The solitary wave is a translatory wave in which the surface lies wholly above the mean water level (see Figure 5.7b). It was first studied in the laboratory by Russel in the 1840's. It is a single, shallow water wave of apparently permanent form which can travel considerable distances with little attenuation. It can be regarded as a limiting case of periodic shallow water waves of finite height (cnoidal waves) if the period or wavelength is stretched out indefinitely as the relative height  $H/d$  is held constant.

The long wave theory has application to tsunami propagation, tidal motion, storm surge, flood waves and the like.

The linearized long wave theory is developed from the basic assumptions that, firstly, the wave height is small so that all nonlinear terms in the governing equations may be neglected, and, secondly, that the wave length is much larger than the water depth so that the vertical particle acceleration may also be neglected. It follows from these two requirements that the horizontal particle velocity is invariant with depth and the pressure is hydrostatic. These simplifications prove most useful in obtaining solutions by numerical methods for unsteady flows and/or flows with complex boundaries. More detailed outlines are given by Stoker (1957) and by Le Mehaute (1976).

### 5.2.13 Numerical Wave Theories

The analytical wave theories discussed up to now satisfy the  $N$ th order boundary conditions on the  $(N-1)$ th order wave form. Some of the numerical wave theories permit the free surface boundary condition for the  $N$ th order solution to be applied to the  $N$ th order water surface. The most prominent among these numerical wave

theories is the stream function theory.

Dean (1965) introduced a numerical method for predicting two-dimensional wave characteristics which is based on a stream function representation of the flow and which has since attained fairly widespread application. This approach somewhat supercedes a not dissimilar technique proposed earlier by Chappellear (1961) and which was based instead on a velocity potential representation. The approach adopted by Dean is capable of generalization and affords a solution where a free surface pressure distribution and uniform current are also prescribed.

In some circumstances numerical models have advantage over purely analytic solutions. Stream function theory is based on a Stokes-type series expansion, in which the dynamic free surface boundary condition is satisfied numerically by a least-square. The kinematic free surface boundary condition is satisfied exactly. This solution can be extended readily to any order, and has a wider range of validity than the similar Stokes model. Aagaard and Dean (1969) used stream function theory to model unsymmetric wave forms. Von Schwind and Reid (1972) and Fenton (1979) have also published some formulations of stream function waves. Dalrymple (1974) has extended the stream function theory to permit simulation of stream function waves on a shear current. Mention should also be made of the somewhat related extended velocity potential method (sometimes termed the EXVP method) described by Lambrakos and Brannon (1974). The method was developed to enable treatment of arbitrary wave profiles which may vary in shape during propagation, or which may have a separately specified crest elevation to wave height ratio. This procedure involves a double Fourier series expansion of the velocity potential. The unknown Fourier coefficients are determined by a least square minimization technique applied to the free surface boundary conditions and carried out over time in the x direction. The technique is useful to deal with, for example, a series of consecutive waves with independent characteristics.

In closing this section it should be added that several researchers have attempted to obtain solutions to a high degree of accuracy by resorting to digital computers. A complete treatment of this subject is beyond the scope of this report. For a more complete discussion of numerical wave theories the reader is referred to Sarpkaya and Isaacson (1981).

#### 5.2.14 Range of Validity and Selection of Wave Theory

The problem of selecting the most suitable wave theory for a particular application invariably arises in engineering situations. This is difficult to resolve since for specified values of  $H$ ,  $T$  and  $d$  different wave theories might better reproduce different characteristics of interest and there can be no unique answer. However, charts have been developed that may greatly assist in selecting an appropriate wave theory. They depict the domains of the various wave theories. Two dimensionless parameters  $H/gT^2$  and  $d/gT^2$  can be formed from wave characteristics  $H$ ,  $T$  and  $d$ . For a given value of  $d/gT^2$ , there is a maximum value of  $H/gT^2$  at which the wave breaks. These dimensionless parameters may be used to determine which wave theory is applicable to a specific problem.

Dean (1970) has compared several wave theories on a theoretical basis. The criterion he used was the closeness of fit of the predicted motion to the complete problem formulation. Since the Laplace equation and bottom boundary condition are exactly satisfied in all the theories considered, the error of fit to the two nonlinear free surface boundary conditions was used as the criterion of validity. The wave theories examined included linear wave theory, Stokes third and fifth order theories, cnoidal (first and second approximations), solitary (first and second approximations) and the stream function theories. Dean found that the first order cnoidal, the linear, the Stokes fifth order and the stream function theories were generally the most suitable over the ranges indicated in Figure 5.8. He emphasizes, however, that the method used to assess the

theories does not necessarily imply the best overall theory, and he also suggests that this kind of comparison may be biased in favor of the lower order theories.

Le Mehaute (1976) has presented a convenient chart showing the approximate limits of validity of various wave theories as shown in Figure 5.9. It is stressed however that Le Mehaute indicates that this plot is not based on any quantitative investigation and so is somewhat arbitrary. Even so, there is some agreement with Dean's comparison in that for higher waves cnoidal wave theory is recommended for the shallow water range and Stokes high order theory for the deep water range.

The Shore Protection Manual (1977) has a chart recommending the ranges of validity of some of the wave theories most commonly used in design (see Figure 5.10).

All hydrodynamically possible nonbreaking waves are shown in these three figures. Actually there is some overlapping of the regions but in these regions, the different theories yield approximately similar results. The decision on which theory is to be used requires some intuition and experience or judgement. If for the sake of comparison, the same force coefficients were used to evaluate wave loads by applying various wave theories, generally the higher order wave theories predict higher drag forces but not necessarily higher inertia forces. To be specific, if drag force dominates the loading pattern, then a higher order theory is sometimes desirable.

Usually, uncertainties in the establishment of design wave parameters far outweigh the relatively minor differences given by the various wave theories. There is some variation in the value of the breaking wave parameter  $H/d$ , or determination of the maximum wave steepness. The criterion for maximum wave steepness adopted by Stokes and used almost exclusively by others is that "waves break when the particle velocity  $u$  at the crest exceeds the wave celerity  $C$ ". For finite



amplitude waves in deep water, this occurs when the angle between tangents to the water surface profile at the crest is  $120^\circ$ . The maximum wave steepness is thus 0.1418 or  $H/T^2 = 0.875$  (based on wavelength for finite amplitude waves).

#### 5.2.15 Comparison with Experiment

The suitability of one theory over another from a theoretical viewpoint is not necessarily reflected in better agreement with experimental data gathered either in the laboratory or in the field. The suitability of a particular theory depends upon which characteristic is being compared. We briefly report some of the most recent comparisons made with laboratory waves and sea waves.

##### 5.2.15.1 Laboratory Waves

Wiegel (1964) describes several comparisons between wave theories and laboratory measurements. Figures 5.12 and 5.13 show some more recent data. Figure 5.12 shows the horizontal velocity profile deep-water wave ( $H/gT^2 = 0.11$ ,  $d/gT^2 = 0.036$ ). Figure 5.13 shows the horizontal velocity profile below the crest of a shallow-water near-breaking wave ( $H/gT^2 = 7.4 \times 10^{-4}$ ,  $d/gT^2 = 1.3 \times 10^{-3}$ ).

Hogben et al. (1974) have already shown that there are only small differences between linear and Stokes V theories in deep-water conditions typical of a North Sea environment. Figure 5.11 confirms this conclusion, showing also good agreement with Fenton's (1979) stream function theory and experiment.

Nonlinear effects are most apparent in shallow-water conditions, particularly near the free surface. Figure 5.12 shows the Airy, long-wave and Goda's (1964) empirically modified form of linear theory; solitary waves of McCowan (1891) and Boussinesq (1871); first and second order of cnoidal theory; third order cnoidal of Keulegan and Patterson (1940), and lastly the stream functions theory. Some

agree quite well with the experiment; others differ by large amounts. Linear theory is satisfactory well below the free surface. Stokes second-order theory is quite inadequate.

#### 5.2.15.2 Sea Waves

Because these theories are used in design as models of extreme sea waves, it is important to compare them not only with regular laboratory-wave data, but also with irregular waves in the real sea. Several recent experiments have made this possible.

Measurements during tropical storm 'Delia' have been correlated with several wave theories by Forristall et al. (1978). Figure 5.13 shows measured velocities below the crests and troughs of 16 large waves, compared with the predictions of Stokes V theory. Trough velocities were predicted quite well, but crest velocities were generally overpredicted, particularly at this, the highest level. Irregular stream function theory, again representing a periodic wave of constant form, also overpredicted crest velocities. Calculations based on a linear spectral model, however, including both frequency and directional spreading, matched the experiment in terms of both spectral shape and extreme value statistics.

Dean et al. (1979) and Bishop et al. (1980) report measurements on the Ocean Test Structure in the Gulf of Mexico, and UK Christchurch Bay Tower. Both indicate a tendency for nonlinear regular wave theories to overpredict particle velocities, and that better agreement may be obtained using spectral models.

As a final comment, it is of practical importance to have an accurate knowledge of particle velocities and accelerations in steep near-breaking waves, especially in the context of wave force calculations. However, it appears that comprehensive comparisons with experiments under such more extreme conditions are relatively unavailable and thus, in spite of the sophistication of wave theories

that may be employed, uncertainties remain in the prediction of particle kinematics for very steep waves.

From the design viewpoint it is reassuring that the design wave approach is conservative, in the sense that particle velocities are overpredicted. It is clear however, that even in conditions where nonlinear effects are apparent, a linear model, based on the theory of directional spectra, can give more realistic results than a nonlinear, but periodic, unidirectional and constant-form model.

### 5.3 Random Waves

In the foregoing sections, long-crested waves of constant height, period and direction were described. These waves present fairly regular behavior. However, the ambient waves on the surface of the ocean are random. The generating mechanism is, predominately, the effect upon the water surface of wind in the atmosphere. The randomness of ocean waves is subsequently enhanced by their propagation over large distances in space and time. Thus ocean waves must be described in a probabilistic manner. Oceanographers have found that the irregular sea can be described by statistical mathematics on the basis of the assumption that a large number of regular waves having different lengths, directions, and amplitudes are superimposed. It should be emphasized that characteristics of idealized regular waves, found in reality only in laboratories, are fundamental for the description and understanding of realistic irregular seas.

We will consider primarily the basic two-dimensional "irregular sea" as generated by a broad-scoped wind. This means that the wave crests are continuous in a breadth-wise direction, and all waves move in the same forward direction (long-crested waves). Of course, as an actual sea moves outward it spreads sideways, losing height, and thins out progressively as the longer waves in the sea tend to outrun the others. If, in the course of its travel, it also meets waves from

other disturbances coming from different directions, as is usually the case, the "short-crested" confused sea results. Whereas this three-dimensional "confused sea" is more prevalent in nature and is important in evaluating long-range history of the motions of a floating body, the two-dimensional "irregular sea" is considered to have maximal effect on a body situated in it.

Figure 5.14 shows a typical record of an irregular sea taken at a fixed point of the ocean. Clearly if the record is very long it is impractical to keep it in its original form. Methods of condensing the gross details of the wave record are required whereas inevitably, after such a process, much detail will be lost.

The condensations of the real sea state need to have the property of stability. The term stability is used to describe a characteristic which does not change too much if the observation is repeated. For example, suppose two wave recorders were placed in the open sea at a distance of, say, 200 feet apart. The water surface - time history of the two records taken at the same time would be completely different. The sea surface records themselves are unstable. On the other hand, such things as the average wave height, mean square water surface fluctuation, etc. of the two records would be very close to being equal (so long as the records were of reasonable length). Such statistical properties are said to be stable.

Probability densities and distributions of sea surface parameters, together with the spectral (or variance-frequency) distribution of the sea surface, have been found to be concise and useful properties of this process. The spectrum is a form of probability distribution and has very desirable stability characteristics. The spectrum retains much information on wave amplitudes and "periods" but loses all information on phase position. Probability distributions, on the other hand, lose all information on wave periods if "wave height" probabilities are computed or vice versa.

There are various characteristics of interest in a record such as Figure 5.14. The zero up-crossing method is the one generally accepted to obtain these characteristics. This method uses the time when the surface wave profile crosses the zero (still water) level in the upward direction. An individual wave height is defined by the vertical difference between the maximum and minimum levels with adjacent zero up-cross points, and the corresponding wave period is defined by the interval of two crossing points. The following are some of the most important statistical data that can be derived from a wave record.

- o The maximum wave ( $H_{\max}$ ,  $T_{\max}$ ), which corresponds to the maximum height in a given wave group;
- o The one-tenth highest wave ( $H_{1/10}$ ,  $T_{1/10}$ ), which corresponds to the average of the heights and periods of the one-tenth highest waves of a given wave group;
- o The significant wave ( $H_{1/3}$ ,  $T_{1/3}$ ), which corresponds to the average of the heights and periods of the one-third highest waves of a given wave group;
- o The mean wave ( $\bar{H}$ ,  $\bar{T}$ ), which corresponds to the mean wave height and period of a given wave group.

### 5.3.1 Wave Height Distribution

The knowledge of the wave height distribution is of great importance since various valuable information can be derived from this distribution. Oceanographers have found that wave heights of an irregular sea follow a Rayleigh distribution, Figure 5.15. Therefore, the wave height probability density functions  $p(H)$  are given by

$$p(H_i) = \frac{2 H_i}{\bar{H}^2} \exp(-H_i^2/\bar{H}^2) \quad (5.36)$$

This may be expressed as the percentage of times a wave height  $H_i$  will occur in all the waves of that series.

The 1/nth highest wave height,  $H_{1/n}$ , is calculated as follows:

$$H_{1/n} = \frac{\int_{H_n}^{\infty} H p(H) dH}{p(H_n)} \quad (5.37)$$

Assuming  $p(H_n) = \frac{1}{n}$  we have

$$H_{1/n} = n \int_{H_n}^{\infty} H p(H) dH \quad (5.38)$$

The results of a calculation based on Equation (5.22) are:

$$H_{1/3} = 1.60 \bar{H} \quad (5.39)$$

$$H_{1/10} \cong 2.03 \bar{H} \quad (5.40)$$

In the design of offshore structures the maximum wave height,  $H_{\max}$  is of great interest. The maximum wave height cannot be determined as a definite value, but can be expressed as the most probable maximum value for a given number of  $N$  waves by the following equation:

$$H_{\max}/H_{1/3} \cong \frac{1}{1.416} [(\ln N)^{1/2} + \frac{1}{2} (\ln N)^{-1/2}] \quad (5.41)$$

$$H_{\max}/H_{1/3} \cong 1.07 \sqrt{\log_{10} N} \quad ; \text{ for large } N \quad (5.42)$$

### 5.3.2 Ocean Wave Energy Spectra

The irregular sea surface may be represented by the sum of a very large number of small-amplitude large waves of different periods or wave lengths, amplitudes, and directions, each individual component following the simple harmonic wave theory regarding wave length, period, and speed. The phase relationships among these various component waves are considered to be completely random. Any seaway can then be characterized by an "energy spectrum" which indicates the relative importance (amount of energy) in the infinite number of different component waves which combine to produce the observed irregular pattern. This in simple terms describes that the total energy of the sea is made up of the sum of the energies of all small, regular waves that make up the sea.

The fundamental importance of the spectrum is that it provides the complete statistical characterization of the sea. The phase lags among various components of the spectrum are random with a uniform probability distribution; that is, there is equal probability of their having any value between 0 and  $2\pi$ . There is no particular physical significance to the values of the phase lags, but the fact that they are random is very important. It introduces an element of probability into the representation which not only makes it realistic but permits the application of probability theory. This application is greatly simplified by the observed fact that successive points at equal intervals of time in an irregular wave record follow approximately the normal or Gaussian distribution. This permits the direct determination of the characteristics of the sea that are of primary interest. First of all, theory shows that the "variance" of statistics, or mean square value  $\sigma^2$  of a wave record (average of sum of squares of deviations from the mean value measured at equal intervals of time) is equal to the area E under the energy spectrum, or one half the area under an amplitude spectrum.

$$\sigma^2 = E = \int_0^{\infty} S(\omega) d\omega = \frac{1}{2} \int_0^{\infty} 2 S(\omega) d\omega \quad (5.43)$$

This means that if we know the spectrum we can immediately determine the mean square value of the seaway record from the spectral area. Alternatively, one can directly compute the mean square value from the record itself, which indicates the area but not the shape of the spectrum.

Various statistical values of visible wave properties can also be obtained from the spectrum by taking advantage of the fact that the peak-to-trough wave heights of a record are found to follow very nearly a so-called "Rayleigh" distribution, Figure 5.15. The excess probability curve for Rayleigh distribution is given in Figure 5.16. In mathematical statistics the following useful relationships have been derived for such a distribution, where E is the area under an energy spectrum and 2E is the area under an amplitude spectrum.

Average apparent wave height, crest to trough

$$\bar{H} = 2.5 \sqrt{E} = 1.77 \sqrt{2E} \quad (5.44)$$

Similarly, the average of the 1/3 highest waves or significant waves height

$$H_{1/3} = 4.0 \sqrt{E} = 2.83 \sqrt{2E} \quad (5.45)$$

And the average of 1/10 highest waves is

$$H_{1/10} = 5.1 \sqrt{E} = 3.6 \sqrt{2E} \quad (5.46)$$

Other visible characteristics, referred to as "apparent" by oceanographers, are obtained from moments of the spectrum.



$$M_n = \int_0^{\infty} \omega^n S(\omega) d\omega \quad (5.47)$$

where n can be any integer. Referring to Equations 5.42 and 5.46, it is evident that  $M_0$  is the area under the spectrum. The characteristics that depend on the moments are affected by the shape, as well as the area, of the spectrum. Thus:

Average apparent period, (average) based on zero up-crossings

$$\bar{T} = 2\pi(M_0/M_2)^{1/2} \quad (5.48)$$

Average apparent wavelength

$$\bar{L} = 2\pi g(M_0/M_4)^{1/2} \quad (5.49)$$

Thus the spectrum of the seaway, which specifies the invisible components of the wave pattern, also defines the properties of the visible pattern which are of interest.

Further details on this subject are beyond the scope of this report. More information may be found in works by Pierson et al. (1955), Marks (1963), Munk (1951), Kinsman (1965), Comstock (1967), Michel (1967, 1968), Dean (1974), Price and Bishop (1974), Wiegel (1975), Sarpkaya and Isaacson (1981), and Dean and Dalrymple (1984).

### 5.3.3 Proposed Wave Spectra

Various oceanographers have proposed analytical expressions for the wave spectra. Most of the proposed spectra may be expressed in one of the two ways:

1. In terms of windspeed, using formulae plus quantitative dependence on wind data to obtain the spectra.

2. In terms of observed significant wave heights,  $H_{1/3}$ , and mean period,  $T$ , thus using only the form of a theoretical spectrum, i.e., in terms of the sea itself.

The wind-speed formula represents the classical approach. The contention is that ocean-wave spectra depend on the velocity of the wind as well as its duration in time and the distance over which the wind is acting on the free surface. This distance is known as fetch. Wave spectra that have reached a steady state of equilibrium, independent of the duration and fetch are said to be fully developed. In what follows some of the better known frequency spectra that have been employed to describe ocean waves are presented.

#### 5.3.3.1 Darbyshire Spectrum (1952)

- o For fully developed sea. Depends only on the characteristic wind speed  $u$ .

- o Equation for spectrum

$$S(f) = A \exp \left[ - \frac{10.79 (f - f_0)}{(f - f_0 + 0.0422)^{1/2}} \right] \quad \text{for } f - f_0 > -0.0422$$

$$S(f) = 0 \quad \text{otherwise}$$

- o  $A$  and  $f_0$  are functions of wind speed  $u$

$$A = 1.169 \times 10^{-5} u^4$$

$$f_0 = 1 / (1.94 u^{1/2} + 2.5 \times 10^{-7} u^4)$$

- o  $f_0$  is the peak frequency, i.e., frequency at which  $S(f)$  is a maximum.

- o Units

$$f_0 \quad \text{Hz}$$

$$u \quad \text{m/s}$$

$$A \quad \text{m}^2/\text{Hz}$$

### 5.3.3.2 Neumann Spectrum (1953)

o For fully developed sea. Depends only on the characteristic wind speed  $u$ .

o Equation for spectrum

$$S(f) = \frac{Kg^2}{f^6} \exp(-B/f^2)$$

o  $B = g^2/2\pi u^2$   
 $K = 2 \times 10^{-5}$

o Peak frequency  $f_0$   
 $f_0 = (B/3)^{1/2}$

o Units

$f_0$	Hz
$u$	m/s
$K$	Hz

### 5.3.3.3 Pierson-Moskowitz Spectrum (1964)

o For fully developed sea. Depends only on the characteristic wind speed  $u$ .

o Equation for spectrum

$$S(f) = \frac{\alpha g^2}{(2\pi)^4 f^5} \exp(-B/f^4)$$

o Phillips constant  
 $\alpha = 8.1 \times 10^{-3}$

o  $B = 0.74 (g/2\pi u)^4$

- o Units
  - $f_0$  Hz
  - $u$  m/s

#### 5.3.3.4 Bretschneider Spectrum (1959)

- o In terms of significant wave height  $H_s$  and peak frequency  $f_0$ . The peak frequency  $f_0$  is empirically related to the significant wave period  $T_s$ .
- o Equation for Spectrum

$$S(f) = \frac{5H_s^2}{16f_0} \frac{1}{(f/f_0)^5} \exp \left[ -\frac{5}{4} \left( \frac{f}{f_0} \right)^{-4} \right]$$

Note: Both the Bretschneider and Pierson-Moskowitz (P-M) equations may be written in general form

$$S(f) = \frac{A}{f^5} \exp(-B/f^4)$$

In this way they differ only in the magnitudes assigned to A and B. For the P-M spectrum A is constant and B depends only on  $u$ , while for the Bretschneider spectrum  $A = 5H_s^2 f_0^4/16$  and  $B = 5 f_0^4/4$ . See Figure 5.17.

#### 5.3.3.5 JONSWAP Spectrum, Hasselmann (1973)

- o P-M spectrum modified to account for the effect of fetch restrictions and to provide for a much more sharply peaked spectrum.

o Equation for spectrum

$$S(f) = \frac{\alpha g^2}{(2\pi)^4 f^5} \exp \left[ -\frac{5}{4} (f/f_0)^4 \right] \gamma^\alpha$$

$$a = \exp \left[ - (f-f_0)^2 / 2\sigma^2 f_0^2 \right]$$

o  $f_0$  is the peak frequency

$$\sigma_a = 0.07 \text{ for } f \leq f_0$$

$$\sigma_b = 0.09 \text{ for } f > f_0$$

o  $\gamma$  is the peakedness parameter, the ratio of the maximum spectral density to that corresponding to P-M spectrum.

o  $\alpha$  characterizes the properties of the high frequency part of the spectrum and determines the total energy content. See Figure 5.18.

Note: The JONSWAP spectrum contains the ISSC (1964) spectrum and the P-M spectrum as special cases. For  $\gamma = 1$  the JONSWAP spectrum equals the ISSC and for  $\gamma = 1$  and  $\alpha = 0.0081$  the JONSWAP spectrum equals the P-M spectrum. See Figure 5.18.

Other parameters of interest for the JONSWAP spectrum are

$$o \quad X = gF/u^2 = \text{dimensionless fetch}$$

$$o \quad F = \text{fetch}$$

$$o \quad u = \text{wind speed}$$

$$o \quad f_0 = 2.84 X^{-0.33}$$

$$\sigma \quad \alpha \quad = \quad 0.066 \quad X^{-0.22}$$

The spectra mentioned so far represent only a concise selection of the various frequency spectra which have been proposed. Others include the Scott (1965) spectrum, the ISSC (1964) spectrum and so on. Ochi and Wang (1976) and Ochi and Hubble (1976) have proposed a further spectrum which depends on six parameters, and which exhibits two peaks, one associated with underlying swell and the other with locally generated waves. This spectrum is the sum of two terms, each specified by characteristic frequency, height and shape parameters.

It is appropriate at this point to mention that the wave spectrum is sometimes present as a period spectrum  $S(T)$  rather than as a frequency spectrum  $S(f)$  or  $S(\omega)$ . These parameters are, however, related to one another. Thus

$$S(T) = f^2 S(f) = (\omega^2 / 2\pi) S(\omega)$$

#### 5.3.3.6 ISSC Spectrum (International Ship Structures Congress, 1964)

o Bretschneider spectrum modified on the premise that the wave period follows a Rayleigh distribution, as does the wave height.

o Equation for spectrum

$$S(\omega) = (173 H_s / T_s^4 \omega^5) \exp(-690 / T_s^4 \omega^4)$$

o  $H_s$  = significant wave height average of the one-third highest waves

o  $T_s$  = significant period, actually the average period of the significant waves

Note: The ISSC spectrum can be obtained from the JONSWAP spectrum by setting  $\gamma = 1$  in the JONSWAP spectrum.

### 5.3.3.7 Ochi-Hubble Spectrum (1976)

- o This six parameter spectrum was derived to describe the wave spectra associated with the growth and decay of a storm including the existence of a swell. It exhibits two peaks and is the sum of two terms, each specified by characteristic frequency, height and shape parameters.

$$S(\omega) = \frac{1}{4} \sum_j \frac{\left(\frac{4\lambda_j+1}{4}\right)^4 \omega_{mj}^{\lambda_j}}{(\lambda_j)} \frac{H_{sj}^2}{\omega^{4\lambda_j+1}} \exp \left[ -\left(\frac{4\lambda_j+1}{4}\right) \left(\frac{\omega_{mj}}{\omega}\right)^4 \right]$$

- o  $j = 1, 2$  stands for the lower and higher frequency components respectively
- o  $H_s$  = significant wave height
- o  $\omega_m$  = modal frequency
- o  $\lambda$  = shape parameter

### 5.3.3.8 Scott Spectrum (1965)

- o Equation of spectrum

$$S(\omega) = 0.214 H_s^2 \exp(a)$$

$$S(\omega) = 0 \quad \text{if} \quad \omega - \omega_p < -0.26 \\ \text{or} \quad \omega - \omega_p > 1.65$$

- o  $a = -\left| \omega - \omega_p \right| / [0.065 (\omega - \omega_p + 0.26)]^{1/2}$

o  $\omega_p$  = spectrum peak frequency

#### 5.4 Short-Crested Waves

The true sea state consists of irregular wave trains of different periods and heights traveling in a number of different directions simultaneously. This condition is generally referred to as a short-crested, or multidirectional sea. The term short-crested evolves from the length of the wave crests perpendicular to the direction of motion, which is short when compared to a unidirectional, or long-crested, sea state with its infinitely long wave crests.

The directional spectrum for short-crested seas is usually generated from the unidirectional, or point spectrum, by the use of a spreading function. The directional spectrum is written as the product of two functions

$$S(f, \theta) = S(f) G(\theta)$$

where  $G(\theta)$  is the spreading function and represents the direction of the wave energy at frequency  $\omega$ , and

$$S(f) = \int_0^{2\pi} S(f, \theta) d\theta \quad (5.50)$$

is the unidirectional wave spectral density. A sketch of a directional spectrum is given in Figure 5.19. Several spreading functions have been proposed. Some of the most widely used spreading functions are given here.

o Cosine-squared

This spreading function was proposed by St. Denis and Pierson (1953) and is given as



$$\begin{aligned}
 G(\theta) &= \frac{2}{\pi} \cos^2 \theta && \text{for } |\theta| < \pi/2 \\
 G(\theta) &= 0 && \text{otherwise}
 \end{aligned}
 \tag{5.51}$$

$G(\theta)$  is a maximum along the direction  $\theta = 0$

o Cosine-power

$$G(\theta) = C(n) \cos^{2n} \left[ \frac{1}{2} (\theta - \bar{\theta}) \right]
 \tag{5.52}$$

where  $\bar{\theta}$  is the direction about which the spectrum is centered and  $C(n)$  is a normalizing function such that

$$\int_{-\pi}^{\pi} G(\theta) d\theta = 1
 \tag{5.53}$$

and is given by

$$C(n) = \frac{1}{2\sqrt{\pi}} \frac{\Gamma(n+1)}{\Gamma(n+1/2)}
 \tag{5.54}$$

There are several other spreading functions proposed by various researchers such as circular normal, Finite Fourier Series, etc. A more detailed description of directional waves and appropriate spreading functions may be found in Sarpkaya and Isaacson (1981).

TABLE 5.2 RESULTS OF LINEAR WAVE THEORY  
(SARPKAYA AND ISAACSON, 1981)

Velocity potential	$\phi = \frac{\pi H \cosh(ks)}{kT \sinh(kd)} \sin \theta$ $= \frac{gH \cosh(ks)}{2\omega \cosh(kd)} \sin \theta$
Dispersion relation	$c^2 = \frac{\omega^2}{k^2} = \frac{g}{k} \tanh(kd)$
Surface elevation	$\eta = \frac{H}{2} \cos \theta$
Horizontal particle displacement	$\xi = -\frac{H \cosh(ks)}{2 \sinh(kd)} \sin \theta$
Vertical particle displacement	$\zeta = \frac{H \sinh(ks)}{2 \sinh(kd)} \cos \theta$
Horizontal particle velocity	$u = \frac{\pi H \cosh(ks)}{T \sinh(kd)} \cos \theta$
Vertical particle velocity	$w = \frac{\pi H \sinh(ks)}{T \sinh(kd)} \sin \theta$
Horizontal particle acceleration	$\frac{\partial u}{\partial t} = \frac{2\pi^2 H \cosh(ks)}{T^2 \sinh(kd)} \sin \theta$
Vertical particle acceleration	$\frac{\partial w}{\partial t} = -\frac{2\pi^2 H \sinh(ks)}{T^2 \sinh(kd)} \cos \theta$
Pressure	$p = -\rho g z + \frac{1}{2} \rho g H \frac{\cosh(ks)}{\cosh(kd)} \cos \theta$
Group velocity	$c_G = \frac{1}{2} \left[ 1 + \frac{2kd}{\sinh(2kd)} \right] c$
Average energy density	$E = \frac{1}{8} \rho g H^2$

TABLE 5.3 SHALLOW AND DEEP WATER APPROXIMATIONS  
TO LINEAR WAVE THEORY  
(SARPKAYA AND ISAACSON, 1981)

	Shallow Water	Deep Water
Range of validity	$kd < \frac{\pi}{10}$ $\frac{d}{L} < \frac{1}{20}$ $\frac{d}{gT^2} < 0.0025$	$kd > \pi$ $\frac{d}{L} > \frac{1}{2}$ $\frac{d}{gT^2} > 0.08$
Velocity potential	$\phi = \frac{\pi H}{k^2 T d} \sin \theta$ $= \frac{gH}{2\omega} \sin \theta$	$\phi = \frac{\pi H}{kT} e^{kz} \sin \theta$ $= \frac{gH}{2\omega} e^{kz} \sin \theta$
Dispersion relation	$c^2 = \frac{\omega^2}{k^2} = gd$	$c^2 = c_0^2 = \frac{\omega^2}{k^2} = \frac{g}{k}$
Wave length	$L = T \sqrt{gd}$	$L = L_0 = gT^2/2\pi$
Surface elevation	$\eta = \frac{H}{2} \cos \theta$	$\eta = \frac{H}{2} \cos \theta$
Horizontal particle displacement	$\xi = -\frac{H}{2kd} \sin \theta$	$\xi = -\frac{H}{2} e^{kz} \sin \theta$
Vertical particle displacement	$\zeta = \frac{H}{2} \left(1 + \frac{z}{d}\right) \cos \theta$	$\zeta = \frac{H}{2} e^{kz} \cos \theta$
Horizontal particle velocity	$u = \frac{\pi H}{T(kd)} \cos \theta$	$u = \frac{\pi H}{T} e^{kz} \cos \theta$
Vertical particle velocity	$w = \frac{\pi H}{T} \left(1 + \frac{z}{d}\right) \sin \theta$	$w = \frac{\pi H}{T} e^{kz} \sin \theta$
Horizontal particle acceleration	$\frac{\partial u}{\partial t} = \frac{2\pi^2 H}{T^2(kd)} \sin \theta$	$\frac{\partial u}{\partial t} = \frac{2\pi^2 H}{T^2} e^{kz} \sin \theta$
Vertical particle acceleration	$\frac{\partial w}{\partial t} = \frac{2\pi^2 H}{T^2} \left(1 + \frac{z}{d}\right) \cos \theta$	$\frac{\partial w}{\partial t} = \frac{2\pi^2 H}{T^2} e^{kz} \cos \theta$
Pressure	$p = -\rho g z + \frac{1}{2} \rho g H \cos \theta$	$p = -\rho g z + \frac{1}{2} \rho g H e^{kz} \cos \theta$
Group velocity	$c_G = c$	$c_G = \frac{1}{2} c$
Average energy density	$E = \frac{1}{8} \rho g H^2$	$E = \frac{1}{8} \rho g H^2$

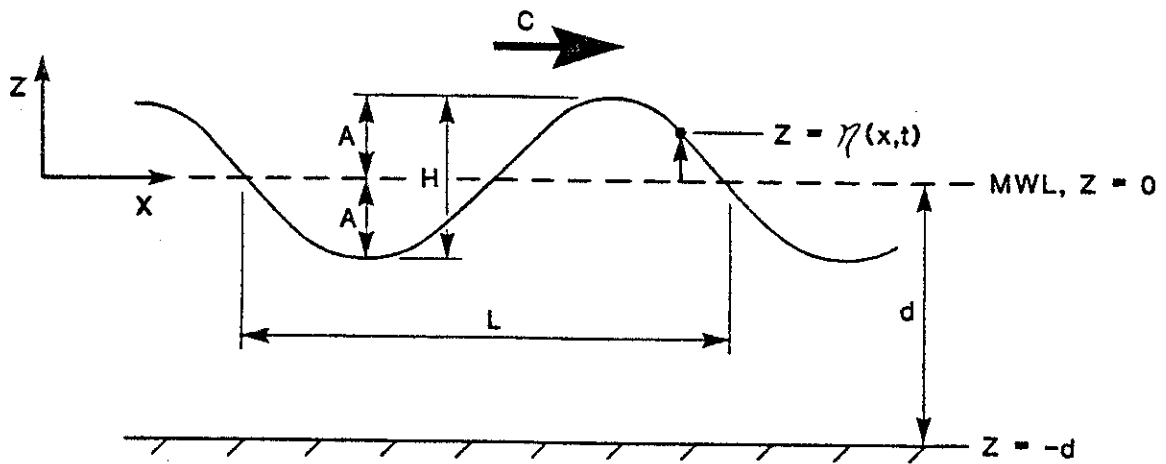


FIGURE 5.1 DEFINITION SKETCH FOR PROGRESSIVE WAVES

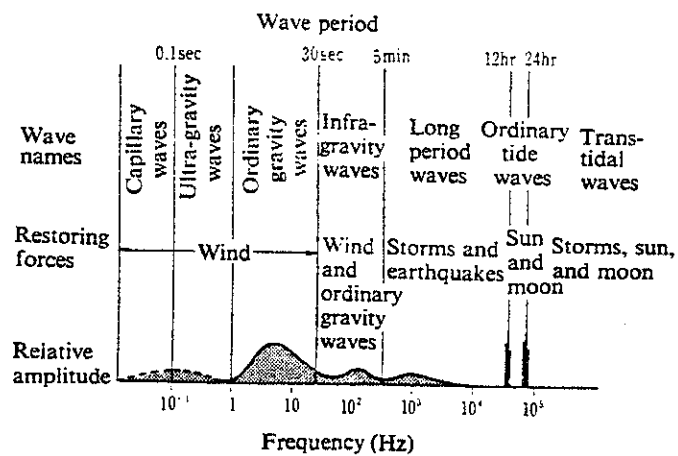


FIGURE 5.2 CLASSIFICATION OF OCEAN WAVES ACCORDING TO WAVE PERIOD (AFTER MUNK, 1951)

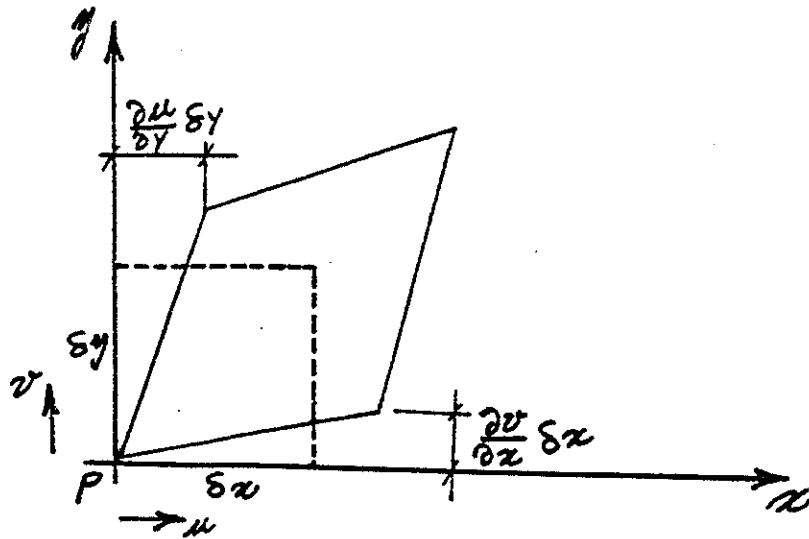


FIGURE 5.3 ANGULAR DEFORMATION WITHOUT ROTATION OF FLUID ELEMENT

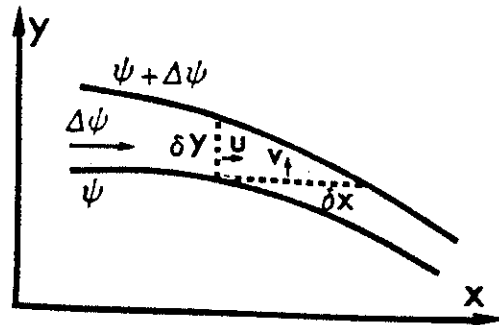
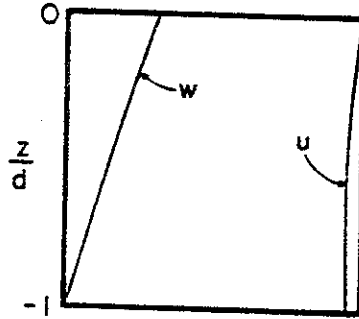
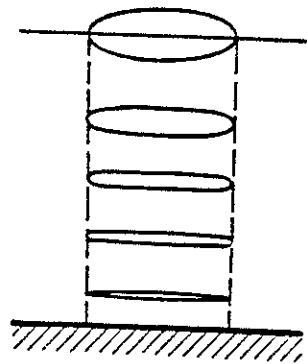
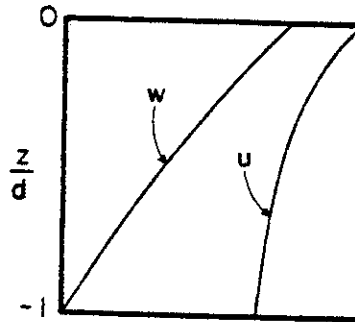
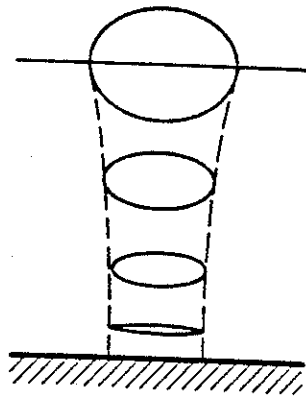


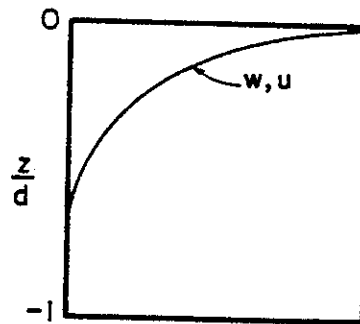
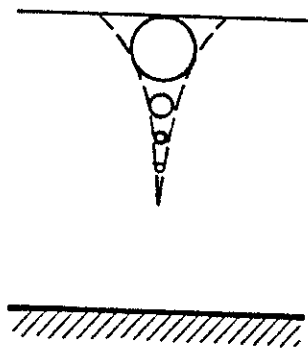
FIGURE 5.4 RELATION BETWEEN  $\psi$  AND VELOCITY COMPONENTS  $u$  &  $v$   
(SARPKAYA AND ISAACSON, 1981)



(a) Shallow water



(b) Intermediate depth



(c) Deep water

FIGURE 5.5 PARTICLE ORBITS AND VARIATION OF PARTICLE VELOCITY AMPLITUDES WITH DEPTH (SARPKAYA AND ISAACSON, 1981)

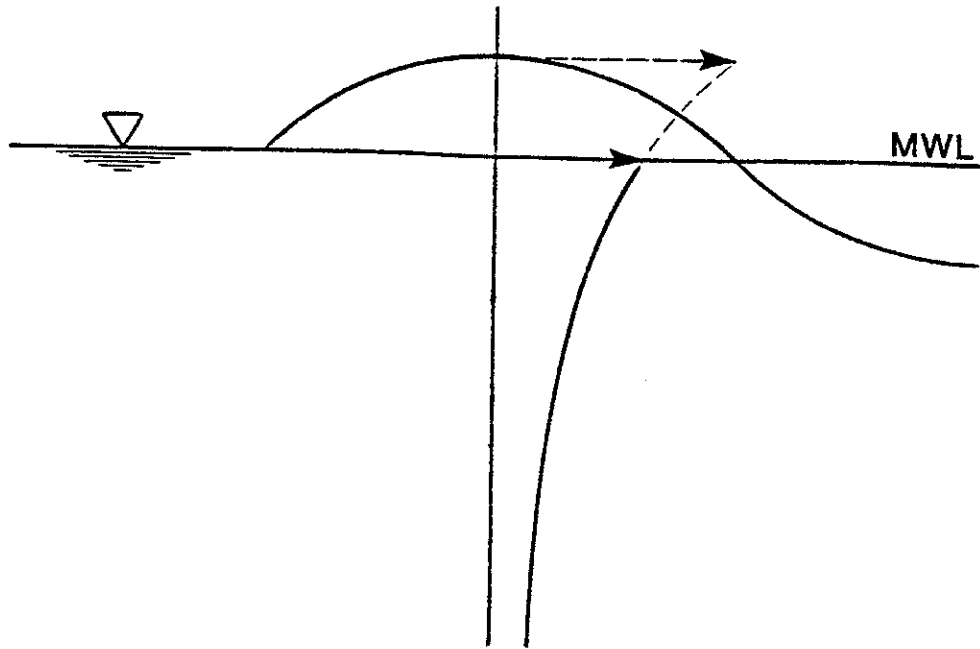


FIGURE 5.6a EXTENDED METHOD

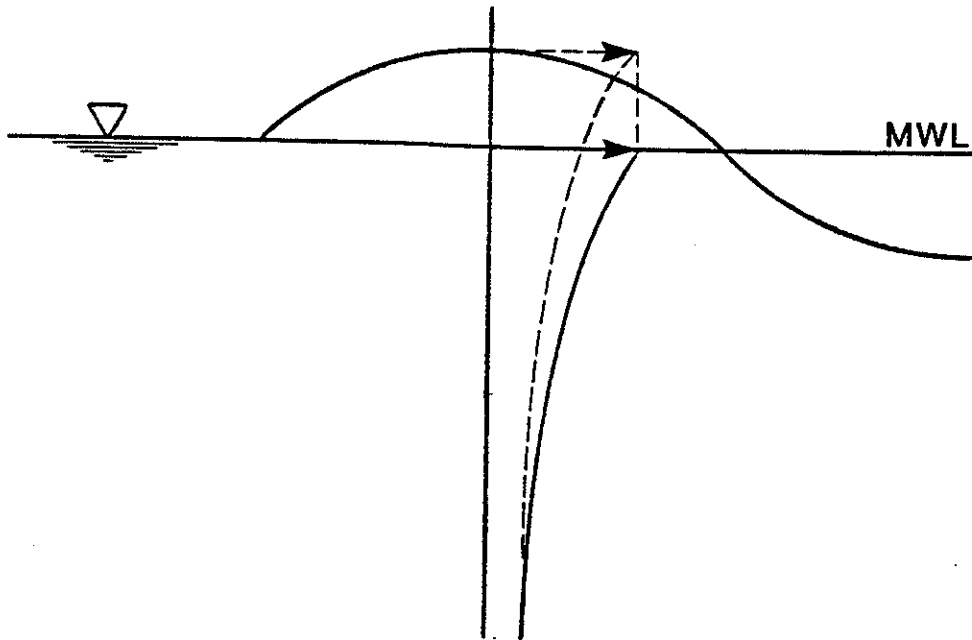


FIGURE 5.6b STRETCHED METHOD

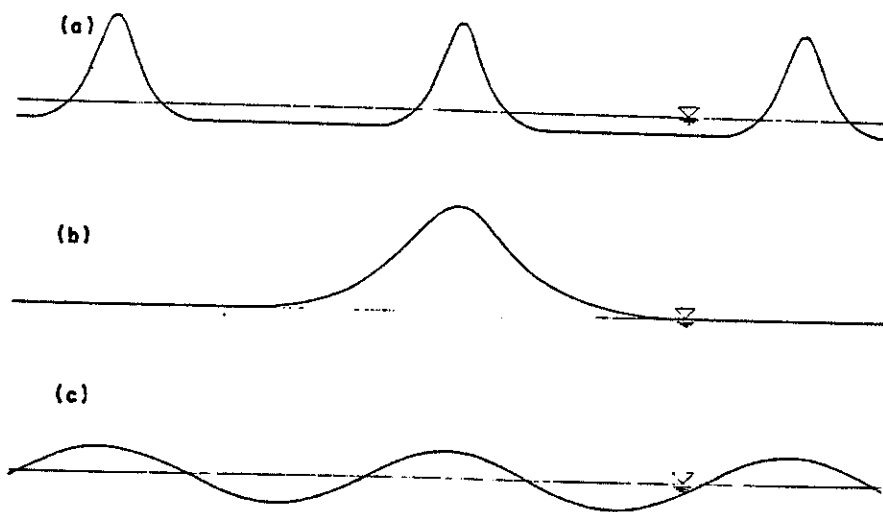


FIGURE 5.7 THE CNOIDAL WAVE PROFILE, TOGETHER WITH ITS LIMITING FORMS. FROM SARPKAYA AND ISACCSON (1981)



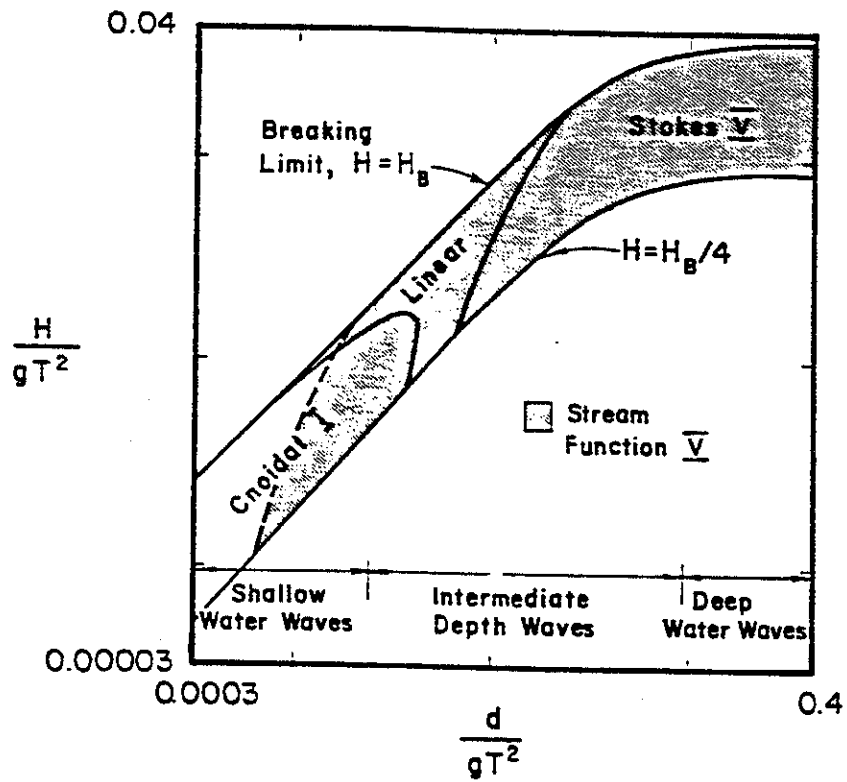


FIGURE 5.8 RANGES OF WAVE THEORIES GIVING THE BEST FIT TO THE DYNAMIC FREE SURFACE BOUNDARY CONDITION. (DEAN 1970)

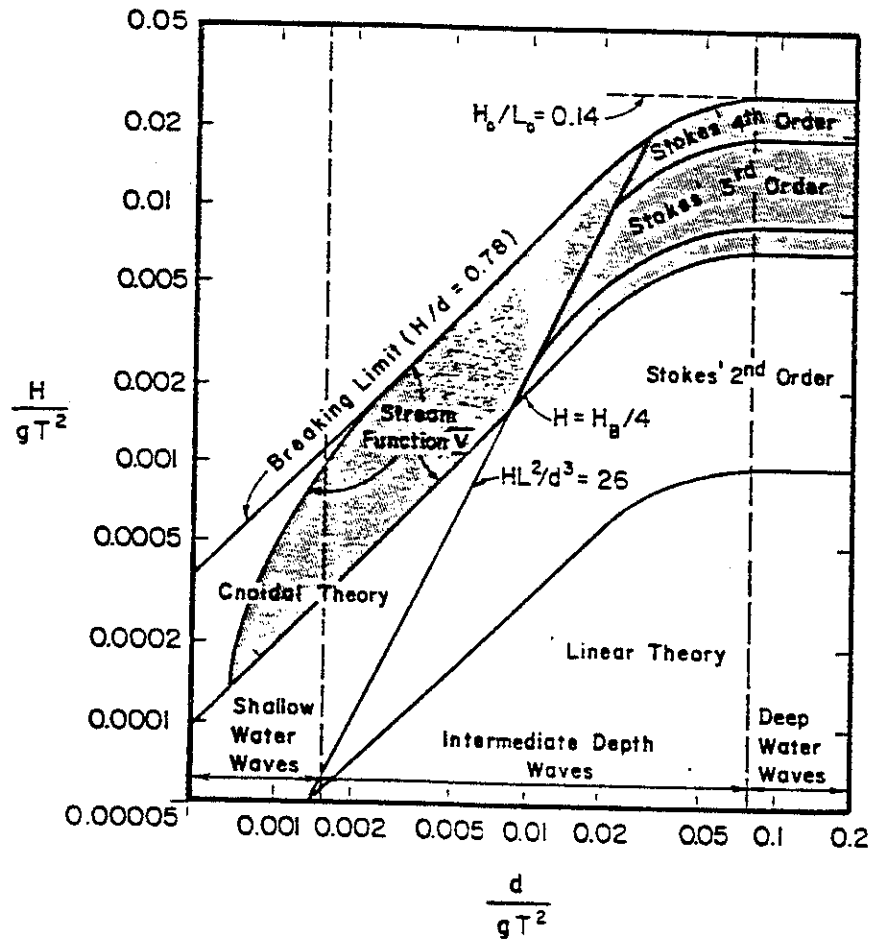


FIGURE 5.9 RANGES OF SUITABILITY FOR VARIOUS WAVE THEORIES AS SUGGESTED BY LE MEHAUTE (1976)

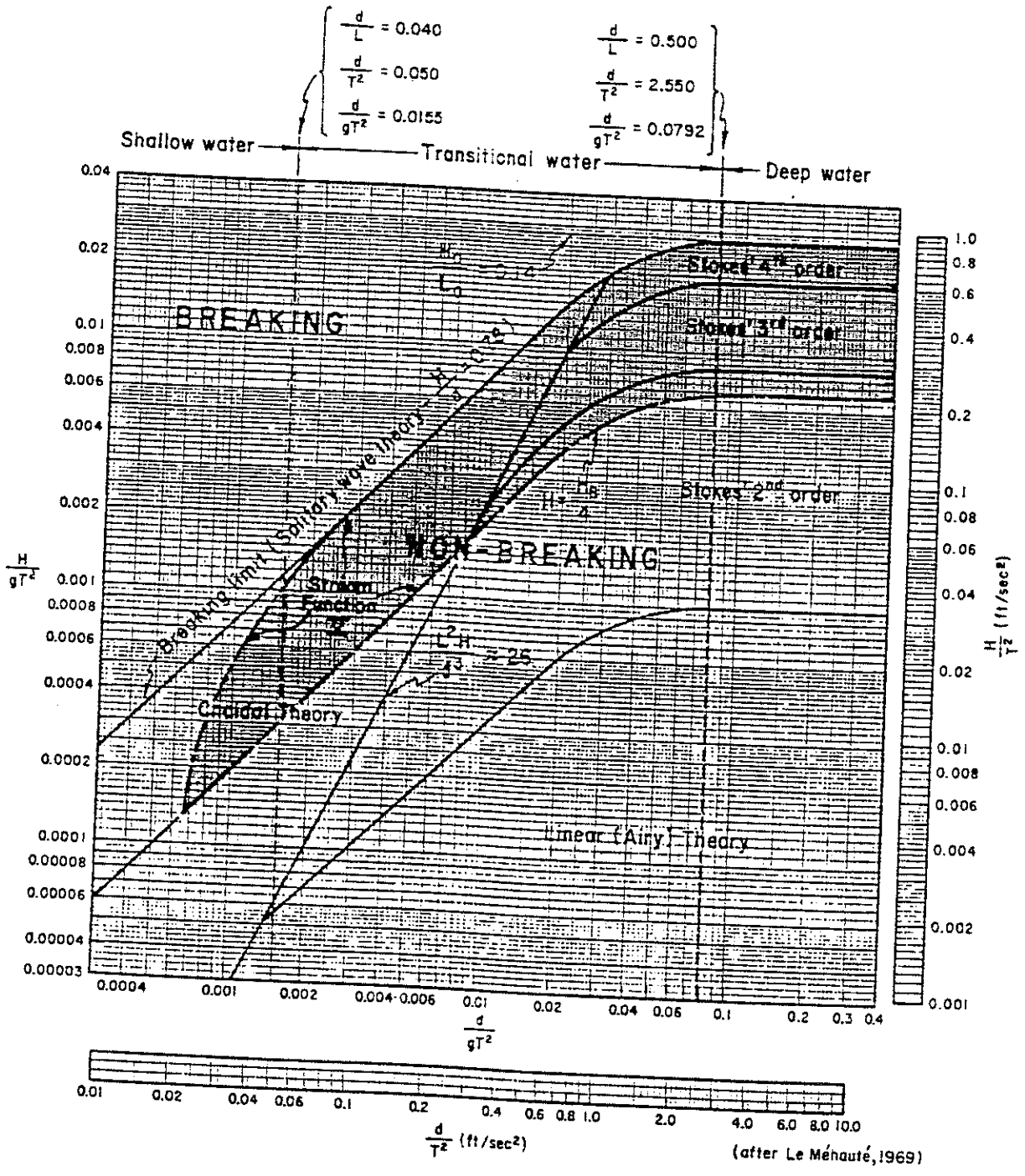


FIGURE 5.10 REGIONS OF VALIDITY FOR VARIOUS WAVE THEORIES.  
(SHORE PROTECTION MANUAL, 1975)

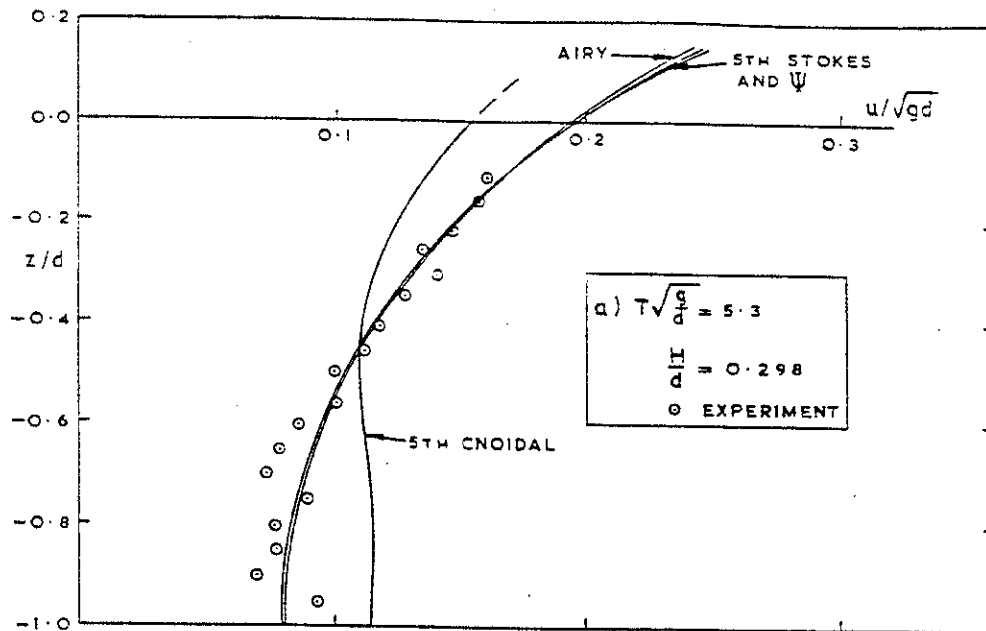


FIGURE 5.11 HORIZONTAL PARTICLE VELOCITY UNDER THE WAVE CREST FOR DEEP-WATER DATA FROM FENTON (1979), IWAGAKI AND SAKAI (1969)

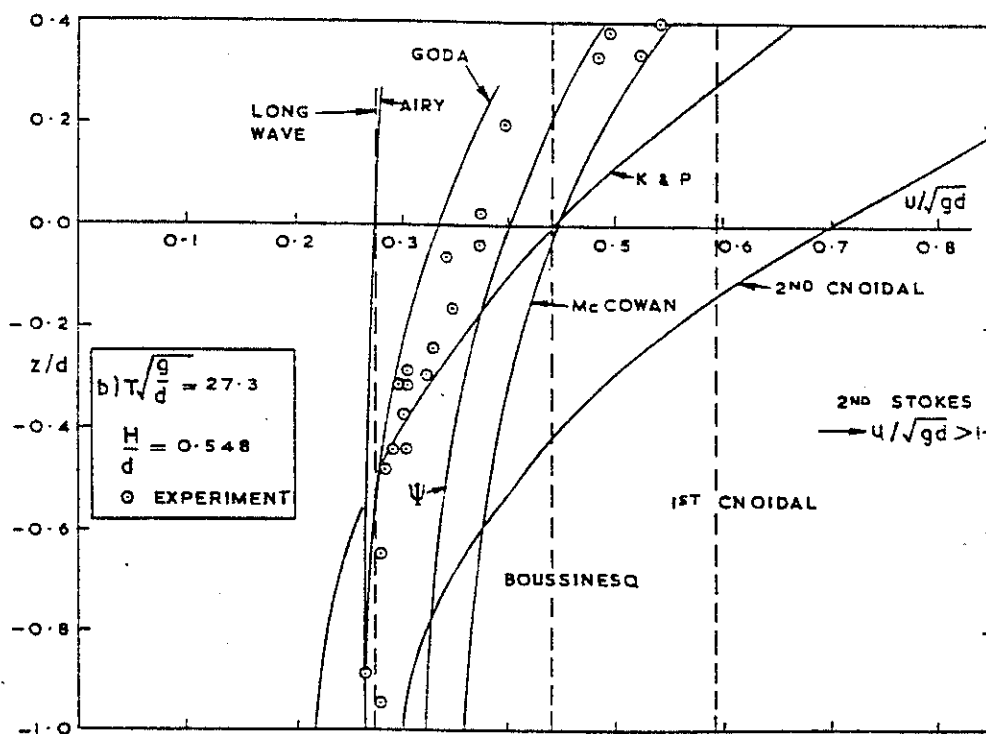


FIGURE 5.12 HORIZONTAL PARTICLE VELOCITY UNDER THE WAVE CREST FOR SHALLOW-WATER FROM LE MEHAUTE ET AL. (1968) AND DEAN (1976)

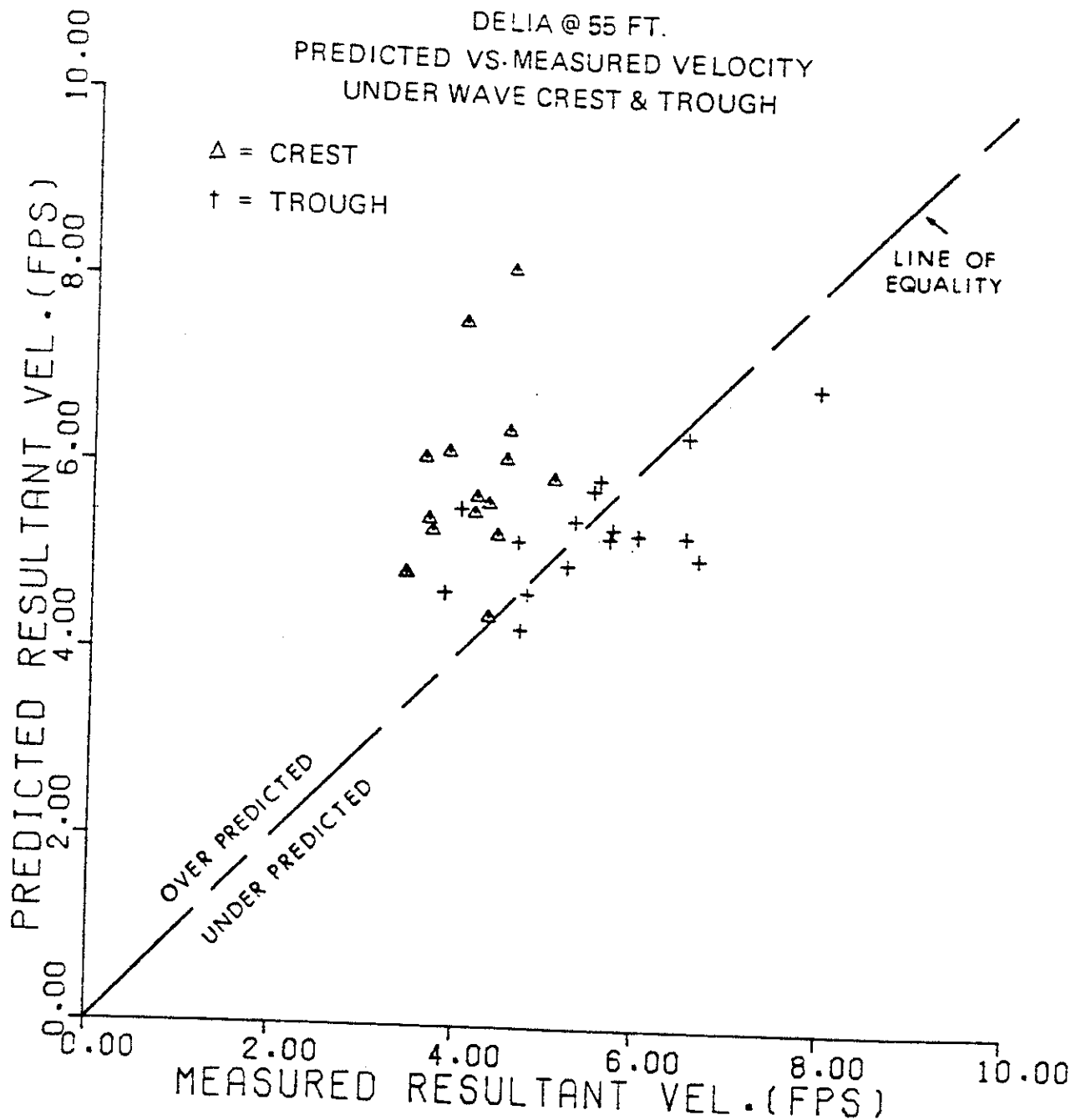


FIGURE 5.13 COMPARISON BETWEEN STOKES FIFTH-ORDER AND MAXIMUM VELOCITIES IN SEA WAVES DURING TROPICAL STORM 'DELIA'. REPRINTED FROM FORRISTALL ET AL. (1978)

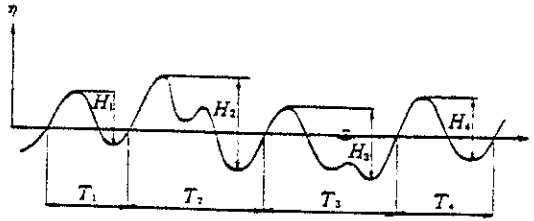


FIGURE 5.14 PROFILE OF OCEAN WAVES  
(HORIKAWA, 1978)

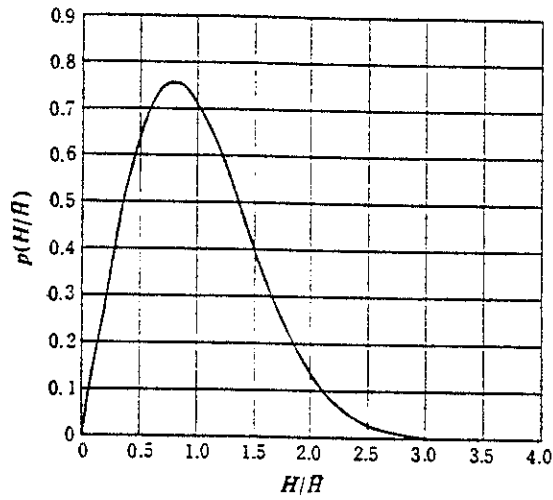


FIGURE 5.15 RAYLEIGH DISTRIBUTION CURVE  
(HORIKAWA, 1978)

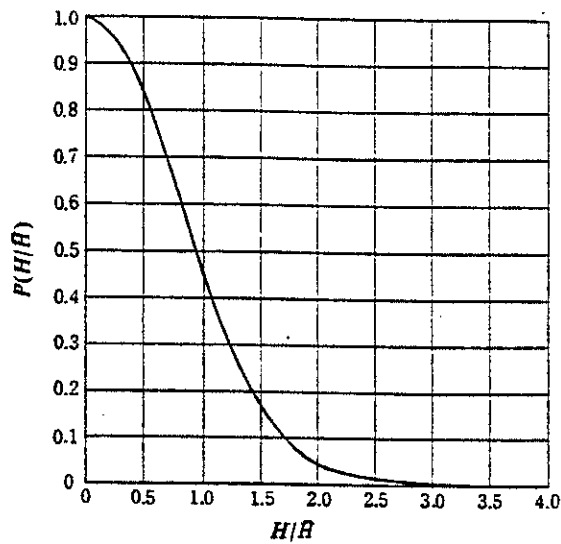


FIGURE 5.16 EXCESS PROBABILITY (RAYLEIGH  
DISTRIBUTION)  
(HORIKAWA, 1978)

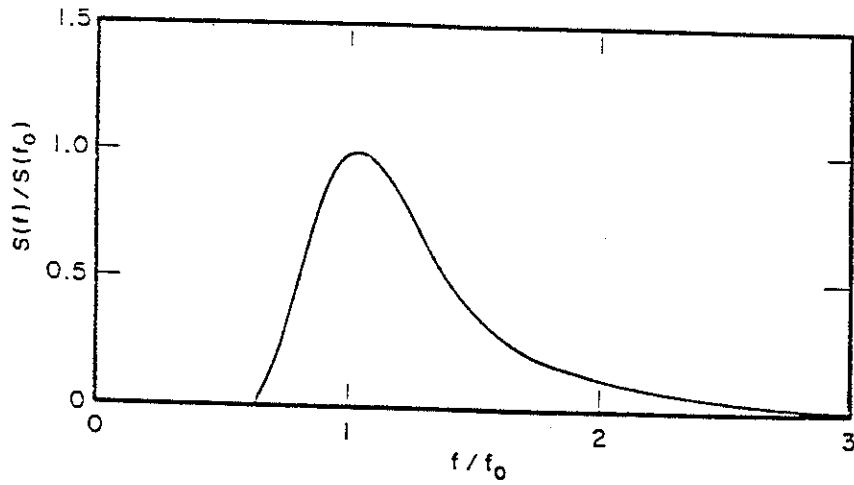


FIGURE 5.17 DIMENSIONLESS FORM OF THE BRETSCHNEIDER AND PIERSON-MOSKOWITZ SPECTRA (SARPKAYA AND ISAACSON, 1981)

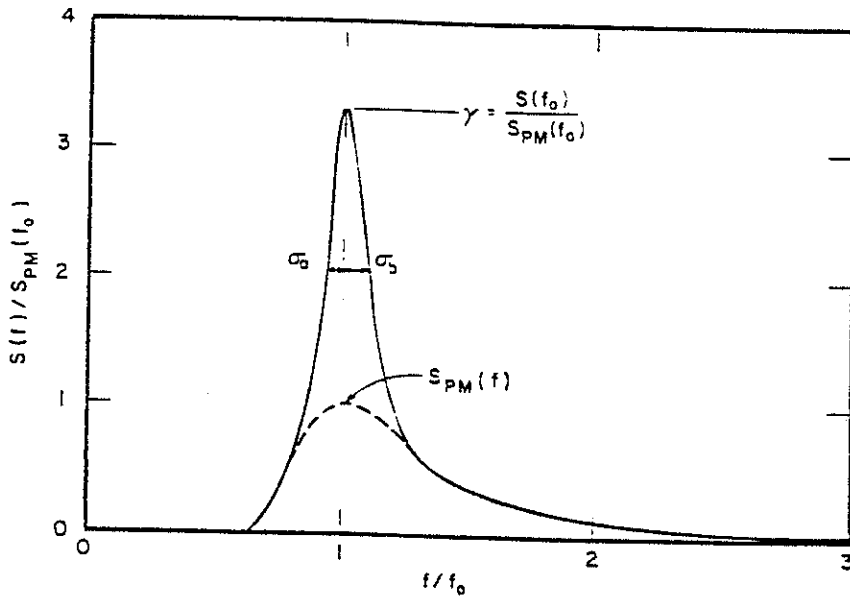


FIGURE 5.18 COMPARISON OF THE JONSWAP AND PIERSON-MOSKOWITZ SPECTRA (SARPKAYA AND ISAACSON, 1981)

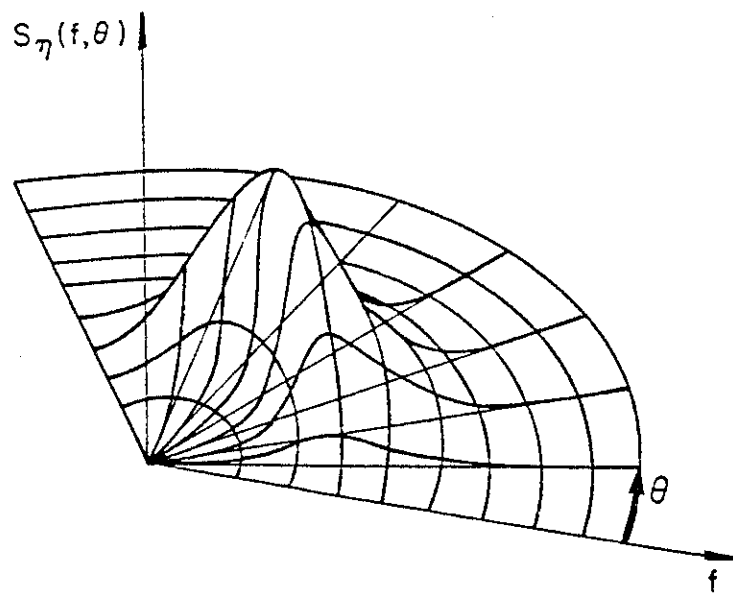


FIGURE 5.19 ILLUSTRATION OF A DIRECTIONAL WAVE SPECTRUM  
(SARPKAYA AND ISAACSON, 1981)



## 6.0 FLUID-STRUCTURE INTERACTION

### 6.1 Effects of Viscosity

If the flow velocities are different on two layers aligned with the flow, the exchange of molecules between them tends to equalize their velocities; that is, the random molecular motion effects a transfer of downstream momentum between them. The process of momentum transfer by the molecular motion is termed viscosity. The viscous force per unit area, termed the shearing stress, is defined as the rate at which the molecules accomplish the cross-stream transfer of downstream momentum per unit area.

A consequence of the existence of fluid viscosity is the "no-slip" condition at the solid surface.

Real fluids have viscosity and cannot move relative to a solid boundary. They separate from the solid boundary under the effect of adverse pressure gradient as momentum is consumed by both wall shear and pressure gradient.

Ludwig Prandtl (1904) showed that at a high Reynolds number the effect of viscosity is concentrated in the boundary layer region of the flow. In the case of bluff bodies such as circular cylinders, boundary layer development results in flow separation and wake development. For this reason the local pressures and resulting forces acting on the body are different than calculated on the basis of the inviscid flow assumption. However, for sufficiently large Reynolds numbers, it is reasonable to assume that within the bulk of the fluid, viscous forces will be negligible by comparison with the inertial forces, and corresponding flow may be considered inviscid.

Nevertheless, a consequence of viscous shear stress is that however large the Reynolds number may be, the fluid velocity on the rigid boundary must still be equal to the velocity of boundary. Thus,

there must exist significant viscous shear in a thin boundary layer at the surface of any body that moves relative to the bulk of the fluid.

This approach provides a scheme for calculating viscous effects, at least for "unseparated" flows at a high Reynolds number; equally important, it gives a rationale for neglecting viscous stress outside the boundary layer. Moreover, if the body is sufficiently regular in shape, its radii of curvature will be much larger than the boundary layer thickness, and the local flow within the boundary layer will be effectively plane. Thus, if one imagines looking at the boundary layer flow, and enlarges it with a magnifying glass or microscope, the details of the flow within this region will become visible, but the overall shape of the body is lost to view and the boundary of the body will appear practically flat within the region of view.

As yet a theoretical analysis of the problem for separated flow is difficult and much of the desired information must be obtained both numerically and experimentally. In this respect, the experimental studies of Morison and his co-workers (1950) on the forces on piles due to action of progressive waves have provided a useful and somewhat heuristic approximation.

## 6.2 Wave Force Regimes

There are basically two different approaches for evaluating wave loads on fixed and floating structures:

1. Empirical formulae, relying heavily on experimental observations, physical insight and dimensional analysis. Examples include the Morison equation and formulae for wave slamming, vortex shedding, etc.

2. Theoretical methods, which solve the boundary value problem describing flow around the structure. These methods are usually based on the classical theory of potential flow. The wave diffraction method falls into this category. It is sometimes necessary to add empirical terms representing non-ideal fluid effects, such as viscous drag.

In this report the attention is focused on the Morison equation and diffraction theory since these are basically two different approaches in use today for computation of fluid-structure interaction.

The ranges of validity of the Morison equation and the diffraction method are largely complementary as can be seen in Figure 6.1. This figure adopted from Garrison (1978) represents a rather convenient method of presentation of the regions of applicability of the inviscid diffraction theory and the Morison equation for the case of a pile. It shows the overlap region bounded by  $H/D = 1.0$  and  $D/L = 0.15$  where both theories are valid and regions at both large  $H/D$  and  $D/L$  where both viscous effects and diffraction effects are important and, consequently, neither theory is valid. However, contours of constant values of wave steepness,  $H/L$ , plotted in Figure 6.1 indicate that the region of large  $H/D$  and  $D/L$  is of little practical importance since the breaking limit for deep water is at about  $H/L = 0.14$ . Thus, Figure 6.1 suggests that viscous effects and diffraction effects should never be important at the same time. It appears that viscous effects should become important only in regions where the Morison equation is valid. Sarpkaya and Isaacson (1981) prepared a similar figure representing the regions of validity of diffraction and separated flow. Their work is shown in Figure 6.2.

The Morison equation is based on the assumption that the kinematics of the undisturbed flow in the region near the structure do not change in the incident wave direction. Since flow velocities and accelerations do in fact vary with a wavelength  $L$ , the assumption implicit in the use of the Morison equation is that the ratio  $D/L$  is

small, where D here denotes a characteristic horizontal dimension of the structure, equivalent say to the diameter of a cylinder. When a body spans a significant fraction of a wavelength, the incident waves generally undergo sufficient scattering or diffraction and wave force calculations should then take such scattering into account. This situation characterizes the diffraction regime of wave-structure interaction and is generally considered to occur when the structure spans more than about a fifth of the incident wavelength. When wave diffraction is important i.e., D/L is not too small, the fluid particle displacements relative to D may themselves become sufficiently small for the effects of flow separation to be minimized or localized.

In brief, various force regimes may be established as follows:

D/L > 1	Condition close to pure reflections
D/L > 0.2	Diffraction increasingly important
D/L < 0.2	Morison equation valid
D/W > 0.2	Inertia increasingly predominant within the Morison equation
D/W < 0.2	Drag predominant within the Morison equation

where W is the orbit width of the water particle given by

$$W = \frac{H}{\tanh \frac{2\pi d}{L}} \quad (6.1)$$

### 6.3 Morison Equation

Morison and his co-workers (1950) conducted some experiments on vertical piles in progressive waves. This work was sponsored by the U.S. Navy based on a problem posed by the Bureau of Yards and Docks. The objective of this study was to develop methods for evaluating wave loads on submerged piles. Morison et al. assumed that the horizontal wave force exerted on the vertical pile is a linear sum of

two forces:

1. A drag force,  $F_D$ , proportional to the square of the horizontal water particle velocity,  $u$ .
2. An inertia force,  $F_I$ , proportional to the horizontal water particle acceleration,  $\dot{u}$ .

Therefore, the force per unit length as a vertical pile could be written as:

$$F = F_D + F_I \quad (6.2)$$

$$F = C_d \frac{1}{2} \rho D |u| u + C_m \rho \frac{\pi D^2}{4} \dot{u} \quad (6.3)$$

where:

- $D$  = pile diameter
- $\rho$  = water mass density
- $C_m$  = inertia coefficient
- $C_d$  = drag coefficient
- $u$  = horizontal water particle velocity
- $\dot{u}$  = horizontal water particle acceleration

The term  $|u| u$  is written in this form to ensure that the drag force component is in the same direction as the velocity.

Other underlying assumptions in formulating the Morison equation are:

- o The equation is for unbroken surface waves.
- o The equation is for a single vertical, cylindrical object, such as a pile, which extends from the bottom upward above the wave crest.

- o The diameter of the pile is small compared to the wave height, wave length and water depth.
- o Coefficients  $C_m$  and  $C_d$  must be obtained experimentally.
- o In force calculations  $u$  is taken as the horizontal wave particle velocity and the convective acceleration terms are often ignored, i.e., it is assumed that

$$\frac{Du}{Dt} \approx \frac{\partial u}{\partial t} \quad (6.4)$$

Considerable uncertainty exists regarding the meaning and application of the inertia force for nonlinear flows in which convective accelerations are not negligible. Isaacson (1979a) has discussed this subject and concluded that the inertia forces calculated in the conventional manner will generally over estimate the actual force.

These basic assumptions represent an over simplification of the complex phenomenon of fluid-structure interaction. In this context the Morison equation is generally regarded as a semi-intuitive engineering expression which is used to approximate the force exerted on a body in a viscous fluid under unsteady flow conditions. However, in spite of these severe assumptions, researchers have not been able to introduce a more appropriate expression to replace the Morison equation. The tendency has been more toward modifying and extending the Morison equation to make it applicable to more complicated situations for which it was never conceived. The application of the Morison equation and its extension to handle more complicated structures is discussed in more detail in sections dealing with wave forces on small bodies (see also Sarpkaya, 1976a, 1976b, 1980, 1981a, 1981b).

It was noted that for structures which are large compared with the wave length, the assumption that the form of the wave is unaffected by the structure is no longer valid. The wave is then scattered by the body and the resultant force is composed of the force due to the incident wave together with the force generated by the scattered component. Wave theories that take this effect into account fall under the general heading of diffraction theory. The diffraction theory, as it has come to be known, refers to the inviscid, incompressible and irrotational (potential flow) solution of fluid-structure interaction. In the linear diffraction theory the solution to the fluid-structure problem is sought such that the linearized free-surface boundary condition is satisfied as well as the kinematic boundary condition on the surface of the body and on the sea floor. Moreover, the waves caused by the presence of the body and/or its motion satisfy a radiation condition at some large distance away from the body. Thus, notwithstanding the possibility of certain numerical limitations in application, the diffraction theory is based on the exact solution to the interaction of either a fixed or floating body with a fluid, but because of its underlying assumptions it admits two fundamental limitations:

1. That arising from the assumption of zero viscosity of the fluid.
2. That arising from the assumption of small amplitude motion as implied by the application of the linearized free-surface boundary condition.

The general diffraction theory is not limited to any specific body shape, although it admits of the two limitations discussed.

It is of interest to consider the diffraction theory's relationship to the Morison equation. Historically the Morison equation was introduced as a semi-intuitive formula for the computation of wave

forces on objects which were small in relation to the wavelength. The Morison equation approach to the calculation of wave forces on a body represents the asymptotic form of the diffraction theory in the limit as the size of the body (or diameter in the case of elongated shapes such as a cylinder) relative to the wavelength approaches zero. Thus, if viscous effects are disregarded, the results of the diffraction theory approach those based on only the linear or local inertia term in the Morison equation as the diameter to wavelength ratio approaches zero.



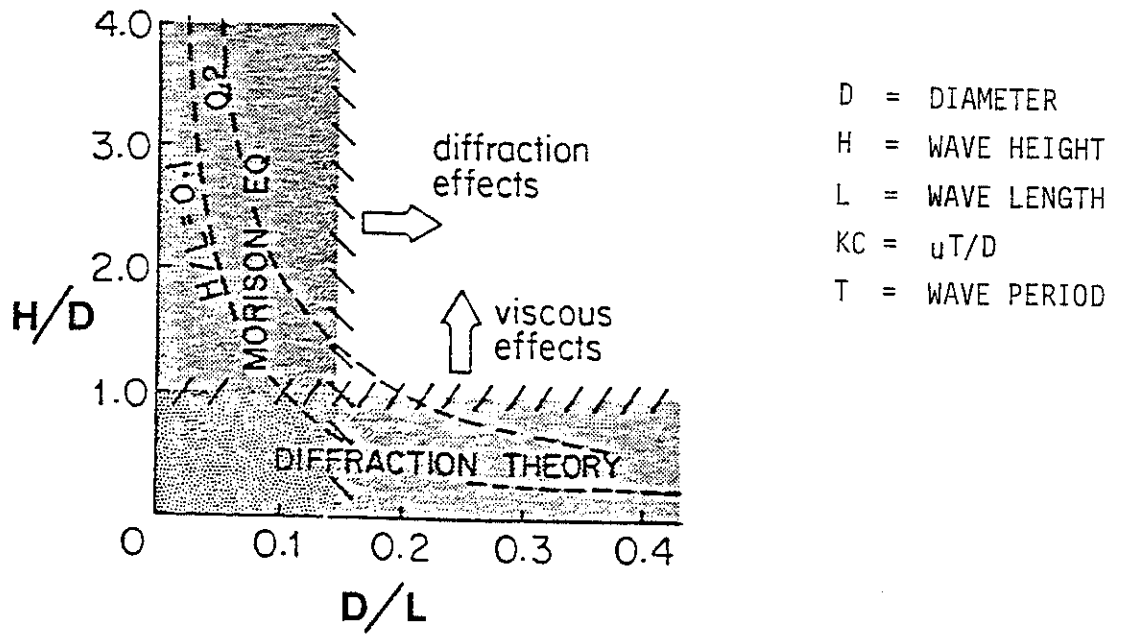


FIGURE 6.1 REGIONS OF VALIDITY - WAVE INTERACTION WITH A PILE (GARRISON, 1978)

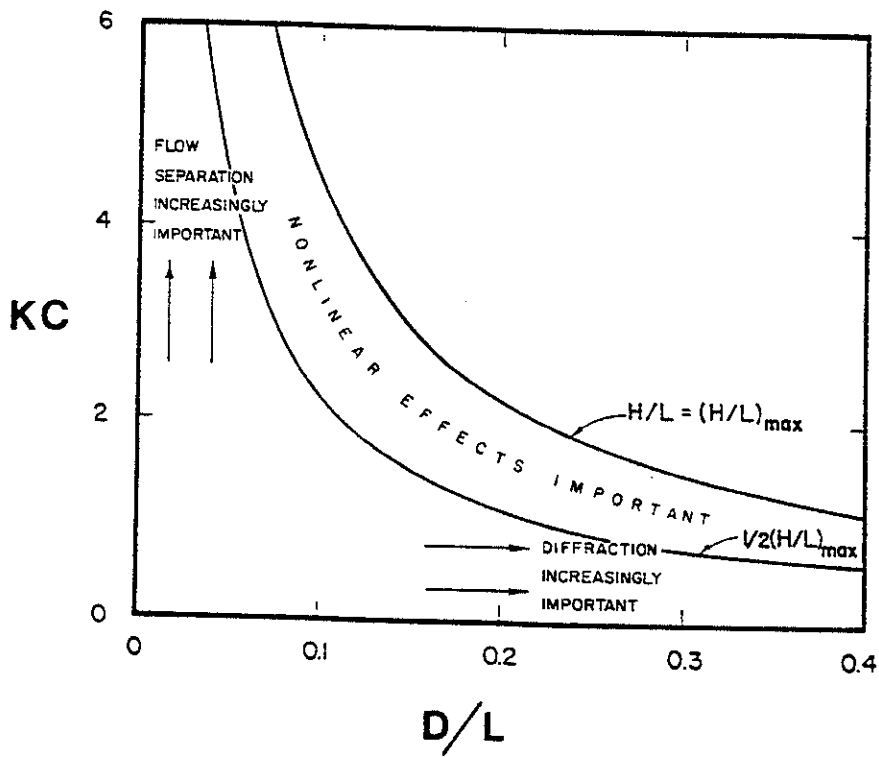


FIGURE 6.2 WAVE FORCE REGIMES (SARPKAYA AND ISAACSON, 1981)



## 7.0 WAVE FORCES ON SMALL BODIES

The word "small" is used with reference to the diameter-wavelength ratio. As such, the diffraction effects are negligible and both drag and inertia forces may be important. The Morison equation is used for estimating wave induced forces on small offshore structures. Application of the Morison equation to complex engineering problems requires knowledge of inherent assumptions and limitations of this equation. Only through this awareness is a clear assessment of the results and their reliability possible.

### 7.1 Application of the Morison Equation

The basic assumption of the Morison equation that the wave force on a cylindrical member can be separated into a velocity squared-dependent drag force and an acceleration-dependent inertia term is a simplification of the complex fluid-structure interaction problem. This equation does not take into account the time history of the fluid flow and the complex unsteady vortex action that is associated with most of the design flow-structure conditions. The equation cannot fully account for flow-structure conditions that are complicated by roughness, inclined members, transverse lift force, and interference effect due to neighboring elements. The equation also cannot represent irregular kinematic conditions where flow is complicated by breaking waves, wave-current interaction, and three-dimensional states. Instead, the Morison equation depends on a pair of adjustable force coefficients to obtain good matching between measured and calculated forces. A more detailed discussion on the validity of the Morison equation is given by Sarpkaya and Isaacson (1981) and Sarpkaya (1967a, 1976b, 1980, 1981a, 1981b).

In spite of all of these shortcomings, in the three decades after the introduction of the Morison equation it has not been possible to replace it with a more appropriate formulation. Current practice still relies heavily on the Morison equation or its extended forms to

determine wave forces on structures. Government and industry regulatory bodies such as the American Petroleum Institute (API), the United Kingdom Department of Energy (DOE), and Det norske Veritas (DnV) of Norway all recommend the use of the Morison equation in designing offshore structures. Moreover, numerous researchers both in laboratory and field conditions have indicated that the Morison equation, used in the appropriate ranges of fluid-structure operating regimes, is a good force predictor given the values of the fluid particle kinematics and the empirical force coefficients. In this regard Sarpkaya (1976b) found that, except over the range of the Keulegan-Carpenter numbers ( $KC = uT/D$  about 10 to 20), for which the wake effects are rather erratic, the Morison equation represents the oscillating forces on the cylinder with surprising accuracy.

The major difficulty in applying the Morison equation is the selection of the appropriate force coefficients from the widely scattered data in literature. This generally requires good judgement and experience in selecting and/or modifying values of the coefficients to fit the particular problem.

Another problem in the application of the Morison equation in the frequency domain approach lies in its nonlinear drag term. A suitable linearization technique, which sometimes involves iterative procedures, should be adopted in a frequency domain application. Some of the most widely used linearization techniques are described in Section 7.7.

## 7.2 Extensions of the Morison Equation

The Morison equation was originally written for force per unit length in a form similar to the following:

$$F = C_m \rho \frac{\pi D^2}{4} \frac{\partial u}{\partial t} + C_d \frac{1}{2} \rho D u^2 \quad (7.1)$$

Shortly thereafter it became:

$$F = C_m \rho \frac{\pi D^2}{4} \frac{\partial u}{\partial t} + C_d \frac{1}{2} \rho D |u| u \quad (7.2)$$

The term  $|u|u$  is written in this form to ensure that the drag force component is in the same direction as velocity for oscillatory flows.

In an attempt to render this equation more general the diameter was replaced by a characteristic cross-sectional area per unit length (projected area),  $A$ , and  $\pi D^2/4$  by a volume per unit length,

$$F = C_m \rho V \frac{\partial u}{\partial t} + C_d \frac{1}{2} \rho A |u| u \quad (7.3)$$

This modification implies that the Morison equation is equally valid for other body shapes. This form of Morison equation represents the static equivalent force that is usually used in the design wave approach for the design of fixed structures.

It was previously mentioned that in the usual Morison equation only the local derivative of the water particle velocity and local acceleration are used and convective accelerations are neglected. The use of the substantial derivative to describe the fluid acceleration,  $Du/Dt$ , has been found to yield better verification than the local acceleration  $\partial u/\partial t$  (see Isaacson 1979a) in computing the inertia forces. Therefore another form of the Morison equation is:

$$F = C_m \rho V \frac{Du}{Dt} + C_d \frac{1}{2} \rho A |u| u \quad (7.4)$$

The standard form of Morison equation assumes that the structure which is experiencing the force is rigid. However, if the structure has a dynamic response or is part of a floating body, its induced motion may be significant when compared with the water particle velocities and accelerations. In this case the Morison equation is

usually written as:

$$F = (C_m - 1) \rho V \dot{(u - X)} + \rho V \ddot{u} + C_d \frac{1}{2} \rho A |u - \dot{X}| (u - \dot{X}) \quad (7.5)$$

where  $X$  and  $\dot{X}$  are structural velocity and acceleration respectively. The first term on the right hand side is the added mass term associated with the acceleration of the relative motion which occurs because of the changing flow around the structure. The term  $(C_m - 1)$  is called added mass coefficient and is customarily denoted as  $C_a$ . The second term on the right hand side is the so called Froude-Krylov force due to the local acceleration of the unsteady flow. The third term gives the drag force due to the relative velocity.

In an attempt to include the effect of a steady current in the hydrodynamic loading process some authors have used the Morison equation in the following form:

$$F = (C_m - 1) \rho V \dot{(u - \dot{X})} + \rho V \ddot{u} + C_d \frac{1}{2} \rho A |V_c + u - \dot{X}| (V_c + u - \dot{X}) \quad (7.6)$$

where  $V_c$  is the current velocity and is assumed to be steady.

The Morison equation in connection with the equation of motion is usually written as

$$m \ddot{X} + C \dot{X} + KX = C_m \rho V \ddot{u} - (C_m - 1) \rho V \dot{X} + C_d \frac{1}{2} \rho A |V_c + u - \dot{X}| (V_c + u - \dot{X}) \quad (7.7)$$

The term  $(C_m - 1) \rho V \dot{X}$  is customarily taken to the left hand side and combined with the inertia term.

$$[m + (C_m - 1) \rho V] \ddot{X} + C \dot{X} + KX = C_m \rho V \ddot{u} + C_d \frac{1}{2} \rho A |V_c + u - \dot{X}| (V_c + u - \dot{X}) \quad (7.8)$$

The term  $(C_m - 1)\rho V$  is referred to as the added mass (see also Section 4.2).

Recently researchers have attempted to improve the Morison equation prediction power by including additional terms to the original equation or altogether formulating new forcing functions that somehow resemble the Morison equation. Sarpkaya (1981b) formulated a three-term and a four-term Morison equation by Fourier analysis of residues (error between the experimental force and theoretical formulation). It was shown through numerous examples, using experimental results obtained in a U-tube, that the new Morison equations reduced the residue significantly in the drag-inertia dominated region where the original Morison equation predictions are not satisfactory.

Horton et al. (1982) formulated a new wave force methodology based on the inertial pressure concept. In this method the pressure distribution on a body is computed from potential flow theory. This pressure distribution is then modified empirically to account for viscous effects. The summation of these pressure forces yields an equation which is quite similar in appearance to the Morison equation.

In light of current improved knowledge on wave flows about structures, extensions to the Morison equation have also been investigated to accommodate complications such as inclined members, transverse lift forces, near surface effects, interference effects, etc. It is also commonly modified for use as a spectral transfer function between frequency domain characterization of wave kinematics and structural response.

It is apparent that the modifications imparted to the Morison equation are bold attempts to employ this equation in situations that were not originally conceived. However, in the absence of any other forcing function, this seems the only way to simulate the complex fluid-structure interaction of small bodies.

### 7.3 Force Coefficients

In the regions where the Morison equation is applicable, force can be computed only if the relevant drag and inertia coefficients are known for the specific structural configurations and design sea states concerned. The determination of drag and inertia coefficients has been a key topic in wave force research since the Morison equation was introduced in the 1950's. Very considerable resources in terms of people, talent and facilities are still involved in this task. With some of the significant research results recently available, investigators are perhaps just beginning to be able to reduce and explain some of the conflicting experimental data and uncertainties about the choice of force coefficient values. Until recently the empirical coefficients in this equation,  $C_m$  and  $C_d$ , depended heavily on data obtained in either small-scale laboratory waves or steady flow in a wind-tunnel. There are well-known difficulties in scaling wave forces measured in the laboratory. In order to achieve similarity with full-scale forces, three parameters have to be identical:

- o  $H/gT^2$  where  $H$  = wave height,  $T$  = wave period,
- o Reynolds number  $Re = uD/\nu$  where  $u$  = typical fluid velocity,  $D$  = member diameter,  $\nu$  = kinematic viscosity,
- o Keulegan-Carpenter number  $KC = uT/D$ .

It is not possible to satisfy all three conditions simultaneously at small scale.

Miller (1976) noted that large Reynolds numbers can be achieved in a wind tunnel, but only in a steady flow ( $KC = \infty$ ). In these conditions it is known that the drag coefficient for a circular cylinder changes dramatically within a "critical" range of Reynolds number, before settling down to a constant plateau value, independent of  $Re$ , in



postcritical conditions. Pearcey (1979b) indicated that a similar transition occurs in oscillatory flow, and that there are important differences between the "subcritical" conditions typical of laboratory waves and the "postcritical" conditions more often encountered at sea. The problem of obtaining data appropriate to offshore conditions has been tackled in two different ways; by using artificially-generated flows in the laboratory, and by experiments in the sea itself.

There are basically three types of flow situation for which some data of varying degrees of quality, covering various ranges of the governing parameter, exists. These are:

- o data obtained with vertical cylinders in laboratory wave channels, often with small amplitude waves;
- o data obtained in the ocean environment either through the instrumentation of the existing platforms or through the use of small scale platforms built specifically for test purposes, e.g. Exxon's Ocean Test Structure, and NMI's Christchurch Bay Tower;
- o data obtained with sinusoidally oscillating planar flow about smooth and rough circular cylinders.

### 7.3.1 Vertical Cylinders with Laboratory Waves

The data obtained with small amplitude laboratory waves have fundamental problems for the following reasons:

- o the range of Reynolds numbers and Keulegan-Carpenter numbers is quite limited;
- o both Re and KC vary with depth as well as with time;

- o often the total in-line force acting on the entire pile, rather than that on a small segment is measured;
- o the kinematics of the flow, calculated through a suitable wave theory is of questionable accuracy; and
- o the orbital motion of the particles and the variation of  $KC$  and  $Re$  along the model pile, in the range of  $KC$  values where the original Morison equation is least accurate, complicates the problem considerably.

### 7.3.2 Ocean Tests

The Ocean Test Structure data was obtained during a large scale experiment undertaken as a joint industry project and conducted by Exxon Production Research (EPR) Company. The highly instrumented 20x40x120 feet steel jacket type platform was installed in 66 feet of water in the Gulf of Mexico. The results of this experiment are reported by Heideman et al. (1979). They used two methods to evaluate the drag and inertia coefficients. The first was the least square error method of each half wave cycle. The second method consisted of the evaluation of  $C_d$  over short segments of wave in which drag force was dominant and  $C_m$  over short segments of the wave in which inertia force was dominant.

The force coefficients exhibited large scatter particularly for  $KC < 20$ . The scatter decreased considerably in the range  $20 < KC < 45$ . It is not clear whether this is a genuine reduction in scatter or whether it is a consequence of the fewer data points in the drag-dominated regime.

Heideman et al. (1979), attributed the scatter in  $C_d$  and  $C_m$  to random wake encounters. It is postulated that if the cylinder encounters its wake on the return half cycle but the current meter does not, then the actual incident velocity will be greater than

measured and the apparent  $C_d$  calculated from the measured force and velocity will be higher than the true  $C_d$ . Conversely, if the current meter encounters the wake on the return half cycle but the cylinder does not, then the apparent  $C_d$  will be too low. Clearly, the encounter of the wake with the current meter and the biasing of the wake by the current are extremely important. This is evidenced by the fact that the values of  $C_d$  and  $C_m$  vary considerably from one half-wave cycle to another even for the same wave. Thus, it is desirable to evaluate  $C_d$  and  $C_m$  with due consideration for the effects of current, wave spreading, and the irregularities superimposed on each wave.

Heideman et al. (1979) concluded that:

- o the Morison equation with constant coefficients can be made to fit measured local forces and kinematics satisfactorily over individual half wave cycles;
- o most of the scatter in the  $C_d$  results can be explained by the random wake encounter concept;
- o local deviations in apparent  $C_d$  are not spatially correlated in any given wave;
- o  $C_d$  results from Sarpkaya's experiments (1976a, 1976b) represent an upper band to  $C_d$  values that may be expected in random three-dimensional oscillatory flow;
- o for  $Re < 2 \times 10^5$ , the apparent  $C_d$  depends on surface roughness and, for members that are nearly in the orbit plane, on  $KC$ ;
- o asymptotic  $C_d$  results from the test data in random three-dimensional oscillatory flow are consistent with steady flow data for the same relative roughness; and

- o  $C_m$  is greater for smooth cylinders than for rough cylinders, while the reverse is true for  $C_d$ .

Figure 7.1 shows the  $C_d$  results from the Ocean Test Structure (OTS) experiment.

### 7.3.3 Laboratory Tests

Sarpkaya (1976a, 1976b, 1978, 1981b), Rance (1969) and Garrison et al. (1977) designed laboratory experiments in which the waves were replaced by a simple unidirectional oscillatory flow, thus eliminating one of the length scales (wavelength), together with restrictions on the steepness parameter  $H/gT^2$ . This gave greater freedom with the two remaining parameters, allowing a good range of Keulegan-Carpenter and Reynolds numbers to be achieved (though only Sarpkaya, in his later experiments, reached postcritical plateau conditions). Sarpkaya's and Rance's experiments were mounted in a U-tube and pulsating water tunnel respectively, while Garrison force-oscillated a cylinder in still water. (This last experiment has been criticized by Sarpkaya and Collins (1978) because the forces may have been contaminated by the effects of high-frequency mechanical vibration).

These laboratory experiments had the advantages of being highly repeatable and controlled, but two important features of free waves were lacking. The particle motions were unidirectional instead of orbital, and uniform instead of varying with immersion depth and phase position in the wave. Pearcey (1979a) has discussed some of the similarities and major differences to be expected between these two types of motion. He has suggested that the variability observed in both the in-line and transverse forces, particularly in sea waves, is associated with an inherent variability in the effects of vortex shedding and convection. These effects are likely to depend strongly on the lengthwise coherence of the vortices, which in turn is likely to be strongly influenced by random three-dimensional features of

real sea waves. Thus although planar flow experiments have been of enormous value in improving our understanding of vortex flows, of their sensitivity to roughness, and of the Reynolds and Keulegan-Carpenter numbers, this very sensitivity has emphasized the need for confirmatory experiments in real sea waves.

In 1976, Sarpkaya (1976a, 1976b) reported the results of a comprehensive series of experiments with a sinusoidally oscillating flow about smooth and rough circular cylinders and demonstrated clearly the dependence of  $C_d$ ,  $C_m$ , and the lift coefficient  $C_L$  on the Reynolds number, Keulegan-Carpenter number, and relative roughness.

Recent laboratory experiments on rough cylinders include those by Sarpkaya U-tube tests (1978), Heideman et al. (1979), Pearcey (1979b), Nath and Wankmuller (1982), Nath (1980, 1981, 1982, 1983a, b, c, d, and 1984), and Nath et al. (1984).

#### 7.4 Sources of Uncertainty

The major sources of uncertainty in values of force coefficients that have caused the large scatter of these data according to Sarpkaya (1980) are:

- o The inaccurate determination of the fluid particle kinematics in many laboratory and ocean tests
- o The nonuniform techniques in deriving force coefficient data
- o Experimental error
- o Inexact description of the complex flow
- o Incomplete parameterization of the force coefficients.
- o Force model

Hudspeth (1983) has also reviewed environmental loads on ocean platforms with emphasis on uncertainties that exist in the current methods and procedures to estimate hydrodynamic forces on both small

and large displacement members.

#### 7.4.1 Fluid Particle Kinematics

Due to difficulties of accurately measuring ambient wave kinematics in experimental wave force measurement programs, most of the studies required that the kinematics used in the correlation of measured forces with the Morison equation be established through the use of some suitable wave theory. As a result different wave theories will, in general, produce different pairs of force coefficients for the same data. In field measurements, the situation is further complicated by the presence of ocean currents and the three-dimensionality of sea waves which will distort the values of local kinematics from that represented by a two-dimensional wave theory.

#### 7.4.2 Experimental Methods

Different techniques have been used by researchers in deriving force coefficients from force measurement data and are expected to produce different results, Ramberg and Niedzwecki (1979). The technique originally employed by Morison, et al. to obtain  $C_m$  and  $C_d$  was to set the measured force equal to either the drag or inertia component when the other was theoretically zero. Keulegan and Carpenter (1956, 1958) later separated the measured force into its Fourier components whose amplitudes could then be used to determine the force coefficients. With this method, a residual or remainder force, not accounted for by the original Morison technique, was identified both in amplitude and frequency. Another technique calls for fitting the Morison equation to the measured force record in a least-square error sense with  $C_m$  and  $C_d$  as the curve fit parameter. Each of the above methods is well-known and widely used. However, the different methods will, in general, produce different pairs of coefficients for the same force record. Even for one-dimensional harmonic flow conditions such as Sarpkaya's U-tube experiments, a 4 percent difference in the drag coefficient was obtained by comparing both the

Fourier and the integral least-square method (Sarpkaya, 1976a).

#### 7.4.3 Experimental Error

There are a number of possible situations which could result in experimental errors that could affect the force coefficients. Errors could result from measurement of the sea surface, calibration of the force transducers, error in measuring the fluid particle kinematics, etc. One possibility of experimental error is simply instrumentation sensitivity and the low magnitudes of forces and other variables during periods of small waves. Dean (1976) showed that depending on the wave and cylinder characteristics, data can be well or poorly conditioned for resolving drag or inertia coefficients, and it is believed that much of the scatter in the reported coefficients may be from data that was poorly conditioned for resolving them.

#### 7.4.4 Inexact Description of Complex Flow

The inexact description of the fluid-structure interaction by the Morison equation itself contributed a certain amount of uncertainty in determining the force coefficients. One source of uncertainty is the existence of vortex-generated lift or transverse force which is not included in simple forms of the Morison equation. In particular, the previously-described disturbance-sensitive region of vortex formation near the range of the Keulegan-Carpenter number from about 10 to 20, is often associated with large lift forces and asymmetry in the in-line forces.

There are additional hydrodynamic complexities encountered in wave flows that are not sufficiently described by the Morison equation, but add to the uncertainty in deriving force coefficients. The eccentricity of the water particle orbits and the orientation of the structural cylinder with respect to the orbits can cause asymmetric flow about the cylinder axis. This means that the wake is not necessarily always sweeping back and forth over the cylinder

(Pearcey, 1979b). Another complexity is represented by the flow not being always uniform along the span. This variation of flow along the span can introduce three-dimensional effects in a number of ways that influence the force coefficients. The instantaneous velocities and accelerations can have an axial variation which can alter the flow forces away from the distribution predicted using one-dimensional flow results. The other three-dimensional effect can arise from the wake which may be swept back over or near one segment of the cylinder after being generated at another segment under different flow conditions.

Another source of uncertainty concerns the theoretical influence of convective acceleration terms on the inertia force. The inertia force as applied to the Morison equation is usually taken as proportional either to the local (temporal) fluid acceleration or to the total (local plus convective) fluid acceleration at a point in nonlinear waves. Even though these may differ significantly from each other in typical design waves, no formal justification exists for adopting one over the other. Isaacson (1979a) derived a complete expression for the inertia force acting on a body in an unsteady nonuniform flow of an inviscid fluid. He found that the force depends on convective acceleration terms, although the force is not necessarily proportional to the total (i.e., local plus convective) acceleration at a point. However, he also found that for most wave conditions, these calculated forces are generally less than forces taken as proportional to the local fluid acceleration.

#### 7.4.5 Incomplete Parameterization of the Force Coefficients

Early researchers attempted to develop relationships between the differing values of the force coefficients used in the Morison equation and the Reynolds number parameter. Although some of the variation of the coefficients can be accounted for through the use of the Reynolds number, it became obvious that the relatively clear relationship which can be obtained in steady flow cannot be



replicated in oscillating flow. The pattern of scatter associated with experimental data on wave forces from oscillating flow has been somewhat more controlled by more recent experiments which includes both the Keulegan-Carpenter and the Reynolds numbers. Recent experiments suggest that other dimensionless parameters may be determined to further order the results of experiments and lend toward yet more precise methods for evaluating the force coefficients.

A critical review of the published data on the drag and inertia coefficients,  $C_d$  and  $C_m$ , has been undertaken by the British Ship Research Association (BSRA, 1976). A tabulated documentation of results from the BSRA investigation is shown in Table 7.1. A summary of most of the prominent laboratory and field tests on the study of wave force coefficients was provided with the values of the key parameters, associated test conditions, as well as their reliability and application to practical structures. Results from some of the more recent full scale tests (e.g., Exxon Ocean Test Structure, Conoco Test Structure) have been added to the list.

Hogben, et al., (1977) provide suggested values of  $C_d$  and  $C_m$  in relation to the corresponding values of the Keulegan-Carpenter number, KC, and the Reynolds number, Re, based on the BSRA study.

The KC and Re numbers are considered to be the best dimensionless parameters for parameterizing the values of force coefficients.

A review of drag and inertia forces on circular cylinders was conducted by Garrison (1980 and 1982) in which he presented the new data obtained in tests on rough cylinders at large Reynolds numbers. His results are compared with Sarpkaya and OTS data and conclude that the simple oscillatory flow data presented in the paper appear to be consistent with the wave force data measurements on the ocean test structure. He further shows that  $C_d$  values decrease sharply for  $Re > 2 \times 10^5$  in opposition to Sarpkaya data that became independent of Re in this range.

The Morison equation is important to offshore technology because it provides a basis for predicting fluid loadings due to waves, which are a crucial consideration for designing ocean structures. Government and industry regulatory bodies all have recommended the use of the Morison equation in designing offshore structures. However, proper values of drag and inertia coefficients are needed for safe calculation of wave forces by the Morison equation. In the foregoing discussion a brief review of existing data was presented and to be honest this is only the tip of the iceberg. A huge amount of data is being generated every day by various industry entities and it looks like the amount of confusion will get worse before it gets better. In spite of this enormous amount of data, it appears that when a real design condition arises the coefficients recommended are always the same and sometimes one may wonder if all this effort and expenditure are justified.

However, the engineer needs to obtain these force coefficients for his design. There are guidelines available which relieve some of the burden from the engineer and, by giving clear instructions, make life easier for the designer. One of these step-by-step instructions is given by Sarpkaya and Isaacson (1981). They suggest the following steps for selection of force coefficients  $C_m$  and  $C_d$  that, after all, coincide with the recommended values as suggested by regulatory agencies such as API, DnV, and UK DTI.

For smooth vertical cylinders it is recommended that:

- o A suitable wave theory (e.g. Stokes, 5th, stream function) be used to calculate the local KC and Re values prevailing at a given depth at the center of a cylinder segment,
- o Figure 7.2 adopted from the Shore Protection Manual (1977) or similar curves (Sarpkaya, 1976) may be used to obtain local drag

and inertia coefficients for corresponding KC and Re values,

- o for  $Re > 1.5 \times 10^6$ , the coefficients  $C_d = 0.62$  and  $C_m = 1.8$  be used,
- o the total in-line force acting on the entire member may be calculated by summing the forces acting on all segments,
- o the transverse force can be calculated in the same manner. For  $Re > 1.5 \times 10^6$  a lift coefficient of 0.2 is recommended.

For marine roughened vertical cylinders, it is recommended that:

- o The effective diameter of the cylinder (essentially the average diametral distance between the protrusions) be first estimated or determined as accurately as possible on the basis of past experience with structures at the same site; and
- o the total force acting on the cylinder be calculated, as previously described, through the use of a suitable wave theory, the Morison equation, apparent diameter of the pipe, and the drag and inertia coefficients. Experimentally obtained force coefficient data in function of KC and Re are given by Sarpkaya and Isaacson (1981) Nath and Wankmuller (1982), Nath (1980, 1981, 1982, 1983a, b, c, d, and 1984), and Nath et al. (1984). Suitable force coefficients are also recommended by regulatory agencies.
- o It is recommended that for large values of KC and Re a lift coefficient of  $C_L = 0.25$  be used.

Table 7.2 shows recommended values of  $C_d$  and  $C_m$  by various regulatory agencies.

## 7.6 Effects of Wave Orbital Motion, Current, Orientation, Marine Growth, and Interference

### 7.6.1 Effect of Wave Orbital Motion

The nature of flow is much more complex for a circular cylinder in waves than in the steady flow condition, and a well defined relationship between the drag coefficient and Reynolds number does not exist. In particular, the flow close to the cylinder is likely to be strongly influenced by two specific flow phenomena not present in steady flow: the water particle motions are orbital, and the oscillatory nature of the flow causes the wake of the cylinder to be swept back and forth over the cylinder.

The boundaries between the flow regimes in oscillatory flows and the associated fluid behavior are not clearly established as are those in steady flows. However, the published values of drag coefficients in waves still show an overall trend with the Reynolds number which is broadly similar to that found in steady flow where the drag coefficient decreases considerably with the Reynolds number over the approximate range  $10^4 < Re < 10^6$  (see Figure 7.2).

However, the differences in flow phenomena between oscillatory and steady flows are extremely important. These qualitative differences between steady and oscillating flow result in the quantitative differences in the force coefficient used in the Morison equation. There is an important distinction between the vortex phenomena observed for steady flow and those likely to occur for oscillatory flow. This is pointed out by Pearcey (1979a).

### 7.6.2 Effect of Current

A speculative generalization of the Morison equation concerns the combined waves and currents. It is ordinarily assumed (as recommended by API) that the Morison equation applies equally well to

predict flow with a mean velocity and that  $C_d$  and  $C_m$  have constant values equal to those applicable to rigid, stationary cylinders in wavy flows. This, in turn, implies that  $C_d$  and  $C_m$  are independent of the convection of vortices and its attendant consequences. The fact that this is not necessarily so is clearly evidenced by the measurements of Mercier (1973), Sarpakaya (1977) and Verley and Moe (1979). Clearly, extensive work is needed to determine the role played by the current, the validity of the Morison equation, the appropriate force coefficients, etc. Until such time as this is accomplished, the general practice within the offshore industry is to use the modified, biased Morison equation along with force coefficients obtained in wavy flows.

### 7.6.3 Effect of Member Orientation

In the original Morison equation, the velocity and acceleration components are defined to be at right angles to the vertical member axis. The vertical and tangential components are ignored in the force evaluation. A limited number of approaches to the problem have been proposed by Borgman (1958), Chakrabarti, et al. (1975) and others for applying the Morison equation to inclined members. A summary of the different approaches was reported by Wade and Dwyer (1976). Hoerner, (1965) proposed the independence or cross-flow principle or the "cosine law" which states that the normal pressure forces are independent of the tangential velocity for subcritical values of the Reynolds number based on the normal component of the velocity. The flow-independence principle has been commonly accepted for subcritical flow conditions but rejected for transitional flows. The recent wind tunnel data by Norton et al. (1981) shows that the flow-independence principle is valid, at least for cylinder inclinations up to  $50^\circ$  (the angle between the cylinder axis and the ambient flow velocity) as long as the Reynolds number based on the normal component of the velocity, remains entirely within either the subcritical or postcritical flow regime.

Studies on wave forces coefficient associated with inclined members are very limited. It is suggested by Hogben, et. al. (1977) that the values of drag and inertia coefficients should be found with the Reynolds number and Keulegan-Carpenter number evaluated from the cylinder diameter and the maximum normal velocity component.

In the case of oscillating members whereby the Morison equation with relative velocity is used, the  $C_m$  and  $C_d$  are customarily evaluated using the Re and KC based on wave water particle velocity only. This approach is adopted because the velocity of the structure is not known a priori and Re and KC cannot be evaluated based on relative velocity. Of course this will create further uncertainty in the correct representation of the forces. To eliminate this problem testing of the model structure with expected velocities is appropriate. This will allow more realistic  $C_m$  and  $C_d$  coefficients to be found.

#### 7.6.4 Effect of Marine Growth

Marine growth may be classified into two types: 'hard' growth includes barnacles, shell-fish and corrosion products, while 'soft' pliable growth consists mainly of seaweed. Marine growth both increases the effective diameter of a member, and may alter the flow over its surface, perhaps causing earlier flow separation. It is customary to allow for this increased diameter in design, but only recently have experiments revealed the often startling changes associated with the flow field. Marine growth may be characterized as shown in Figure 7.3, by:

- o A typical roughness height,  $k_r$ , defined as a representative maximum height of protrusion from an imaginary smooth surface to which the roughness is assumed to be attached;
- o the thickness of accumulated growth, giving an increase in cylinder diameter from  $D$  to  $(D + r)$ .

Values of  $k_r$  range from approximately 0.04 inch, for poorly painted, galvanized or very lightly rusted surfaces, up to about 2 inches for heavily fouled surfaces. Cylinder diameters,  $D$ , on jackets, semisubmersibles and tension leg platforms are in the range

$$20 < D < 400 \text{ inches}$$

The relative roughness,  $k_r/D$ , is consequently in the range

$$10^{-5} < k_r/D < 10^{-1}$$

Growths, mainly of the flexible variety, up to 8 inches thick have formed in less than 2 years in some areas and peak growth rates of 1 - 2 inches per month have been measured.

Generally the type and extent of growth are functions of the sea area (salinity, temperature, available nutrients) and of the depth below the surface (oxygen and/or light). The stronger growth occurs nearer the surface. Figure 7.4 shows the typical distribution of marine growth on a submerged member. It was mentioned earlier that a common design practice is to allow for increases in diameter up to a maximum of 4 - 12 inches, depending upon the sea area and immersion depth of the structural member involved. Experiments have been conducted in Sarpkaya's U-tube (1978), in laboratory and sea waves by Heideman et al. (1979) and Pearcey (1979b) respectively, at large Reynolds numbers. Recent experiments on rough cylinders include those by Nath and Wankmuller (1982), Nath (1980, 1981, 1982, 1983a, b, c, d, and 1984), and Nath et al. (1984). The results show that "hard" roughness increases the drag coefficient substantially, in some cases doubling the wave forces, even after allowing for the effective increase in diameter.

As in steady flow, the critical Reynolds number decreases as the relative roughness increases. In post-critical conditions the drag coefficient  $C_d$  reaches a constant plateau value. Sarpkaya's

plateau values, however, are higher than those shown in Figure 7.5. This figure summarizes results of a number of steady-flow experiments. Even at  $KC = 100$ , where near-steady flow conditions might be expected, Sarpkaya's values are still some 50 percent larger. In the discussion of his paper Sarpkaya (1978) revealed that he could achieve steady-flow values, but only at exceptionally high Keulegan-Carpenter numbers (around 1000). Experiments in large-amplitude laboratory waves by Pearcey (1979b) tend to support Sarpkaya's high values. OTS results by Heideman et al. (1979) however, obtained in real sea waves and also shown in Figure 7.5, agree well with the lower steady-flow values. Again these differences may be associated with the degree of coherence in the vortex wake and wave encounter phenomenon. The lower OTS values may be due to random three-dimensional effects on vortex-shedding and their convection and wave encounter phenomenon.

Pearcey (1979b) also reports some recent preliminary experiments on soft forms of marine growth, and suggests that these may increase wave loads still further. This additional increase may be associated with inertial effects, as the fronds of seaweed are swept back and forth.

#### 7.6.5 Interference and Shielding Effect

The forces on a member in close proximity to another will be affected by the wake field. It is possible for the vortices in the wake from the first member to excite the dynamic response of the member behind it, leading to an effective increase in the forces computed from the Morison equation. Conversely, it is possible that a small member surrounded on all sides by larger members will be shielded and experience a smaller force. It is probable that the effects of interference or shielding are negligible if the separation is greater than both the diameter of the larger member and the water particle orbit diameter. In most cases only the drag component of the wave induced force will be changed. A careful review of flow interference



between two circular cylinders in various arrangements has been presented by Zdravkovich (1977) where an extensive list of references may be found.

#### Added Mass of Group of Members in Close Proximity

If several members are placed close together, for instance, conductor tubes in an offshore oil production platform, there will be a tendency for a portion of the mass of water enclosed by them to act as part of the structure. This will lead to an effective increase in the inertia coefficient  $C_m$  for all the members. The actual increase will vary with the configuration, but for conductor tubes 2.5 feet in diameter arranged on a square grid with 7 feet center to center the inertia coefficient has been found to be as high as 3.0.

The potential flow theory may be used to determine the inertia coefficient for each cylinder through the use of the method of images and complex variables (see Robertson 1965, Dalton and Helfinstine 1971, Spring and Monkmeyer 1974, Yamamoto 1976, Yamamoto and Nath 1976, and Dalton 1980).

Gibson and Wang (1977) carried out a series of tests to determine the added mass of a series of tube bundles.

### 7.7 Linearization of the Morison Equation

As discussed in Section 7.2, the Morison equation includes a nonlinear drag expression arising from the velocity square term. For a frequency domain analysis, this nonlinear term must be linearized. Basically, the linearization process relies on the minimization of the error between the nonlinear term and its linear approximation. The linearized drag term in the Morison equation is usually written as

$$F_D = C_d \frac{1}{2} \rho A |u| u \approx C_{d1} \frac{1}{2} \rho A u \quad (7.9)$$

where  $C_{d1}$  is the linearized drag term.

Krylov and Bogoliubov (1943) described an equivalent linearization technique in connection with nonlinear vibration problems. They hypothesized that the work dissipated by nonlinear force during one cycle of oscillation should be equivalent to the work dissipated by the linearized force during the same cycle of oscillation. This idea has been used extensively in the linearization of the Morison equation as will be seen later.

Some other researchers have adopted the least square minimization technique for linearizing the Morison equation. This method is based on minimizing the error between the experimental force and the theoretical formulation, thereby obtaining the coefficients of linearization.

Another widely used linearization method is based on the "Describing Functions" technique. Electrical engineers for years have been dealing with the linearization of nonlinear input. In this method, the input is expressed in its Fourier components and only a few terms of this expansion are used as a linear representation of the nonlinear phenomenon. Gelb and Vander Velde (1968) give a detail definition of describing functions technique in connection with electrical circuits. In applying this method to the Morison equation it is customary to retain only the first term of the Fourier series and assume the higher order terms to be negligible.

Borgman (1967) used the least square minimization technique to linearize the drag term in the basic form of the Morison equation where no current or relative velocity was involved. He concluded that

$$|u|u \cong u_{rms} \sqrt{\frac{8}{\pi}} u \quad (7.10)$$

or

$$C_{dl} = C_d u_{rms} \sqrt{\frac{8}{\pi}} \quad (7.11)$$

Malhotra and Penzien (1970) followed Borgman's approach to linearize the Morison equation with relative velocity. They obtained

$$\left| u - \dot{X} \right| (u - \dot{X}) = (u - \dot{X})_{\text{rms}} \sqrt{\frac{8}{\pi}} (u - \dot{X}) \quad (7.12)$$

The same result can be obtained using equivalent linearization of Krylov and Bogoliubov (1943).

For regular waves a linearization provided by Thompson (1972) based on equating the energy dissipated by the viscous damping to that of the nonviscous damping with harmonic motion is given by

$$\left| u \right| u = \frac{8}{3\pi} u_0 u \quad (7.13)$$

where  $u_0$  is the amplitude of the oscillatory velocity. Paulling (1981) indicates that this linearization may be used for regular platform and wave motion.

Tung and Huang (1973) extended Borgman's technique to include current and wrote expressions for the linearized drag force as well as a modified wave energy density spectrum in the presence of current.

Wu and Tung (1975) followed Malhotra and Penzien's approach to obtain a statistical linearization of the Morison equation including relative velocity and current.

Blevins (1977) proposed a linearization method similar to the describing functions technique based on expansion of the relative velocity in its Fourier components and retention of the first term of this series.

Daring and Huang (1979) followed the equivalent linearization technique of Krylov and Bogoliubov to linearize the Morison equation

with relative velocity and current. They applied this method to regular sea only. However, their method can be extended to random sea without major difficulty.

Krolikowski and Gay (1980) extended the Blevins approach to include current in the relative velocity. They applied this improved linearization technique to marine risers in both regular and random sea states.

It should be mentioned that in linearizing the drag force in the Morison equation where a relative velocity term is used an iterative process is needed to converge to linearization coefficients. The iteration is needed because at the start of the linearization process the structural velocity is unknown. Usually the displaced configuration of the structure under some static loads is used to initialize the iteration.

Gudmestad and Connor (1983) reviewed the linearization methods and the influence of current on the nonlinear hydrodynamic drag force. They note that in linearizing the Morison equation through equivalent linearization techniques, terms emerging from nonlinear drag force having frequencies  $2\omega_p$ ,  $3\omega_p$ , etc. are not accounted for in a frequency domain analysis. Here  $\omega_p$  represents the peak frequency of the exciting wave. However, for deepwater structures, these terms may increase the force spectral density near the fundamental natural period of the structure and thereby increase the response of the structure considerably (see also Sigbjomsen et al., 1978; Mes, 1978; Smith, 1978).

## 7.8 Vortex Shedding On Flexible Cylinders

Many of the of the offshore structures now being designed and built include a variety of circular cylinders. When water flows past a cylinder, a periodic wake is formed by vortices shed from alternate sides of the cylinder. Shedding of the vortices gives rise to an

alternating force perpendicular to the direction of the flow propagation. This transverse force is known as lift force, in contrast to the in-line force which is applied in the direction of the flow propagation (See Figure 7.6). Figures 7.7 and 7.8 show the initiation of vortex shedding and the alternate shedding of vortices and its relation to the lift force. If the condition is right a cylinder may undergo sustained oscillation under the action of these lift forces.

Problems that are caused by vortex shedding and the vortex-excited oscillations of marine structures often have been ignored in the past, largely because reliable experimental data and design methods have not been available. However, as marine construction has moved into deeper water and into harsher operating environments such as the North Sea, the need to design slender, flexible structures and structural members against vortex shedding-related problems has increased in importance. The steady and unsteady vortex-excited hydrodynamic forces and their associated deflections and vibrations cause amplified stress levels and fatigue, and they often lead to structural damage and eventually to failure.

Many types of marine structures are susceptible to vortex-excited oscillations. These include the risers and conductor tubes that are employed in oil exploration and production, deepwater pipelines, and members of jacketed structures. Deepwater piling installations and driving operations also are hampered sometimes by problems arising from vortex shedding.

The phenomenon of vortex shedding on cylindrical marine structures has received considerable attention in recent years. The importance of vortex shedding lies in the associated lift forces which are dynamic in nature. When the vortex shedding frequency brackets the natural frequency of a flexible or flexibly mounted cylinder, the cylinder takes control of the shedding process causing vortices to be shed at a frequency close to or at one of its natural frequencies.

This phenomenon is called vortex shedding "lock-in" or synchronization. Under "lock-in" conditions, large resonant transverse oscillations occur and lift forces are amplified due to increased vortex strength and spanwise correlation along the cylinder. Large in-line oscillations are usually associated with resonant oscillations in the transverse direction. This is attributed to a substantial increase in the in-line drag under these conditions. Large responses in both directions give rise to oscillatory stresses. If these stresses persist for a long enough period of time, significant fatigue damage occurs.

New marine structures have long flexible cylindrical members and therefore are susceptible to resonant hydroelastic oscillations in both current and wave environments. When a particular design is likely to undergo hydroelastic oscillations, most engineers either try altering the design to offset its natural frequency from the shedding frequency or use vortex suppressors. Both solutions can be quite expensive and the latter may not be that effective. On the other hand, in some cases, hydroelastic oscillations are not that dangerous and such measures may not be necessary. In either case, a reliable analytical model to predict vortex shedding induced oscillations and associated stresses is highly needed at this stage.

#### 7.8.1 Theoretical Background

The separation of flow and alternate vortex shedding phenomenon is intrinsic to the flow itself and has been known at least since the times of Leonardo da Vinci. Almost 100 years ago, Strouhal (1878), in connection with his work on a special method of creation of sound, discovered that there is a relationship between the frequency of vortex shedding, the velocity of flow, and the diameter of the cylinder. This relationship which is known as the Strouhal number,  $St$ , is given by:

$$St = f_v D/u \quad (7.14)$$

where  $f_v$  is the vortex shedding frequency,  $D$  is the cylinder diameter, and  $u$  is the flow velocity. His data showed that the Strouhal number is nearly constant for a wide range of values of  $D$  and  $u$ . Strouhal's own data suggested a value of about  $St \approx 0.185$ . The characterization of the vortex shedding process by a simple frequency is a practical simplification. The Strouhal number is a function of the Reynolds number for a given body. Figure 7.9 shows the relationship between the Strouhal number and the Reynolds number.

Other parameters that have been found to be of major importance in determining the amplitude of oscillations and the range of synchronization for a given body are

$$V_r = u/f_n D \quad (\text{reduced velocity}) \quad (7.15)$$

$$K_s = m / \pi D^2 \quad (\text{stability parameter}) \quad (7.16)$$

$$R_p = m / \pi L D^2 (C_L^0)_{rms} \quad (\text{response parameter}) \quad (7.17)$$

where  $V_r$  is the reduced velocity,  $u$  is the flow velocity,  $f_n = 1/T_n$  is the natural frequency of the body,  $D$  is the cylinder diameter,  $m$  is the effective mass of the cylinder,  $C_L^0$  is the lift coefficient of a stationary cylinder in the hydrodynamically similar flow.

Vortex shedding on cylinders can be induced by waves as well as currents. In the past, most of the attention in both research and design was given to hydroelastic oscillations produced by vortex shedding in currents. Recently, Sarpkaya and Rajabi (1979) have shown that vortex shedding in harmonic flow is at least as important. They established vortex shedding "lock-in" for an elastically mounted cylinder in two-dimensional harmonic flow. Their results indicated that perfect "lock-in" occurs at a reduced velocity  $V_r (=u/f_n D)$  of 5.5. At this condition, the amplitude of the lift coefficient is amplified by nearly a factor of 2 as compared to a

fixed cylinder in a hydrodynamically similar flow.

Studies on cylinders undergoing hydroelastic oscillations concentrated more on the response rather than the force. Rajabi (1979) studied both response and lift forces on smooth and rough cylinders in harmonically oscillating flow. He correlated the response of the rough and smooth cylinders with the response parameter  $R_p$ . Figure 7.10 shows the relationship between the ratio of amplitude of oscillations to cylinder diameter against the response parameter  $R_p$ . Zedan et al. (1980) used a cantilever pile to experimentally study the hydroelastic oscillations in waves. The results showed that "lock-in" can be established at a reduced velocity  $V_r$  somewhere between 5.5 and 7.5 depending on the water depth parameter "kd" (= wave number x depth). Using the cantilever pile test data, Zedan and Rajabi (1981) were able to establish the lift forces in that experiment. At "lock-in", it was shown that the lift coefficient is monoharmonic with a frequency equal to the expected vortex shedding frequency at the Reynolds,  $Re$ , and Keulegan-Carpenter,  $KC$ , numbers of the test. The amplitude of the lift coefficient at "lock-in" conditions was amplified by a factor of 1.6 to 1.93 (for different tests) as compared to a stationary cylinder in harmonic flow at the same  $KC$  and  $Re$  numbers. Angrilli and Cossalter (1981), conducted similar tests in waves but at a much smaller scale. Their results generally agreed with those of Zedan et al. (1980) and Zedan and Rajabi (1981).

The lift forces and responses induced by vortex shedding in current are studied by Griffin (1982) and King (1977).

The lift frequency is generally equal to the vortex shedding frequency  $f_v$  which can be predicted from the Strouhal number versus Reynolds number correlation. Therefore, the excitation lift force can be approximated by a monoharmonic function of time with a frequency equal to  $f_v$  (CIRIA Report (1980), Hallam et al. (1978), Blevins (1977)). This is particularly correct in regions of  $Re$  where



vortex shedding is predominantly periodic or at "lock-in" condition. The amplitude of the lift coefficient on a fixed cylinder is a function of Reynolds number; this relation is given in the CIRIA Report (1980) and Hallam et al. (1978). For a flexible cylinder undergoing hydroelastic oscillations at "lock-in", the lift forces are amplified and become more periodic (monoharmonic) because of stronger vortices and better spanwise vortex correlation. There are no systematic data available in the literature to describe the lift amplification in this case.

The in-line force acting on a cylinder usually is described by the well-known Morison equation (1950). The validity of this equation, for fixed cylinders in waves or two-dimensional harmonic flows has been demonstrated by Sarpkaya and Isaacson (1981). For flexible cylinders, it is customary to use the relative velocity between the fluid particles and the oscillating cylinder (in the direction of wave propagation) in the Morison equation instead of the particle velocity. Also, an inertia term is added to the Morison equation to account for the effects of cylinder oscillation on surrounding fluid. When a current is present, a widely accepted practice is to add its velocity component in the in-line direction to the wave particle velocity in the Morison equation. The validity of these modifications of the Morison equation is not yet established.

The use of the Morison equation in the manner described earlier to represent the in-line force under vortex shedding "lock-in" is still inadequate. Experimental results have shown a substantial increase in the in-line response when "lock-in" was achieved in the transverse direction. This is customarily explained by a substantial increase in the in-line drag coefficient. A similar increase in the in-line response was noticed in the case of cross flow vortex-excited oscillations produced by a current. Fischer et al. (1979) studied the hydroelastic oscillations for model piles in a steady current. For low flow velocities, the measured and predicted tip in-line deflections agreed when the pile was effectively stationary in the

transverse direction. When the critical flow velocity for the onset of transverse hydroelastic oscillations was exceeded, the measured in-line steady deflection was almost twice the predicted deflection using the same drag coefficient as before. This has been explained by Griffin (1982) as an increase in the drag coefficient due to resonant cross flow oscillations. The in-line drag amplification has been measured under a variety of conditions and results were reported by Griffin and Ramberg (1975). Griffin (1980) has discussed the problem in detail. The ratio of the drag coefficient of a cylinder undergoing hydroelastic oscillations  $C_{da}$  to that of a stationary cylinder  $C_d$ , was correlated with the amplitude and frequency of the transverse response. The correlation is given by

$$C_{da}/C_d = 1 \quad \text{for } W_r < 1 \quad (7.18)$$

$$C_{da}/C_d = 1 + 1.16 (W_r - 1)^{0.65} \quad \text{for } W_r > 1 \quad (7.19)$$

where:  $W_r = (1 + 2 \bar{z}/D)/(V_r St)$ ;  $\bar{z}$  = amplitude of transverse oscillations;  $D$  = cylinder diameter;  $V_r$  = reduced velocity; and  $St$  = Strouhal number. Sarpkaya (1981c) suggested the following correlation,

$$C_{da}/C_d = (1 + 2 \bar{z}/D) \quad (7.20)$$

The in-line drag correlations discussed above were developed for hydroelastic oscillations in steady flows. No similar correlations were developed for hydroelastic oscillations in waves. Since the phenomenon is similar in waves and currents, it can be hypothesized that the above correlations are applicable in both flows. Although this hypothesis is questionable, it can be adopted until better correlations are available in wave flows. Furthermore, it should be mentioned that the expression proposed by Sarpkaya was developed based on experimental data from a low Reynolds number flow and its use in connection with high Reynolds number flows is beyond the limits for which it was conceived.

### 7.8.2 Forcing Functions Model

Several mathematical models have been proposed. Noteworthy among them are works by Hartlen and Currie (1970), Skop and Griffin (1973), Iwan (1974), Iwan and Blevins (1974), Parkinson (1974), Naudascher (1974), Currie et al. (1974), Eaton (1974), Blevins and Burton (1976). These models usually do not include the analysis of the flow field and the fluid mechanical arguments invoked in their evaluations are not altogether convincing. Thus their worth should be measured not so much by their capacity to obtain functional relations among significant parameters that lead to the basic understanding of the phenomenon but by their ability to produce results which are qualitatively similar to those obtained experimentally.

The most noteworthy among the oscillator models is the one proposed by Hartlen and Currie (1970) where a Van der Pol-type soft nonlinear oscillator for the lift force is coupled to the body motion by a linear-dependence on cylinder velocity. The model has its roots in mechanics and electricity rather than in the equations of fluid motion.

Recently Rajabi et al. (1983) introduced a model for representation of the vortex shedding induced lift forces based on the latest available experimental data. They used this model to predict the response of marine risers in the transverse direction due to vortex shedding. The lift amplification was considered at or near the "lock-in" conditions. The model also allowed for the evaluation of drag amplification due to transverse oscillation at "lock-in" conditions.

In their model the transverse force per unit length was split into two parts; namely, a lift force  $F_L$  and a resisting force  $F_r$ . Therefore,

$$F_{\text{trans}} = F_L - F_r \quad (7.21)$$

The lift force per unit length was represented by

$$F_L = \frac{1}{2}\rho D u^2 C_L^0 (C_L/C_L^0) \cos(\omega_V t - \theta) \quad (7.22)$$

Where  $\rho$  = water density;  $\omega_V$  = predominant circular lift frequency  
 $C_L/C_L^0$  (lift amplification parameter) = the ratio of the actual lift coefficient of the oscillating cylinder to the lift coefficient of a stationary cylinder in hydrodynamically similar flow;  $u$  = water particle velocity amplitude in the direction of flow propagation;  $\theta$  = a phase angle;  $t$  = time; and  $D$  = diameter.

In this equation  $u$  is a function of elevation since it varies along the cylinder. The Airy wave theory provides a simple expression for its variation.  $C_L^0$  is a function of both the Reynolds and Keulegan-Carpenter numbers ( $Re$  and  $KC$ ), which vary along the cylinder.  $C_L^0$  can be obtained from the two-dimensional harmonic flow data of Sarpkaya (1976) based on local values of  $Re$  and  $KC$ . The predominant lift frequency is assumed to be equal to the dominant vortex shedding frequency, i.e.  $2\pi f_V$ . For fixed cylinders, Sarpkaya (1976a, 1976b) and others (Isaacson and Maul, 1976) found that the lift force is generally periodic but not exactly monoharmonic, and that the ratio of dominant shedding (lift) frequency to the wave frequency ( $f_V/f_W$ ) is a function of both  $Re$  and  $KC$ . These results were confirmed by recently published data on vertical cylinders by Torum and Reed (1982). The CIRIA Report (1980) and Hallam (1978) give an empirical correlation based mostly on Sarpkaya's data. This correlation can be used to predict the dominant vortex shedding frequency. Since  $Re$  and  $KC$  vary along the cylinder, one expects to obtain a number of possible shedding frequencies. The closest of these frequencies to the lowest mode natural frequency of the cylinder can be chosen as the lift frequency. This model assumes "lock-in" with one of the cylinder modes and that perfect correlation exists along the cylinder.

The lift amplification parameter  $C_L/C_L^0$  has been shown by Sarpkaya et al. (1981) to be a function of  $KC/KC^*$ .  $KC^*$  is simply equal to  $KC$  at perfect synchronization. It is obvious that  $KC/KC^*$  equals the corresponding ratio of reduced velocities i.e.  $V_r/V_r^*$ . Figure 7.11 shows  $C_L/C_L^0$  versus  $V_r/V_r^*$  based on harmonic flow data of Sarpkaya (1976a, 1976b), Rajabi (1979), and wave data of Zedan and Rajabi (1981). For a cylinder  $V_r^*$  is the reduced velocity at the location on the cylinder where the shedding frequency is chosen to be the dominant. Since  $V_r$  varies along the cylinder, one expects to obtain different amplification parameters along the cylinder.

This lift model can be used either for waves or current. In the case of current,  $u$  will be replaced by the local current velocity  $V_c$ , and  $C_L^0$  is the lift coefficient produced by a current on a fixed cylinder.  $C_L^0$  is a function of  $Re$ , and is given in the CIRIA Report (1980) and Hallam (1978). The dominant lift frequency  $\omega_v$  is evaluated as in the case of waves, with the exception of the use of the Strouhal number - Reynolds number correlation to find all possible shedding frequencies along the cylinder. There are no systematic data available on  $(C_L/C_L^0)$  for this case, therefore a value of 1 may be assumed until better data are found.

As a result of cylinder oscillations in the transverse direction, a resisting force is generated which can be represented by the Morison type equation in the form

$$F_r = \frac{1}{2} \rho C_d D \left| \dot{z} \right| \dot{z} + \rho \frac{\pi D^2}{4} (C_m - 1) \ddot{z} \quad (7.23)$$

Where  $z$  represents the transverse response of the cylinder and dot represents partial differentiation with respect to time.

The modified Morison equation may be employed to describe the hydrodynamic loading in the in-line direction. Therefore,

$$\begin{aligned}
 F_y(x,t) = & \frac{1}{2} \rho D C_d (C_{da}/C_d) \left| (u - V_c - \dot{y}) \right| (u + V_c - \dot{y}) \\
 & + \rho \frac{\pi D^2}{4} C_m \dot{u} - (C_m - 1) \ddot{y}
 \end{aligned}
 \tag{7.24}$$

where  $V_c$  = steady current speed,  $y$  = displacement in the in-line direction,  $C_m$  = inertia coefficient,  $C_d$  = drag coefficient for a stationary cylinder,  $C_{da}/C_d$  = drag amplification parameter. Figure 7.12 shows a schematic of the local axis system used to define vortex shedding forcing functions on flexible cylinders.

The coefficients  $C_m$  and  $C_d$  are functions of  $Re$  and  $KC$  which vary along the cylinders. The drag amplification may be obtained from correlations presented previously.

Summary of literature giving explicit  $C_M$  and  $C_D$  values (the  $C_M$  and  $C_D$  force, and  $R$  and  $K_c$  have been evaluated using the maximum horizontal wave particle values given are applicable to the calculation of the horizontal component of wave orbit velocity at the still water level), unless otherwise stated).

AUTHOR	LOCATION	SEA STATE	STRUCTURE	$K_c$ and $R_e$	$C_D$	$C_M$	Reliability/wave theory
Reid (1958)	Gulf of Mexico	Small amplitudes sea waves $2 < H < 4$ ft $3 < T < 5$ s Wind speed 10-30 mile/h Current 0.5 - 0.7 ft/s at surface	Vertical cylinder clamped above water with other end loose $D = 8.625$ in.	$K_c = 10-20$ , $R_e = 10^5 - 2 \times 10^5$	0.53 Standard deviation 0.20	1.47 Standard deviation 0.36	Measured wave force records and those calculated using constant mean $C_M$ and $C_D$ values given showed good agreement; linear spectral technique was used, with the effect of a current considered in the analysis. Inertial force was about double the drag force. Structural vibration was observed and allowed for in the analysis.
Wiegell et al (1957)	Pacific coast of California at Davenport	Storm waves $5 < H < 20$ ft $9 < T < 17$ s $45 < d < 50$ ft Wind waves superimposed on the swell.	Vertical cylinder $D = 6.625$ in., 1.0, 2.0, 5.0 ft, with test section at various depths	$K_c = 8-40$ , $R_e = 3 \times 10^4 - 9 \times 10^7$ , evaluated at test section level using maximum Airy orbital velocity.	0.1-5.0 Extremes of scatter. Average about 0.5-0.7 at $R_e = 5 \times 10^5$ , increasing to 1.0 and above at smaller $R_e$	0.7-6.0 Extremes of scatter. 2.5 given as mean value of a Gaussian distribution	Local forces, calculated using linear wave theory and average values of $C_M$ and $C_D$ differed from measured forces by up to about 100%. The large scatter was attributed to roughness, turbulence, wind waves and shallow water effects. Effect of a current was not considered. Structural vibration, which resulted in fatigue failure, was observed.
William (1965)	Gulf of Mexico	Confused sea on two wave trains Observed H and T $3 < H < 8$ ft $5 < T < 8$ s $d = 38$ ft Wind speed 10 knots Current 0.55 ft/s at surface	Vertical cylinder suspended in the water $D = 2.5$ ft	$K_c = 5-15$ , $R_e = 3 \times 10^5 - 10^6$	(a) 0.32 Current not considered (b) 0.60 Current considered (c) 0.75 Current considered and phase correction between force and wave recorded included (d) 1.79 Best results from (b) and (c) averaged	(a) 1.53 Current not considered (b) 1.54 Current considered (c) 1.36 Current considered and phase correction between force and wave recorded included (d) 1.53 Best results from (b) and (c) averaged	Large scatter in $C_D$ and $C_M$ values from different wave force record analyses; correlation between calculated and measured force varied from poor to very good for individual records. A linear spectral method of data analysis was used. $C_D$ values were significantly affected by current; $C_M$ appeared to be unaffected by the current. Structural vibration, which resulted in fatigue failure, was observed.

TABLE 7.1

Fig. 2

FIELD STUDIES

AUTHOR	LOCATION	SEA STATE	STRUCTURE	$K_c$ and $R_e$	$C_D$	$C_M$	Reliability/wave theory
Bretschneider (1967)	Calif, coast, Davenport	Storm waves 5<H<20 ft 9<T<17 s 45<d<50 ft	Vertical cylinders D = 1, 2 ft	$K_c = 8-10, R_e = 10^5-10^6$ evaluated using linear theory values beneath the wave crest, considering variation with depth	0.4-1.5 Higher values more probable	2-5 Lower values more probable	$C_D$ at 1% level = 0.5-20%, $C_M$ values were unsatisfactory. Probabilistic approach considering peak drag and inertial forces and linear wave theory
Asgard and Dean (1969)	Gulf of Mexico wave projects I and II	Hurricane storm waves 6<H<40 ft 6<T<17 s d = 30, 100 ft	Vertical cylinders d = 30 ft D = 1, 2, 3, 4 ft d = 100 ft D = 3.7 ft	$K_c = 15-50, R_e = 10^4-10^7$ evaluated using Stokes fifth order theory values beneath the wave crest, considering variation with depth	1.2-0.5 decreasing with $R_e$ For in-line force	1.33 For in-line force	Calculated forces averaged over H, T, d agreed to within 10% of measured total forces. Calculated and measured local force maxima agreed to within 50%. Effects of currents not considered. Stream function wave theory to be used with wave force evaluation technique given
Evans (1969)	Gulf of Mexico wave projects I and II	Project I 10<H<20 ft 6<T<10 s d=30 ft Project II 25<H<45 ft 10<T<17 s d=100 ft	Vertical cylinders D = 1, 2, 3, 4 ft Vertical cylinder D = 3.7 ft	$K_c = 20-50, R_e = 10^5-2 \times 10^6$ , evaluated using Stokes fifth order theory wave crest and trough values. $K_c = 10-30, R_e = 10^5-5 \times 10^6$ , evaluated using Stokes fifth order theory values beneath the wave crest, considering variation with depth	0.5  0.58 Standard deviation 0.33	1.5  1.76 Standard deviation 1.06	Wave force project I. Calculated total forces were generally within 10% of the measured forces, and usually conservative Wave force project II. $C_M$ and $C_D$ were averaged over H, T, d but varied appreciably with H, T, d. Agreement between measured local forces and those calculated using local $C_M$ and $C_D$ values was quite good. Maximum total forces calculated using mean $C_M$ and $C_D$ values generally agreed to within 10% of measured forces and were usually conservative Wave force projects I and II. Wave theory to be used depends on wave characteristics, and is one of Chappelier, Stokes fifth order, linear or McCowan, to be used in the wave force evaluation technique given. Effects of currents were not considered
Grace & Casciano (1969)	Hawaii coast	Small sea waves 1.7<H<5.6 ft 11<T<16 s d=25 ft	Sphere on seabed D=8 in	$K_c = 6-60, R_e = 6 \times 10^4 - 9 \times 10^5$ , evaluated using Stokes third order theory maximum orbit velocity at the centre of the sphere.	0.7	1.2	Peak forces calculated using Stokes third order wave theory were generally within 25% of the measured forces. The wave force was drag dominant; a constant value of $C_M$ was assumed. The same H, T for different waves gave $C_D$ values differing by over 100%.



FIELD STUDIES

Author	LOCATION	SEA STATE	STRUCTURE	$K_c$ and $P_c$	$C_D$	$C_M$	Reliability/wave theory
Wheeler (1969)	Gulf of Mexico wave force project II	Hurricane storm waves 20<H<40 ft 10<T<17 s d=99 ft	Vertical cylinder d = 3.7 ft	$K_c=24-65, R_e=2.5 \times 10^6$ $5 \times 10^6$	0.6 Smaller ( $\approx 0.4$ ) at surface	1.2-2.0 Varying with depth	Measured and calculated maximum local forces differed by up to 40% in high waves. A linear spectral method of data analysis was used. Effect of currents was not considered.
Mudspeth et al (1974)	Gulf of Mexico wave force projects I and II	Hurricane storm waves 10<H<40 ft 6<T<17 s d=33, 100 ft	Vertical cylinders d = 30 ft D = 1, 2, 3, 4 ft d = 100 ft D = 3.7 ft	$K_c=10-70, R_e=10^4-10^7$ , evaluated using Stokes fifth order theory values beneath the wave crest, considering variation with depth.	1.2-0.5 decreasing with $R_e$	1.1	Methods and results of data analysis using linear spectral wave theory and stream function wave theory were compared. The standard deviation between measured and calculated forces was smallest for the $C_M$ and $C_D$ values given using the stream function theory
Kim and Hubbard (1975)	Pass Straits, Australia	Small amplitude sea waves 2.55<H<9.87 ft (significant height) h.35<T<8.70 s (dominant period) d = 7.25 ft at test section. Current = 1 ft/s	Vertical cylinder D = 12.75 in.	$K_c=12-80, R_e=2.5 \times 10^5$ $8.0 \times 10^7$ , evaluated using measured velocity at test section	0.61 Standard deviation 0.24	1.2 Standard deviation 0.22	$C_D$ was stated to be constant and independent of $R_e$ above $R_e=2 \times 10^5$ . Agreement between measured and calculated force was good in the drag dominated part of the wave cycle, and fair in the inertia dominated part. Orbit velocity was measured.
Heideman, Olsen and Johansson (1979)	Gulf of Mexico, Ocean Test Structure	Storm waves 9<H<24 ft 6<T<12 s water depth, 66 ft	Vertical cylinders D = 16 in 1/5 scale prototype	$K_c=5-48, R_e=2 \times 10^5 - 8 \times 10^5$ Evaluated by measured velocity at test section.	1.5-0.68 mean values for clean members, decreasing with $K_c$ . 1.8-1.0 mean values for fouled members, decreasing with $K_c$	1.51-1.65 mean values for clean members. 1.25-1.43 mean values for fouled members	Wave force coefficients calculated based on measured kinematics with a current meter 4.67 ft away from force transducer. Large scatter at low $K_c$ , but decreases considerably at high $K_c$ . Agreement between calculated and measured force traces was very good. Calculation of total force using Stokes fifth order theory overpredicts the measured total force by 10%.
Olmart & Gratz (1979)	Gulf of Mexico, Conoco Full Scale Test Structure	Hurricane storm waves 18<H<35 ft 6.0<T<10.5 s water depth, 177 ft	Vertical cylinder d = 36 in.	$K_c=5-17, R_e=3 \times 10^5 - 3 \times 10^6$ , evaluated by measured velocity at test section.	mean value of 0.7 for $1 \times 10^6 < R_e < 3 \times 10^6$ 0.06 for $3 \times 10^5 < R_e < 1 \times 10^6$	1.5	Wave force coefficients were calculated based on kinematics measured by current meters 5 ft from force transducer. $C_D, C_M$ showed considerable scatter. There was some sign of $C_D$ dependence on $R_e$ .

TABLE 7.1 (CONT'D)

(BSRA, 1976)

LABORATORY STUDIES

Author	Location	Sea State	Structure	$V_c$ and $K_c$	$C_D$	$C_M$	Reliability/wave theory
Morison et al (1950)	Laboratory	Linear sinusoidal waves $0.1 < d/\lambda < 0.5$ $h, 0 < d/H < 18.2$	Vertical cylinder $0.01 < d/\lambda < 0.04$ $0.2 < D/H < 0.8$	$K = 4-25, R = 2 \times 10^3$ $8 \times 10^5$ , evaluated using measured velocity at test section	1.626 to 4.14	1.508 to 0.197	Measured moments and moments calculated using linear wave theory and constant $C_M$ and $C_D$ values derived for individual waves agreed well over a wave cycle. $C_M$ and $C_D$ did not correlate well with $d/\lambda, D/\lambda$ or $R_e$ .
O'Brien & Morison (1952)	Laboratory	Linear sinusoidal waves $0.2 < H < 0.4$ ft $0.6 < T < 2.2$ s $0.9 < d < 1.3$ ft	Spheres on bottom of water channel $0.030 < D < 0.125$ ft	$K = 1-4, R = 1.9 \times 10^3 - 7.8 \times 10^3$ , evaluated using maximum orbital velocity at centre of sphere	0.8-3.0	0.9-1.6	Measured forces and forces calculated using linear wave theory and constant $C_M$ and $C_D$ values derived for individual waves agreed well over a wave cycle. Alternative derivation methods gave $C_M$ values varying over 100% for the same wave and $C_D$ value.
Keulegan and Carpenter (1958)	Laboratory	Linear sinusoidal standing wave $0.10 < U_M < 0.75$ m/s	Horizontal cylinders and flat plates submerged under standing wave $0.5 < D < 3.0$ in.	$K = 2-120, R = 4 \times 10^3 - 3 \times 10^4$ , evaluated from values of $U_M$ given.	0.7-2.2 cylinders, 1.8-11.5 plates. Presented as functions of $K_c$ .	0.6-2.6 cylinders, 1.1-5.0 plates. Presented as functions of $K_c$ .	Agreement between the measured forces on the cylinders and those calculated using linear wave theory was excellent except near $K = 15$ , where the largest difference was about 20%. The agreement for flat plates was not so good. Phase variation was considered, but $C_M$ and $C_D$ departed significantly from mean values only for cylinders near $K = 15$ . Eddy shedding was related to variation in $C_M$ and $C_D$ , and to $K_c$ .
Paape and Breusers (1967)	Laboratory	(a) Structure oscillated in still water $0.5 < T < 3.0$ s Semi-amplitude $0.01-0.20$ m (b) Linear sinusoidal waves $0.43 < T < 0.80$ s $0.007 < H < 0.075$ m $d = 0.300, 0.406, 0.555, 0.775$ m	(a) Horizontal cylinder and plate $D = 0.075$ m (b) vertical square piles $D = 0.025, 0.046, 0.063$ m	(a) $K_c = 0.8-16.7, R = 7 \times 10^3 - 2.7 \times 10^4$ , evaluated using the amplitude of oscillation (b) $K_c = 1-10, R = 10^3 - 7 \times 10^5$ , instantaneous values at maximum force	(a) 0.5-2.0 cylinder, 3-13 plate. Presented as functions of $K_c$ . (b) Not considered	(a) 1.0-2.5 cylinder, 1-4 plate. Presented as functions of $K_c$ . (b) Not considered	Results of experiment (a) agreed with the results of Keulegan and Carpenter. Doubt was cast on the use of Morison's equation due to uncertainties in $C_M$ and $C_D$ . It was recommended that model wave force should be used in design with $H/D$ as independent parameter. Wave theory was not considered.
Jen (1968)	Laboratory	Regular and irregular small waves $0.063 < H < 0.305$ ft $0.9 < T < 2.0$ s $d = 3$ ft	Vertical cylinder $b = 6$ in.	$K = 0.4-2.2, R = 5.6 \times 10^3 - 2.5 \times 10^6$ , evaluated using Airy theory deep water approximation.	Drag negligible	2.0	Linearized force r.m.s. values were in good agreement with the measured values, justifying the neglect of drag. Spectral analysis of two irregular waves also gave $C_M = 2.0$

Author	Location	SEA STATE	STRUCTURE	$K_c$ and $R_e$	$C_D$	$C_M$	Reliability/wave theory
Rance (1969)	Laboratory	Pulsating water tunnel	Vertical cylinders 0.025 < D < 0.3 m	$K = 9-230$ , from $a/D$ values quoted; $R_e = 1 \times 10^5 - 7 \times 10^5$ , instantaneous values at maximum force.	0.4-7.0 as a function of $a/D$ and $R_e$ , 0.4-1.7 for $K_c > 60$ .	2.0	Assuming a constant value for $C_M$ reduced the scatter in $C_D$ . Drag was dominant; results were good only for $K_c$ greater than about 60. $a/D$ was shown to affect critical $R_e$ significantly. Transverse lift force was also given as a function of $a/D$ and exceeded in-line force at $R_e$ less than 10. Wave theory was not used.
Shank and Herbich (1970)	Laboratory	Linear sinusoidal waves $1.5 < \lambda/d < 6.0$ $0.01 < H/\lambda < 0.11$ $d = 13, 18, 24$ in.	Rectangular and semi-cylindrical model oil storage tanks D = 8 in.	$K = 0-11$ , $R_e = 2 \times 10^3 - 2 \times 10^6$ , evaluated using maximum orbit velocity at centre of object.	Drag negligible	1.2-2.2 Optimum value 1.8	Agreement between measured forces and forces calculated using linear wave theory was good. Force increased with $H/\lambda$ and $\lambda/d$ , but $C_M$ was independent of these parameters.
Subbelle et al (1971)	Laboratory scaled 1:30 on Froude's scale law	Linear sinusoidal and irregular waves $2 < H < 16$ m $6 < T < 1/8$ s $d = 20$ m Full-scale values	Vertical cylinder D = 1 m Full-scale	$K = 6-105$ , $R_e = 9.2 \times 10^5 - 5.0 \times 10^6$ full scale, $R_e = 5.6 \times 10^3 - 3.0 \times 10^4$ model scale	0.6-3.0 Values in irregular waves considered to be higher.	0.8-2.1 Values in irregular waves considered to be higher.	The actual $C_M$ and $C_D$ range of values varied with the methods of derivation, which included linear, Stokes third and fifth order wave theory and stream function wave theory. Use of $C_M$ and $C_D$ obtained from Keulegan and Carpenter's curves from $K$ values resulted in a maximum difference of 10% between measured and calculated local forces. Several $C_M$ and $C_D$ pairs were shown to predict the same force.
Johnson (1972)	Laboratory	Linear sinusoidal waves $11.7 < d/H < 65.6$ $0.4 < d/\lambda < 2.5$	Vertical cylinders $d = 0.25, 0.50, 0.67$ ft, top 3 ft below still water level.	$K = 1-12$ , $R_e = 3.5 \times 10^4 - 1.6 \times 10^5$	Drag negligible	2.0	The measured forces agreed to within 20% of the forces calculated using linear wave theory. A theoretical formula for the wave force was derived assuming drag was negligible and $C_M = 2.0$ .
Chakrabarti and Tam (1973)	Laboratory	Linear sinusoidal waves $3 < H < 10$ in. $1.0 < T < 3.5$ s $d = 47.25$ in.	Vertical cylinder D = 81 in.	$K = 0.1-0.7$ , $R_e = 10^5 - 10^6$	Drag negligible	2.0 for $D/\lambda = 0.2$	Agreement between theoretical and experimentally measured forces was excellent. Wave forces were evaluated by diffraction analysis, using linear wave theory.
Mercier (1973)	Laboratory	Low speed constant stream $d = 10$ in.	Vertical cylinder oscillated parallel and transverse to stream D = 0.5, 1.0 in.	$K$ not considered, $R_e = 6 \times 10^3 - 1.3 \times 10^4$ , stream velocity value ( $U_0$ ), interaction with oscillation not considered.	1.0-2.5 transverse oscillations, 1.0-5.0 parallel oscillations	0-1.5 transverse oscillations, 0.2-0.8 parallel oscillations	$C_M$ and $C_D$ were found to depend on the velocity and direction of the stream and the amplitude of oscillation. Drag force correlated with $\rho U_0^2$ ( $\rho =$ fluid density). Wave theory was not used.

TABLE 7.1 (CONT'D)

LABORATORY STUDIES

AUTHOR	LOCATION	SEA STATE	STRUCTURE	$K_c$ and $K_r$	$C_D$	$C_M$	Reliability/wave theory
Garrison et al (1974)	Laboratory model scale 1:120	Linear sinusoidal waves simulating full-scale conditions of $21 < H < 29$ m $14 < T < 17$ s $d = 120$ m	Model of Condeep oil production platform structure. $D = 12$ m for towers at water line	$K = 0.5, R = 3 \times 10^7$ - $9 \times 10^7$ full scale, $R = 2.3 \times 10^6 - 6.9 \times 10^6$ model scale	1.0 Assumed value	2.0 Assumed value	Agreement between calculated and measured forces and moments on the model was excellent. Diffraction analysis using linear wave theory was applied to the large base to obtain the velocity field for the platform supporting towers. The drag force was very small.
Snrykhaya and Tuter (1974)	Laboratory	One-dimensional simple harmonic flow Amplitude = 11 in. $T = 2.86$ s $d = 20$ in.	Horizontal cylinders extended across the horizontal limb of a U tube $1.0 < D < 2.5$ in. Spheres hung on wires in the horizontal limb of a U tube $1.25 < D < 3.975$ in.	$K = 0.50, R = 0 \cdot 10^4$ , evaluated using the amplitude of the simple harmonic flow.	0.0-2.1 cylinder, 0.0-0.8 sphere. Presented as functions of $K_c$	0.8-2.1 cylinder, 1.0-1.5 sphere. Presented as functions of $K_c$	Lift forces up to 1.5 times drag force were measured up to $K$ values of about 20. Measured and calculated forces agreed to within 15%; the difference was largest at $K = 12$ for cylinders and between $K = 12$ and 22 for spheres. Generally agreement was excellent.
Chakrabarti et al (1975)	Laboratory	Linear sinusoidal waves $h < 13$ in. $1.5 < T < 3.0$ s $d = 5$ ft	Cylinders held at various inclinations, in line with and normal to the waves $D = 3, 5, 7.5$ in.	$K = 0.5 \cdot 20, R = 5 \times 10^3 - 5 \times 10^4$ , calculated using maximum horizontal velocity averaged over the length of the cylinder.	0-2.5	1.0-2.5	Large scatter in $C_M$ and $C_D$ values. Morison equation used in three-dimensional vector form with velocity component normal to the axis of the cylinder. Measured and calculated mean forces agreed to within 10% using $C_M$ and $C_D$ values for individual waves.
Bekita (1975)	Laboratory	Small amplitude regular waves $5 < H < 42$ cm $0.9 < T < 5.0$ s $0.005 < H/\lambda < 0.1$ $d = 133$ cm	1/60 scale model of jacket structure with cross framing, with 15 conductor tubes and with no conductor tubes, at various incidences to the flow.	$K = 10-100, R = 10^3 - 3 \times 10^4$ , evaluated using maximum velocity at still water level as given by Stokes fifth order theory and the diameter of the main column.	0.6 Representative of whole structure; smaller when conductor tubes included.	1.6 Representative of whole structure; smaller when conductor tubes included.	$C_M$ and $C_D$ showed a markedly different correlation with $K$ from that obtained by Keulegan and Carpenter. Morison's equation was used in three-dimensional vector form with velocity component normal to the axis of the cylinder. Current drag was considered separately. Application of model results to prototype is uncertain.

Author	LOCATION	SEA STATE	STRUCTURE	$K_c$ and $v_c$	$C_D$	$C_M$	Reliability/wave theory
Sarpkaya (1976)	Laboratory	One-dimensional simple harmonic flow $T=5.272$ s	Smooth and rough horizontal cylindrical extended across the horizontal limb of a U tube, larger than that used in Sarpkaya and Tutler (1974).	$K_c=0.200, R=10^{-4}$ $7 \times 10^5$ , evaluated using the amplitude of the simple harmonic flow. Frequency parameter $\beta_1=R/K_c$ and roughness Reynolds number $U_{M1}k/v$ also shown to be important data correlation parameters.	0.5-2.0 Presented as functions of $R, K_c$ , and $k_r/D^2$	0.7-1.9 Presented as functions of $R, K_c$ , and $k_r/D^2$	Very little data scatter; lift coefficient and Strouhal number also found to be functions of $R, K_c$ and $k_r/D$ . Lift forces can be large and must be considered in design; Strouhal number varied between 0.15 and 0.45. Agreement between measured and calculated forces was excellent except between $K_c$ values of about 10 and 20. These discrepancies were largely attributed to eddy shedding associated with large lift forces and shedding of single vortices.

TABLE 7.1 (CONT'D)

TABLE 7.2

Approaches to Design Practice in Static Wave Force Calculation  
(Space-Frame Structures, Deep Water)

	API RP2A (April 1977)	DNV Rules (July 1974)	U.K. DTI Guidance Notes (March 1974)
Wave kinematics:	"defensible" (e.g., Stokes 5th, Stream Function)	Stokes 5th	"Appropriate to the water depth"
Drag coefficient, $C_d$ :	0.6-1.0 (not smaller than 0.6)	0.5-1.2	"Reliable experi- mental results"
Inertia coefficient, $C_m$ :	1.5-2.0 (not smaller than 1.5) Recognizes that $C_d$ , $C_m$ depend on wave theory.	2  Other $C_d$ , $C_m$ acceptable with different wave theory. $C_d > 0.7$ at high Reynolds No.	

(SARPKAYA AND ISAACSON, 1981)

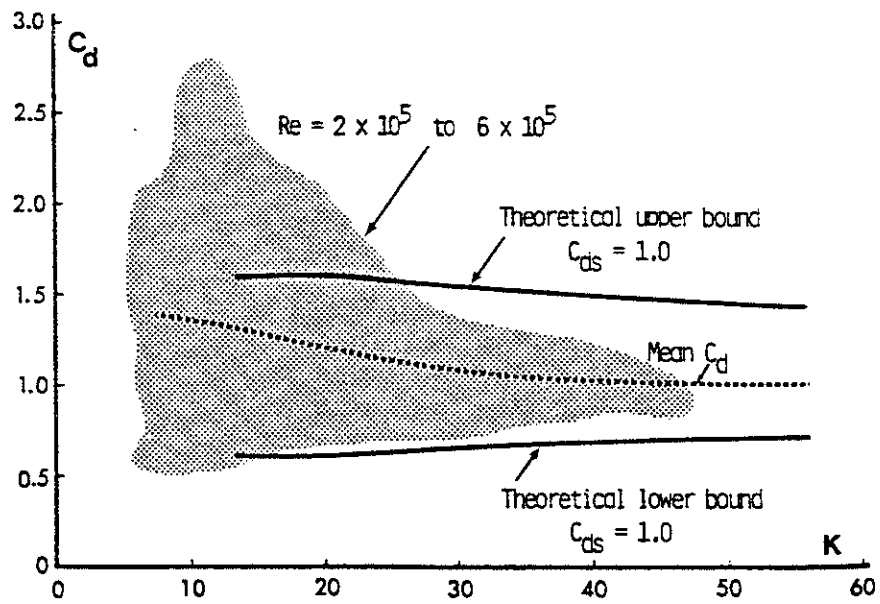


FIGURE 7.1 OCEAN TEST STRUCTURE RESULTS  
(SARPKAYA AND ISAACSON, 1981)

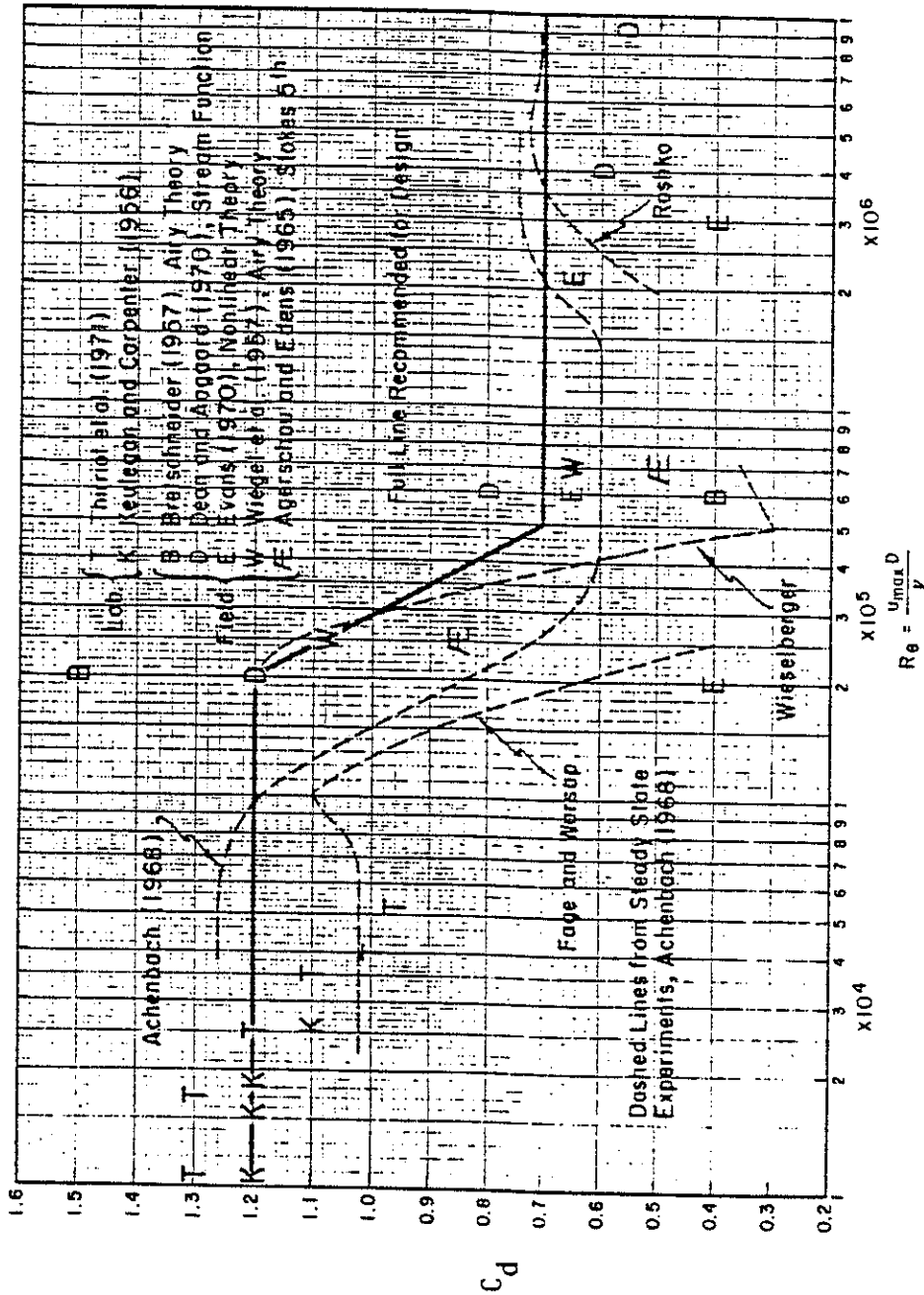


FIGURE 7.2 VARIATION OF DRAG COEFFICIENT,  $C_d$ , WITH REYNOLDS NUMBER,  $Re$   
 (SHORE PROTECTION MANUAL, 1977)



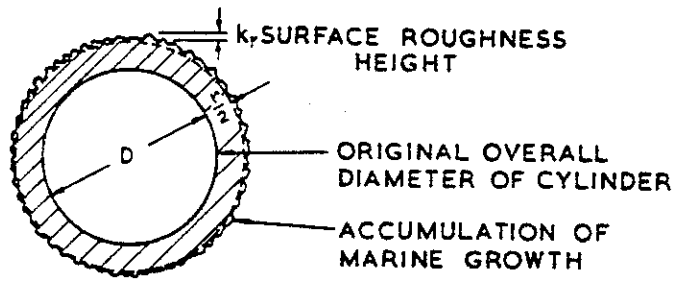


FIGURE 7.3 MARINE ROUGHNESS DEFINITION (MILLER, 1976)

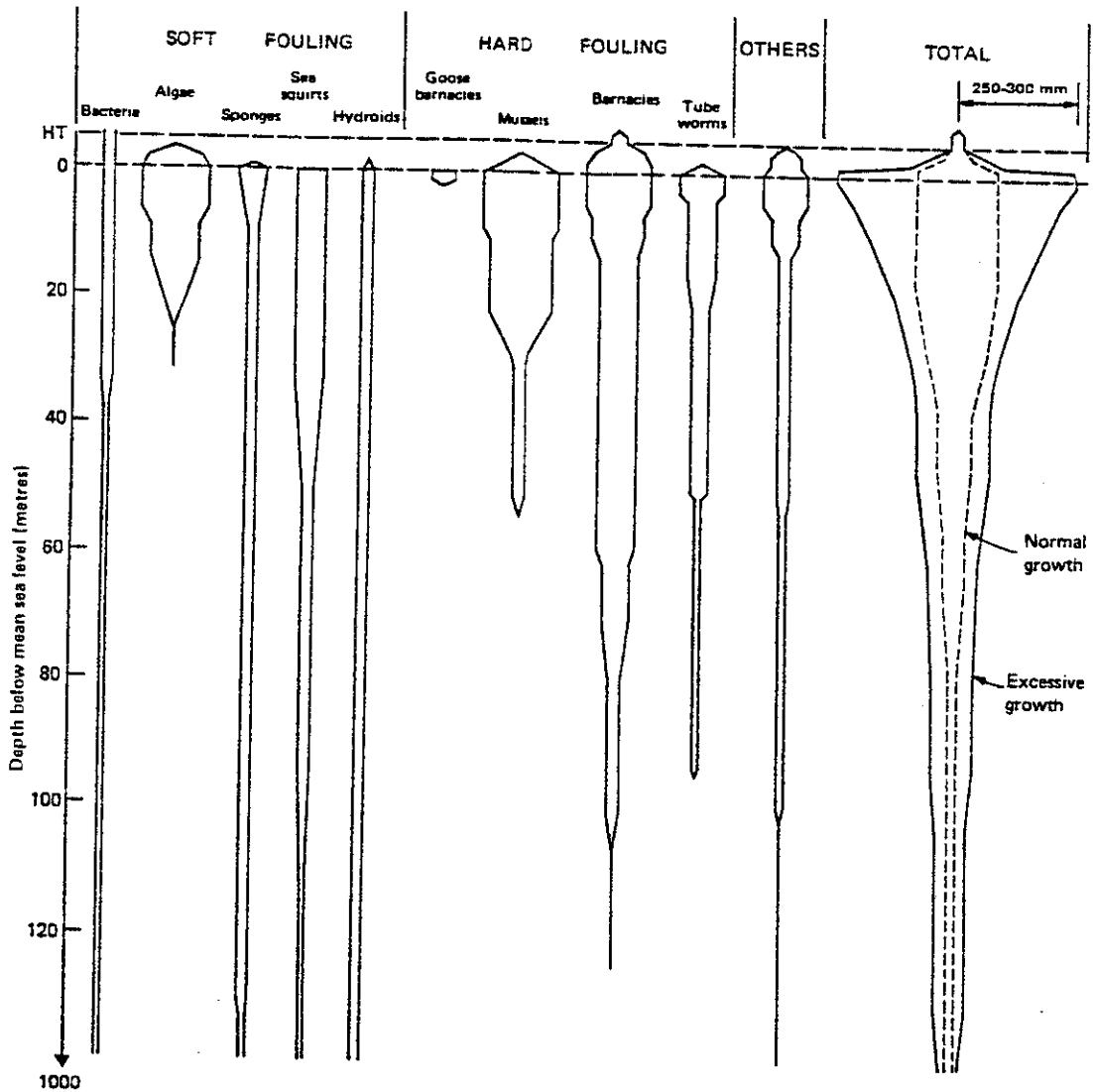


FIGURE 7.4 TYPICAL DISTRIBUTION OF MARINE GROWTH (HALLAM ET AL., 1978)

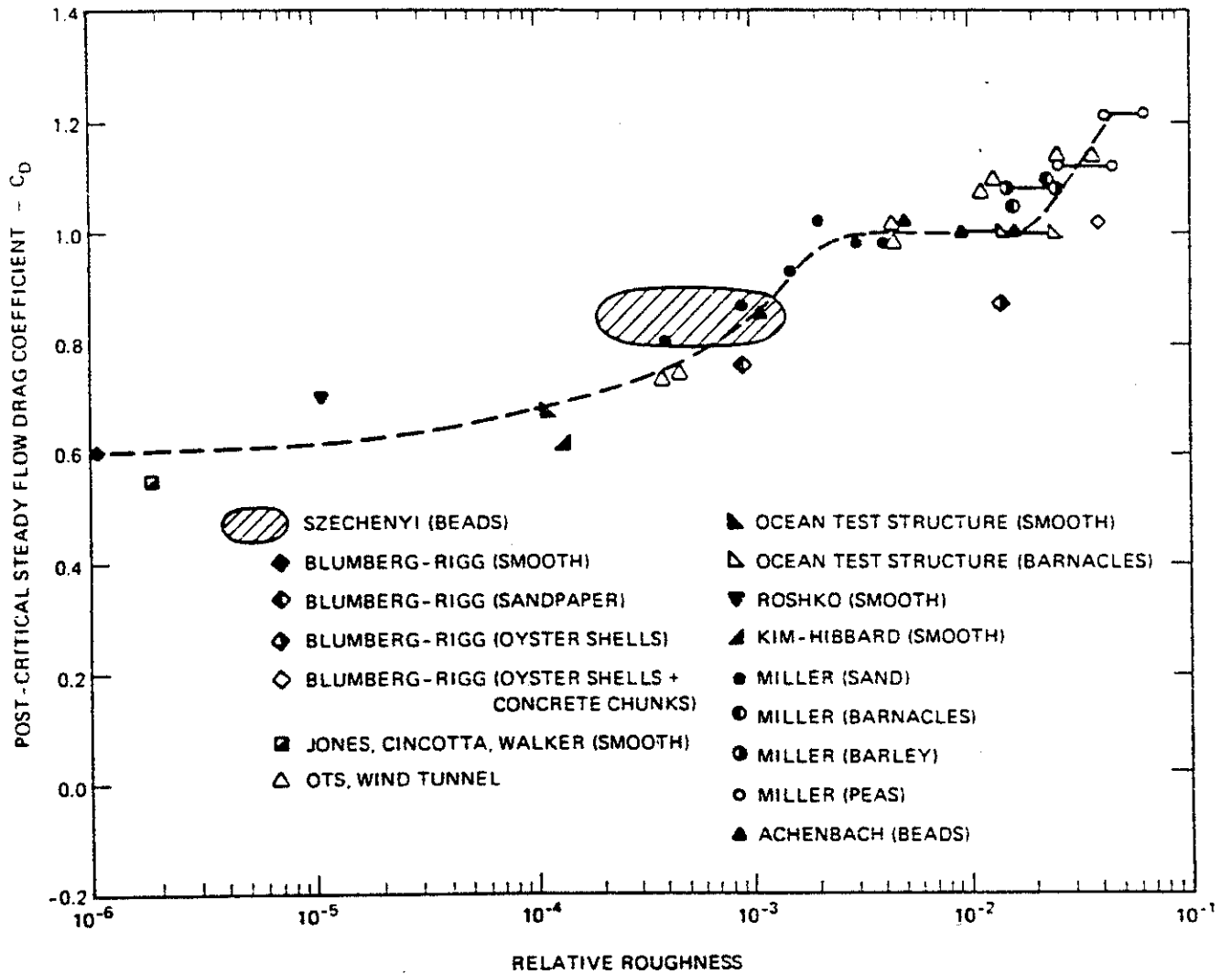


FIGURE 7.5 POST-CRITICAL DRAG COEFFICIENT FOR CYLINDERS IN STEADY FLOW: DEPENDENCE ON RELATIVE ROUGHNESS  $k_r/D$  (REPRINTED FROM STANDING, 1981)

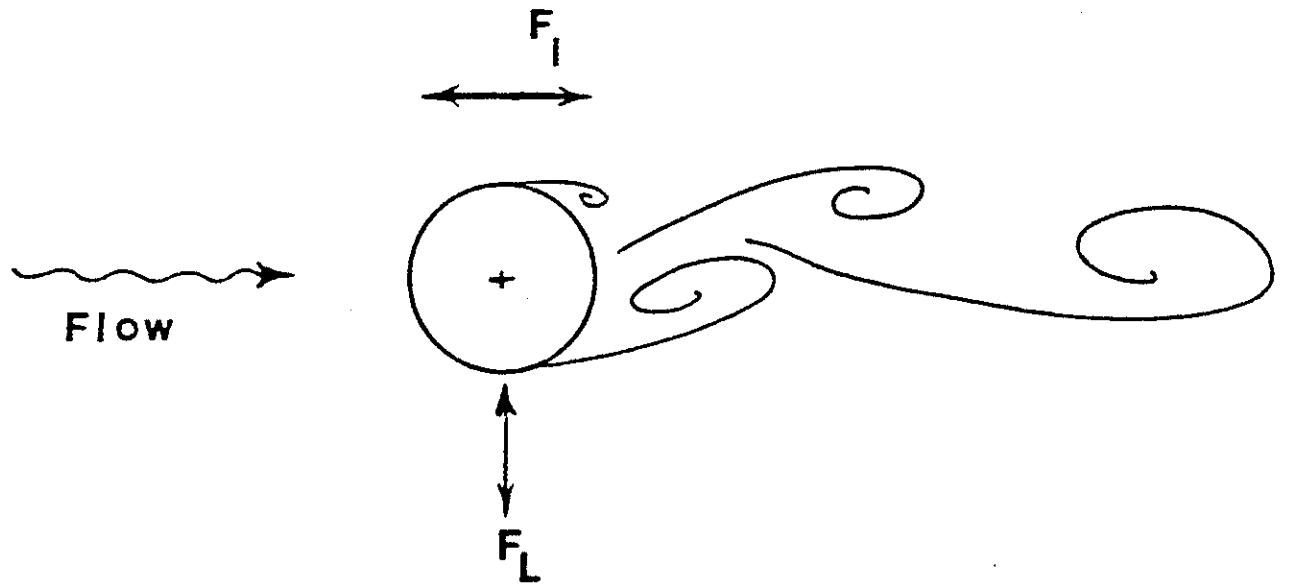


FIGURE 7.6 ALTERNATING VORTEX SHEDDING AND RESULTING LIFT AND IN-LINE FORCES

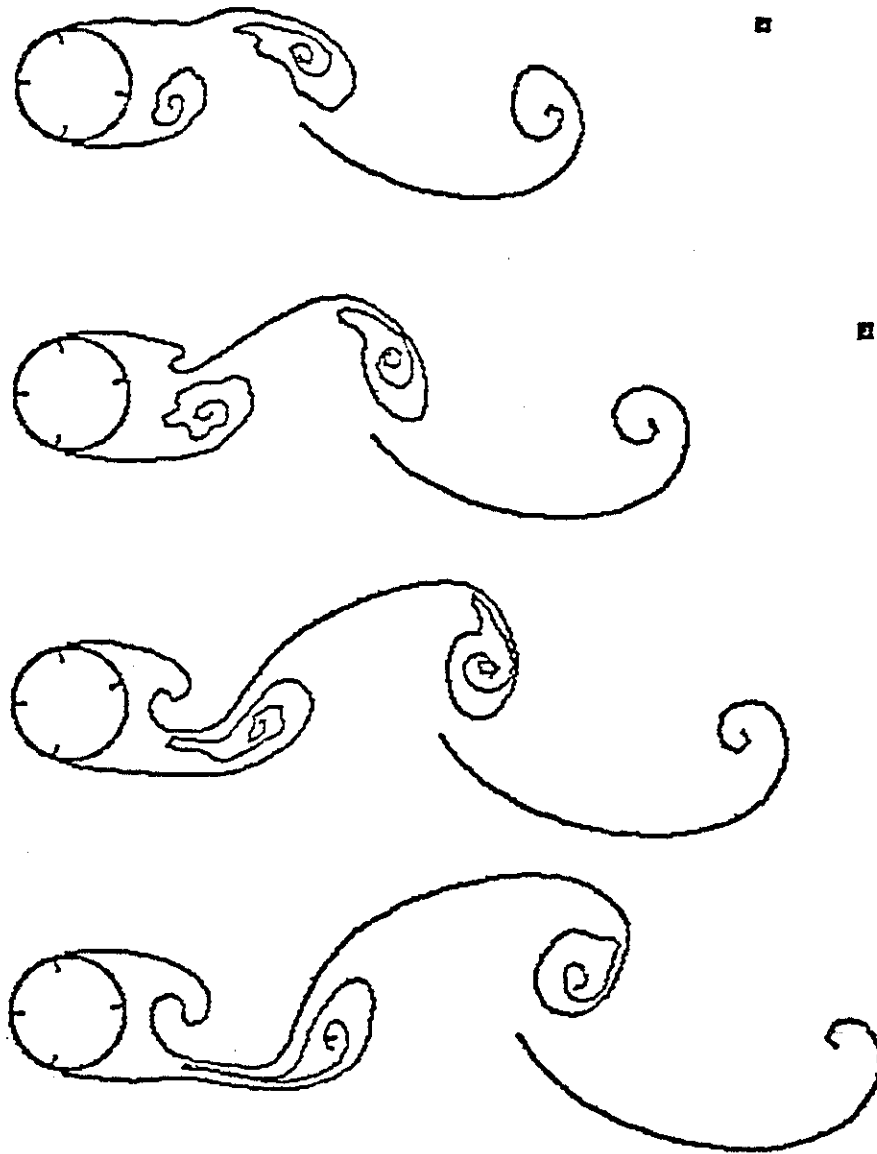


FIGURE 7.7 INITIATION OF VORTEX SHEDDING AFTER SHOAF (1978)

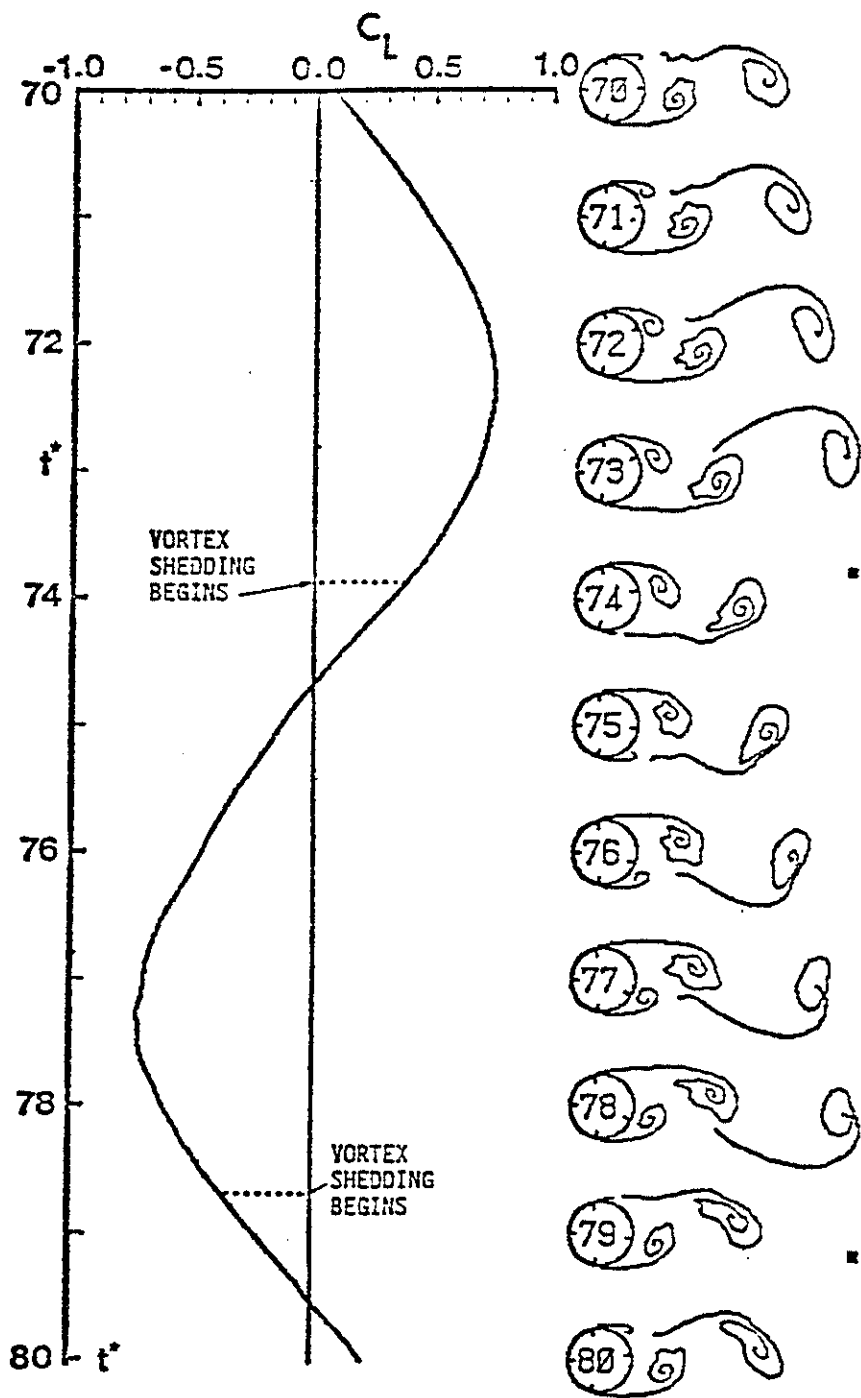


FIGURE 7.8 ALTERNATE SHEDDING OF VORTICES AND ITS RELATION TO THE LIFT FORCE AFTER SHOAF (1978)

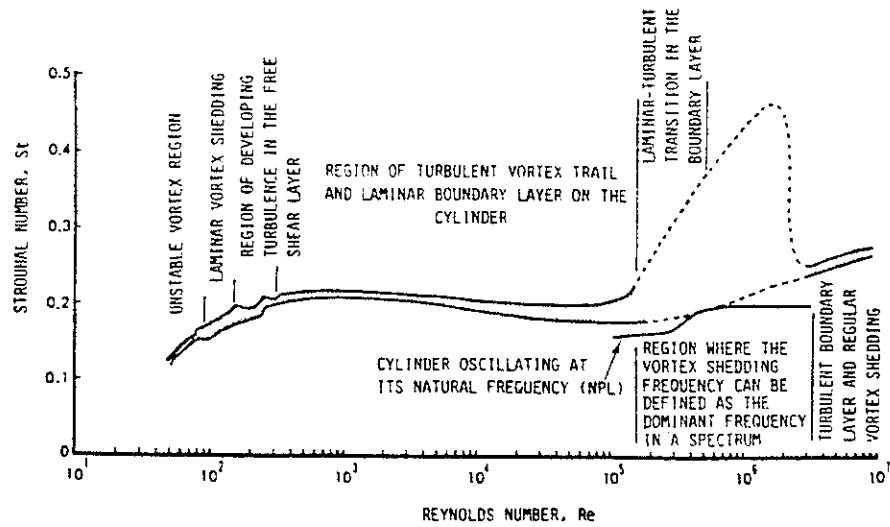


FIGURE 7.9 STROUHAL NUMBER VERSUS REYNOLDS NUMBER (LIENHARD, 1966)

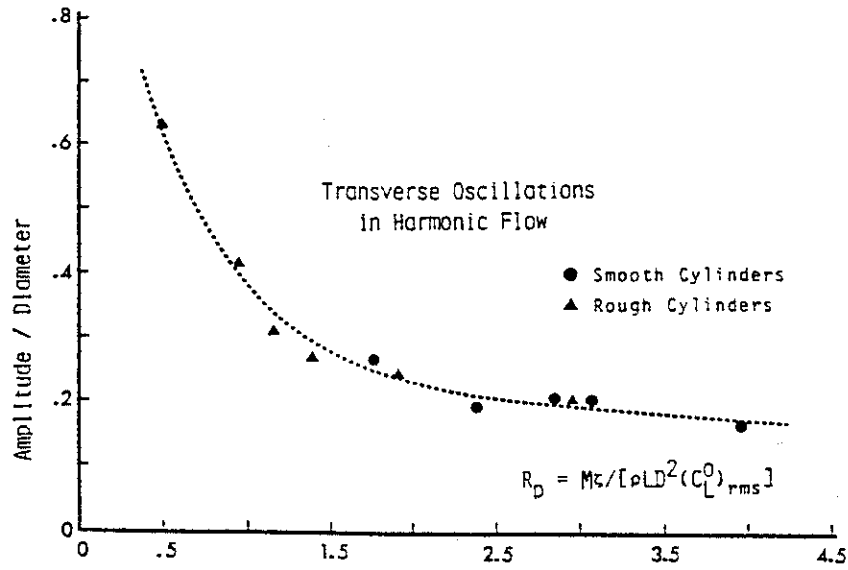


FIGURE 7.10 FREE TRANSVERSE OSCILLATIONS OF CIRCULAR CYLINDERS IN HARMONIC FLOW (RAJABI, 1979)

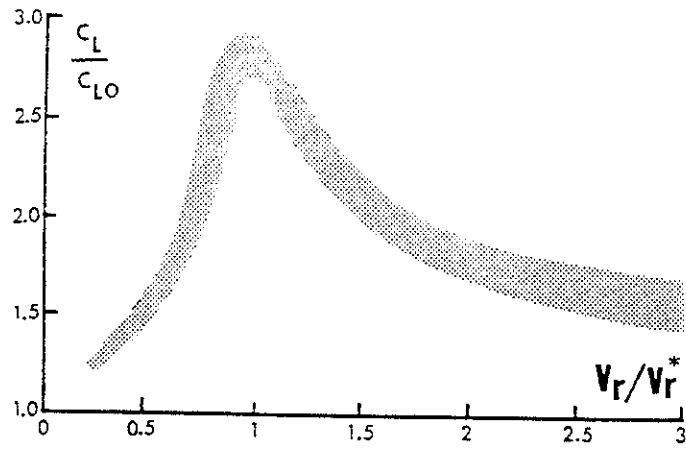


FIGURE 7.11 LIFT AMPLIFICATION CORRELATION (SARPKAYA ET AL. 1981)

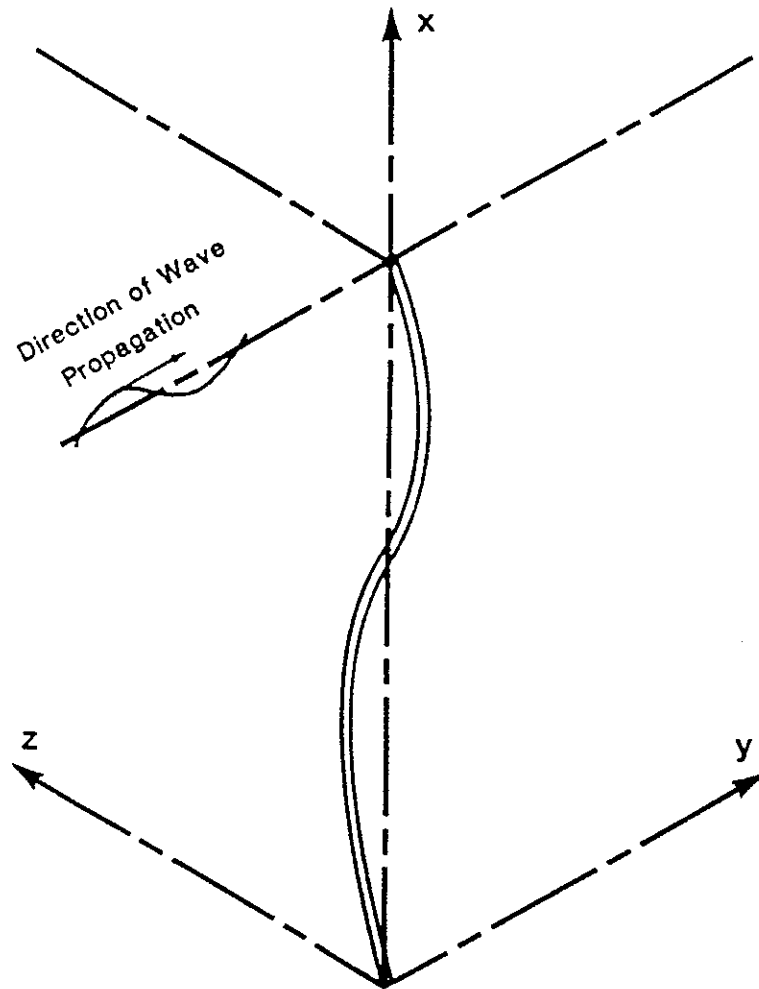


FIGURE 7.12 SCHEMATIC OF LOCAL AXIS SYSTEM FOR FLEXIBLE CYLINDERS





## 8.0 WAVE FORCES ON LARGE BODIES

### 8.1 Introduction

The forces that act on a platform hull are of two principal types: wave-induced, or excitation; and motion-induced, or reactions. If the platform is freely floating, the forces are all hydrodynamic; if the platform is moored, there is, in addition, a mooring reaction.

Hydrodynamic forces are separable according to the role played by viscosity. If the viscosity is not significant, the forces are derived on the assumption that the fluid is inviscid and can be described in terms of a velocity potential. If the viscosity plays a nonnegligible (yet far from dominant) role, the forces derived on the assumption of inviscid fluid can sometimes be suitably adjusted by an amount which, at the present state of knowledge, can be given only in an empirical form. If, on the other hand, the viscosity plays a dominant role, the hydrodynamic forces have purely empirical expressions and the concept of a velocity potential ceases to have meaning. In which specific category a force falls depends essentially on the geometry of the body, its orientation to the flow and its depth of submergence.

If the ratio  $D/L$  is small, say less than  $1/5$ , where  $D$  is a characteristic horizontal dimension of the body and  $L$  denotes the wavelength, then the member falls into the category of "small bodies". In this case the viscous forces are predominant and the Morison equation is usually employed to evaluate hydrodynamic loads on small bodies. The inherent assumption in this approach is that the kinematics of the undisturbed flow in the region near the structure do not change in the incident flow.

However, when a body spans a significant fraction of a wavelength, the incident waves generally undergo significant scattering or diffraction and wave force calculations should then take such

scattering into account. This situation characterizes the diffraction regime of wave-structure interaction and is generally considered to occur when the structure spans more than about a fifth of the incident wave length,  $D/L > 1/5$ . This is in contrast to the interaction of waves with a slender structural element, in which case flow separation dominates the loading behavior but beyond the immediate vicinity of the element, the wave train remains relatively unaffected. These two regimes of wave-structure interaction give rise to two distinct approaches by which wave force problems are treated. The first of these two has been described in detail in Chapter 7.0 and the second approach concerning the diffraction regime is treated in this chapter.

## 8.2 Wave Diffraction Theory

The terms "wave diffraction" and "wave radiation" are often used in a narrow sense, to distinguish between waves scattered by a fixed structure, and the waves generated by an oscillating structure. This distinction arises largely through the use of linear wave theory, which allows the two processes to be decoupled and linearly superimposed. The wave diffraction and radiation processes are closely related, and the criteria and methods of solution are almost identical. In the following discussion, therefore, it is both convenient and concise to refer to the combined process as one of "wave diffraction".

Wave diffraction becomes important when the diameter  $D$  of a structural member is large in relation to the wavelength  $L$ : roughly when the ratio  $D/L > 0.2$  (see Section 6.2). The Morison equation no longer predicts the wave force on the diffracting member satisfactorily, in terms of either its amplitude or phase, and the diffracted wave field may affect other nearby members. Results based on linear wave diffraction theory are then more satisfactory. There is no simple relationship between the wave force and particle kinematics in the undisturbed wave, as assumed by the Morison

equation. The full hydrodynamic boundary value problem has to be solved. Wave forces are expressed in terms of a velocity potential, describing the diffracted wave field. There are explicit analytic solutions in a few special cases, but in most practical design situations, the problem has to be solved numerically.

Computer programs, suitable for use in design, have been based on integral equation, conformal mapping, finite element and hybrid techniques. These methods and the underlying theory are described fully in survey papers by Mei (1978) and Isaacson (1979b). The following brief summary also discusses experimental validation and practical applications of these methods, and recent attempts to develop a higher-order theory.

### 8.3 Linear Wave Diffraction Theory

The linear diffraction problem arises when the wave height is assumed sufficiently small for linear wave theory to apply.

The main assumptions are:

- o ideal fluid (inviscid, incompressible, and irrotational flow),
- o wave height and structure motions are small, so that the equations may be linearized,
- o incident wave is regular and unidirectional,
- o uniform water depth,
- o structure has no mean forward speed, and there is no current.

Letting, as in Chapter 5.0, the velocity vector  $\bar{q}$  be expressed as

$$\bar{q} = \text{grad } \phi \quad (8.1)$$

the problem reduces to the determination of a velocity potential  $\phi(x,y,z,t)$  which satisfies the Laplace equation

$$\nabla^2 \phi = 0 \quad (8.2)$$

within the fluid region. The solution is subject to boundary conditions which specify the behavior of the flow at infinity, at the surface and bottom of the sea, and at the wetted surface of the hull.

The boundary conditions at infinity and at the bottom pose no problem; those at the surfaces of the sea and hull can be satisfied by splitting the potential into components; thus, for a non-transiting body subject to wave action,

$$\phi = \phi_w + \phi_d + \phi_b \quad (8.3)$$

where the subscripts w, d and b denote incident wave, diffracted wave and body motion, respectively. The incident wave potential defines a wave train in the absence of the hull; the diffracted wave potential defines how the presence of the fixed hull disturbs the incident wave train; and the body potential describes the flow field that is generated by the oscillatory motions of the hull in still water. The sum of the incident and diffracted wave potentials is sometimes called the excitation potential,

$$\phi_e = \phi_w + \phi_d \quad (8.4)$$

The sum of all three potentials must satisfy the following boundary condition on the wetted surface of the hull:

$$\frac{\partial \phi}{\partial n} = V_n \quad (8.5)$$

in which n is the normal to the surface (outward for body) and  $V_n$  denotes the velocity of the body in the direction of the normal. The spatial and temporal aspects of the velocity potential can be separated as

$$\phi(x,y,z;t) = \phi_0(x,y,z) \exp(-i\omega t) \quad (8.6)$$

where  $\omega$  is the circular frequency of the regular wave under consideration. The same factoring can also be applied to the individual potential components related to the incident and diffracted waves and to that generated by the oscillations of the hull.

The wave potential, diffracted potential and body potential are sometimes called "incident wave", "scattered wave", and "radiated wave" potentials, respectively.

The wave forces and moments on the hull are obtained by integrating the pressure  $p(x,y,z;t)$  over its time-varying submerged surface. Thus,

$$F_j(t) = - \int_s p n_j ds \quad (j=1,2,\dots,6) \quad (8.7)$$

where  $ds$  is an element of the hull surface and  $n_j$  are the components of a generalized normal vector defined as

$$\begin{aligned} n_1 &= n_x \\ n_2 &= n_y \\ n_3 &= n_z \\ n_4 &= zn_y - yn_z \\ n_5 &= xn_z - zn_x \\ n_6 &= yn_x - xn_y \end{aligned} \quad (8.8)$$

Here,  $n_x, n_y, n_z$  are the direction cosines of the normal to the surface, and  $x,y,z$  are distances from the c.g. of the platform. The pressure  $p$  comes from the Bernoulli equation as discussed in detail in Chapter 5.0. Several serious computational difficulties arise in seeking to derive the hydrodynamic forces on a given hull shape, among which may be noted:

- o The boundary condition on the hull is a function of its motions, which are themselves the goal of the solution.
- o The Bernoulli equation is nonlinear.

As it stands, the problem is mathematically intractable and must be simplified if it is to be solved. The first simplification introduced is the linearization of the Bernoulli equation by dropping the squared velocity term, a step that limits the validity of the theory to waves of small height. This restriction is often forgotten in engineering practice.

The wave diffraction and body motion potentials can be derived directly only for very simple bodies. No way has been found to construct such potentials for a hull oscillating in waves: what is usually done is determine the diffraction potential of the restrained hull in waves and the body potential of the oscillating hull in calm water and combine them. By this strategem, the boundary condition at the hull surface is satisfied not at all instants but only on the average, i.e. in the mean positions. If the motions are small (as is assumed to be the case), the error is negligible.

The use of linearized Bernoulli equation, the expression of the velocity potential and associated variables in the form of Equation (8.2) involving a separation into undisturbed incident wave, scattered wave by static structure, and radiated wave as the structure responds in each of its degrees of freedom constitutes the basis of diffraction theory. Consequently there are three contributions to the hydrodynamic force:  $F_j^{(w)}$  (Froude-Krylov force),  $F_j^{(d)}$  from the diffracted wave, and  $F_j^{(b)}$  associated with the motion of the platform. The first two are usually combined to give a total wave force or "exciting force", harmonic in time:

$$F_j^{(e)} = (f_j^{(w)} + f_j^{(d)}) \exp(-i\omega t) = f_j^{(e)} \exp(-i\omega t) \quad (8.8)$$

The motion-dependent forces are proportional to the structure's response  $X_k$ , and are conventionally decomposed into components in phase with the velocity and acceleration of each mode.

$$F_j^{(b)} = \sum_{k=1}^6 [-A_{jk} \ddot{X}_k - B_{jk} \dot{X}_k] \quad (8.9)$$

where the coefficients  $A_{jk}$  and  $B_{jk}$  are taken as real. These are termed the "added mass" and "damping" coefficients, respectively, since they assume corresponding roles in the equation of motion. The added mass and damping coefficients are found from expressions

$$A_{jk} = \text{Re} \left[ \frac{i\pi}{\omega} \int_S \phi_k n_j ds \right] \quad (8.10)$$

$$B_{jk} = \text{Im} \left[ i\rho \int_S \phi_k n_j ds \right] \quad (8.11)$$

where  $\phi_k$  is the body potential associated with mode  $X_k$ . There are various relationships between these coefficients. For example, reciprocal relationships

$$A_{jk} = A_{kj} \quad (8.12)$$

$$B_{jk} = B_{kj}$$

are described by Vugts (1970). The so-called Kramers-Kronig relationship between added mass and damping is treated by Ogilvie (1964), and the Haskind relationship between the coefficients and wave forces is presented by Newman (1962). These relationships may be put to practical use, either to check the accuracy of numerical estimates or to reduce the number of calculations. In some circumstances, however, these relationships can be satisfied even though the numerical values of the coefficients may be grossly

inaccurate.

The structure's response  $X_k$  now satisfies the equations of motion

$$\sum_{k=1}^6 (M_{jk} + A_{jk}) \ddot{X}_k + B_{jk} \dot{X}_k + C_{jk} X_k = f_j^{(e)} \exp(-i\omega t) \quad (8.13)$$

$$j = 1, 2, \dots, 6$$

where  $M$  and  $C$  represent structural mass and stiffness matrices, respectively.

The advantage of writing the equation of motion in this way relates to the fact that the forces and moments associated with  $\phi_w$  and  $\phi_d$  comprise the exciting force  $F^{(e)}$  on the body, and this is identical to what it would be if the body were fixed. The exciting force could be determined in the same manner as in the fixed body case, but the calculation does not require  $\phi_d$  to be determined explicitly.

#### 8.4 Hydrodynamic Solutions

Hydrodynamic solution pertains to evaluation of the coefficients and excitation force in the equation of motion described by Equation (8.13).

The parameters of hydrodynamic inertia and wave damping can always be determined experimentally, but this is not a convenient procedure during the design process. For this purpose, prediction of these parameters based either on theory or empirical relationships is preferred.

There are three basic theoretical methods by which we may seek to determine the hydrodynamic inertia and wave damping of a hull of arbitrary form:



1. By a rigorous analytical solution to the boundary value problem.
2. By conformal transformation of the exact solution for a simple body to that for the arbitrary shape.
3. Through representation of the hull by a distribution of periodic singularities in a uniform flow and derivation of the action on the bounding surface between the flow.

#### 8.4.1 Analytic

Rigorous solutions for the parameters of hydrodynamic inertia and wave damping derived from velocity potentials of the body motions have been obtained only for a relatively few bodies of simple analytical description, the most complex one for which the full set of body motion potentials were derived being that of a submerged ellipsoid close to the surface by Newman (1961). Other solutions are reported in Table 1 of St. Denis (1975) and Table 3 of Hogben et al. (1977).

These solutions also include wave diffraction by an isolated vertical circular cylinder extending from the seabed and piercing the free surface. This was treated initially by Havelock (1940) for the deep water range, then by Omer and Hall (1949) for the shallow water range and subsequently by MacCamy and Fuchs (1954) for general depths. Omer and Hall were concerned with predicting the wave runup around a circular island and presented a comparison of their prediction with observed tsunami runup around the island of Kauai. The work of MacCamy and Fuchs is widely referred to in the wave force literature, not only because their study was the first pertaining to arbitrary depths, but also because emphasis was given to the wave-induced loads on the cylinder.

In this regard, Ursell's (1949) work on two-dimensional models of a heaving horizontal cylinder is worth mentioning.

#### 8.4.2 Strip Theory

If the hull is slender, there is a way to avoid analytical difficulties and that is to invoke the so called strip hypothesis, which implies that the flow is everywhere in plane normal to the axis of slenderness. This method is particularly suitable for elongated bodies (such as semisubmersible pontoons) and for ships of conventional form. This method assumes that the ship's beam and draft are small compared with its length.

The strip, or cross-flow hypothesis was apparently introduced by Lewis (1929), but its application to ship motions is due to Korvin-Kroukovsky (1961). Its present refined form, which applies to all motions except surge, is due to Salvesen, Tuck and Faltinsen (1970), and results obtained by these authors correlate very well with data derived from tests with ship models. Inasmuch as the strip technique is also relatively simple to employ, it has become the established method for ship hulls, and has even been applied uncritically to the blunt hulls with which some platforms are fitted. In strip theory the ship is divided along its length into a number of sections (or strips), around each of which the flow is assumed to be two-dimensional. Results from all sections are combined to give overall coefficients and wave forces. Two-dimensional solutions for individual sections are based on either:

- o Conformal Mapping
- o Frank Close-Fit Method
- o Schwartz-Christoffel Method

##### 8.4.2.1 Conformal Mapping

In the application of the strip hypothesis, the known solutions for the hydrodynamic inertia and wave damping of circular cylinders and plates are transformed by conformal mapping to sections which closely approach in form those of the actual hull. For the present purpose,

the required known solutions are those corresponding to the motions of sway, heave and roll. Conformal mapping extends the Ursell's (1949) cylinder solution to the Lewis forms (1929). More general sections are treated by Tasai (1960) and Porter (1960).

#### 8.4.2.2. Frank Close-Fit Method

The Frank close-fit method is based on integral equation techniques and can be applied to any section shape and water depth. The hull contour can be accurately mapped by the technique developed by Frank (1967), according to which the shape of a section is first replaced by a prism of a modest number of sides (in practice, up to about twelve); pulsating sources are then disposed along the sides and the corresponding velocity potential is derived. The technique has been further refined by Faltinsen (1969), who succeeded in eliminating some anomalies inherent in the original formulation.

#### 8.4.2.3. Schwartz-Christoffel Method

The methods of Tasai (1960), Porter (1960) and Frank as modified by Faltinsen are all accurate and adaptive within the intrinsic limitations of the strip hypothesis, to almost any form. Of course, this flexibility implies longer computations. But when the hull sections vary abruptly in curvature (as occurs, for example, when they are of rectangular shape or when bilge keels or similar extensions are fitted), the extended Joukovsky transformation does not lead to a good fit unless it is carried out to an extremely large number of terms, with a consequent gigantic increase in the computational work over that required for a conventional hull. In such a case, a superior transformation namely that of Schwartz-Christoffel is used. St. Denis (1975) described this method in more detail and Table 2 of his paper also includes the hydrodynamic coefficients for some of the bodies derived through the application of this method.

#### 8.4.3 Three-Dimensional Problem: Vertical Wall Boundaries

The potential solution is expressed in separable form

$$\phi = \phi_H(X,Y) \cosh k(d-Z) \exp(-i\omega t) \quad (8.14)$$

where the  $\phi_H$  is usually determined by boundary element or finite element techniques. Hwang and Tuck (1970) and Chen and Mei (1974) have applied these methods in the analysis of harbors and man-made islands.

#### 8.4.4 Three-Dimensional Problem: Axisymmetric Structures

When the body has a vertical axis of symmetry (i.e. the Z-axis) the potential solution may be written as:

$$\phi = \sum_{j=0}^{\infty} \phi_{Rj}(r,Z) \cos j\theta \exp(-i\omega t) \quad (8.15)$$

where  $(r,\theta)$  are cylindrical polar coordinates about that vertical axis. The added mass, damping and wave forces depend on only the first two terms of the series (i.e.  $j=0,1$ ), but local pressures and particle kinematics require many more terms. Individual contributions  $\phi_{Rj}$  have been evaluated by Chenot (1975) using finite element techniques. Fenton (1978) applied a boundary element method, and Kokkinowarchos (1978) used a Fourier expansion for evaluation of  $\phi_{Rj}$ .

#### 8.4.5 General Three-Dimensional Problem

The solutions obtained so far have a wide range of applications, but it eventually becomes necessary to take up the case of bodies of arbitrary geometry in order to deal with the variety and complexity of design configurations encountered in the modern offshore

structures. Such treatment must necessarily be based on a numerical approach. These techniques can, in principle, model a quite arbitrary shape, and take full account of flow interaction between members. They usually require sophisticated computer programs. In practice, computer run costs and mesh-size limit definition of the structure's shape. These computer programs have been based on the boundary element method (BEM), finite element method (FEM), finite difference method (FDM) and hybrid element method (HEM).

#### 8.4.5.1 Boundary Element Method (BEM)

The BEM, sometimes called boundary integral method, integral equation method, wave source method, etc., has a long history. It is based on the classical theory of Green's function which defines the potential of source and sink.

In describing the wave source approach, we first note that a fundamental result of potential theory is that the velocity potential of the waves  $\phi$  may be represented as due to a continuous distribution of point wave sources over the immersed body surface. This result is described by Lamb (1945) (see also Wehausen and Laitone, 1960). If the potential of the fluid due to a point source of unit strength located at the point  $p = (\bar{x}, \bar{y}, \bar{z})$  is known, then on account of the linearity of the problem this may be amplified to any required strength and then superposed with any number of other wave sources. The velocity potential due to the whole (continuous) distribution of sources over the body surface is then given as

$$\phi(X) = \frac{1}{4\pi} \int_S f(p)G(X,p)ds \quad (8.16)$$

Here  $X$  represents a point  $(x,y,z)$  on  $S$ ,  $G(X,p)$  is the Green's function of a point wave source of unit strength located at the point  $p = (\bar{x}, \bar{y}, \bar{z})$ ;  $f(p)$  is the unknown source strength distribution function, and  $ds$  is a differential area on the immersed body

surface. The Green's function, which is singular at the source point  $p$ , must itself satisfy the Laplace equation, the bottom and linearized free-surface boundary conditions, together with the radiation condition. Such a Green's function was developed by John (1950) and may be expressed either in terms of an integral or as an infinite series. For a more detailed discussion of Equation (8.15) and functions appearing in it, the reader may wish to refer to Garrison (1978) or Sarpkaya and Isaacson (1981).

In a numerical model the structure's surface is divided into small plane area elements (facets), as shown in Figure 8.1. A pulsating fluid source is placed at the center of each facet, and the source strengths are calculated so as to satisfy the normal velocity condition as described by Equation (8.5) at each point of the structure's surface. The source flow field represents the diffracted wave.

The method has now become firmly established in design practice. More detailed descriptions are provided by Garrison and Chow (1972), Hogben and Standing (1974), Hogben et al. (1974), Garrison (1974a), and Standing (1978). Attention is also drawn to a review paper by Hogben et al. (1977) in which are tabulated some available diffraction programs based on the wave source method. These include programs by Lebreton and Cormault (1969), Garrison and Rao (1971), Garrison and Chow (1972), Garrison (1974a), Van Oortmerssen (1972), Hogben and Standing (1974), Faltinsen and Michelsen (1974), and Van Oortmerssen (1976a, b).

Additional information on this subject may be found in the work by Garrison and Stacy (1977), Garrison (1978), and Garrison (1982).

#### 8.4.5.2 Finite Element Method (FEM)

The finite element method has found increasing use in treating many diffraction problems. The general method has been described in

detail in the text by Zienkiewicz (1977), and has been reviewed in the context of fluid flow problem by Shen (1977). Surveys by Mei (1978), Zienkiewicz et al. (1978) and Brebbia and Walker (1979) describe the application of the finite element and "hybrid" element method to the wave diffraction problem.

In FEM the boundary value problem is re-expressed as a variational principle. A suitable functional is extremised in order to determine certain interpolation coefficients, which describe the solutions within each element. A mesh of finite elements has to be constructed throughout the fluid. There is some choice in the element shapes and interpolation functions to be used. Zienkiewicz (1977) gives a complete description of these elements.

One important factor of wave diffraction problems concerns modeling the infinite extent of the ocean or radiation condition at infinity. Four methods have been used with the finite element method to ensure that the radiation condition is satisfied. These are as follows:

1. Finite distance radiation, boundary.
2. Analytical series solutions for exterior region.
3. Boundary integral solution for exterior region.
4. "Infinite" elements.

The first such approach is the simplest and most direct: "radiation" boundaries are taken to lie at some reasonably large but finite distance from the body, and the radiation condition is applied directly at these boundaries. This method has been found to give surprisingly accurate results. In the second and third methods listed above, sometimes termed "hybrid element" methods, the fluid region is divided as sketched in Figure 8.2, into an interior region in the vicinity of the body, and an exterior region extending to infinity. A finite element analysis is used only in the interior region and this is matched to an alternative representation of the exterior region. When the matching boundary forms a circular

cylinder for three-dimensional or horizontal plan problems, or forms a plane  $x = \text{constant}$  for vertical plane problems, the potential in the exterior region may readily be expressed as an analytical series with unknown coefficients, Chen and Mei (1974). This corresponds to the second method listed above. Alternatively, the third method involves expressing the potential in the exterior region in terms of a singularity distribution over the matching boundary, and thus the matching boundary may now possess a more general shape. The fourth method involves "infinite" elements in which the outermost elements themselves extend to infinity, and possess exponentially decaying interpolation functions which ensure that the radiation condition is satisfied, Bettess (1977). Hara et al. (1979), have reviewed the alternative methods outlined above and present a comparison of results based on the alternative approaches.

#### 8.4.5.3 Finite Difference Method (FDM)

At this point mention is made in passing of the finite difference technique which has occasionally been employed in wave force calculations. Raichlen and Naheer (1976) have used it extensively for the related harbor resonance problem. Chan and Hirt (1974), and Miner et al. (1979) have used finite difference methods for various vertical plane problems. It appears that the finite difference methods do not have the power of the corresponding finite element methods and have not been developed as extensively.

#### 8.4.6 Computational Considerations on FEM and BEM

The finite element methods generally compare reasonably well with the integral equation methods. The finite element method generally requires greater preparation in setting up a particular configuration, but this is offset by the fact that it may be more flexible, for instance, in being able to accommodate variable depths in the region near the body. Both approaches can give accurate results and both involve approximately the same order of computer



effort. For a two-dimensional problem, this may be indicated as follows. If  $N$  sources are used to describe a body contour in the wave source method, then a matrix equation of rank  $N$  must be solved, corresponding to the interaction of each source with all the others. In contrast, if  $M$  elements are used to describe the corresponding fluid region in the finite element method, then a matrix equation of rank  $M$  is to be solved, with  $M$  typically larger than  $N$  (corresponding to an area rather than a contour being discretized). But now the matrix equation is symmetric and banded and the overall order of computer effort is not too different. Similar comments apply to three-dimensional problems: now a finite fluid volume must be discretized in the finite element method, whereas a surface is discretized in the wave source method. In this case the hybrid element methods, or the use of infinite elements, are essential in order to avoid too large a matrix rank.

#### 8.4.7 General Comments on Various Numerical Methods

Each method has a number of advantages and disadvantages, including the following:

- o The finite difference approach is perhaps the most straightforward. It requires no elaborate functional or Green's function, and is readily extended to include, for example, non-linear free-surface effects.
- o The finite element method allows greater flexibility in the choice of mesh points. The finite difference method is generally restricted to rectangular elements.
- o Both the FEM and FDM methods require a mesh throughout the fluid. The BEM requires a mesh over the body surface only, and uses a correspondingly smaller matrix. This advantage is offset, however, by the complexity of the Green's functions in that matrix.

- o Certain resonance conditions have to be avoided. The BEM for example, is known to fail at certain "irregular frequencies", corresponding to internal wave modes, see John (1950). Mei (1978) and Ogilvie and Shin (1978) mention that these frequencies are often outside the range of interest and are quite easy to avoid. However, they cause few practical difficulties.
- o The FEM and FDM are particularly suited to problems involving small finite bodies of water (for example, the sloshing of liquid in tanks), but the radiation condition at infinity causes difficulties, as described above.

## 8.5 Applications and Experimental Validation

Various applications and validation of linear diffraction theory are reviewed by Standing (1981) and Sarpkaya and Isaacson (1981). Following is a brief summary of the most important results.

Linear wave diffraction theory often agrees remarkably well with experiment. This has been a major factor for its increasing popularity for use in offshore design. Papers listed in Table 8.1 contain some of these comparisons, and have been chosen to illustrate the range of applications and conditions in which these methods have been tested. The following conclusions have been drawn.

- o Linear wave diffraction theory generally predicts wave forces, added masses and damping, response motions and associated structural stresses very well, provided the Keulegan-Carpenter number remains small, and the motions are too large. There is often particularly good agreement in deepwater wave conditions (also see Section 5.2.13).
- o Nonlinear features of the wave are most obvious at, or just below, the free surface, and they attenuate rapidly with depth.

There may be however, quite serious nonlinear effects in large-amplitude shallow-water waves.

- o Responses of floating structures are usually predicted better than the associated added mass and damping. The main reasons are as follows. First, the structure does not respond to high-frequency forces, so that nonlinear higher harmonics are filtered out; secondly, the response equations are often dominated by the Froude-Krylov wave force, buoyancy stiffness and structural mass terms, and are less sensitive to added mass and damping.
- o Natural-frequency response, especially roll response of ships, may be predicted rather poorly. This happens when the wave-radiation damping is small, and the response depends on viscous damping and vortex-shedding. Empirical damping coefficients may be required.
- o Inglis and Price (1980) show that strip theory methods represent conventional ship forms quite well but Faltinsen and Michelsen (1974) mention that this is not the case for a square box. There are however, discrepancies between the coefficients predicted by two and three-dimensional theories at low wave frequencies as emphasized by Inglis and Price (1980).
- o Experiments on a gravity platform model carried out by Garrison et al. (1974) and Garrison and Stacy (1977) showed a small steady uplift force (see Figure 8.3), attributed to second-order pressures. Garrison et al. (1975) showed that pipelines and other bottom-mounted structures may be similarly affected.
- o Garrison et al. (1974), (1975) used a hybrid technique to analyze a gravity platform basing tower loads on the Morison equation, and caisson loads on diffraction theory. This hybrid approach is often more accurate and efficient than either the

diffraction or the Morison method on its own. Semisubmersibles and tethered buoyant platforms have also been analyzed in a similar way. Such an application is reported by Standing (1981), and some of the results are shown in Figure 8.4.

- o Hogben and Standing (1975) showed that drag loads, acting between the mean and instantaneous water levels, may contribute significantly to the maximum overturning moment on a surface-piercing structure.
- o Wave diffraction theory is valid for all values of  $D/L$ , and may be used to estimate the mass coefficient  $C_m$  for a member of unusual shape when  $D/L$  and the effects of diffraction are small. In these circumstances there may be advantages in using a simplified form of the source potential as defined by Garrison and Stacy (1977), in which the free surface is treated as a rigid "lid".

Figures 8.3 and 8.4 show two typical applications of three-dimensional wave diffraction theory compared with experiment. Figure 8.3, based on results from the work by Garrison and Stacy (1977), shows the maximum horizontal force  $f_1$ , vertical force  $f_3$ , overturning moment  $f_5$  on a Condeep-type gravity platform. Results cover three wave periods and a range of wave heights. A hybrid model was used (see above), and several small nonlinear terms were included. For example, wave kinematics were based on Stokes V theory, and there was a mean uplift force calculation from the quadratic term in the Bernoulli equation. This mean force caused the maximum upwards force (marked UP) to differ from the maximum downwards force (DN).

Figure 8.4 from the experiments carried out by Standing (1978), shows the surge response and oscillatory cable tensions for a tethered buoyant platform. Again, a hybrid Morison/diffraction model was used, but this time including only linear terms and with zero drag.

Potential theory has been used extensively for prediction of semisubmersible and tension leg platform motion characteristics. Some researchers have applied this theory in conjunction with the Morison type formulation to evaluate wave loads on the smaller members of semisubmersibles and tension leg platforms. Table 8.2 summarizes some of the applications of these theories to semisubmersibles and tension leg platforms.

## 8.6 Nonlinear Wave Effects

One of the important limitations of the diffraction methods outlined in preceding sections is that they are based on small amplitude wave theory and the associated assumption of linearity. The severe wave heights encountered in practice have led to some consideration being given to extensions to deal with steep (nonlinear) waves.

Comments on the possible effect of wave nonlinearities on design wave loads on typical gravity platforms have been made by Hogben and Standing (1975), Garrison and Stacey (1977) and Garrison (1978). Hogben and Standing compared linear and Stokes fifth order theory predictions of the inertia force on a column and concluded that the difference for typical North Sea design wave conditions is not large. However, one important effect of wave nonlinearity is that for a given wave period nonlinear wave theory predicts a different (longer) wavelength than does linear theory. Garrison and Stacey have pointed out that the higher order components of a nonlinear wave are expected to have little effect on a typical well-submerged caisson on the seabed and they suggest using the first order component of Stokes fifth order theory (which has the appropriate wavelength) in place of linear theory itself in the diffraction calculation. The columns of a typical structure lie in the inertia range and so can be calculated by a nonlinear wave theory on the basis of the Morison equation as was described in Chapter 7.0. Although such an approach lacks mathematical rigor, its use is justified in that it does produce empirically satisfactory results

and serves as a basis for a practical design procedure.

Another effect of wave nonlinearities on surface-piercing structures is that forces calculated by integrating pressures up to the still water level on the one hand, or up to the instantaneous free surface on the other, may differ noticeably from each other. Again, Hogben and Standing (1975) have illustrated this difference for the limiting case of inertia force predictions. Formally, this difference is a second order quantity, and is thus of the same order as other second order force contributions which are neglected in the linear diffraction theory. This effect is discussed further in the chapter that follows.

Linear diffraction theory may be more unreliable for the relatively steep waves encountered in shallower water or for large structures extending up to the free surface, and a more serious investigation of nonlinear effects then becomes necessary. The important features of the nonlinear effects then become necessary. The important features of the nonlinear problem can formally be investigated by extending the diffraction theory to a second approximation on the basis of the Stokes expansion procedure in a manner analogous to the derivation of Stokes second order wave theory (Section 5.2.7).

TABLE 8.1  
SOME COMPARISONS BETWEEN LINEAR WAVE DIFFRACTION  
THEORY AND EXPERIMENT

Author	Structure and Theory Types	Date Presented
	<u>A. Strip/2-dimensional Programs:</u>	(Including some results at non-zero forward speed)
Vugts (1968) (1970)	Ship sections (mapping method)	Coefficients, wave forces, surface elevation and response
Salvesen, Tuck, Faltinsen (1970)	Ship sections (Frank close-fit)	Coefficients, responses, bending moments, shear stresses
Keuning and Beukelman (1979)	Barges (Frank close-fit and Lewis form)	Coefficients, wave forces, responses
Faltinsen and Michelsen (1974)	Square-plan caisson (Frank close-fit)	Coefficients, wave forces, responses
	<u>B. 3-dimensional Programs</u> a) <u>Fixed structures:</u>	(Zero forward speed only)
Garrison et al. (1974) (1977)	Condeep-type gravity platform	Forces and moments
Boreel (1975)	Pyramidal storage tank	Pressures, surface elevation
Hogben and Standing (1975)	Square and circular-plan columns	
Ohkusu (1974)	Groups of cylinders	Forces and moments
Huntington and Thompson (1976)	Circular cylinder in multidirectional waves	Forces, moments, pressures
Apelt and Macknight (1976)	Caisson in shallow water	Forces and moments

TABLE 8.1 (Continued)

Author	Structure and Theory Types	Data Presented
	<u>b) Floating structures:</u>	
Garrison (1974a)	Disc buoy	Heave and pitch motions
Van Oortmerssen (1976)	Tanker	Coefficients, wave forces, responses
Pinkster and Van Oortmerssen (1976)	Barge	Wave forces and responses
Keuning and Beukelman (1979)	Barges	Coefficients
Faltinsen and Michelsen (1974)	Square-plan caissons	Coefficients, wave forces, responses
Standing (1979)	Wave energy device (quasi 2-dimensional)	Responses, power absorbed, reaction forces
Hogben and Rowe (1979)	Tethered buoyant platforms	Responses, tether tensions
	<u>c) Flexible structures:</u>	
Eatock-Taylor and Duncan (1980)	Vertical column	Coefficients for rigid-body and bending modes
	<u>C. Part-Empirical:</u>	
Chakrabarti (1973)	Range of simple bodies on sea-bed	Wave forces and moments



TABLE 8.2  
APPLICATION OF DIFFRACTION THEORY AND THE MORISON EQUATION  
TO SEMISUBMERSIBLES AND TENSION LEG PLATFORMS

Year	Author(s)	Body	Modes of Action, $\tau$	Boundary Conditions Water	Boundary Conditions Body	Wave Direction	Remarks
1969	Burke Chevron Oil Field Research	Semi	1-6 Frequency domain	unbounded	submerged	arbitrary	Linearized Morison equation
1971	Hoofst NSMB	Slender Member Semi	1-6 Frequency domain	unbounded		arbitrary	Potential theory
1973	Kim & Chou	Semi	Frequency domain	deepwater	submerged	head sea	Strip theory Frank close-fit method
1974	Van Opstal et al. Shell Exploratie	Semi	1-6 Frequency domain	unbounded			Long wavelength approach Sufficiently accurate for $Ka \leq 0.6$ A program package
1977	Paulling NSMB	Cylinder Semi TLP	1-6 Time domain	unbounded	submerged	arbitrary	Morison Equation
1980	Liu, Chen, Y.N. Shin, Chen, P.C. (Paulling) ABS	TLP	1-6 Frequency and Time Domain	unbounded	surface submerged	arbitrary	Morison-type equation with a linearized drag term for small- diameter bracing 3-D source-sink method for large- displacement part
1980	Carlisen and Mathisen DnV	Semi	1-6 Frequency domain	unbounded	surface submerged	arbitrary	The Morison equation for $L/D < 5$ No interaction effects between members Strip theory Frank close-fit method 3-D Source-Sink theory for large bodies Slender body diffraction theory (not yet in wide spread use)
1981	Tein, Chou Chianis, Teymourian Brown & Root	Arbitrary shape Semi TLP	1-6 Frequency domain	unbounded	surface submerged	arbitrary	3-D source-sink method (Garrison's program) Strip theory Frank close-fit method

TABLE 8.2 (Continued)

Year	Author(s)	Body	Modes of Action, i	Boundary Conditions Water	Body	Wave Direction	Remarks
1981	Burns SOCAL	TLP	2 Stochastic	unbounded		beam sea	Morison equation Simplified analysis sway motion only Viscous drift
1981	Isaacson U. of British Columbia	arbitrary shape	1-6 Time domain	shallow water	surface submerged	arbitrary	Steep (nonlinear) wave Initial condition problem using time-stepping procedure.
1981	Pinkster NSMB	arbitrary shape Semi	1-6 Frequency domain	unbounded	surface submerged	arbitrary	3-D potential theory Wave drift force calculated by direct integrating method
1982	Malaeb Texas A&M	TLP	1-6 Frequency and Time domain	unbounded		arbitrary	The modified Morison equation Member diameters 3.5m - 16m No member interaction
1982	Angelides, Chen, Will McDermott	TLP	1-6	unbounded	submerged	arbitrary	The modified Morison Equation No member interaction
1982	Salvesen, Von Kerczek Yue Science Applications	Cylinder Arbitrary shape TLP	1-6 1-2 Time domain	unbounded	surface submerged	arbitrary	Potential flow-Frequency domain hybrid-element method Viscous force-New viscous drag formula Non-linear time-domain Surge motion Regular sea only
1982	Garrison	Arbitrary shape Vertical cylin- der Semi TLP	1-6 Frequency domain	unbounded	surface submerged	arbitrary	3-D Source-Sink method MacCamy-Fuches' method Froude-Krilov force for the end force on truncated cylinders Morison equation (linearized)
1983	Patel Lynch LCMT	TLP	1-6 Frequency domain			arbitrary	The Morison equation slender member approach No hydrodynamic interference between members

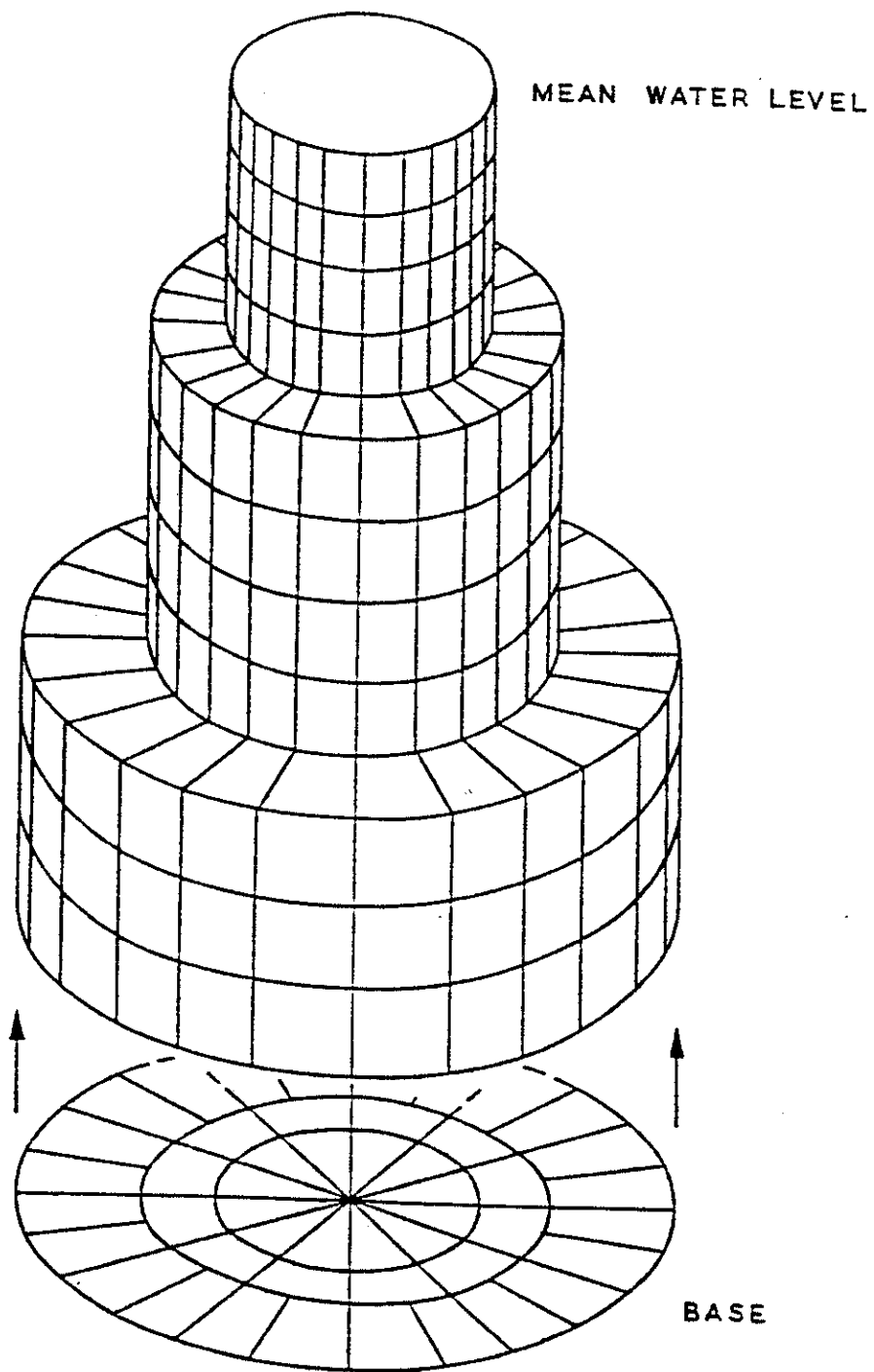


FIGURE 8.1 WAVE DIFFRACTION THEORY: EXAMPLE OF FACET MODEL, FLOATING PRODUCTION PLATFORM (STANDING, 1981)

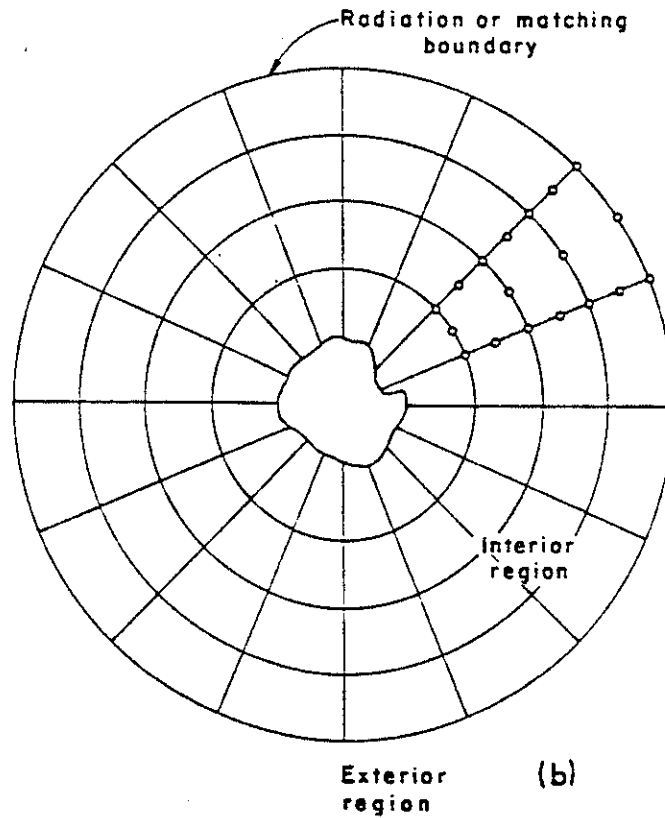
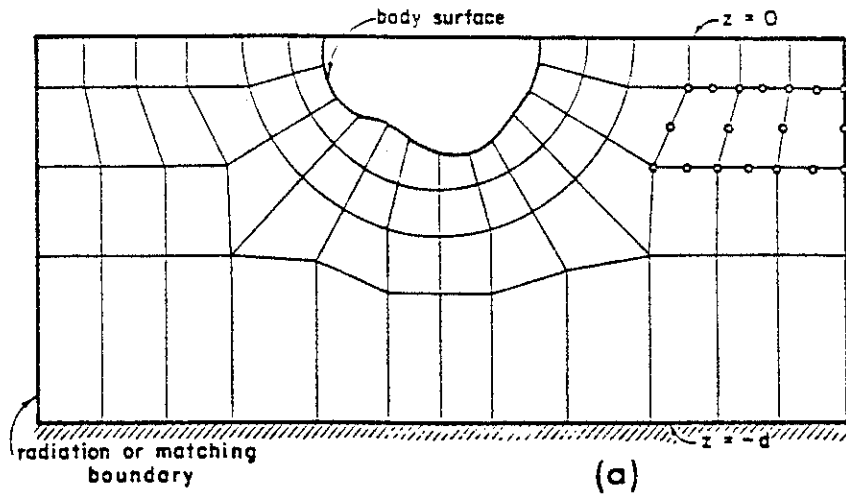


FIGURE 8.2 ILLUSTRATION OF FINITE ELEMENT MESHES FOR (a) A VERTICAL PLANE PROBLEM, AND (b) A HORIZONTAL PLANE PROBLEM. ELEMENT NODE AND RADIATION BOUNDARY REPRESENTATIONS ARE INDICATED. (SARPKAYA AND ISAACSON, 1981)

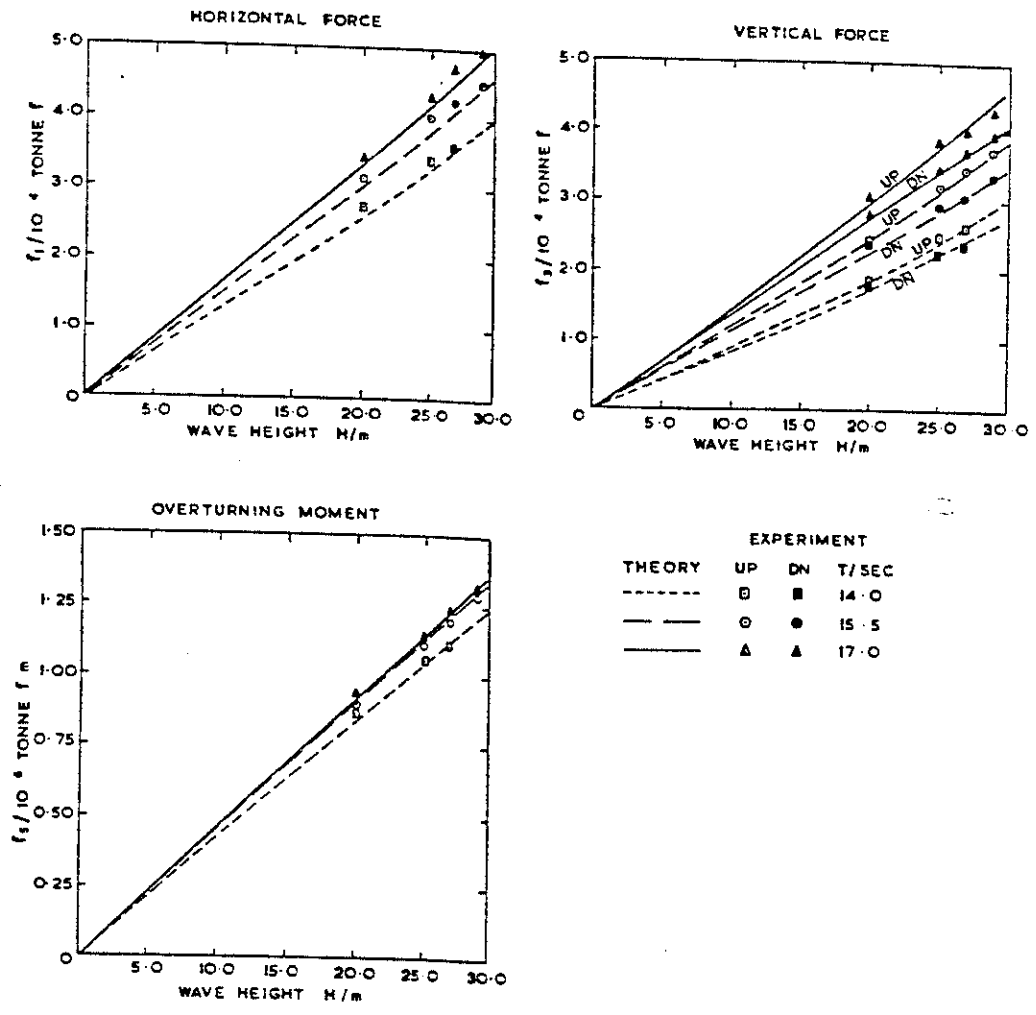


FIGURE 8.3 WAVE FORCES ON A GRAVITY STRUCTURE: THEORY AND EXPERIMENT (GARRISON & STACY, 1977)

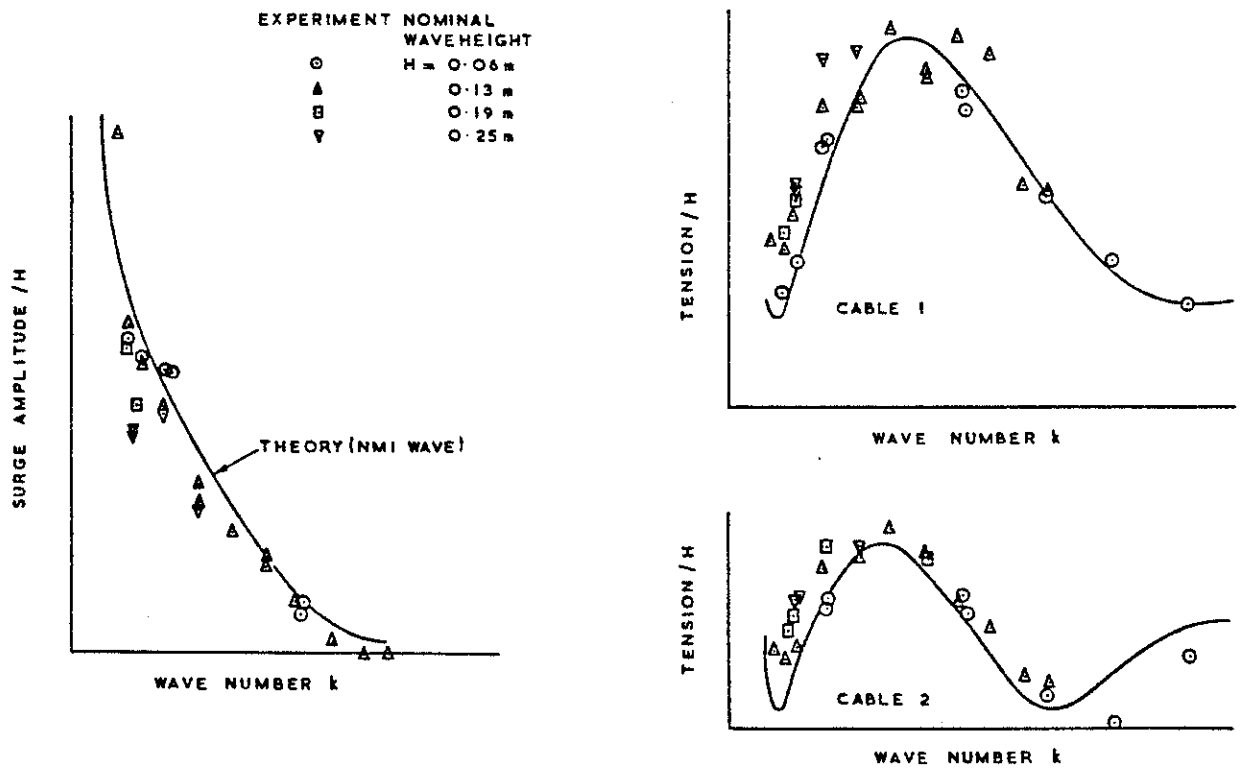


FIGURE 8.4 COMPARISON BETWEEN THEORY AND EXPERIMENT, TETHERED BUOYANT PLATFORM SURGE AMPLITUDE AND MOORING CABLE TENSION (STANDING 1981)

Under the action of environmental forces, a TLP or semisubmersible usually experiences three types of motion, namely, (1) "first order motions", i.e. oscillations at wave frequencies, (2) "slow drift oscillations" associated with some higher order (nonlinear) wave effects and (3) steady horizontal offset stemming from wind, current and/or mean second order wave drift forces. First order wave loads and associated first order motions are discussed in detail in other sections of this report. The purpose of this chapter is to review the origin, relative significance and computational aspects of various nonlinear hydrodynamics phenomena that lead to mean and/or slowly varying drift forces. As pointed out by Lundgren, et al. (1982), these forces are characterized by having small values, generally having a mean value different from zero, varying with much lower frequencies than the waves and causing large horizontal motions of moored structures such as a TLP or semisubmersible.

In potential flow theory, it is assumed that the water is inviscid, i.e. viscous effects are neglected. One group of drift forces stem from the fact that, in reality, water is a viscous fluid so that localized viscous phenomena often occur even in an otherwise ideal potential flow. Another group of drift forces, which have nothing to do with viscous effects, are associated with the nonlinearities already inherent in a potential flow. It may be recalled in this connection that the potential flow theory involves two basically nonlinear free surface boundary conditions as discussed in detail by Sarpkaya and Isaacson (1981) and others:

$$\frac{\partial \eta}{\partial t} + \frac{\partial \phi}{\partial x} \frac{\partial \eta}{\partial x} - \frac{\partial \phi}{\partial z} = 0 \quad \text{at } z = \eta \quad (9.1)$$

$$\frac{\partial \phi}{\partial t} + \frac{1}{2} \left[ \left( \frac{\partial \phi}{\partial x} \right)^2 + \left( \frac{\partial \phi}{\partial z} \right)^2 \right] + g\eta = f(t) \quad \text{at } z = \eta \quad (9.2)$$

in which  $\eta(x,t)$  is the free surface elevation measured from the still

water level,  $z=0$ . In the so-called "linear" or "small amplitude" wave theory, the nonlinear terms in these equations are neglected and, in addition, the equations are written at  $z=0$  rather than at  $z=\eta$ . A more rigorous solution of the potential flow equations can be obtained by expressing  $\phi$  as

$$\phi = \epsilon \phi^{(1)} + \epsilon^2 \phi^{(2)} \quad (9.3)$$

in which

$$\begin{aligned} \phi^{(1)} &= \text{first order velocity potential} \\ \phi^{(2)} &= \text{second order velocity potential} \\ \epsilon &= \text{a small parameter } (\epsilon \ll 1) \end{aligned}$$

While one particular type of potential flow drift force is directly related to  $\phi^{(2)}$ , others can be determined on the basis of  $\phi^{(1)}$  only, i.e. without having to construct  $\phi^{(2)}$  explicitly, as will be discussed in some detail shortly.

With the foregoing background information in mind, wave related drift forces can now be classified as follows as pointed out by Lundgren, et al. (1982), Pinkster (1981), Chakrabarti and Cotter (1983) and others.

## 9.1 Viscous Drift Forces

These forces are important mainly in connection with slender members and in the presence of relatively large wave heights and/or a combination of waves and currents.

### 9.1.1 Wave Drag Drift

Consider a partially submerged circular cylinder such as a column of a TLP or semisubmersible. The length of the wetted part of the column is  $h$  at mean water level and  $h+\eta$  in the presence of waves



with, as previously indicated,  $\eta$  = free surface elevation. According to the Morison formula, the drag force acting per unit length of the cylinder is given by

$$F_D = \frac{1}{2} \rho C_d D u |u| \quad (9.4)$$

in which  $u$  = water particle velocity,  $D$  = diameter and  $C_d$  = drag coefficient. To calculate the total drag force,  $F_D$  must be integrated along the wetted length of the column. For small wave heights, the integration may be performed along the "mean" wetted length  $h$  without introducing serious errors into the calculation. The drag force thus calculated has a zero mean value over a wave period  $T$ . When the wave height is not small, the integration must be performed along the "instantaneous" wetted length  $(h+\eta)$ . The drag force calculated on this basis always has a positive mean value because positive values of  $u$  are accompanied by positive values of  $\eta$  and vice versa. As pointed out by various investigators, this mean value represents the dominant drift force acting on a TLP or a semisubmersible.

### 9.1.2 Current-Wave Drift

In the presence of a small current with velocity  $V_c$ , the product  $u|u|$  in the Morison equation would have to be replaced by  $(u + V_c)|u + V_c|$ . Note that  $V_c$  is always positive whereas  $u$  is positive over half of the period and negative over the other half. Consequently, the mean value of  $(u + V_c)|u + V_c|$  over a complete period is a positive quantity that is larger than  $(V_c^2 + u^2)$ . In other words, the drag force associated with the wave-current combination is larger than the sum of the drag forces that would be produced by the wave and current acting individually. The net difference, which represents the effect of the "wave-current interaction", can be approximated as

$$F_{wc} = \frac{1}{2} \rho C_d D \frac{4}{\pi} u_m V_c \quad (9.5)$$

per unit length of the column as shown by Lundgren, et al. (1982). The quantity  $u_m$  in this equation is the maximum horizontal orbital velocity at the particular point under consideration.

## 9.2 Potential Flow Drift Forces

In potential flow theory, there are three types of forces acting on a moving body, namely, forces associated with incident, diffraction and radiation waves, respectively. In a purely linearized approach, these forces can be calculated separately and then superposed to determine their combined contribution. These so-called first order wave loads are directly proportional to the wave height. Nonlinear theory, on the other hand, predicts a number of higher order loads (proportional to the square or higher order powers of the wave height) in addition to the first order wave loads. These nonlinear load terms are usually referred to collectively as "second order drift forces" or "potential flow drift forces".

Before going into a detailed description of these forces, it is useful to recall that the Bernoulli equation which defines the hydrodynamic pressure at an arbitrary point of the flow, takes on the following form in a potential flow:

$$p = \rho \frac{\partial \phi}{\partial t} + \frac{1}{2} \rho (\nabla \phi)^2 \quad (9.6)$$

The total wave load acting on a body is determined by simply integrating  $p$  over the entire wetted surface of the body. As previously mentioned, the wetted surface of a partially submerged body varies with time due to the variation of the free surface elevation  $\eta$ . Finally, the wave loads acting on a moving body are indirectly dependent on the motion of the body itself since that motion affects the position and orientation of the body with respect to the wave profile.

With the foregoing observations in mind, it would now be possible to state that of the six principal potential flow drift forces listed below, the first five can be determined on the basis of the first order velocity potential only, whereas the sixth one is a function of the second order potential.

### 9.2.1 Wave Elevation Drift

Consider a partially submerged body such as a column of a TLP or semisubmersible. If the linear pressure term in the Bernoulli equation is extended from the mean water level to the instantaneous free surface  $z = \eta$ , the integral of that pressure around the body has a nonzero mean value when averaged over a wave period  $T$ . Assuming that the pressure varies linearly with depth, this so-called "wave elevation drift force" can be determined by simply integrating the quantity  $(\frac{1}{2} \rho g \eta^2)$  around the waterline of the body.

### 9.2.2 Velocity Head Drift

This particular force is associated with the second (nonlinear) term in the Bernoulli equation. It is calculated as the integral of  $(\frac{1}{2} \rho q^2)$  over the mean wetted surface of the body, where  $q^2 =$  square of water velocity at the body surface due to the first order velocity potential,  $(u^2 + v^2 + w^2)$ .

### 9.2.3 Body Translation Drift

In the case of a moving body, the position of the body relative to the pressure field varies due to the motion of the body itself, thus causing some second order variations in the wave loads. Those load variations that are associated with the translational components of the motion, when averaged over a wave period  $T$ , define the so-called "body translation drift". Letting  $X_i$  (1,2,3) denote Cartesian coordinates and  $x_i$  (1,2,3) translational components of the body's motion, the product  $x_i \cdot (\partial p / \partial X_i)$  may be viewed as a pressure

term which, when integrated over the mean wetted surface, leads to the body translation drift.

#### 9.2.4 Body Rotation Drift

This force is similar to the one above except that one now deals with the rotational components of the body's motion rather than the translational ones.

#### 9.2.5 Slowly Varying Wave Drift Forces

The four types of drift forces considered above may have an oscillating component as well as a nonzero mean value. Oscillating drift forces, which usually have very low frequencies, occur only in irregular seas (i.e. in the presence of a group of waves as opposed to a single wave), as demonstrated by Remery and Hermans (1971) and Pinkster (1981). To illustrate the concept, let us first note that all four drift forces considered above involve products of the type PQ in which P and Q are first order quantities with discrete components,

$$P = \sum_i p_i \cos(\omega_i t - \phi_i) \quad (9.7)$$

$$Q = \sum_i q_i \cos(\omega_i t - \psi_i) \quad (9.8)$$

Thus,

$$PQ = \frac{1}{2} \sum_i \sum_j p_i q_j \cos[(\omega_i + \omega_j)t - \phi_i - \psi_j] + \cos[(\omega_i - \omega_j)t - \phi_i + \psi_j] \quad (9.9)$$

The second term in this expression varies with the low frequency  $(\omega_i - \omega_j)$  which, with the right combination of i and j, may concei-

vably be very close to one of the natural frequencies of a TLP or semisubmersible (such as surge, sway or yaw frequencies) thus resulting in resonant behavior. While the amplitudes of these low frequency drift forces are usually quite small, the amplitudes of the resulting oscillations may reach alarmingly large proportions.

#### 9.2.6 Effect of Second Order Potential

The five drift forces listed in the preceding sections are all associated with the first order velocity potential. There is a sixth drift force which differs from the first five in that it is related to the second order velocity potential. To calculate this force, the second order pressure gradient,  $\rho (\partial\phi^2/\partial t)$ , is integrated over the mean wetted surface of the body.

The drift force associated with the second order potential has a zero mean value. Accordingly, it consists mainly of a low frequency oscillating component somewhat similar to the slowly varying drift force associated with the first order potential and discussed in the preceding section.

#### 9.2.7 Relative Significance of Wave Drift Forces

As discussed in detail in Section 6.2 of this report, the precise physical nature of the hydrodynamic forces acting on a body depends on the ratio (D/L) in which L is the wave length and D denotes a characteristic horizontal dimension of the body such as the diameter of a circular cylinder. In the case of a slender cylinder with  $D/L < 0.2$ , the incident wave is not disturbed appreciably by the presence of the cylinder, except in a small region where viscous effects become dominant. The Morison equation is then used to calculate the hydrodynamic loads acting on the cylinder. For larger values of D/L, diffraction effects take on a more dominant role, thus requiring that the hydrodynamic loads be calculated on the basis of incident diffraction and radiation waves. The foregoing considerations apply

to both first and second order wave forces.

A semisubmersible or TLP is essentially a framed structure that is made up of vertical and horizontal members usually referred to as columns and pontoons, respectively. In some cases, there may also be inclined members usually referred to as bracings. The column diameter is of the order of 50 to 80 feet in a properly designed TLP, and perhaps a little less than that in a semisubmersible. On the other hand, wave lengths corresponding to wave periods of 5 to 20 seconds are of the order of 130 to 2000 feet. It is seen that, in terms of the values of the D/L ratio, the columns of a TLP or semisubmersible would behave as "small bodies" for larger wave periods and as "large bodies" for smaller wave periods. In intermediate cases, both diffraction and viscosity effects would probably be equally significant.

The four types of potential flow drift forces listed above are all "second order" wave forces, i.e. they are approximately proportional to the square of the wave height. The wave drag drift force, on the other hand, is a "third order" force. According to Lundgren, et al. (1982), it may even be viewed as a "fourth order" force since the drag coefficient  $C_d$  varies too, and is approximately proportional to the wave height. It should be emphasized, however, that the abstract "order" of a force is not necessarily an accurate indicator of the actual magnitude of that force in any given application. According to Ferretti and Berta (1981), the wave drag drift force, which is of viscous origin, is the dominant drift force on a TLP or semisubmersible. This contention seems to be supported by a numerical example presented by Lundgren, et al. (1982), in which the total potential drift force acting on a particular circular column is found to be only 15 percent of the wave drag drift force acting on the same column. It should be emphasized, however, that the ratio D/L is approximately equal to 0.04 in that numerical example, i.e. it is much smaller than 0.2 thus indicating that viscous effects would indeed be expected to be the dominant factor in the particular case

under consideration. As D/L increases, diffraction effects would gradually take on a more dominant role. According to Pinkster (1981), wave drift forces cannot be predicted correctly on the basis of viscous effects only.

According to API (1984), the mean drift force acting on a semisubmersible hull may be evaluated from the formula

$$F_{\text{mds}} = C_{\text{mds}} \sum D^2 \left( \frac{H_s}{T_s} \right)^2 \quad (9.10)$$

in which  $H_s$  and  $T_s$  denote significant wave height and period, respectively,  $D$  is the column diameter and  $C_{\text{mds}}$  is a "dimensional" constant. While API does not state the specific origin of this formula, the following observations seem to be pertinent: The formula appears to be an empirical (as opposed to analytical) one. The ratio  $(H_s/T_s)$  is an indirect measure of water particle velocities, indicating that the drift force is essentially proportional to the square of the velocity. The force depends on the waterline dimensions of the columns (as represented by  $D$ ) but is independent of either the shape or size of the submerged section of the semisubmersible. The force is also independent of either the translational or rotational displacements of the vessel. The foregoing observations seem to suggest that API's formula for mean drift force is intended to represent mainly the wave drag drift force stemming from viscous effects around the columns.

When a time domain method is used and all nonlinear hydrodynamic effects are taken into consideration, the wave drift forces are accounted for automatically so that one need not have to worry about them separately. When the frequency domain approach is used, however, the situation is different. The calculation of static offsets associated with wind, current and mean wave drift forces represents the first item of business in a frequency domain analysis. The RAO's are then calculated by assuming that the vessel

is undergoing small oscillations about this "static" configuration. As far as oscillating drift forces are concerned, what is relevant in a frequency domain analysis is the so-called "slowly varying wave drift forces" which are associated with wave groups (as opposed to a single wave) as pointed out in Section 9.2.5. These forces can most conveniently be analyzed in terms of "quadratic transfer functions" as discussed in detail by Pinkster (1981).



## 10.0 WIND LOADS

A detailed knowledge of the wind climate at a particular location is essential in estimating the wind forces on a fixed or floating platform.

### 10.1 Description of Wind

The wind description should include a velocity profile and the wind spectra. The statistical wind speed data is useful in some cases such as for a long transoceanic voyage. Though wind is mostly considered as steady in nature, the dynamic part of the wind may cause amplification of responses in a compliant structure such as a semisubmersible or tension leg platform. In such cases, knowledge of the wind spectra may be quite useful in determining the mooring and tendon forces.

#### 10.1.1 Wind Speed

Wind speed is often characterized as "sustained" and "gust". The sustained wind speed is defined as the average wind speed in a sampling time usually of one minute, whereas the gust speed is the average for a much shorter duration (usually 3 seconds). The terms "N years sustained wind speed" and "N years gust wind speed" are used to refer to a statistical recurrence period of N years. Wind speed is always referred to a standard elevation, usually 30 feet (or 10 meters) above the still water level (SWL). The wind profile is then determined by using empirical relationships. DnV (1977) recommends the following relationship in the absence of detailed field data:

$$(V_z)_{\text{sustained}} = V_{10} (0.93 + .007z)^{1/2} \text{ for } z \leq 150 \text{ m} \quad (10.1)$$

$$(V_z)_{\text{gust}} = V_{10} (1.53 + 0.003z)^{1/2} \quad (10.2)$$

where  $V_z$  is the wind speed at a height  $z$  meters above SWL and  $V_{10}$  is the reference wind at a standard elevation of 10 meters above SWL. API RP 2A (1982) recommends the following formulation,

$$V_z = V_{30} \left[ \frac{z}{30} \right]^{1/n} \quad (10.3)$$

where

$V_z$  = wind speed at height  $z$  feet above SWL

$V_{30}$  = wind speed at a reference height of 30 feet above SWL

$1/n$  = an exponent, usually assumed to be between 1/13 and 1/7 depending upon sea state, related to the distance from land and duration of the design wind velocity. The exponent is approximately equal to 1/13 for gusts and 1/8 for sustained wind in the open ocean.

Velocity profile is sometimes determined by using a height coefficient, as recommended by ABS (1980) and API RP 2P (1984), and is given by

$$V_z = C_h \cdot V_{30} \quad (10.4)$$

Recommended values of height coefficients,  $C_h$ , for various heights are listed in Table 10.1.

### 10.1.2 Wind Spectra

In general, the wind speed is considered to remain constant over a certain length of time and the wind force is calculated as a quasi-static force based on the sustained (one minute average) speed. In reality, however, the wind speed is unsteady, and may produce slowly varying components with a very high natural period.

This dynamic wind force may cause significant amplification of surge, sway or yaw motions in compliant structures such as TLP's or semisubmersibles and exert higher forces on the moorings. Three of the most well known formulations of wind spectra are attributed to Davenport, Harris, Simiu and Leigh (1984). Their formulations are described below:

Harris Spectrum

$$S_V(n) = 4 \cdot K_w \cdot V_{30} \cdot L (2+f^2)^{-5/6} \quad (10.5)$$

Davenport Spectrum

$$S_V(n) = \frac{4 K_w V_{30}^2}{n} \cdot \frac{f^2}{(1+f^2)^{4/3}} \quad (10.6)$$

where

$S_V(n)$  = velocity power density function (ft<sup>2</sup>/second)

$n$  = fluctuation frequency (1/seconds)

$K_w$  = wind surface stress coefficient  
 = 0.0020 for rough sea  
 = 0.0015 for moderate sea

$V_{30}$  = average 1 hour wind speed (feet/second) at an elevation of 30 feet

$L$  = length scale dimension  
 = 5900 feet, for Harris Spectrum  
 = 4000 feet, for Davenport Spectrum

$$f = \text{non-dimensional frequency}$$

$$= \frac{nL}{V_{30}}$$

Simiu Spectrum (Simiu and Leigh 1984)

$$\frac{n S_V(z, n)}{v_*^2} = \begin{cases} a_1 f + b_1 f^2 + d_1 f^3 & f \leq f_m & (10.7a) \\ c_2 + a_2 f + b_2 f^2 & f_m < f < f_s & (10.7b) \\ 0.26 f^{-2/3} & f \geq f_s & (10.7c) \end{cases}$$

The friction velocity  $v_*$  is given by

$$v_* = \frac{k_v \overline{v_{ref}}}{\text{Ln} \frac{Z_{ref}}{Z_0}} \quad (10.8)$$

where,

$k_v$  = von Karman constant ( $\approx 0.40$ )

$\overline{v_{ref}}$  = mean velocity of wind at reference elevation

$Z_{ref}$  = reference elevation

$Z_0$  = roughness length

The roughness length  $Z_0$  is generally provided by specifying the value of sea drag coefficient  $K$ , defined as

$$K_{r1} = [k_v / \text{Ln} (Z_{ref} / Z_0)]^2 \quad (10.9)$$

The mean wind speed at any elevation 'Z' can be modelled as

$$\overline{v}_Z = \overline{v}_{ref} \cdot [\text{Ln}(Z/Z_0)/\text{Ln}(Z_{ref}/Z_0)] \quad (10.10)$$

The various constants of the equation (10.7) are given by the following expressions

$$a_1 = \frac{4 L_u \beta}{Z} \quad (10.11)$$

$$\beta_1 = 0.26 f_s^{-2/3} \quad (10.12)$$

$$b_2 = \frac{\frac{1}{3} a_1 f_m + \left( \frac{7}{3} + \text{Ln} \frac{f_s}{f_m} \right) \beta_1 - \beta}{\frac{5}{6} (f_m - f_s)^2 + \frac{1}{2} (f_m^2 - f_s^2) + 2f_m (f_s - f_m) + f_s (f_s - 2f_m) \text{Ln} \frac{f_s}{f_m}} \quad (10.13)$$

$$a_2 = -2 b_2 f_m \quad (10.14)$$

$$d_1 = \frac{2}{f_m^3} \left[ \frac{a_1 f_m}{2} - \beta_1 + b_2 (f_m - f_s)^2 \right] \quad (10.15)$$

$$b_1 = \frac{-a_1}{2f_m} - 1.5 f_m d_1 \quad (10.16)$$

$$c_2 = \beta_1 - a_2 f_s - b_2 f_s^2 \quad (10.17)$$

$$\beta = \frac{\overline{v}^2}{v_*^2} \quad (10.18)$$

$$f = nZ / \overline{v}_Z \quad (10.19)$$

where

$L_u$  = integral scale of longitudinal wind velocity fluctuations  
(in direction of mean wind speed)

$\beta$  = coefficient defining mean square value of turbulent  
fluctuation in terms of friction velocity  $v_*$

$f$  = non-dimensional frequency given by equation (10.19)

$f_s$  = non-dimensional frequency above which equation 10.7c is  
valid and is ( $\approx$ ) 0.2

$f_m$  = non-dimensional frequency at which the product of  $nS_v$  is  
maximum, (i.e. derivative of the function  $nS_v$  vanishes).  
Measurements at elevations of interest in platform design  
suggest that  $f_m \approx 0.05$  to  $0.09$

$n$  = frequency

$S_v$  = spectrum

$v$  = longitudinal wind velocity

— = denotes mean value

## 10.2 Wind Force Calculation

The wind force is usually calculated as a drag force, which is proportional to the drag coefficient, air density, windage and the square of the wind speed. Thus wind force  $F_{wind}$  may be written as

$$F_{wind} = K_{air} C_d A_{wind} (v_{wind})^2 \quad (10.20)$$

where

$$K_{air} = \frac{1}{2} \rho_{air}$$

$C_d$  = drag coefficient which depends on the geometrical shape of the body; sometime referred to as shape factor  $C_s$ . Typical values of shape factor are listed in Table 10.3.

$A_{wind}$  = wind exposed area or windage. Typical wind exposure areas for a semisubmersible platform are illustrated in Figure 10.1.

$V_{wind}$  = wind velocity at the center of wind exposed area

The value of  $K_{air}$  depends on the units used for the wind velocity  $V_{wind}$  and the wind force  $F_{wind}$ . The relative values of the factor " $K_{air}$ " are summarized in Table 10.2.

The following four guidelines for calculating wind areas are quoted from API RP 2P (1984):

1. The projected area of all columns of a column stabilized unit should be included.
2. The blocked in projected area of several deck houses may be used instead of calculating the area of each individual unit. However, when this is done, a shape factor,  $C_s$  of 1.10 should be used.
3. Isolated structures such as derricks and cranes should be calculated individually.

4. Open truss work commonly used for derricks, masts and booms may be approximated by taking 60 percent of the projected block area of one face.

In the absence of data related to the shape factor, the coefficients recommended by ABS (1980) which are listed in Table 10.3 may be used for wind force calculation. The drag coefficients recommended by DnV (1981), CIRIA (1980), and Hallam (1978) for current force calculations are summarized in Table 11.1 and may be used for wind force estimation as well.

The wind speed at different levels should be determined by methods outlined in Section 10.1.1 before calculating the wind force on individual objects. On any floating vessel there are many objects that are shielded partially or fully by another object or objects upwind of it.

Thus the wind force  $F_{wind}$ , on a platform with "N" number of items exposed to wind can be estimated as shown below (see also Chou et al. 1983):

$$F_{wind} = \sum_{i=1}^N K(V_i)^2 (C_s)_i (C_{sh})_i A_i \quad (10.21)$$

where

- $V_i$  = wind velocity at centroid of  $A_i$
- $(C_s)_i$  = shape factor for ith object
- $(C_{sh})_i$  = shielding factor for ith object
- $A_i$  = area of ith windage, see Figure 10.1
- $K$  = value in accordance with Table 10.2

The recommended shape coefficients for various geometries are summarized in Table 10.3. Shielding coefficients should be used when



adjacent objects exposed to wind lie close enough behind the first one. Use of the shielding coefficient is generally left to the discretion of the designer. For units with columns, however, ABS (1980) recommends not using any shielding allowance. If desired, the shielding factors may be determined when two members are located one behind the other in the direction of wind and the center-to-center distance "x" is less than seven times the width (or diameter)  $d_{ww}$  of the windward member. The shielding factor recommended by DnV (1981) is:

$$\begin{aligned}
 (C_{sh})_i &= 1 - \frac{d_{ww}}{d_{lw}} \left(1 - \frac{x}{7d_{lw}}\right) && \text{for } d_{ww} < d_{lw} \\
 &= \frac{x}{7d_{lw}} && \text{for } d_{ww} \geq d_{lw} \\
 &= 1.00 && \text{for } x \geq 7d_{lw}
 \end{aligned} \tag{10.22}$$

where  $d_{lw}$  is the width (or diameter) of the leeward member and  $d_{ww}$  is the width (or diameter) of the windward member.

### 10.3 Discussion of Wind Force Calculation Methods

The methods outlined in the preceding sections can only be used as an estimating tool due to a lack of knowledge of the precise values for shape factors, shielding factors and height coefficients. Thus, the wind force calculation is often verified by wind tunnel tests. Most of the published literature, based on wind tunnel tests of floating vessels, is related to column stabilized semisubmersible units. Two important trends of those studies are described below:

1. Numata et al. (1976) found that wind force estimation by equation (10.20) is conservative, as shown in Figures 10.2 and 10.3. Bjerregaard et al. (1981) confirmed the previous findings. They found that wind forces on semisubmersibles at

Large angles of heel, in general, are considerably smaller than those predicted by DnV and other rules.

2. Bjerregaard et al. (1981) were able, through wind tunnel model tests on various semisubmersibles, to show that the lift force contributes significantly to the wind overturning moment on a semisubmersible. This effect is not taken into account in the empirical methods outlined in Section 10.2.

Table 10.1  
Height Coefficients for Wind Speed Profile (ABS, 1980)

Meters		Feet		Height Coefficient $C_h$
Over	Not Exceeding	Over	Not Exceeding	
0	15.3	0	50	1.00
15.3	30.5	50	100	1.10
30.5	46.0	100	150	1.20
46.0	61.0	150	200	1.30
61.0	76.0	200	250	1.37
76.0	91.5	250	300	1.43
91.5	106.5	300	350	1.48
106.5	122.0	350	400	1.52
122.0	137.0	400	450	1.56
137.0	152.5	450	500	1.60
152.5	167.5	500	550	1.63
167.5	183.0	550	600	1.67
183.0	198.0	600	650	1.70
198.0	213.5	650	700	1.72
213.5	228.5	700	750	1.75
228.5	244.0	750	800	1.77
244.0	256.0	800	850	1.79
>256		>850		1.80

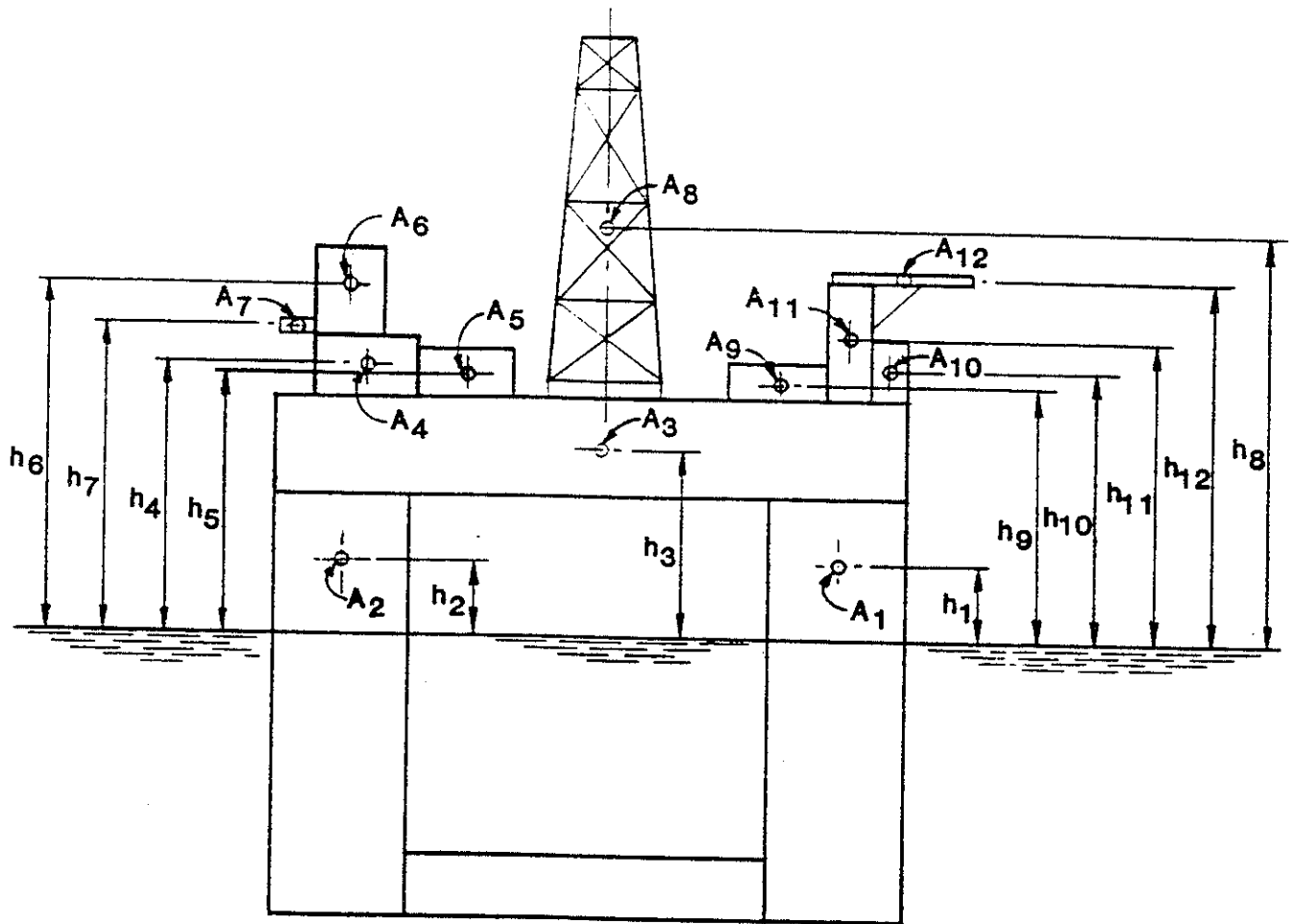
\* The height is the vertical distance from the design water surface to the center of wind exposed area A as defined in Section 3.5.2c, ABS (1980)

Table 10.2  
 Values of the Factor "K<sub>air</sub>"

A <sub>wind</sub>	F <sub>wind</sub>	V <sub>wind</sub>	"K <sub>air</sub> "	Unit
ft <sup>2</sup>	lbs	knots	0.00338	English
ft <sup>2</sup>	lbs	mph	0.00256	English
m <sup>2</sup>	N	Km/h	0.0473	Metric
m <sup>2</sup>	Kg	m/s	0.0623	Metric

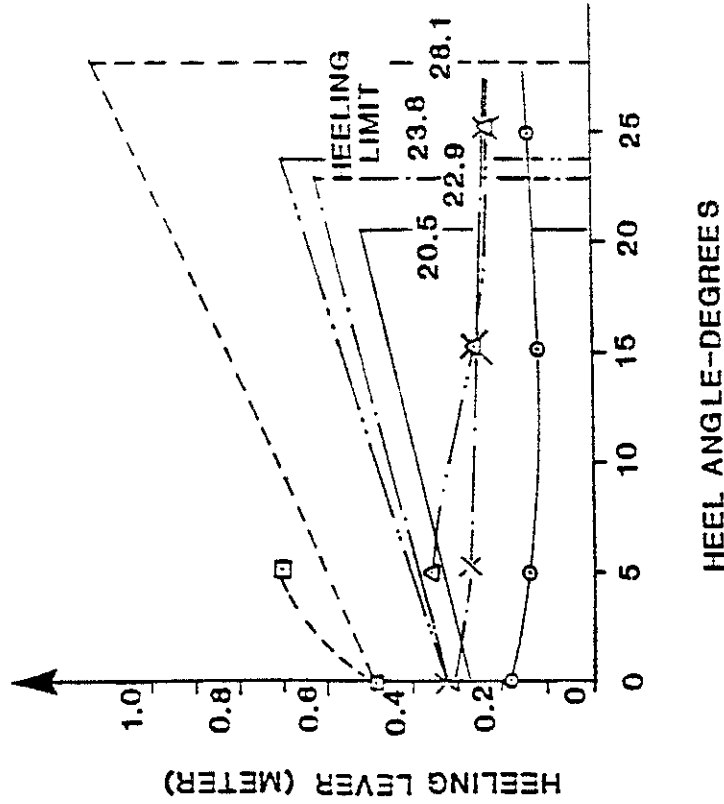
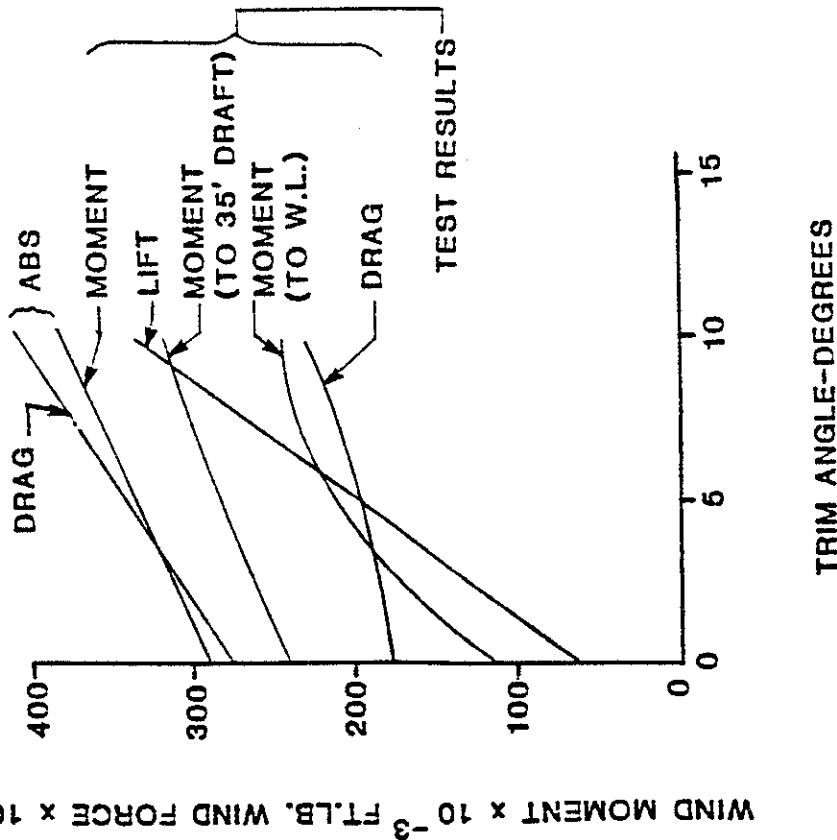
Table 10.3  
 Shape Factor C<sub>s</sub> (ABS, 1980 and API RP 2P, 1984)

Shape	C <sub>s</sub>
Cylindrical shapes	0.5
Hull (surface type)	1.0
Deckhouse	1.0
Isolated structural shapes (cranes, angles, channels, beams, etc.)	1.5
Underdeck areas (smooth surfaces)	1.0
Underdeck areas (exposed beams and girders)	1.3
Rig derrick (each face)	1.25



**WIND EXPOSED AREAS**  
**FIGURE 10.1**

MODEL TESTS	ABS	
□	---	6.43m
△	---	9.00m
×	---	10.85m
○	---	15.25m



NUMATA et al. (1976)

VARIATION OF WIND FORCES WITH TRIM ANGLE, 70 FT. DRAFT, 60 KNOT WIND

WIND HEELING LEVERS OBTAINED FROM WIND TUNNEL TEST AND FROM ABS WIND FORCE CALCULATIONS

FIGURE 10

## 11.0 CURRENT LOADS

Any structure, fixed or floating, is subjected to the current load which is a drag force. The drag force is proportional to the drag coefficient  $C_d$ , density of the water  $\rho_{\text{water}}$ , projected area  $A_c$  in the direction of the current and, the square of the current velocity  $V_c$ . Thus, to estimate current force, the important parameters are the current velocity profile and the geometry and shape of the submerged part of the structure.

### 11.1 Current Profile

The current velocity profile should be based on field data. In the absence of such measured data, the current velocity profile, as recommended by API (1982), may be determined as follows:

$$(V_c)_x = (V_c)_s \left( \frac{x}{d} \right)^{1/7} \quad (11.1)$$

where

$(V_c)_x$  = current velocity in ft/sec (m/s) at distance  $x$  in ft (m) above mudline

$(V_c)_s$  = current velocity in ft/sec (m/s) at water surface

$x$  = distance in ft (m) above mudline

$d$  = distance in ft (m) from water surface to mudline

The quantities  $x$ ,  $d$ ,  $(V_c)_x$  and  $(V_c)_s$  are illustrated in Figure 11.1.

## 11.2 Drag Coefficients

The in-line force due to a current is proportional to the member drag coefficient  $C_d$  which depends on the shape of the member and the Reynolds number  $Re$ . The coefficient  $C_d$  is not constant and varies as shown in Figure 11.2, for a smooth right circular cylinder. CIRIA (1980) shows that the fluid flow is basically divided into laminar and turbulent flow and also identifies four ranges of fluid flow on the basis of the Reynolds number. These ranges are as follows:

Subcritical range	$Re < 10^5$
Critical range	$10^5 \leq Re \leq 8 \times 10^5$
Supercritical range	$8 \times 10^5 < Re \leq 8 \times 10^6$
Postcritical range	$8 \times 10^6 < Re$

For all practical purposes, in offshore engineering applications, the fluid flow is either in the supercritical or in the postcritical range. In these ranges, the drag coefficients for a smooth cylinder vary from 0.25 to 0.60. The drag coefficient increases with roughness on the cylinder surface and marine growth as shown in Figures 11.3 and Figure 11.4 (see Olsen, 1974; Miller, 1976; CIRIA, 1980; Hallam et al., 1978). The  $C_d$  values are based on experimental research work and some typical scattering of these values in the subcritical and critical ranges is shown in Figure 11.5. Similar scatter is reported in the literature for other regions, such as the supercritical and postcritical ranges. This leads sometimes to the use of two quite different values of  $C_d$  in the same fluid flow region.

For members with cross sections other than circular, it is even more difficult to select a value of  $C_d$ . The data base for these sections is quite limited.  $C_d$  values recommended by DnV (1981), CIRIA (1980) and Hallam et al. (1978) for right circle cylindrical, square, triangular, hexagonal, octagonal and decagonal sections are summarized in Table 11.1 and can be used for estimating the drag



force.

### 11.3 Current Force Calculation

The in-line current force  $F_{\text{current}}$  can be estimated using the following equation:

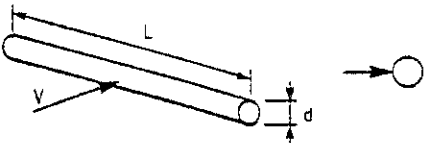
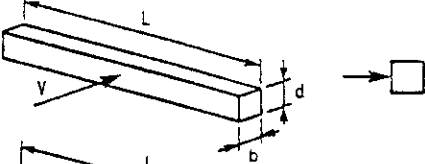
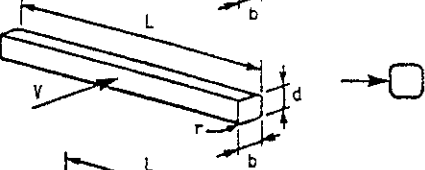
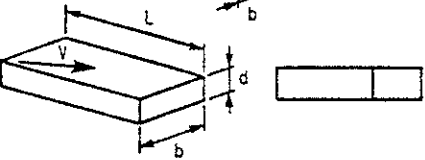

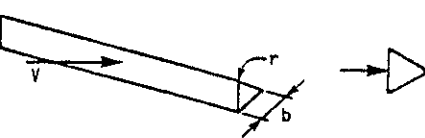
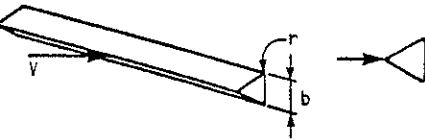


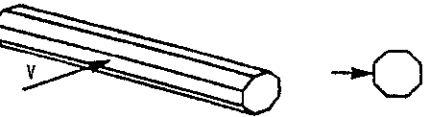

$$F_{\text{current}} = \frac{1}{2} \rho_{\text{water}} C_d A_c V_c^2 \quad (11.2)$$

where the quantities  $\rho_{\text{water}}$ ,  $C_d$ ,  $A_c$  and  $V_c$  are described in Section 11.0.

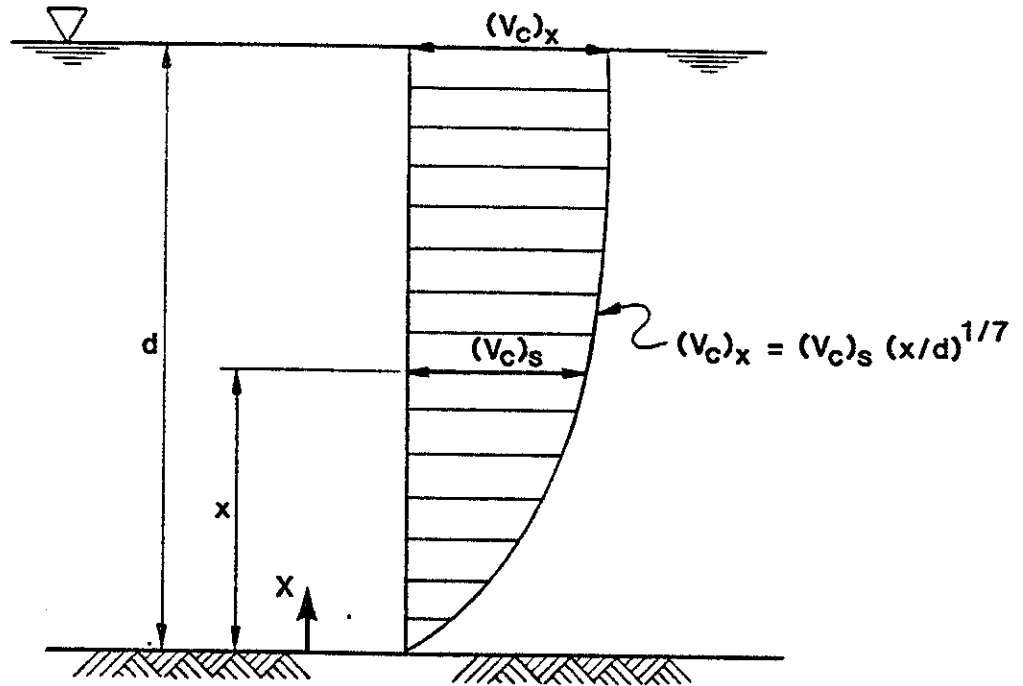
The  $C_d$  value may be chosen from Table 11.1 and the current velocity should be obtained from the design current profile.

In certain current-flow conditions, there is a dynamically-stable situation in which vortices are shed alternately from either side of the structural member around which the stream is passing. This vortex shedding generates transverse forces which can result in large strains in flexible components, particularly if the frequency coincides with the natural frequency of the structural system. This phenomenon is elaborated on in Chapter 7 of this review.

TABLE 11.1 DRAG COEFFICIENTS  
(CIRIA, 1980, HALLAM ET AL., 1978, DnV, 1981)

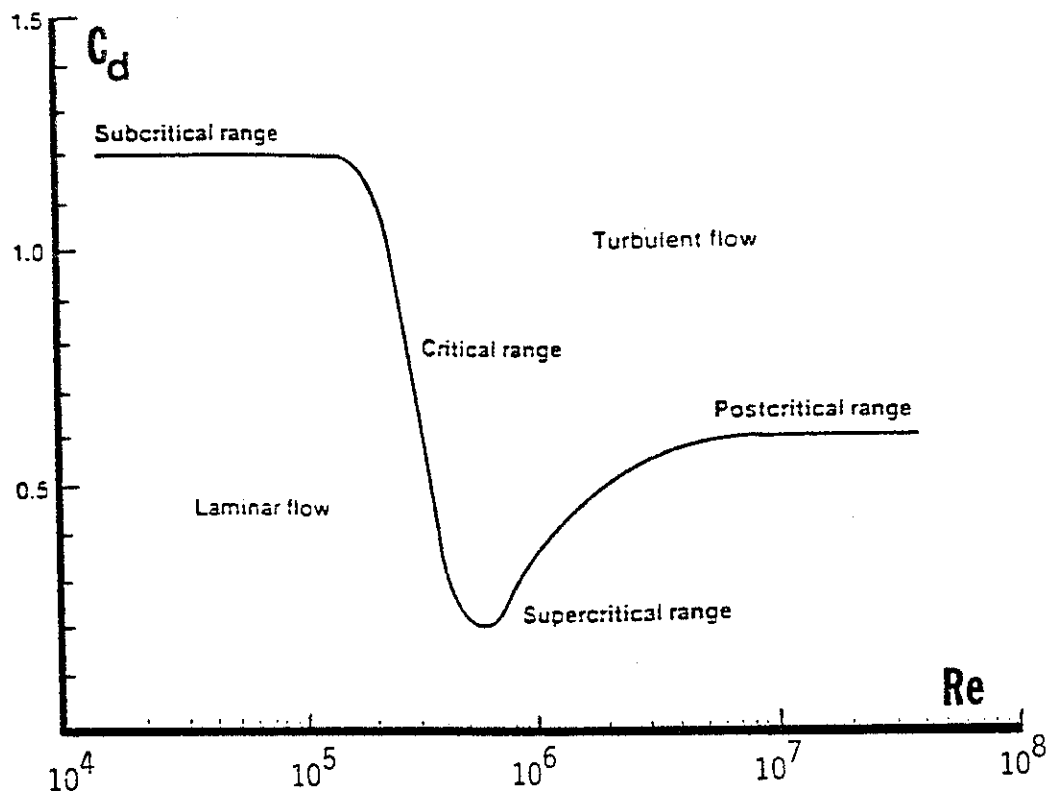
Shape of Member	Current Direction	$C_d$
Right circular Cylinders		$0.7 K_L *$
Flat bars, rolled sections, other sharp-ended sections		$2.0 K_L *$
Rectangular parallelepiped with corner radius $r$ ( $0 < r < d/2$ ), as shown in sketch		$2.0 K_L K_r K_b *$
Quadratic box, one diagonal parallel to flow		$1.5 K_L *$
Rectangular parallelepiped, diagonal of the cross- section parallel to current flow		1.6
Prism with cross-section of Equilateral triangle		2.0 (sharp edge)
		$1.9 \left( \frac{r}{b} = 0.08 \right)$ $1.3 \left( \frac{r}{b} = 0.25 \right)$
Prism with cross-section of Equalateral triangle		1.3 (sharp edge and $\frac{r}{b} < 0.08$ )
Prism with cross-section of hexagon		1.3
Prism with cross-section of hexagon		0.8
Prism with cross-section of octagon		1.4
Prism with cross-section of decagon		1.1

\*  $K_L = 0.5 + 0.1 (L/d)$ ; for  $L/d < 5$   
 $= 1.0$ ; for  $L/d \geq 5$   
 $K_b = 1.0$ ; for  $b/d \leq 2$   
 $= (8-b/d)/6$ ; for  $2 < b/d < 5$   
 $= 0.5$ ; for  $b/d \geq 5$   
 $K_r = 1.0$ ; for  $r/d \leq 0.10$   
 $= (4.3 - 13 r/d)/3$ ; for  $0.10 < r/d < 0.26$   
 $= 0.35$ ; for  $r/d \geq 0.26$



**CURRENT VELOCITY PROFILE (API, 1982)**

**FIGURE 11.1**



Reynolds number  $Re = \frac{DV_c}{\nu}$

where,  $D$  = member diameter  
 $V_c$  = fluid particle velocity  
 $\nu$  = kinematic viscosity of water

FIGURE 11.2 DRAG COEFFICIENT VARIATION  
 THE DRAG COEFFICIENT CAN VARY WIDELY WITH SEVERAL  
 PARAMETERS AS YET NOT FULLY CORRELATED. IN  
 PARTICULAR IT EXPERIENCES ABRUPT CHANGE WITH  
 THE TRANSITION FROM LAMINAR TO TURBULENT FLOW.

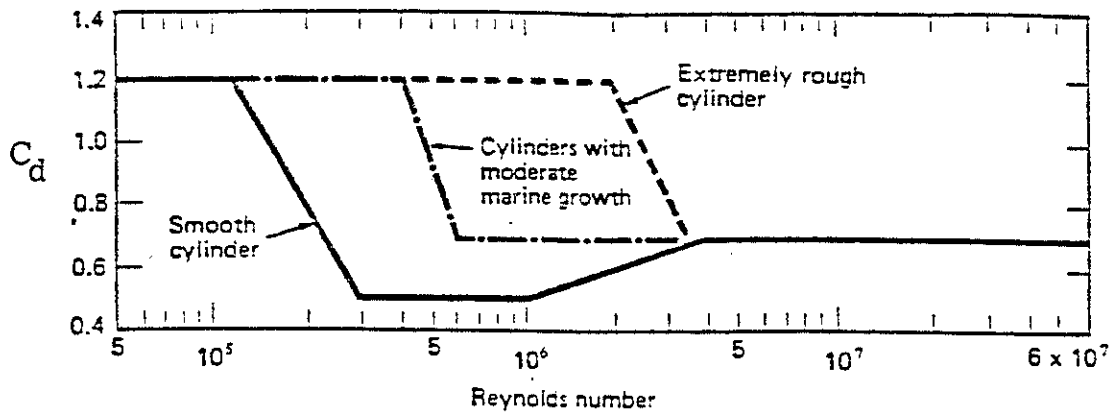


FIGURE 11.3 DRAG COEFFICIENT VALUES RECOMMENDED BY OLSEN, 1974 (SEE ALSO MILLER, 1976 AND BSRA, 1975)

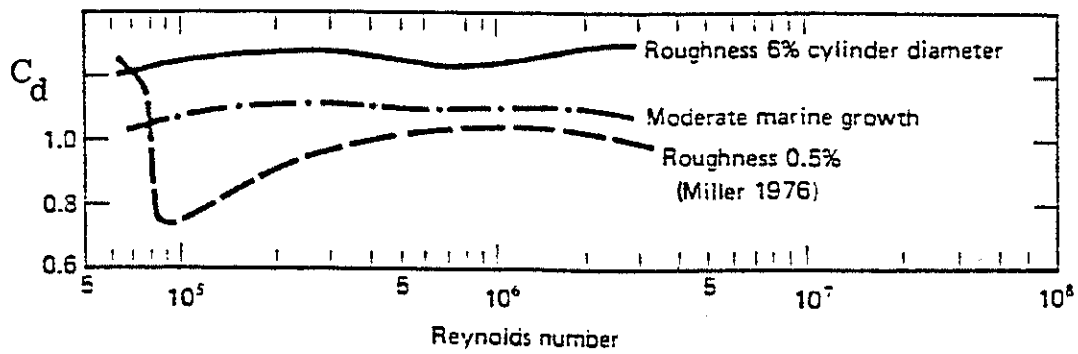
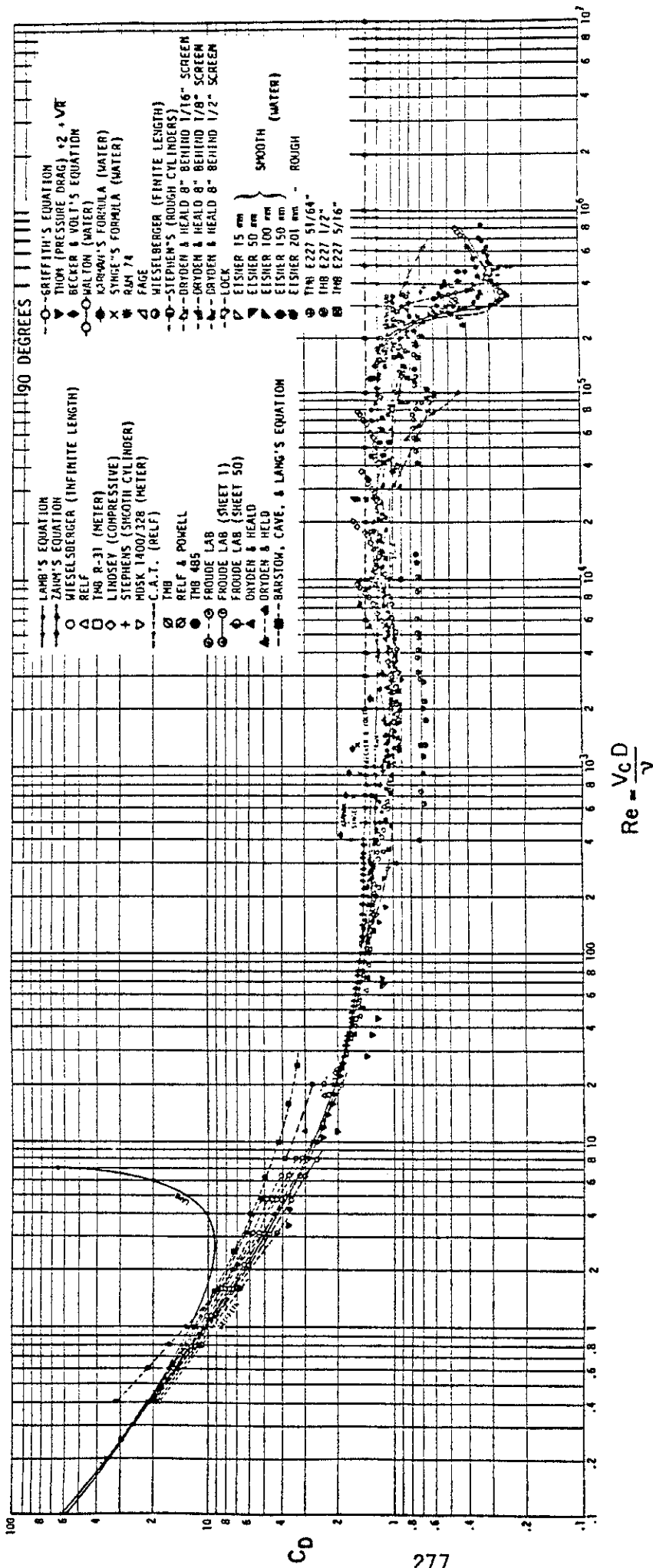


FIGURE 11.4 EFFECT OF ROUGHNESS AND MARINE GROWTH ON  $C_d$  VALUES



DRAG COEFFICIENT OF CIRCULAR CYLINDERS

FIGURE 11.5

STABILITY ANALYSIS

The stability of a floating platform is primarily measured by the metacentric height (GM), which is a function of the platform center of gravity above keel (KG), center of buoyancy above keel (KB) and the water plane moment of inertia of the surface piercing members. The quantities KG, KB and GM are illustrated graphically in Figure 12.1. The expression for the metacentric height, GM, is given by:

$$GM = KB + \frac{I_{WP}}{\Delta} - KG \quad (12.1)$$

where  $I_{WP}$  is the water plane area moment of inertia and  $\Delta$  is the volumetric displacement.

The effective metacentric height, GM, of a semisubmersible vessel may be reduced by the presence of sloshing liquids in the vessel tanks. With rolling (or pitching), the center of gravity of the liquid shifts towards the low side. This will cause the platform center of gravity to move in the same direction and thus reduce the effective metacentric height and the righting arm. The correction required in the metacentric height due to the sloshing of liquids is called the "free surface correction". This is added to the vertical center of gravity of the vessel above the keel (KG), resulting in an equivalent reduction in the metacentric height. The same discussion may be offered for a TLP during floatout or towout operation.

The free surface correction (FSC) for a floating vessel with liquid in tanks, is given by:

$$FSC = \frac{\sum_{i=1}^N (I_T)_i}{\delta_{liquid} \Delta} \quad (12.2)$$

where

$(I_T)_i$  = moment of inertia of liquid plane in the  $i$ th tank about the tank heeling or trimming axis

$\delta_{\text{liquid}}$  = specific volume of the liquid in the tank

$\Delta$  = displacement of the vessel

$N$  = number of tanks

Thus the corrected metacentric height,  $GM_{\text{corrected}}$ , will be given by:

$$GM_{\text{corrected}} = GM - FSC \quad (12.3)$$

For a semisubmersible or a TLP in floatout and towout mode, the columns and bracings in a vertical plane are the surface piercing members in the operating load condition. The water plane moment of inertia of these surface piercing members is proportional to the square of the distance of the columns and bracings from the heeling axis.

It should be emphasized that a positive metacentric height only indicates stability of the vessel in the immediate neighborhood of the instantaneous position under consideration. It does not give any real indication as to how the vessel would behave under larger angles of heel. Often the range of stability, which is the angular range over which a floating vessel will have positive static stability, gives an important indication of the angle to which the vessel could heel before capsizing. The range of stability for a floating vessel is indicated in Figure 12.2. A floating vessel may be stable for a particular load condition. This does not necessarily mean that it will have adequate stability for another loading condition. With the change of imposed loading (e.g. on-deck payload), the draft,



displacement, center of buoyancy, water plane moment of inertia, and center of gravity may all change. This will result in a change of the metacentric height and other stability related parameters such as the righting moment and the range of stability. Thus the stability of a floating vessel has to be checked for all conceivable loading conditions the vessel may be expected to encounter (e.g., towing, operating and survival conditions).

## 12.1 Stability Requirements

During the design of any floating vessel the stability will be evaluated in its intact as well as in the damaged condition. Intact stability requirements are generally enforced for the operating condition as well as the tow condition; whereas damaged stability requirements will govern the compartmentation so as to prevent capsizing of the vessel in the event of damage of one compartment adjacent to the sea.

### 12.1.1 Intact Stability

Various regulatory agencies have set specific criteria for stability evaluation of floating vessels. These criteria are, in general, similar to each other. DnV (1981) recommends the following stability criteria concerning the intact stability of semisubmersible vessels:

- o the static equilibrium heel angle due to wind should not exceed 15 degrees;
- o the second intercept (see Figure 12.2) of the righting moment and the heeling moment curves should not occur at an angle less than 30 degrees;
- o the metacentric height should be at least 1.0m ( $\approx$ 3.0 feet) in all operating and transit conditions. The metacentric height should not be less than 0.3m ( $\approx$ 1.0 feet) in any temporary

position; and

- o the area under the righting moment curve to the second intercept, or down flooding angle should not be less than 30 percent in excess of the area under the wind heeling moment curve to the same limiting angle (see Figure 12.2). Wind heeling moment should be determined on the basis of 100 year storm data; if 100 year storm data are not available, a wind velocity of 100 knots may be used. The wind force calculation is outlined in Section 10.

#### 12.1.2 Damaged Stability

To check the adequacy of water tight compartmentation, various regulatory agencies require a stability analysis with a specified number of compartments (usually one adjacent to the sea) flooded. This analysis will confirm that the vessel will not capsize as a result of progressive flooding due to damage in a specified number of compartments.

In assessing the damaged stability of column stabilized units, the regulatory agencies require the extent of damage (DnV, 1981) to be assumed as:

- o Columns, pontoons and bracings are flooded when damage occurs at any level between 5.0 meters ( $\approx$ 16 feet) above the maximum draft and 3.0 meters ( $\approx$ 10 feet) below the minimum draft specified in the operating manual;
- o Only the columns, pontoons and bracings on the periphery of the unit are damaged and the damage is in an exposed area of structure;
- o Vertical damage extent not to exceed 3.0 meters ( $\approx$ 10 feet) occurring at any level between 5.0 meters ( $\approx$ 16 feet) above and

3.0 meters ( $\approx$ 10 feet) below the water line;

- o Horizontal damage extent not to exceed 3.0 meters ( $\approx$ 10 feet) measured along the periphery of the column or pontoon; and
- o Horizontal penetration not to exceed 1.5 meters ( $\approx$ 5 feet) measured radially from the shell.

ABS (1980) specifies that the vessel will be considered to have adequate compartmentation if the unit possesses sufficient reserve buoyancy in the damaged condition to withstand an additional overturning moment due to a 50 knot wind. The water line in the damaged equilibrium condition should be below the lower edge of any opening through which downflooding may take place.

#### 12.1.3 Additional Intact Stability Criteria

Goldberg and Tucker's (1974) intact stability criteria for SWATH (Small Waterplane Area Twin Hull) ships may be considered for other semisubmersibles. The criteria presented by them was based on the following considerations of the hazards due to:

- o beam winds combined with rolling; and
- o large off-center loads.

When the heeling arms, due to wind heel, are superimposed on the plot of the vessel's righting arm, as shown in Figure 12.3, and an assumption is made for the angle of rolling into the wind,  $\theta_R$ , the following must be satisfied:

- o the heeling arm at the intersection of the heeling arm and righting arm curves (point C) must not exceed six tenths of the maximum righting arm.

- o area  $A_1$  is to be not less than 1.4 times area  $A_2$  ( $A_2$  extends  $\theta_R$  degrees to windward from point C and  $A_1$  extends from C to the angle of downflooding or the angle of second intercept of the curves (point D), whichever is the less).

The roll angle associated with the storm wind and sea conditions is expressed as  $\theta_R$ . A value of  $25^\circ$  was used by Sarchin and Goldberg (1962) for U.S. Naval surface ships, but for SWATH ships (as for air-cushion vehicles in displacement mode) a value of  $15^\circ$  seems more reasonable.

Large off-center loading can arise from lifting heavy weights over the side or end. The criteria are similar to the above except that the heeling arm is due to the off-center load rather than the wind heeling moment, and are as follows:

- o the angle of heel at the intersection of the curves (point C) must not exceed  $15^\circ$ ,
- o the heeling arm at point C must not exceed six tenths of the maximum righting arm,
- o the reserve of dynamic stability (corresponding to area  $A_1$ ) up to the angle of downflooding or the angle of second intercept, whichever is the less, must not be less than four tenths of the total area under the righting arm curve up the same angle.

## 12.2 Comparisons of Existing Stability Criteria

Four of the regulatory authorities who have published stability regulations are:

- o American Bureau of Shipping (ABS, 1980)
- o U.K. Department of Energy (DOE, 1974)
- o Norwegian Maritime Directorate (MD, 1973)

- o Det norske Veritas (DnV, 1981)

Summaries of those four authorities' stability requirements are compared by Ghosh et al. (1979) and are reported in Table 12.1. Due to recent accidents of the Alexander Kjelland and Ocean Ranger, the Norwegian Maritime Directorate is in the process of implementing some additional stability criteria which are not included in the comparison Table 12.1. The additional criteria will require that (column stabilized) platforms be provided with a way of providing buoyancy in the deck structure so as to make it possible to remain afloat after the loss of buoyancy equivalent to the volume of the whole or major part of any column. This loss of buoyancy should be assumed to occur when the platform is at the maximum operating draft and with the allowable maximum vertical center of gravity.

### 12.3 Discussion of Stability Analysis

The current practice regarding stability assessment of semisubmersible vessels is essentially "static" in nature, in the sense that at each displaced position of the vessel, a comparison is made of the righting forces and the disturbing forces corresponding to winds. To avoid capsizing of the vessel, the righting energy must exceed the heeling energy by a margin of 30 percent. In actuality, the vessel is in motion and various other environmental effects are acting on it concurrently with the sustained wind force. These include:

- o Wind Gusts
- o Forces and motion of the vessel due to the prevailing sea states.

The 30 percent margin of safety (of righting energy over heeling energy as discussed in Section 12.1.1) is provided to account for the dynamic/quasi-dynamic effects associated with wind gust, wave induced loads and the forces associated with vessel motion. Many within the industry consider this margin of safety (see Bell, 1974) too

conservative.

A SNAME sponsored research study (see Numata et al., 1976) has, however, established the adequacy of the current approach for evaluating stability of semisubmersibles. Laboratory tests have shown that the empirical criterion of stability for the configurations investigated may even be too severe, thus possibly penalizing the load carrying capacity of the semisubmersible vessels. However, a reduction in the safety margins cannot be justified due to a lack of rigorous, analytical/rational procedures for stability investigations and a wide variation in the structural configurations of the present and future semisubmersible vessels. With the recent accidents of the Alexander Kjelland, Ocean Ranger and Glomar Java Sea, no relaxation of the present stability requirements of various classification societies is expected. More stringent rules are forthcoming as mentioned earlier in Section 12.2.

TABLE 12.1 (Ghosh et al 1979)

COMPARISON OF STABILITY CRITERIA FOR SEMISUBMERSIBLE BARGE

ITEM NO.	REQUIREMENT	AUTHORITY	AMERICAN BUREAU OF SHIPPING (A.B.S.S.)	UNITED KINGDOM DEPARTMENT OF ENERGY (D.O.E.)	NORWEGIAN MARITIME DIRECTORATE (M.D.)	DET NORSKE VERITAS (D.N.V.)
1	Wind Speeds: - Minimum wind speed to be assumed for operational condition at an offshore location.		36 m/sec. (25.8 m/sec. may be considered for sheltered location)	35 m/sec	70 knots (= 36.04 m/sec)	35 m/sec
2	Minimum wind speed to be assumed for extreme weather survival condition.		51 m/sec.	50 m/sec	100 knots (= 51.48 m/sec)	50 m/sec
3	Wind speed to be assumed for flooded/damaged condition.		25.8 m/sec	25 m/sec	50 knots (= 25.74 m/sec)	25 m/sec
4	Wind Heeling Moment: - Method to be used to determine wind heeling moment.		Either by calculation (using a method described in these rules) or by wind tunnel tests.			By calculation, using a recognized method. The suggested method of calculation is described in these rules. This is not obligatory.
5	Variation of Wind Moment with Angle of Heel: -		To be calculated for a sufficient number of heel angles to define the curve.	To be calculated for a sufficient number of heel angles to define the curve.	Proportional to cosine of angle of heel.	The suggested method of calculation in these rules describes calculations at different angles of heel.
6	Heeling Directions and Wind Directions to be Examined: - For intact stability calculations.		The (wind heeling moment) calculation should be performed in a manner to reflect the range of stability about the most critical axis.		Cross curves of stability shall be prepared for the horizontal axis which gives the most severe requirement regarding stability.	Wind heeling moment curves are normally to be calculated for the wind directions parallel to the unit's two main axes in the horizontal plane. When there is other wind direction is more unfavourable curves referred to such directions are to be calculated.
7	For Damaged Stability Calculations.		Wind from any direction.	Wind from any direction.	Wind applied from the most severe horizontal direction regarding damage.	Acting in the direction to which the unit will heel/trim on account of flooding.

TABLE 12.1 (Ghosh et al 1979)  
COMPARISON OF STABILITY CRITERIA FOR SEMISUBMERSIBLE BARGE (CONTINUED)

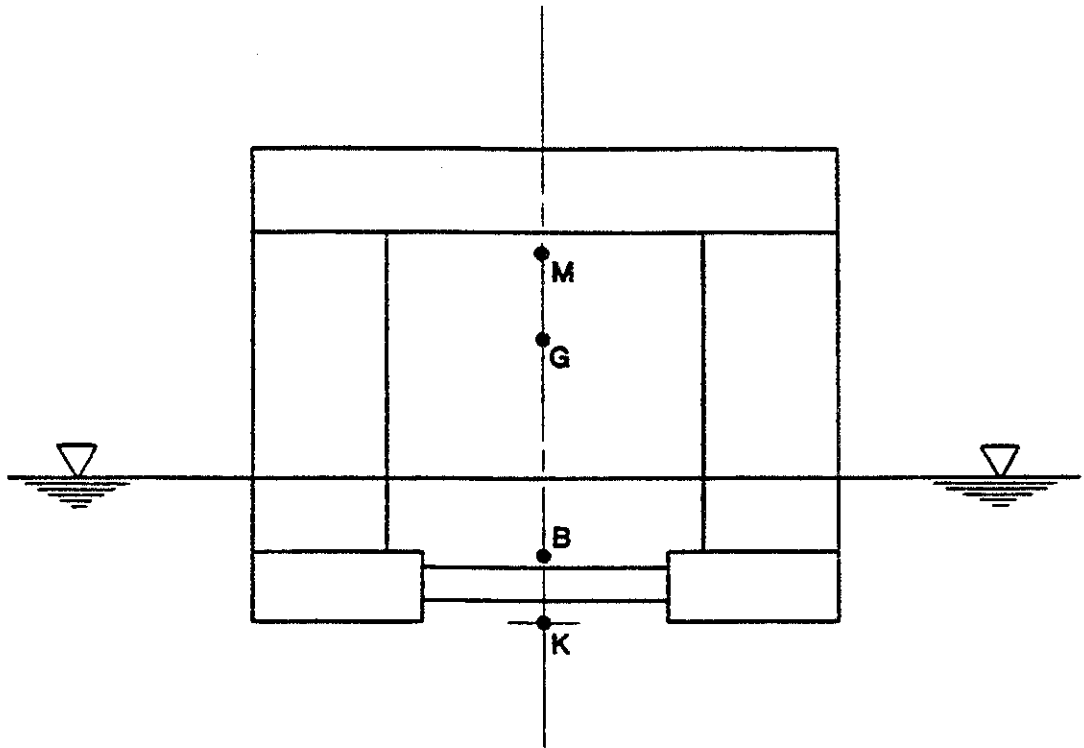
ITEM NO.	REQUIREMENT	AUTHORITY	AMERICAN BUREAU OF SHIPPING (A.B.S.)	UNITED KINGDOM DEPARTMENT OF ENERGY (D.O.E.)	NORWEGIAN MARITIME DIRECTORATE (M.D.)	DET NORSKE VERITAS (D.N.V.)
8	Initial Metacentric Height, GM, for every condition of loading.		To be positive	To be positive		> 0.3 m
9	For each condition of loading the static angle of heel due to the wind speed which is required to be assumed for the condition (see items 1 and 2 of Table 1) shall comply with either (a) and/or (b): - (a) amplitude of the angle of heel (b) ratio (freeboard at static angle of heel)/(freeboard of the unit with no heel)				< 12° > 0.5	
10	For the survival condition with wind speed as item 2, area ratio, area (A + B)/area (B + C) For all other conditions, with wind speed as item 1, area ratio area (A + B)/area (B + C)		> 1.3 > 1.3	> 1.3 > 1.3	> 1.3	> 1.3
11	Number of compartments to be assumed flooded at any one time. Description of the compartments which require to be considered floodable.		one, two, or more depending on positions of watertight divisions in way of assumed damage. those which may be damaged (see item 17)	one any one watertight compartment	normally two (see below) (a) those which may be damaged (see item 17); (b) one compartment beyond the damage. (Regulation is not specific whether (a) and (b), or alternately (a) or (b) is required.	one, two or more depending on positions of watertight divisions in way of assumed damage. Those which may be damaged (see item 17) or any one compartment adjacent to the sea.



TABLE 12.1 (Ghosh et al 1979)

COMPARISON OF STABILITY CRITERIA FOR SEMISUBMERSIBLE BARGE (CONTINUED)

ITEM NO.	REQUIREMENT	AUTHORITY	AMERICAN BUREAU OF SHIPPING (A.B.S.)	UNITED KINGDOM DEPARTMENT OF ENERGY (D.O.E.)	NORWEGIAN MARITIME DIRECTORATE (M.D.)	DET NORSKE VERITAS (D.N.V.)
12	Extent of Assumed Damage  (i) Peripheral location  (ii) Vertical location  (iii) Vertical extent of damage  (iv) Circumferential extent of damage to a cylindrical member having diameter = D  (v) Damage penetration		At any point on the exposed periphery of the unit			At any point unless it is obvious that damage can not take place.
			(presumably) at the level of the waterline before damage.			Within the zone from 1.5 m below lowest waterline to 5 m highest waterline.
			Any watertight flat within 1.5 m of normal operating drafts will be damaged.			Not less than 4.5 m, but sufficient to damage one watertight flat.
			$\pi D/4$			2.3 m
			1.5 m			$\pi D/6$
13	Require-ments after flooding  With wind heeling moment (see item 3 and item 7 of Table 1) applied after flooding.					
			The lower edge of any opening through which downflooding may occur shall not be immersed.	Any opening through which downflooding may occur shall not be submerged.	For the equilibrium flooded condition: - area (A + B) > area (B + C)	For the equilibrium flooded condition: - GM > 0.3 m



**K - KEEL**

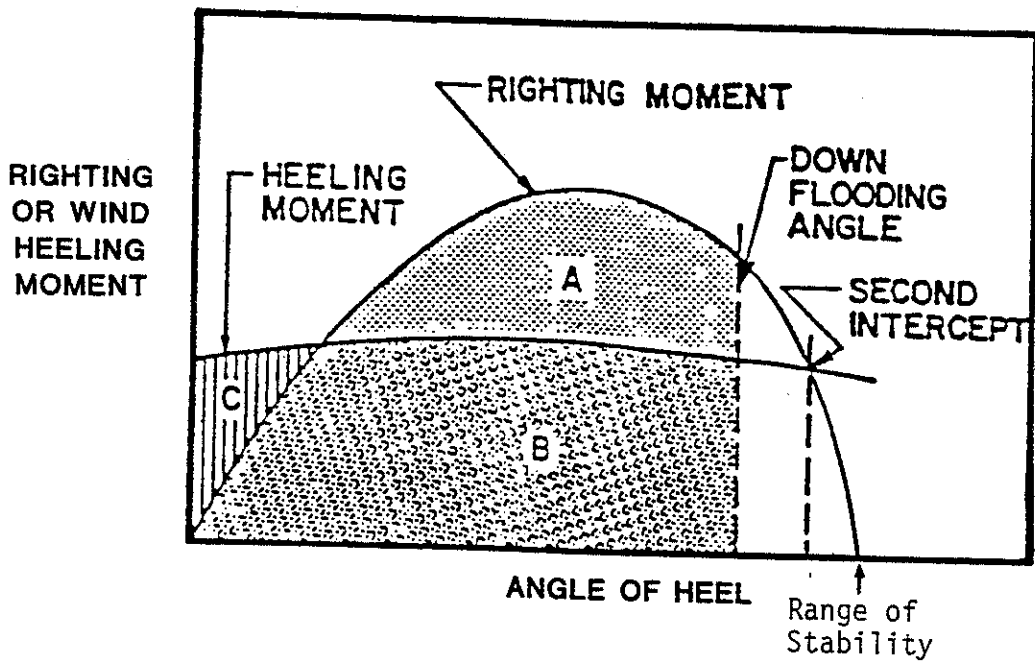
**B - CENTER OF BUOYANCY**

**G - CENTER OF GRAVITY**

**M - METACENTER**

**DEFINITION SKETCH FOR CENTER OF BUOYANCY AND METACENTER**

**FIGURE 12.1**



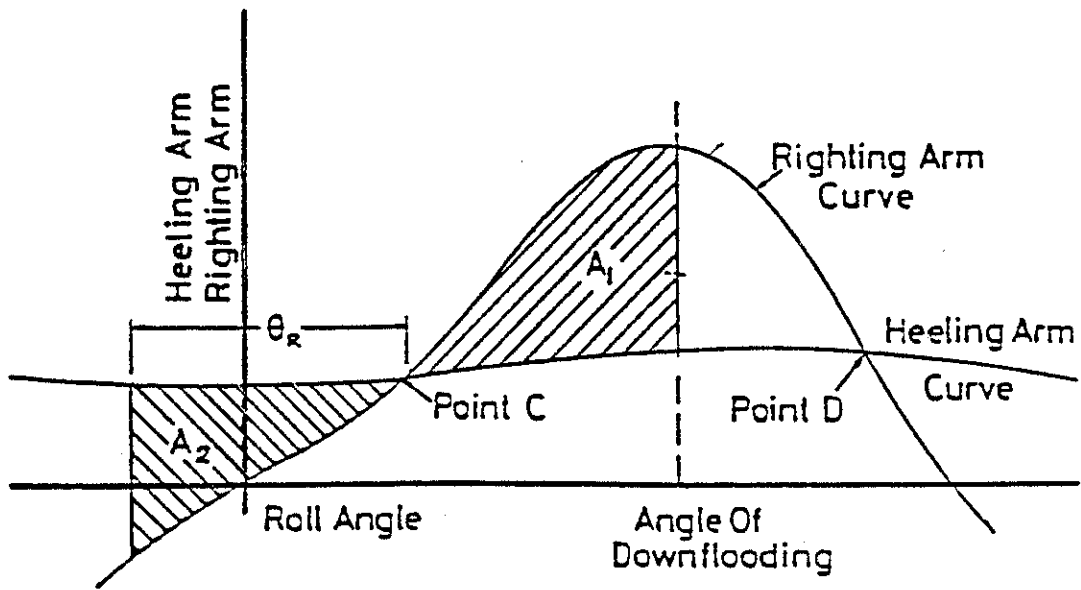
$$\text{AREA (A+B)} \geq 1.3 \text{ AREA (B+C)}$$

$$B(1 + \frac{A}{B}) \geq 1.3B(1 + \frac{C}{B})$$

$$\frac{A}{B} \geq .3 + 1.3 \frac{C}{B}$$

**DYNAMIC STABILITY CURVE**

**FIGURE 12.2**



**STABILITY CURVE**

**FIGURE 12.3**

MOORING SYSTEM ANALYSIS

The factors predominant in the design of any mooring system must include the correct application of the analytical methodology as related to the project objective and requirements. From an operations standpoint, the factors considered should include realistic expectations based on ordinary offshore practices and specific installation requirements. Other significant parameters influencing the design should include minimization of cost, reduction of the mooring system weight, and adherence to existing space requirements.

This chapter presents a general overview of mooring system analysis and design for deepwater moored structures. Specifically, the application to semisubmersible and tension leg platform structures will be addressed. Only the more common mooring systems will be presented. These will include the catenary and vertical pretensioned mooring systems.

Catenary Mooring System - Catenary mooring systems are used in deep water for semisubmersibles and for TLP's during their installation operations. The catenary mooring systems of today can be comprised of any or all of the following materials; chain, wire rope, and synthetic lines. Drag anchors are frequently used, but in some instances, piles or explosive embedment anchors are better suited. Depending on the application, large displacement surface buoys or smaller in-line buoys may be used. Catenary systems are generally easy to deploy, but through the use of buoys, the process is made even easier. In this case, the mooring system is deployed first by a separate vessel, and then the platform is brought in and engaged to the system simply by running hawsers to the buoys. Once the system is tensioned, it is fully operational. In the event the platform must leave the site (bad weather or repairs) it must only slack down and disengage at the buoy. The mooring system stays in place. Hybrid systems consisting of synthetic line and chain or wire rope

have been very successful in keeping the overall weight of the system to a minimum and simplifying deployment. Figures 13.1 and 13.2 show a hybrid mooring system in slack and pretension configurations respectively. Figure 13.3 shows details of a hybrid mooring system.

Vertical Pretensioned Mooring System - The vertical pretensioned mooring system is used in deep water for tension leg platforms (see Figures 3.15 to 3.18). This system is extremely well suited for limiting the heave, roll, and pitch responses of the moored platform. It is, however, difficult to deploy (requiring a temporary catenary mooring system during installation) and is quite expensive. Also due to the large pretension force exerted by the mooring system, the design of the hull structure requires special attention.

### 13.1 Design Methodology For Catenary Mooring Systems

There are six major steps in the design of a catenary mooring system once a particular type of mooring system is selected. These steps are briefly listed below.

1. Environment Direction Study - Based on the client supplied design criteria pertaining to the directions of wind, waves, and current, a worst case environmental loading condition for design is selected. A tentative mooring pattern is chosen at this step.
2. Platform Motion Response to Waves - By temporarily ignoring the mooring system, an analysis is performed to determine the frequency domain first order motions of the semisubmersible and to establish a data file for subsequent motion analysis in the time domain. The details of this task depend on whether the platform is treated as a large body or an assemblage of small bodies. In the latter case, in which the hydrodynamic loads acting on the platform are calculated from the Morison equation, the equations of motion must first be linearized as discussed in detail in Section 7.7.

3. System Stiffness Study - A catenary mooring system is intended to be effective more against mean and slowly varying drift forces than in connection with first order motions produced by first order wave loads. For purposes of preliminary analysis, the mooring system is often modeled as a set of horizontal springs and the hydrodynamic loads acting directly on the mooring lines are neglected. In designing a catenary mooring system for a given platform, a general study is conducted by considering a realistic set of horizontal springs and determining the motion characteristics of the platform in each case. This leads to displacement versus spring constant relationships of the type illustrated in Figure 13.10. These relationships, used in conjunction with the requirements of the client (such as maximum allowable static and dynamic excursions for the platform) give a good idea as to what spring stiffness would be most desirable for the mooring system of the particular platform under consideration.
4. Mooring System Force Balance - A static solution is obtained for the horizontal components of the static tensions in all mooring lines at the optimum pattern for the environmental design loading condition.
5. Selection of Actual Mooring Line Configuration - Based on the stiffness and tension requirements found in previous analyses and the operational criteria specified by the client an actual mooring line configuration is chosen.
6. Verification of Design By Time Domain Analysis - A time domain analysis incorporating the effects of the first and second order wave forces, the wind and current forces and the newly designed mooring system (with nonlinear characteristics) is executed as a final check on the client's requirements for maximum allowable excursions and allowable mooring line tensions.

The overall process of catenary mooring system design is summarized in Figure 13.4.

## 13.2 Design Criteria

The client-specified design criteria consist of performance and environmental specifications, safety factors for mooring components, and mooring line candidates. These are explained below.

- o Environmental design criteria: The client must specify a maximum environmental condition consisting of wind, waves, and current which is to be used for design.
  - Sustained wind velocity and a description of the exposed vessel for load calculation.
  - Wave height given as a statistical value such as significant wave height (average of the highest 1/3).
  - Surface current velocity and a description of the vessel's submerged geometry for load calculation.
  - Subsurface current profile as a function of depth and direction. This may be very important for small semisubmersibles in deep water where the ratio of hydrodynamic load on the mooring lines is a large percentage of the total hydrodynamic loads for the platform system.
  
- o Safety factors (S.F.) on mooring components: These values may be based on manufacturer's recommendations, client's requirements, or experience.
  - Typically synthetic lines have a S.F. of 5 or more for operating conditions, and a S.F. of 3 for survival conditions.
  - Chain usually carries a S.F. of 3.
  - Wire rope usually carries a S.F. of 2.



- o Mooring line candidates: Based on previous in situ performance or client's requirements, mooring systems of synthetic, wire rope, chain, or any combination of the three.

### 13.3 Preliminary Analysis

#### 13.3.1 Mooring Pattern Selection

Initially, a study must be performed to determine the sensitivity of mooring line loads to current, wind, and waves. This is done to establish a worst case environmental loading condition and to determine from this an optimum mooring pattern. The greater part of the loads on the vessel (and the mooring lines themselves) will result from the current when velocities exceed 2 knots. Emphasis should be placed on current, therefore, when determining the mooring pattern. The subsurface current profile may be very important for deepwater cases and especially when small semisubmersibles such as the Navy's or Air Force's (as described in Section 3.2.1) are considered. The subsurface current should also be considered for deepwater TLP's. A typical mooring pattern selection process and development of a sample design environmental condition are given below for a catenary system.

Current force and moment data are computed from current velocity specified by the client. Typical force and moment data scaled to a 1-knot current are shown in Figure 13.5 for all directions. From the given data, curves are generated to show individual horizontal line tensions for various mooring patterns. A 4-point catenary mooring pattern of  $55^\circ$  (measured with respect to the vessel longitudinal) is used as an example and is shown in Figure 13.6. The curve in Figure 13.7 shows the individual line tensions which result from a typical 3-knot current from all directions.

The client-supplied wind force and moment data should be based on a particular speed and all directions. Typical wind data are shown in

Figure 13.8. From this data, a set of curves is generated to show the horizontal mooring line tensions for the 55° pattern. These results are shown in Figure 13.9. As the wind is shifted through all headings from 0 to 180°, the maximum tension is experienced by line No. 1 at a heading of 55°. This corresponds to a wind acting in line with the mooring line.

Based on prior experience with wave forces on vessels, beam seas are usually chosen for design purposes.

An overall environmental design condition can now be defined. For this example, wind should be studied at 55°, waves from 90° and current from 20° (based on a limitation of 50 kips horizontal tension due to current alone). This condition is summarized below and in Figure 13.9.

SAMPLE ENVIRONMENTAL LOADING CONDITION

	<u>MAGNITUDE</u>	<u>DIRECTION</u>
Current	3 Knots	20°
Wind	24 Knots	55°
Waves	Based on client supplied significant wave height for irregular sea state	90°

13.3.2 Frequency Domain Analysis

The analysis of the motion response of a semisubmersible or TLP is not a uniquely defined task in that the sea state under consideration may be regular or irregular, the mathematical formulation of the problem may be linear or nonlinear, and the analytical approach used may be in the frequency or time domain. In preliminary analysis, the frequency domain approach is usually preferred due to its simplicity

and cost effectiveness. However, since this approach requires that the mathematical formulation of the problem be completely linearized, a relatively costly time domain analysis is often performed in the final design stage to account for some of the more significant nonlinearities that are inevitably ignored in a frequency domain analysis.

When the platform is treated as a "large body", a frequency domain analysis usually involves the following four steps for any specific wave frequency under consideration:

1. From the incident, diffraction and radiation wave theories, obtain the hydrodynamic load terms and the added mass and damping matrices.
2. From a combination of mooring system characteristics and hydrodynamic characteristics of the platform, obtain the stiffness matrix.
3. Write the six linearized equations of motion.
4. Solve these equations to determine the RAOs and phase angles for the six principal displacement components of the vessel.

When the platform is treated as an assemblage of "small bodies", the first of the four steps listed above would have to be modified as follows:

Determine the added mass matrix of the platform by using the appropriate  $C_m$  coefficient for each individual member and linearize the drag terms as outlined in Section 7.7.

An irregular sea state is generally viewed as made up of a finite number of regular waves. The analysis outlined above is repeated for each component wave frequency and the results are combined in a

probabilistic sense and in accordance with the wave amplitudes suggested by the particular wave spectrum under consideration.

Wave drift forces can be one of the more significant external forces which are overcome by mooring line tension and should therefore be considered in mooring system design. This is especially true for a platform in beam seas.

### 13.3.3 System Stiffness Study

In this part of the design, calculations are performed to determine the general mooring characteristics of the vessel and its proposed optimum mooring pattern as it relates to individual line stiffness. This is done to assist in the preliminary determination of mooring line configuration and size.

In preliminary analysis, the mooring lines are modeled as horizontal linear springs placed at each fairlead location and orientated with the optimum mooring pattern angle. Again, for a small semisubmersible in deep water the assumption of linear springs to model the mooring may not be valid. It may be better to use the stiffness generated from a load displacement table. The effects of first and second order wave forces from the beam direction (typically the most severe) are studied. The steady state effects of wind and current can be neglected from the analysis based on the fact the steady forces will be balanced out by the static tension.

A range of horizontal line stiffnesses should be studied. The range of values which are used (Example: From 0.1 to 1.0 kips/foot) will be based upon experience gained in similar type analyses. For each value of horizontal line stiffness two parameters will be investigated. These are, 1) the amplitude of the sway motion of the vessel - to obtain maximum excursion information, and 2) the horizontal tension in the line of highest loading - for allowable tension information. As an example, Figure 13.10 shows typical sway

motion (as a function of horizontal line stiffness) results. This figure shows what value of horizontal line stiffness is needed in order to satisfy the maximum excursion criteria. The initial line tensions or static tensions in each analysis are set to balance the mean wave drift force. Therefore, the sway results represent the displacements caused by dynamic wave forces only. As an example, the maximum line tension shown in Figure 13.11 represents a typical horizontal line tension due to the first and second order wave forces. This type of figure provides a means of estimating the dynamic component of line tensions based on mooring line stiffness.

#### 13.4 Mooring Line Design

This section describes the procedures which are used in determining the mooring line configurations and sizes for a particular vessel. Initially a mooring line is configured and sized based on the results of static analysis. Finally, a complete dynamic analysis in the time domain is run to verify the design. These steps form an iterative procedure.

##### 13.4.1 Mooring System Force Balance

A mooring system force balance is performed to determine the relationship between mooring line tension and the prescribed environmental forces which are used for design. These forces include those due to current, wind, and mean wave drift. This is a static balance procedure and is one of the preparatory steps in mooring system analysis and design. A computer program can be used to compute the lowest necessary static tension values for all mooring lines to keep the vessel over a defined location when subjected to the design environmental loads. The environmental effects due to current, wind, and mean wave drift, are treated as steady state forces.

#### 13.4.2 Mooring Line Force-Deflection Characteristics

The next step in the mooring system design after performing the static balance is to select a mooring line configuration and determine its force-deflection or stiffness characteristics. Three basic parameters are considered when selecting an initial line configuration. These are, 1) operational feasibility, 2) ease of deployment and recovery, and 3) performance.

The stiffness characteristics of the various mooring configurations can be efficiently determined by a computer program. If synthetic rope is used in the system, an extensible catenary formulation must be considered in the solution of the problem. Drag on the underwater mooring due to the current may or may not be considered.

The program should compute a series of values which describe the force-deflection characteristics of the various mooring line configurations. These values, which give the mooring line reactions at the vessel for a given range of displacements from a known starting position, can then be used by the time domain motion analysis program to account for nonlinear effects in the restoring force terms.

#### 13.4.3 Time Domain Motion Analysis

The linear wave theory is based on the assumption that the wave height is infinitely small. On the other hand, wave heights of 80 to 100 feet are often used to simulate extreme storm conditions. Does this mean that the linear wave theory is basically inadequate? Not necessarily. For example, the linear theory is generally considered adequate for the purpose of motion analysis under "operating conditions" including, in particular, the calculation of the fatigue life of both the vessel and the mooring system. Under extreme storm conditions, however, one usually needs a more elaborate analytical approach, namely, a time domain analysis to account for the

complexities of the particular physical problem under consideration. These complexities include:

- o Nonlinearities associated with finite wave height.
- o Viscous damping and other nonlinear hydrodynamic phenomena.
- o Nonlinear mooring system characteristics.
- o Nonlinearities associated with large rigid body rotations of structural components.
- o Material nonlinearities (synthetic rope).

The equations of motion of the time domain approach differ from those of the frequency domain approach in two important ways, namely, 1) the load terms are reevaluated at each time step by using the latest available information concerning the velocities and accelerations of both water particles and structural components and, 2) the added mass and damping matrices, which are usually frequency-dependent in the frequency domain approach, are modified in such a way as to make them meaningful and useful in the more general time domain approach. The equations of motion are then integrated by a step-by-step numerical technique over a sufficiently long time interval. The results obtained are compared with those of previous frequency domain analyses and if possible, with experimental data. (See Chapter 4.0 for a more detailed discussion of frequency and time domain approaches).

## 13.5 TLP Tendons

### 13.5.1 Description of Tendon System

A TLP is held in place by a set of vertical pretensioned mooring lines usually referred to as "tendons". The tendons are arranged in

groups called "legs". The number of legs in a given TLP and the number of tendons per leg depend on many factors including platform configuration, loading conditions, service requirements, redundancy considerations, etc.

An individual tendon is composed of three major components, namely a main body and two connection devices, one at each end for interface with the platform and foundation, respectively. The main body may consist of tubulars, solid rods, bar shapes, wire ropes, etc. Also, the material used may be steel, nonmetallic composites, etc. The selection of a particular tendon system would depend on installation and service requirements as well as on motion analysis and structural strength considerations.

#### 13.5.2 Catenary versus Vertical Pretensioned Mooring Systems

Catenary mooring systems are effective against wind, current and second order wave drift forces but are not very effective against first order wave loads. A semisubmersible with a catenary mooring system normally experiences large oscillations in all six degrees of freedom under the action of first order wave loads. While such large motions may be tolerable from the viewpoint of exploration drilling, production platforms cannot function properly unless the vertical motions (i.e. heave, pitch and roll) are drastically reduced.

In a TLP, the hull-deck structure is initially in equilibrium under the action of upward excess buoyancy forces and downward tendon pretensions. As far as the three vertical motion components are concerned, the stiffness of the system is controlled by the geometric and mechanical properties of the tendons (i.e., their number, distribution, cross-sectional area and modulus of elasticity) whereas for the three horizontal motion components the stiffness is directly proportional to the total pretension in the tendon system. A fundamental consideration in the design of a mooring system is minimization of the probability of resonant behavior under the action



of first order wave loads for waves with periods approximately in the 5 to 20 second range. As illustrated previously in Figure 3.24, all six natural periods of a properly designed semisubmersible are larger than 20 seconds. However, only three natural periods of a TLP are larger than 20 seconds (for horizontal motions) whereas the remaining three are smaller than 5 seconds (for vertical motions).

### 13.5.3 Methods of Analysis

Tendons are subjected to a combination of static and dynamic loads. Static loads stem from tendon pretension, tide effects on the hull, and platform offsets associated with wind, current and mean wave drift forces. Dynamic loads arise from a combination of platform motions and hydrodynamic forces acting directly on the tendons.

The analysis of the static behavior of a TLP is a relatively simple task, at least in a conceptual sense. The analysis of the dynamic behavior, on the other hand, is generally considerably more complex. A rigorous analysis of the dynamic stresses in a given tendon would normally require a coupled (or integrated) analysis, i.e. a simultaneous analysis of the overall structural system consisting of the platform, risers and tendons. Such an analysis would normally be highly nonlinear from both structural and hydrodynamic viewpoints and would have to be based on the time domain approach. Computational costs would, therefore, be very high.

As previously pointed out in Chapter 4.0, coupled analysis is still viewed by the industry as the ultimate analytical tool for the final design of a TLP. Accordingly, various companies are currently in the process of developing their own coupled analysis computer programs. For preliminary design purposes, however, a two-stage uncoupled analysis is generally considered adequate. In uncoupled analysis, a platform motion analysis is first performed by idealizing the tendon system as a set of linearly elastic springs. The dynamic response of an individual tendon is then analyzed by specifying time histories

for tendon top forces or displacements in accordance with the results of the preceding platform motion analysis, also taking into account the lateral hydrodynamic loads acting directly on the tendon.

Platform motion analysis may either be in the frequency or time domain, the former approach being considerably more popular due to its simplicity and economy. Tendon analysis may also be carried out in either domain. However, the tendon problem is an inherently highly nonlinear one, so that the frequency domain approach, which requires a complete linearization of the problem, may lead to inaccurate and unreliable results when applied to tendon analysis.

#### 13.5.4 Design Considerations

An important consideration in the design of a tendon system is "redundancy". Since individual tendons may have to be removed periodically for inspection and/or repair purposes, the system must be redundant, i.e. the case of a missing tendon must not cause overstressing either in the remaining tendons or in the hull-deck structure. The analysis of the fatigue life of a TLP must also take into account a realistic assessment of the cumulative time (throughout the design life of the platform) when one or more tendons may be missing.

In addition to the static loads (associated with pretensions, tides and static offsets) wave loads (both first and second order), vortex shedding loads and seismic loads must be taken into consideration. The stresses corresponding to each relevant load combination must remain within the limits specified for that particular load combination by the recommended design practices of the industry.

#### 13.6 Mathieu Instabilities

The principal source of stiffness of a TLP in surge or sway motion is the total tensile force in the tendon system. Letting  $x(t)$  denote

the horizontal displacement of the platform at time  $t$ , the instantaneous horizontal restoring force acting on the platform can be expressed as  $(T_x/L)$  in which  $T$  = total tensile force and  $L$  = length of tendons. The quantity  $(T/L)$  can thus be viewed as the stiffness coefficient (spring constant) of a fictitious horizontal and linearly elastic spring attached to the platform.

Under the action of waves, the hull-deck structure is subjected to time-dependent wave loads in both horizontal and vertical directions. Of these, the vertical one is transferred directly to the tendon system thus making  $T$  a time-dependent force and causing the stiffness coefficient of the fictitious spring to be time-dependent. A mechanical system with time-dependent stiffness characteristics does not have well defined free vibration modes and frequencies. Furthermore, it is known that such a system may become dynamically unstable as discussed by Bolotin (1964), Rainey (1977) and others. In the case of a TLP or any other floating vessel (such as a semisubmersible or a ship), there is a second possible source of instability, namely, the time variation of the phase of the horizontal wave load stemming from the motion of the vessel itself.

The possibility of the so-called "Mathieu instability" in a TLP was apparently first considered by Rainey (1977). Several theoretical and experimental studies have since been reported by Paulling (1982), Richardson (1979), Rowe and Jackson (1980), Hydraulic Research Station (1981), and others. On account of the enormously complex nature of the problem, the theoretical studies are generally based on some drastic simplifying assumptions. In particular, the TLP is usually idealized as a single-degree-of-freedom system in surge or sway and most nonlinearities are ignored. The purpose of the discussion presented herein is to review the essential physical and mathematical aspects of this problem in light of the studies reported in the literature and also look into the possible significance of the so-called "secondary modes" of a TLP with respect to the occurrence of Mathieu instability.

The equation of motion of a TLP in simple surge motion is often written in the form

$$(M + m_a) \ddot{X} + B \dot{X} + \frac{T(t)}{L} X = F(t) \quad (13.1)$$

in which  $M$  = mass of platform,  $m_a$  = added mass,  $B$  = linear damping coefficient and  $F(t)$  = horizontal wave force acting on the platform. In regular waves, the total tendon force can be expressed as

$$T(t) = T_0 + T_1 \cos(\omega t - kX) \quad (13.2)$$

and the horizontal wave force as

$$F(t) = F_0 \sin(\omega t - kX) \quad (13.3)$$

in which  $k$  is the wave number and the quantity  $kX$  represents the phase angle associated with the horizontal motion of the platform. It is seen that this term is a source of nonlinearity in Equation (13.1). Noting that the displacement  $X$  is usually much smaller than the wave length, i.e.,  $kX \ll 1$ , Equation (13.1) can be linearized in  $X$  and rewritten as

$$(M + m_a) \ddot{X} = B \dot{X} + \left[ \frac{T_0}{L} + \left( \frac{T_1}{L} + kF_0 \right) \cos \omega t \right] X = F_0 \sin \omega t \quad (13.4)$$

Note that the bracketed quantity in this equation, which represents the stiffness of the TLP in simple surge motion, is indeed time-dependent due to two different reasons, namely, the variation of the tendon force with time and the phase variation of the horizontal wave force acting on the platform.

The homogenous part of Equation (13.4) can be rewritten as

$$\ddot{X} + 2\varepsilon \dot{X} + \omega_X^2 [1 + 2\mu \cos \omega t] X = 0 \quad (16.5)$$

in which  $\omega_X$  is the undamped circular frequency of the TLP in simple surge motion calculated on the assumption of constant tensile force,  $T_0$ . Equation (13.5) is the well-known Mathieu equation. The possibility of instability of a TLP is determined by the behavior of the corresponding Mathieu equation, i.e., by the relative values of the four principal problem parameters that appear therein, namely,  $\omega$ ,  $\omega_X$ ,  $\mu$  and  $\varepsilon$ .

Since the Mathieu equation is a second order linear homogeneous differential equation, its general solution can be expressed in terms of two linearly independent particular solutions. The physical system (i.e., TLP, ship, etc.) is stable if both particular solutions remain bounded for  $t \rightarrow \infty$  and unstable if at least one solution is unbounded. Transition from stability to instability occurs when the particular solutions are periodic in nature.

Results corresponding to the special case of zero damping are summarized graphically in Figure 13.12 in which the hatched areas correspond to unbounded particular solutions to the Mathieu equation, i.e., to unstable behavior for the TLP. Note that, for small values of the excitation parameter  $\mu$ , instability occurs in the vicinity of integer values of the ratio  $2 T_\omega / T_X = 2 \omega_X / \omega$  in which  $T_\omega$  is the wave period and  $T_X$  the period of the TLP in simple surge motion. Particularly significant in this connection is the so-called "principal region of instability" which begins at  $2 T_\omega / T_X = 1$  and  $\mu = 0$ , i.e., the lowest hatched region in Figure 13.12. In the presence of damping,  $\varepsilon \neq 0$ , instability regions do shrink somewhat as illustrated in Figure 13.13, the principal region shrinking less than the others. It is seen that the presence of linear damping can eliminate the danger of instability for small values of the excitation

parameter  $\mu$  but not for its larger values.

What is the practical significance of these theoretical developments in terms of the actual stability behavior of a realistic TLP structure. It is important to emphasize at this point that the foregoing analysis was based on a drastically simplified mathematical model: Single-degree-of-freedom system, linear damping, no other nonlinearities of either structural or hydrodynamic origin, and regular seas. Accordingly, any theoretical results obtained on the basis of that simplified analysis would have to be used with caution. Also, any experimental results obtained from a particular test model may or may not have any practical significance because the model used may or may not be representative of any realistic TLP structure under realistic environmental conditions. For example, the tests conducted by Rowe and Jackson (1980) were, as pointed out by the authors, designed primarily to "accentuate the factors leading to the instabilities" rather than represent realistic TLP configurations.

After these words of caution, it may be possible to offer a few general observations. In-house studies at Brown and Root indicate that the surge period of a TLP varies approximately in the range 60 seconds  $< T_x < 160$  seconds for water depths of 400 feet  $< L < 6000$  feet. On the other hand, significant wave periods are approximately in the range 5 seconds  $< T_w < 20$  seconds. Using the more critical value of  $T_w = 20$  seconds, one finds that  $0.67 < (2 T_w/T_x) < 0.25$  and this in turn seems to suggest that the TLP would not develop Mathieu instability (except possibly in unrealistically shallow waters) because the parameters  $(2 T_w/T_x)$  always remains substantially below unity.

While the foregoing conclusion sounds quite reasonable, one has to remember that the analysis used was based on a single-degree-of-freedom idealization for the TLP. In reality, the tendon-platform combination is a continuous mechanical system with an infinite number of degrees of freedom as pointed out by Oran (1983). In particular,

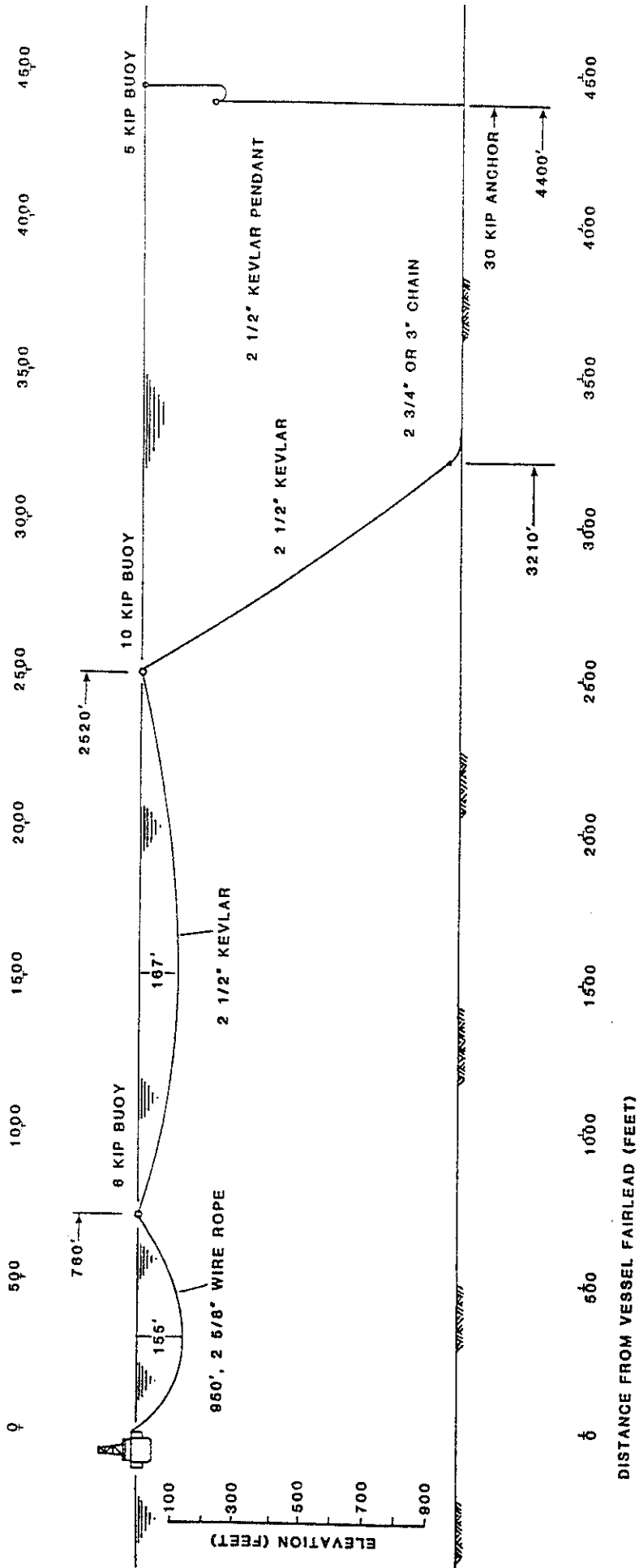
it has an infinite number of vibration modes in the lateral direction, the commonly defined "surge" mode being only an approximation of the so-called "principal lateral" mode. Numerical studies indicate that the periods of the "secondary lateral" modes vary within an extremely wide range as illustrated in Figure 13.11. An interesting question here is: Can Mathieu instability occur through the excitation of a secondary lateral mode? The linearized nature of the analysis used implies the validity of the principle of superposition which in turn suggests that each vibration mode can indeed be excited independently provided, of course, there exists a certain critical relationship between the excitation frequency and the frequency of the particular vibration mode under consideration. If the period of a secondary mode is used for  $T_x$  rather than the surge period, then the ratio  $(2 T_\omega/T_x)$  can easily be made equal to unity or some other positive integer for almost any water depth as seen from Figure 13.14, thus suggesting the possibility of Mathieu instability through the excitation of a secondary lateral mode.

The reasoning outlined in the preceding paragraph must also be used with caution since that reasoning happens to be based on the assumption of linear damping. Wave-structure interaction of the type considered herein usually involves both linear and quadratic damping stemming from wave radiation and drag effects, respectively. Quadratic damping generally has the net effect of bounding the amplitudes of vibration of a mechanical system as also demonstrated by the Hydraulic Research Station (1981) in connection with some special TLP models. However, whether these amplitudes do remain small enough to keep the stresses within allowable limits is of course another question. Also rather unclear in the particular TLP problem under consideration is the precise distribution and magnitude of the drag forces acting on the system.

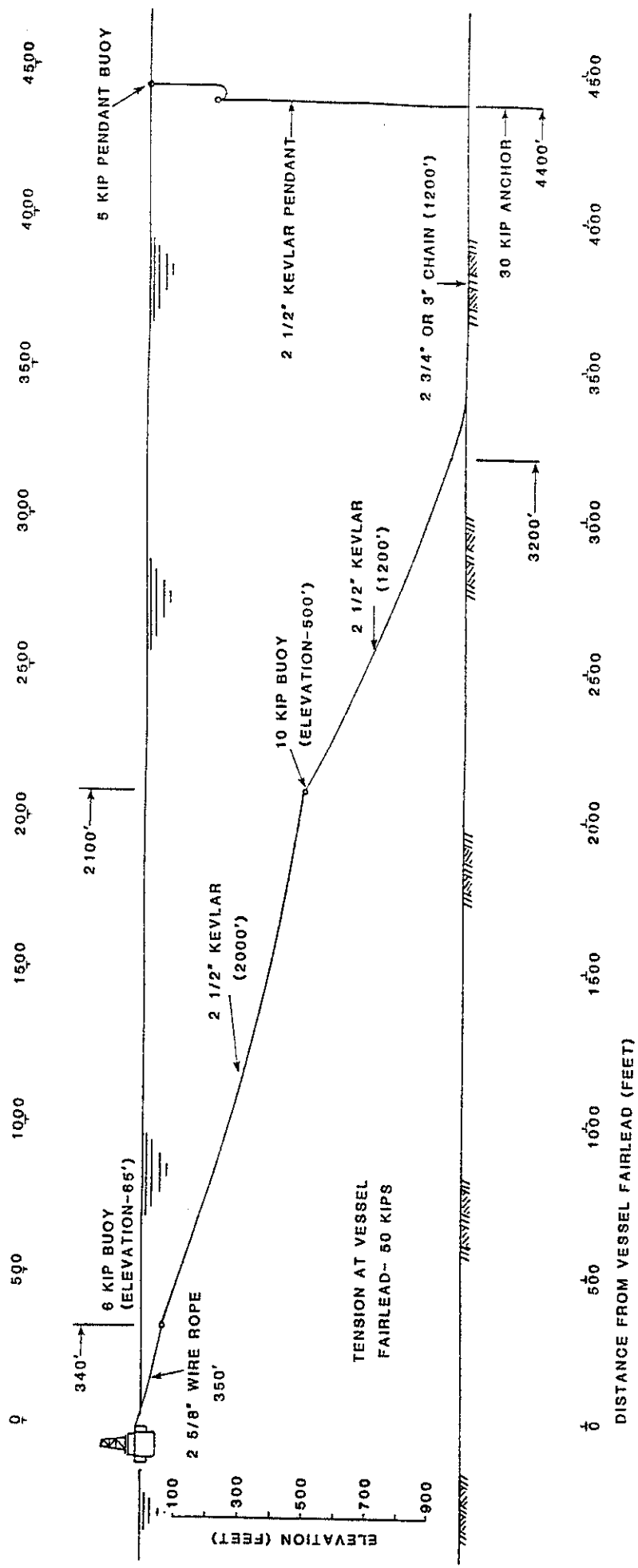
In summary, the information that is currently available concerning the possibility of Mathieu instability in a TLP is still very much incomplete. Development of practical and reliable design criteria on

this subject would require further research along both analytical and experimental paths.

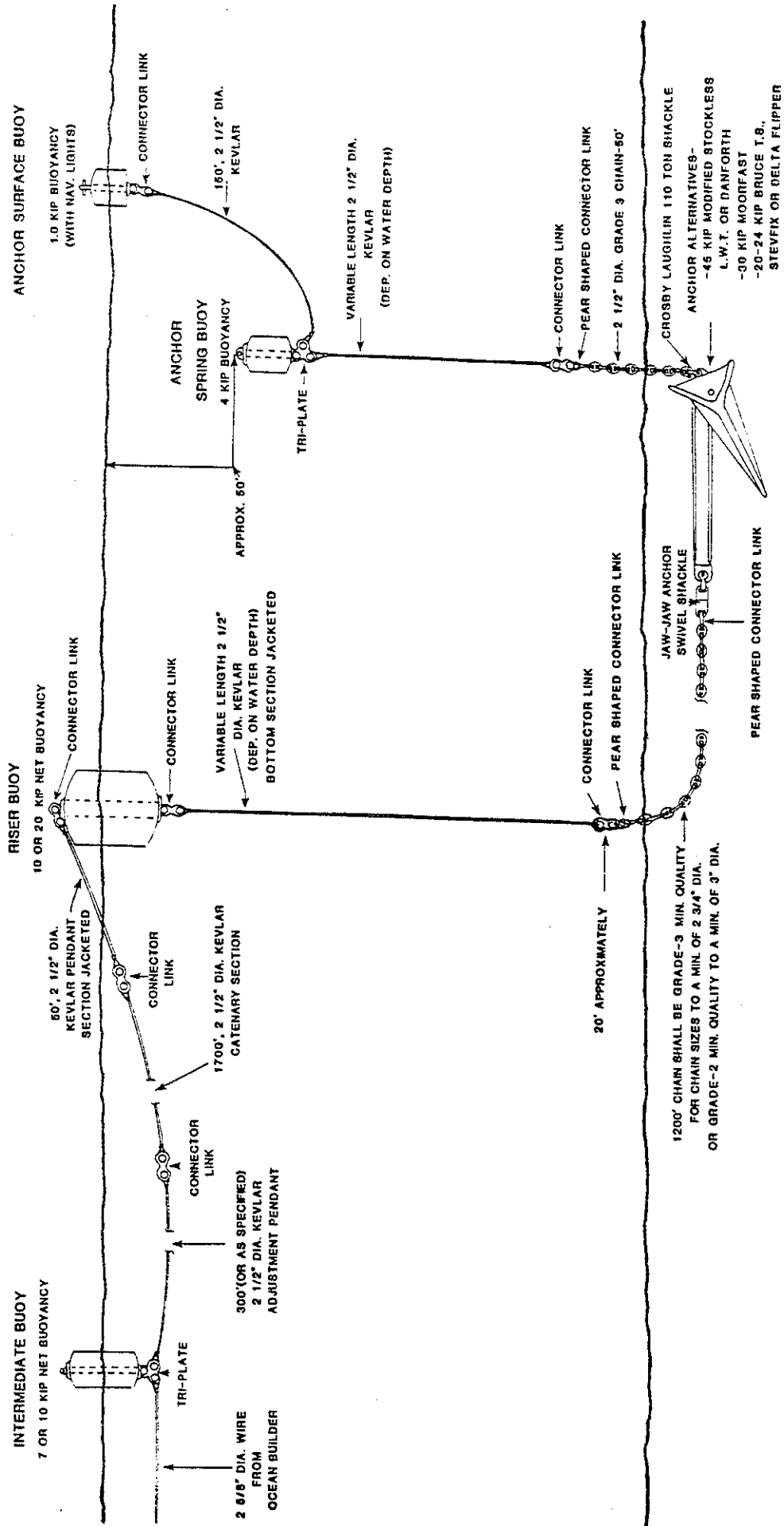




HYBRID MOORING SYSTEM  
 SLACK PROFILE  
 FIGURE 13.1

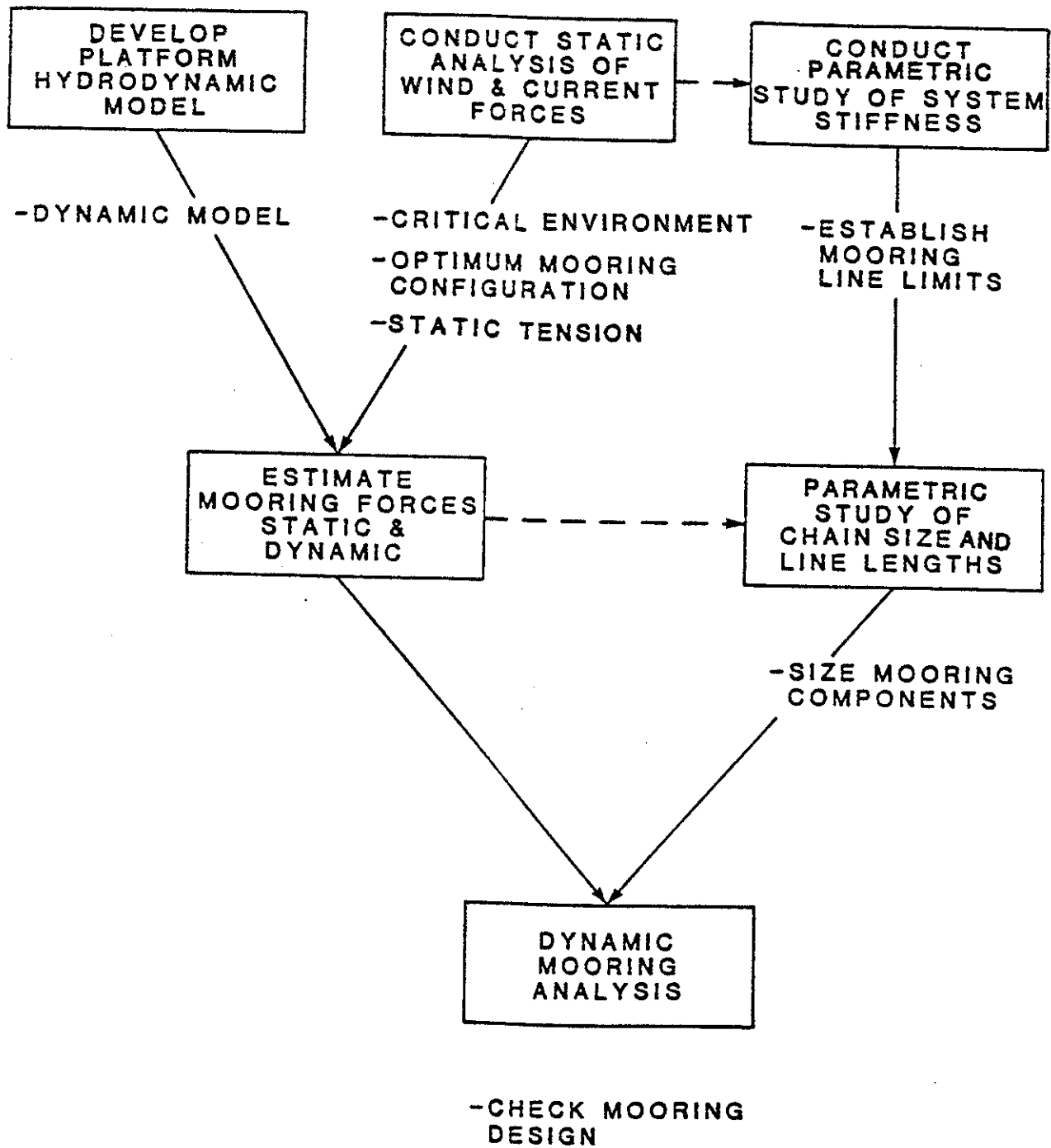


HYBRID MOORING SYSTEM  
 PRETENSION PROFILE  
 FIGURE 13.2



HYBRID MOORING SYSTEM DETAILS

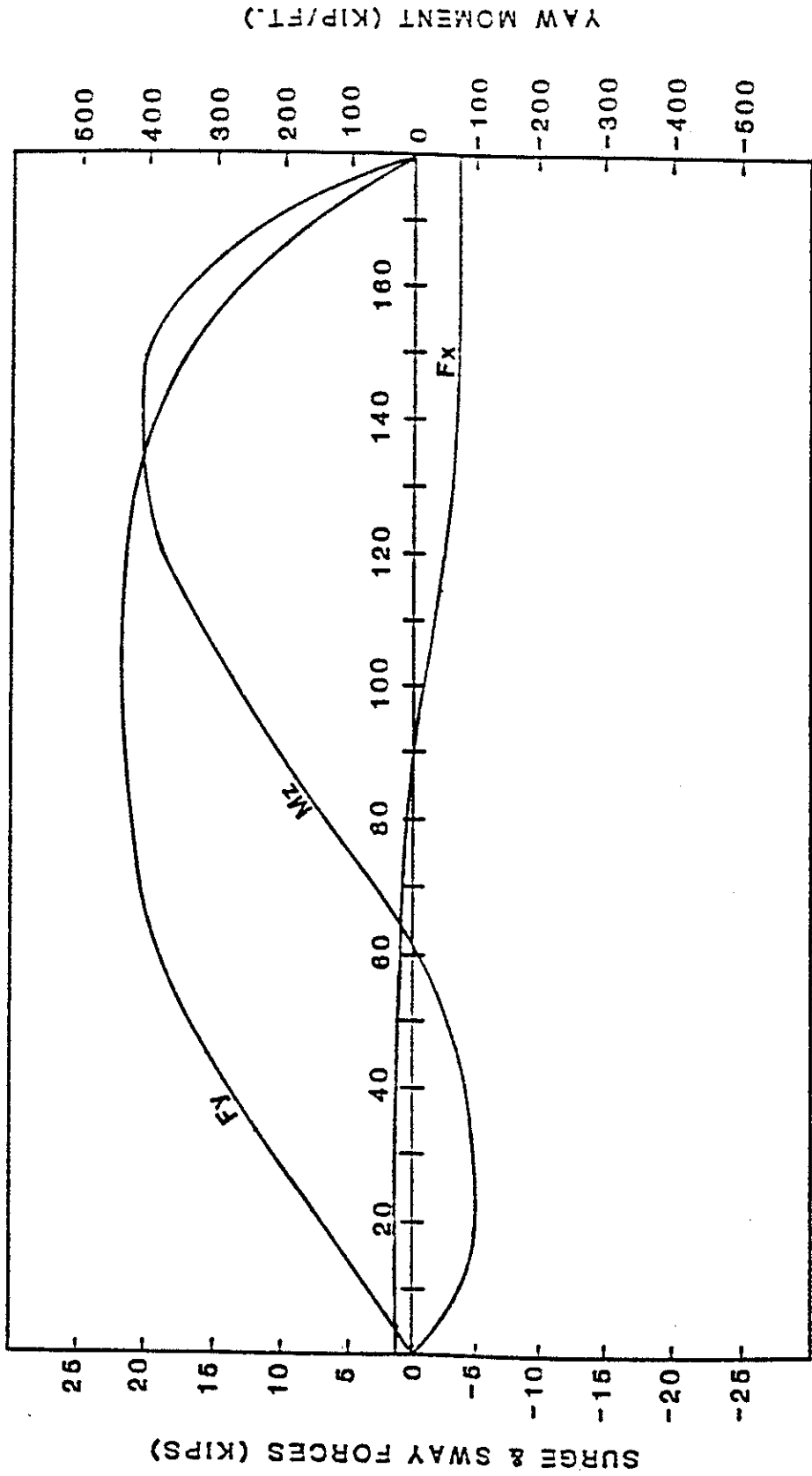
FIGURE 13.3



DESIGN METHODOLOGY FOR CATENARY MOORING SYSTEMS

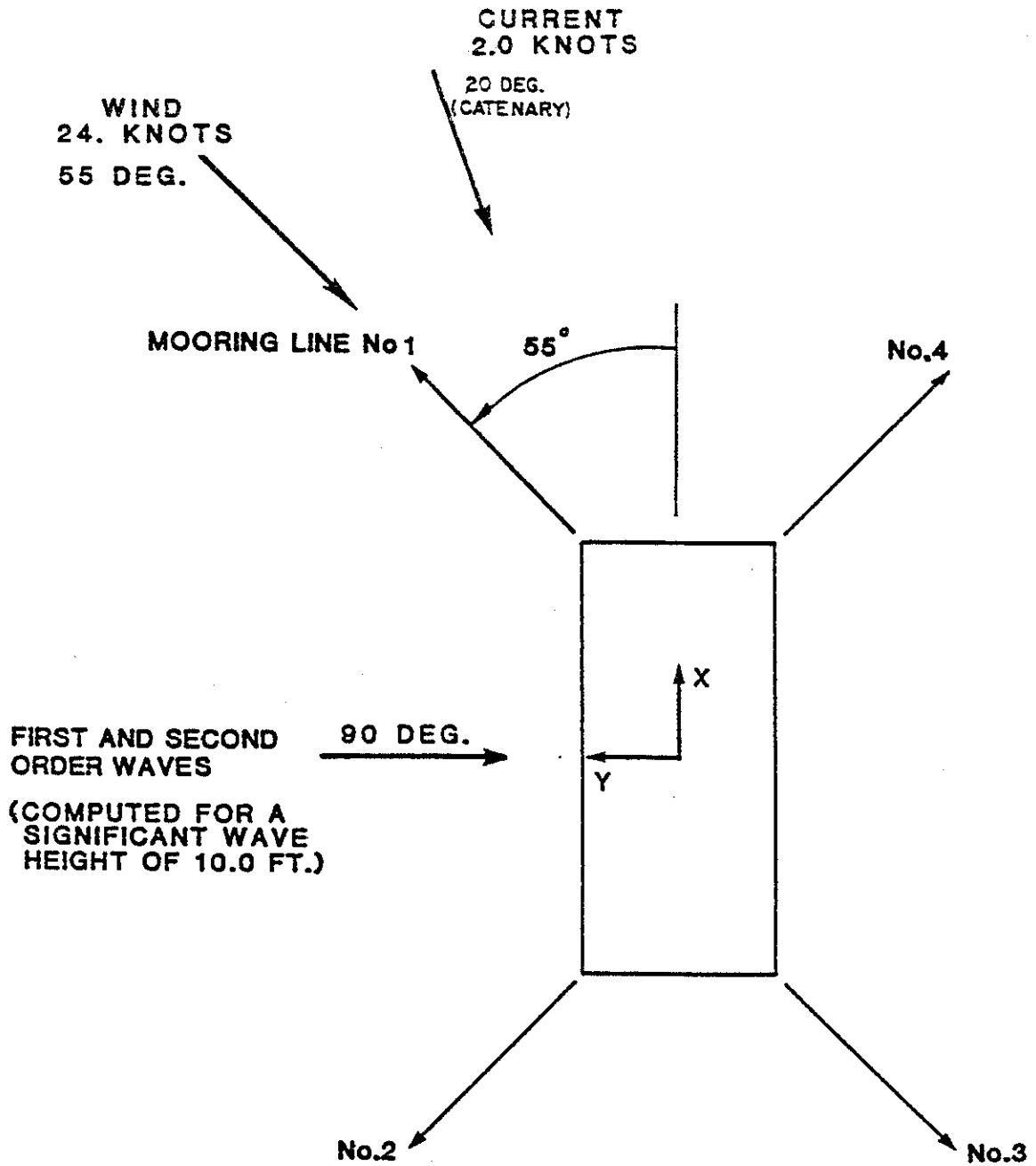
FIGURE 13.4

CURRENT FORCES : 1 KNOT



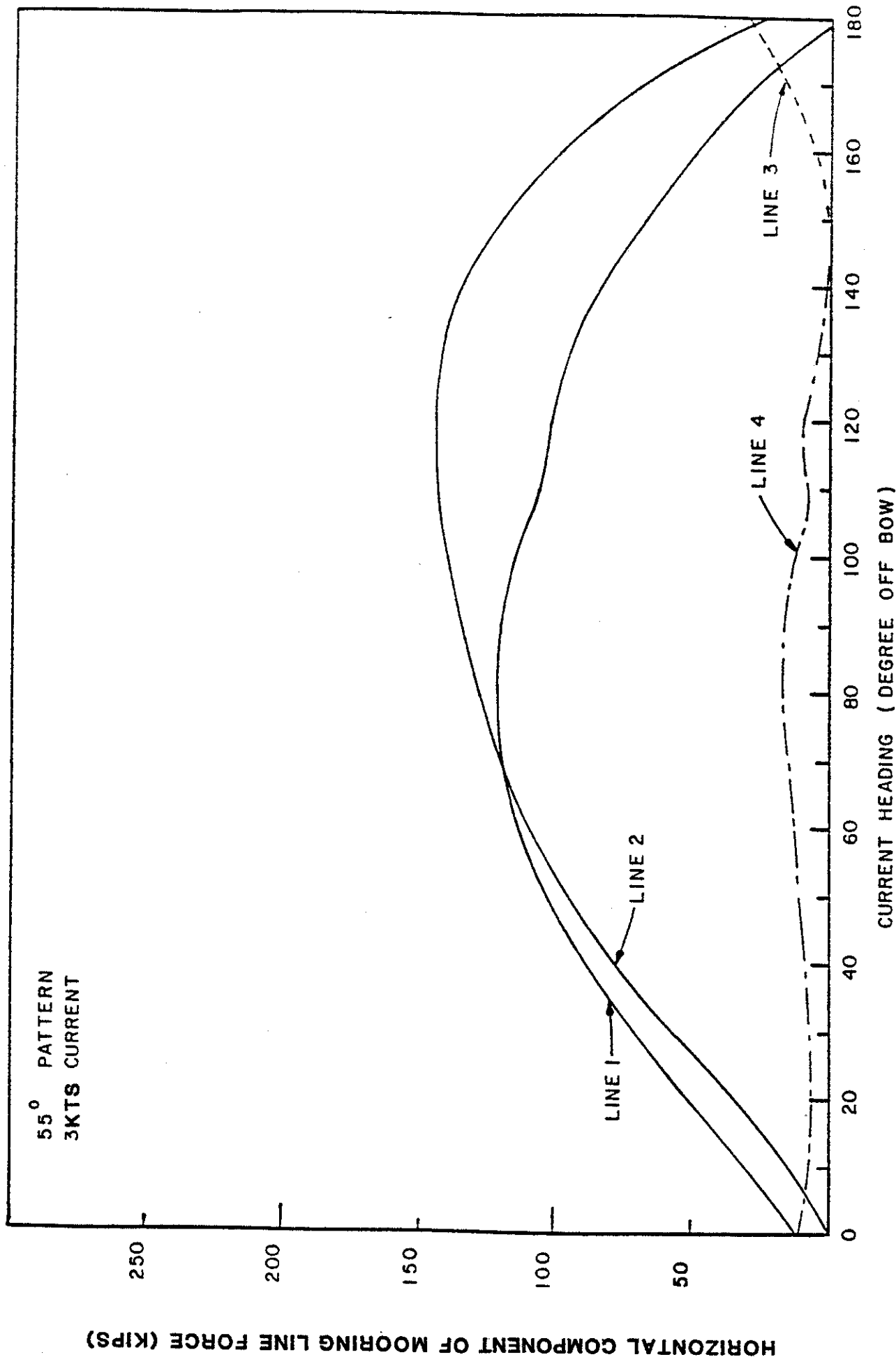
CURRENT FORCES VS. HEADING ANGLE

FIGURE 13.5

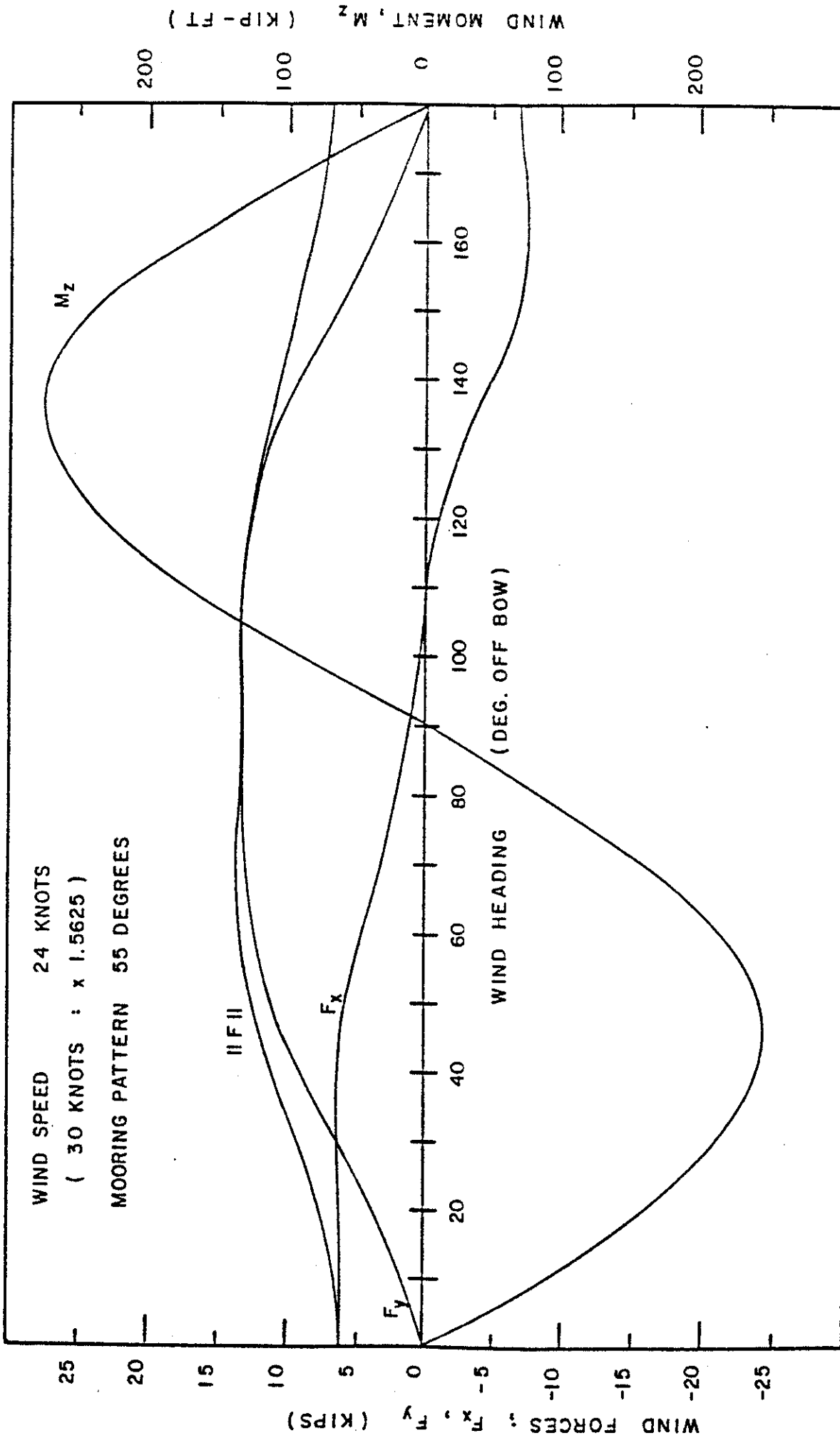


ENVIRONMENTAL LOADING DIRECTIONS  
USED IN MOORING SYSTEM DESIGN

FIGURE 13.6



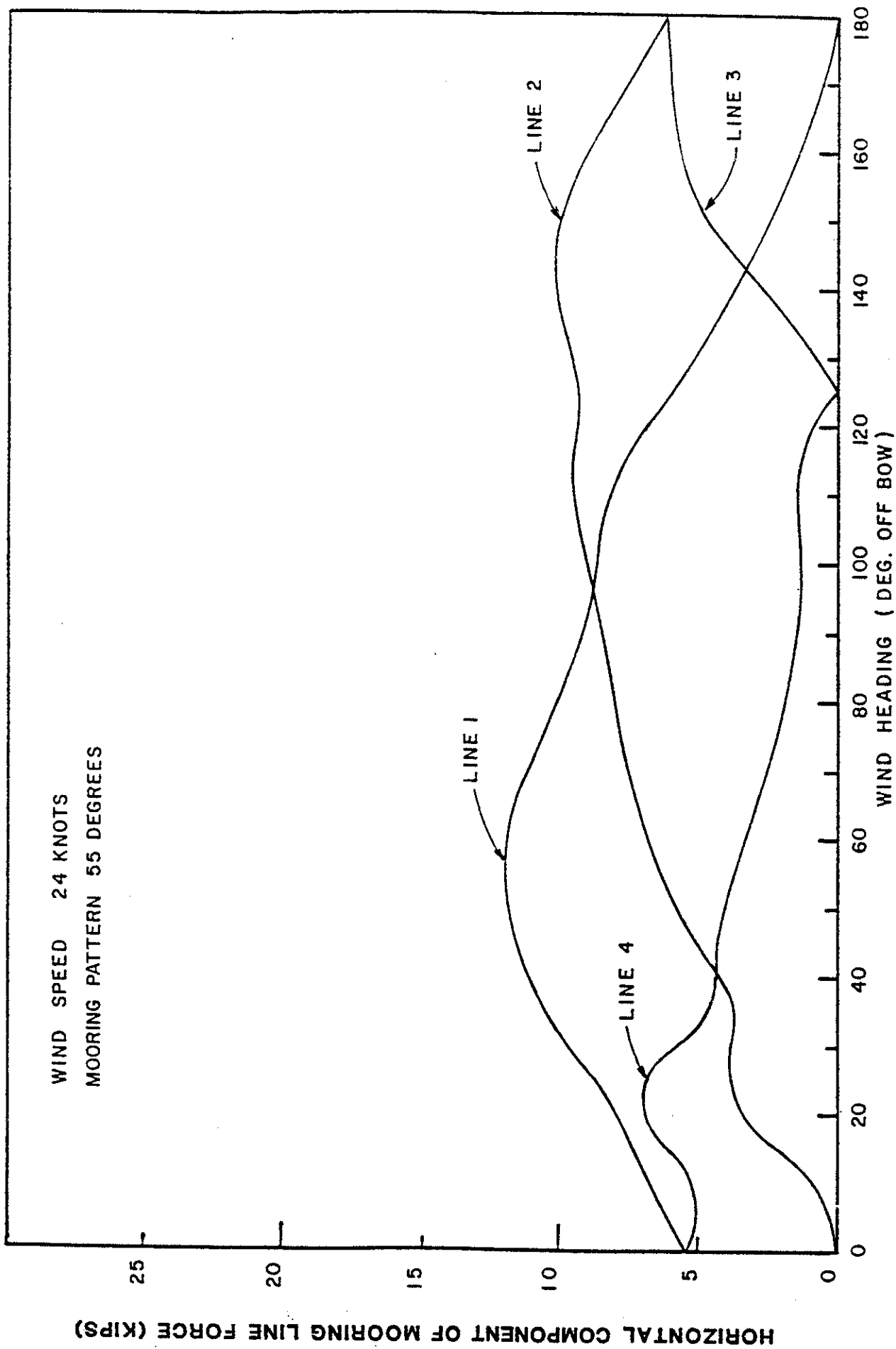
HORIZONTAL LINE TENSIONS DUE TO CURRENT  
WITH 55 DEG. MOORING PATTERN  
FIGURE 13.7



WIND FORCES AND MOMENTS AS A FUNCTION  
OF WIND HEADING

'GU 1'

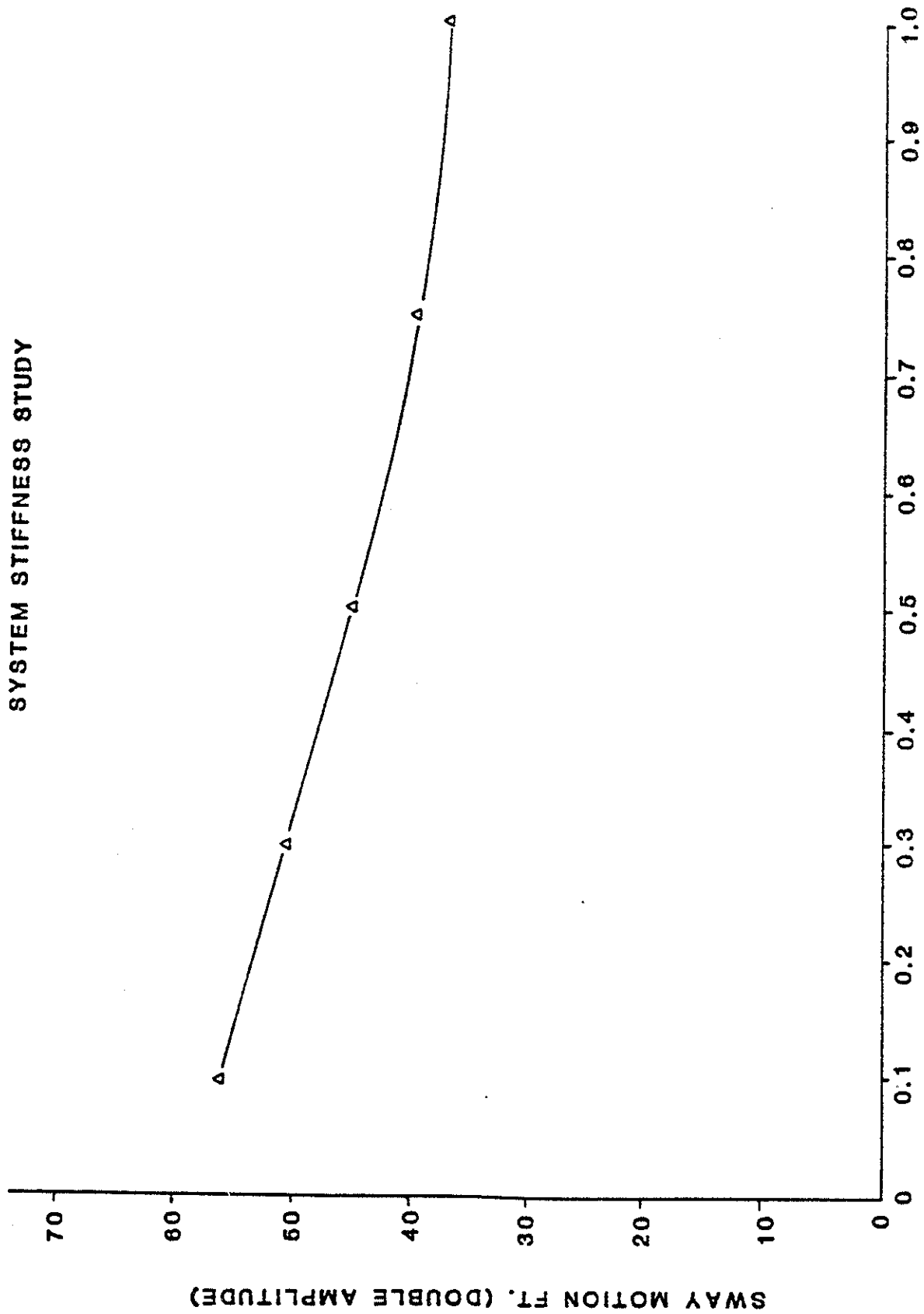




HORIZONTAL LINE TENSIONS DUE TO WIND  
WITH 55 DEG. MOORING PATTERN

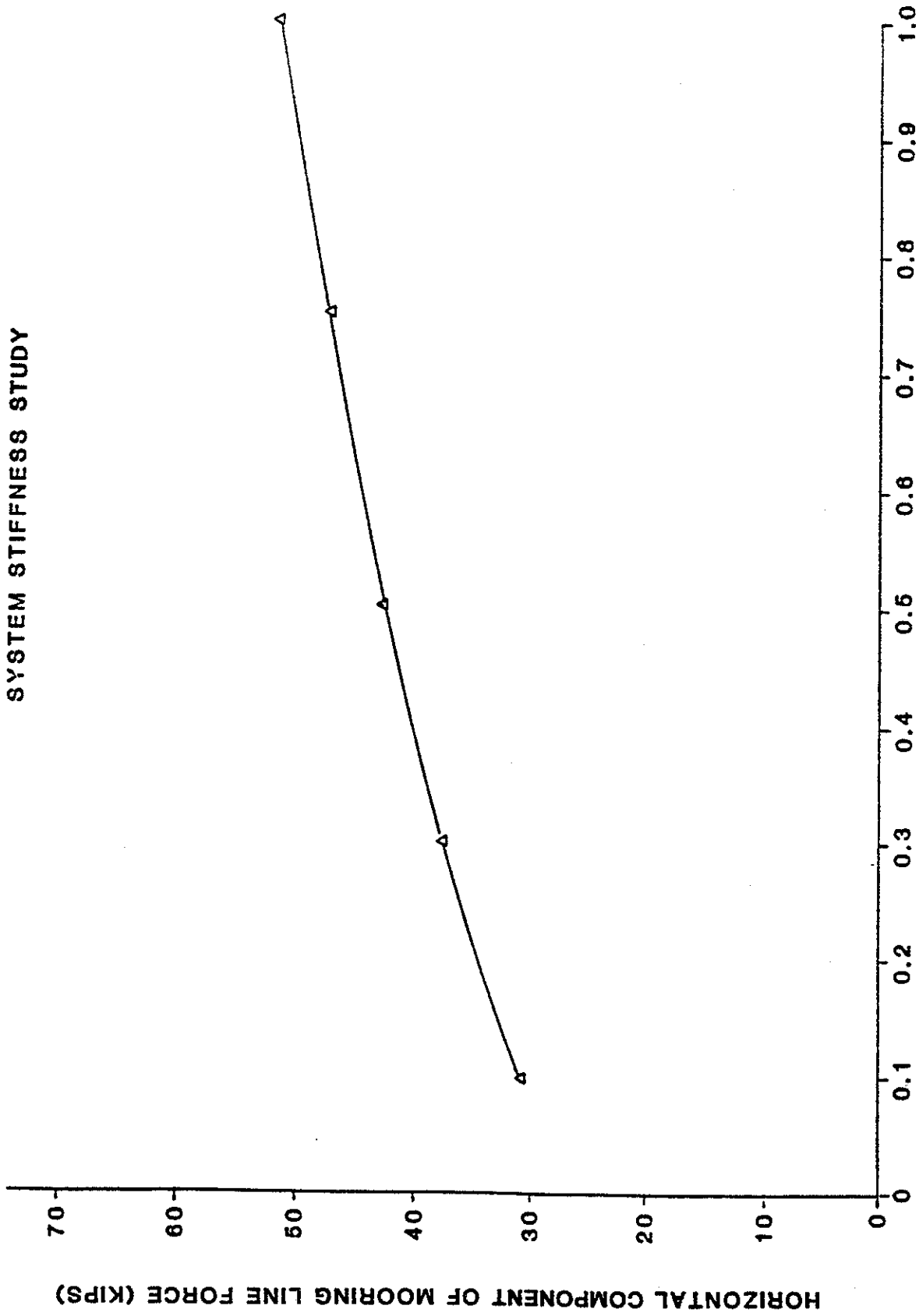
FIGURE 13.9

SYSTEM STIFFNESS STUDY



HORIZONTAL STIFFNESS (KIP/FT.)  
SWAY MOTION DUE TO WAVES AS A  
FUNCTION OF HORIZONTAL STIFFNESS

SYSTEM STIFFNESS STUDY



HORIZONTAL STIFFNESS (KIPS/FT.)  
HORIZONTAL LINE TENSION DUE TO WAVES  
AS A FUNCTION OF HORIZONTAL STIFFNESS  
FIGURE 13.11

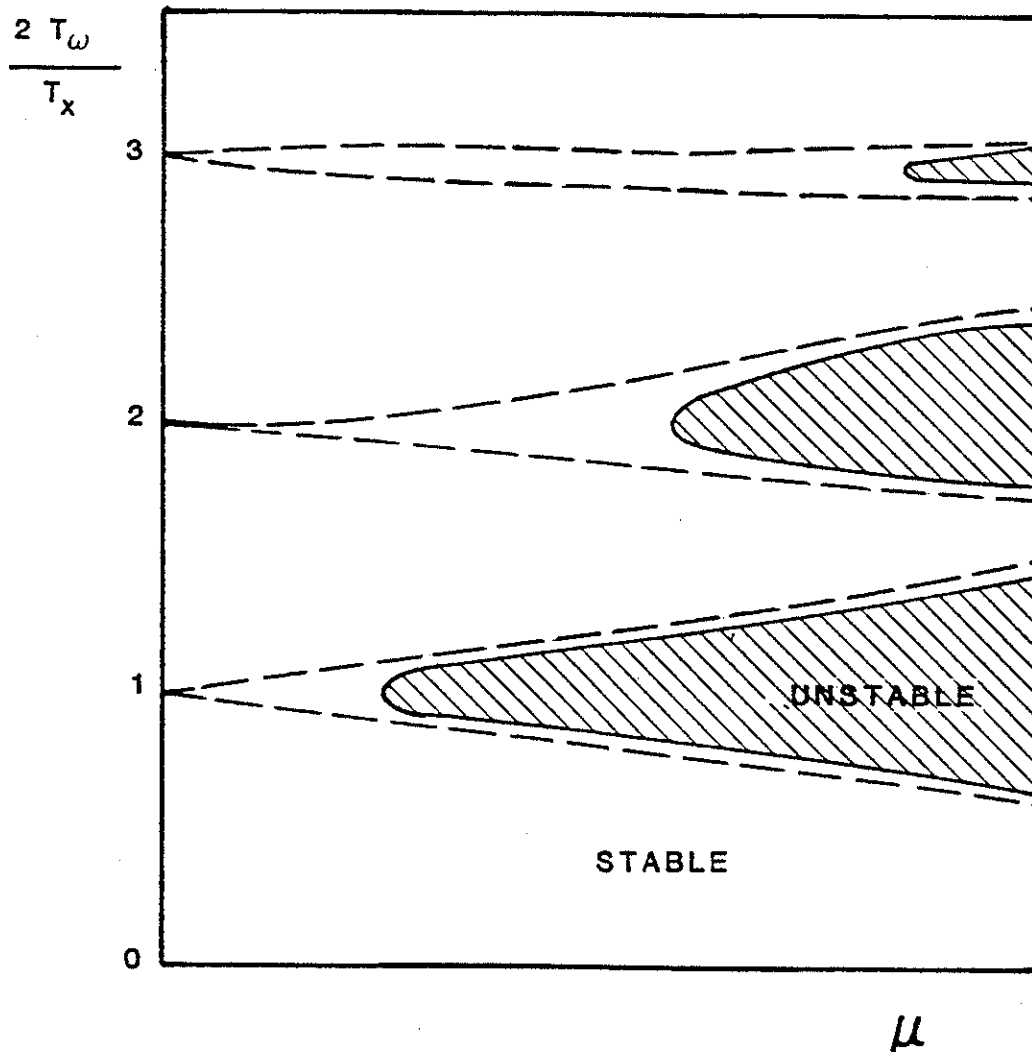


FIGURE 13.12 MATHIEU INSTABILITY REGIONS (SYSTEM WITH LINEAR DAMPING)

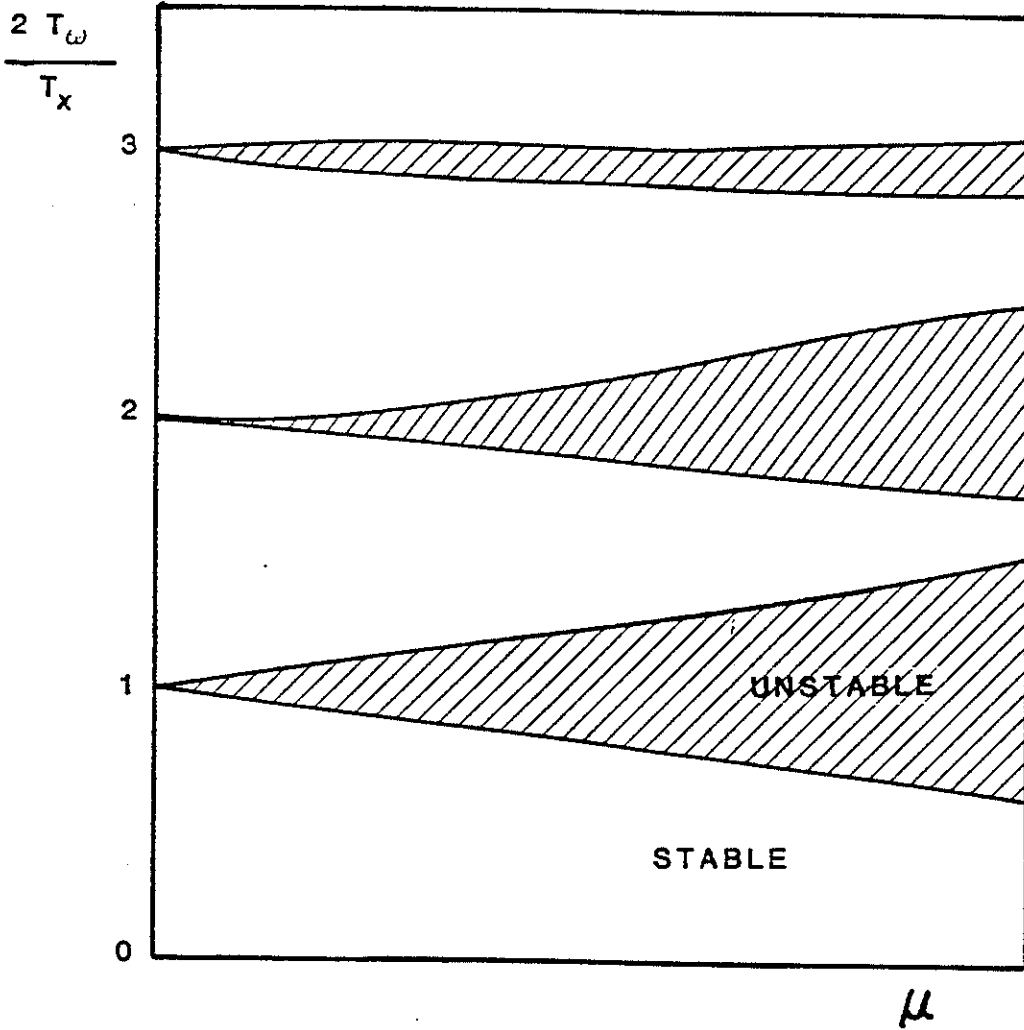


FIGURE 13.13 MATHIEU INSTABILITY REGIONS (UNDAMPED SYSTEM)

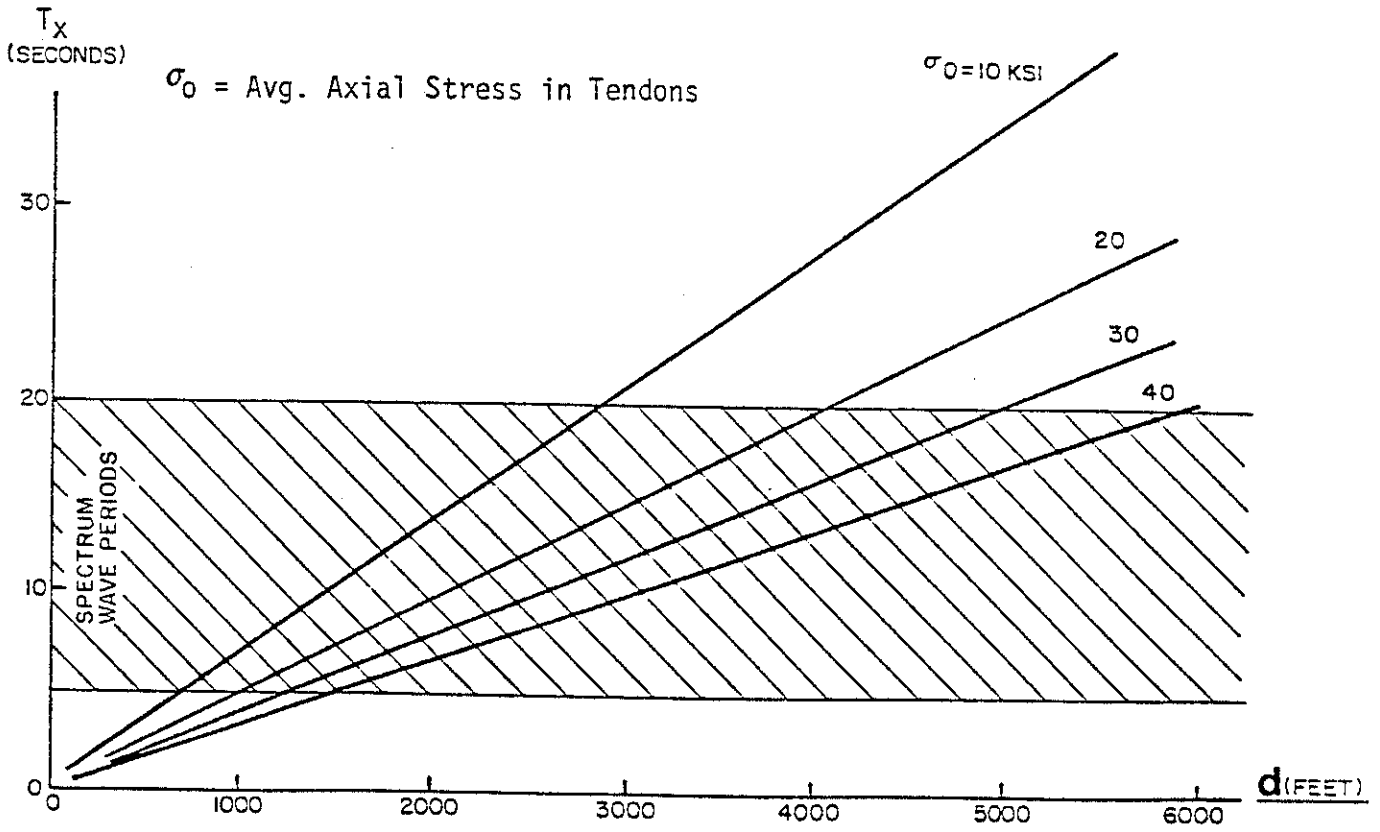


FIGURE 13.14 PERIODS OF SECONDARY LATERAL MODES

## 14.0 STRUCTURAL DESIGN AND ANALYSIS

### 14.1 Introduction

The structural design of a semisubmersible or TLP is considered adequate if the platform meets the requirement of minimum weight and maximum strength during the functional life of the structure. The minimum weight design may be achieved by careful design and analysis of the structure for all the possible loading conditions. The strength requirement can be met if all the components and connections have an adequate safety factor, resist yielding and buckling, and have sufficient fatigue life. To meet these requirements the semisubmersible and TLP structures should be redesigned and analyzed, and resized for all the phases from construction to platform removal (after completion of the mission or due to emergency). The initial member sizing may be based on a conceptual study or on past experience. The initial design will provide the preliminary structural weight estimate required by all the other disciplines involved in the platform design. These include the areas of motion analysis, foundation, tendon and mooring, riser, drilling, etc.

The preliminary design should be followed by detailed structural analysis of the system for all loading conditions. The members should be continuously checked and resized to provide both strength and minimum weight.

The following list summarizes the significant phases which should be considered for the complete design of a semisubmersible or TLP.

- o Hull and Deck Construction
- o Hull and Deck Towout (single-piece or two-piece structure)
- o Hull/Deck Mating (onshore or offshore)
- o Module Installation
- o Platform Towout (damaged and undamaged configuration)
- o Platform Installation

- o Platform In-place (operating or extreme storm)
- o Removal of Platform (reversal of installation procedure)

The following sections describe a procedure for the structural design and analysis of semisubmersible and TLP vessels.

#### 14.2 Catalog of Loading and Weight Estimates

Semisubmersible and TLP structural components must be designed for the loads applicable to each phase discussed in the previous section. At the start of the design activity all loads and weights must be identified and tabulated. Major loads can be categorized as follows:

- o Environmental loads. These include wind, wave and current loads.
  - Wind loads. Appropriate wind speed should be used for each loading condition and geographical location.
  - Wave loads. The wave forces acting on the hull of the vessel should be calculated by an appropriate motion analysis program. Wave spectra may be used for the load calculations.
  - Current loads. Current velocity profiles and appropriate drag coefficients should be used to derive the total current loads.
  - Seismic loads.
- o Permanent loads. These loads comprise the dead weight of structure, facilities, machinery, equipment modules, piping, risers' tension, ducting, anodes, etc. These loads should have appropriate values for each loading condition.



- o Moveable loads. In this category, the major loads to be considered in the design are the drilling derrick substructures and any other moveable deck equipment.
- o Variable operating loads. These comprise the drilling and production material weights such as liquid mud, sack mud, drill water, diesel fuel, tank storage, etc. The magnitude of these loads varies depending on the environmental condition considered. The location of the loads remains unchanged.
- o Live loads. These loads comprise consumables or equipment which are temporarily placed on open deck areas. The live loads may be reduced by area live load reduction factors, when designing subsidiary support members.
- o Mooring loads for semisubmersibles.
  - Static pretension
  - Variations due to changes in M.W.L.
  - Effects due to current and wind loads
  - Dynamic variations due to wave loads
- o Tendon loads for TLP's. The tendon loads consist of:
  - Static pretension
  - Variable static tendon tension associated with changes in mean water level (M.W.L.).
  - Static offset tendon tension (setdown). This is the tension induced by a steady current and/or wind force.
  - Dynamic tendon tension. This is induced by the action of waves passing through the structure.
- o Inertial loads. These loads are due to the structural accelerations induced by the environmental loads.
- o Ballast loads and buoyancy loads. These loads depend on the specified drafts associated with different loading conditions.

- o Construction and installation loads.

### 14.3 Hydrodynamic Loads Generation

Waves affect the semisubmersibles and TLP's in two distinct ways: through hydrodynamic loads acting on the underwater portion of the vessel, and through motion-induced structural inertia forces acting on the overall structure.

The computation of motion-induced structural loads is straightforward, since these loads depend simply on the mass distribution of the structure and the motion responses of the platform. The computation of hydrodynamic loads, on the other hand, is somewhat more complex and depends on whether the platform is treated as a small or large body. These loads are affected by diffraction and radiation phenomena, hydrostatic pressure perturbation, effects from moorings, and effects of fluid viscosity.

Wave forces may be considered as being composed of first-order and second-order wave forces, producing respectively the high and low frequency oscillation motions for the vessel. Second-order wave forces, also known as slow drifting forces, are generally small compared to first-order wave forces. The low frequency nature of the excursion motion due to second-order wave forces suggests that the excursion-induced inertial forces are also likely to be small compared to those due to first-order wave forces. Thus, it is sufficient to consider first order wave forces for the purpose of predicting the maximum dynamic stress and fatigue life for the platform.

Wave diffraction and hydrodynamic interactions are important to the semisubmersible and TLP. Therefore, advanced potential fluid theories are employed to compute hydrodynamic coefficients and wave forces. Various analytical programs have been developed for semisubmersibles and TLP's using either a 2-D or 3-D source-sink method.

The selection of proper methods for evaluating hydrodynamic forces and coefficients depends on the geometry of the hull and the degree of sophistication desired. For instance, the sophisticated 3-D source and sink method, suggested by Faltinsen (1974) and Garrison and Stacey (1974), can be used to calculate the added mass, damping coefficients, and wave forces. Alternately, these forces and coefficients can be obtained by judicious selection of 2-D methods.

In the case of a "large body", a direct application of the 3-D potential flow method appears to be desirable because it is capable of modeling any geometric shape. However, the modeling procedure could be cumbersome and the computer costs prohibitive. On the other hand, 2-D methods are cost effective and reasonably accurate, provided care is taken in selecting methods capable of modeling the important physical process.

The effects of viscous damping on the semisubmersible and TLP motion near resonance have proven to be rather significant as indicated by Tein et al. (1982), since wave damping effects are small in both high frequency regions (heave, roll, and pitch natural frequencies) and low frequency regions (surge, sway, and yaw natural frequencies).

When the platform is treated as a "small" body, the wave force evaluation is based on the Morison equation. In this method it is inherently assumed that:

- o Structural members are widely separated so that the hydrodynamic interaction among members is negligible; i.e., the fluid force acting on one member is not affected by the presence of other members. Thus, the total force and moment may be computed by vectorial summation of those acting on each individual member.
- o The cross-sectional dimension of a member is small in comparison with the wavelength so that the pressure, velocity and acceleration on the surface of the member may be approximated by

nominal values evaluated at the centerline of the cylindrical members.

The restoring forces and moments of a semisubmersible or TLP consist of two parts: those due to hydrostatic properties of the vessel, and those due to the constraints of the mooring system. The former can be expressed in terms of area and moments of water plane and metacentric heights; the latter can be expressed in terms of the pretension and stiffness.

The hydrodynamic loads are usually predicted using a frequency domain approach. Since wave diffraction and hydrodynamic interactions are important to the semisubmersibles and TLP's, diffraction potential fluid theories are usually used as the primary tool in determining the hydrodynamic load. Provision should also be made for viscous damping in view of its effect on the motion response.

When the hydrodynamic loads are calculated from the Morison equation, the problem is complicated by the fact that the distribution of these loads around the cross section of a member is not known although their distribution in the axial direction is known. For the analysis of the local shell behavior of a member, it becomes necessary to make an assumption concerning the missing load distribution. This assumption may be based on experimental results and/or theoretical results obtained from the diffraction theory.

In summary, as far as structural design and analysis are concerned the main problem is twofold:

- o How to provide a set of structural loads that are consistent with the motion analysis, and
- o How to efficiently process the massive amount of data.

In this regard the integrated motion-structural analysis methods come into the picture. This subject is briefly described in the next section.

#### 14.4 Integrated Motion-Structural Analysis Methods

In the structural design and analysis of a semisubmersible or TLP two distinct models should be considered. These are the hydrodynamic model and the structural model. With the hydrodynamic model, the primary concern is the accurate representation of the underwater hull geometry. In constructing the structural model, the primary concern is the accurate representation of the overall platform structural rigidity and weight distribution. Nevertheless, these two models must be consistent with each other in terms of weight distribution, geometry representation and load distribution. It should be emphasized that the semisubmersible and TLP are free-free systems in that motion induced inertial forces are delicately balanced by hydrodynamic forces. Inconsistencies between models could tilt the delicate balance thus resulting in a meaningless structural analysis. To achieve such consistency, an integrated motion-structural analysis approach is needed. This integrated procedure not only ensures the consistency of the analytical models, but also allows the entire analysis to be performed through data interfaces and automatic data generations. The system integration is achieved by interfacing the motion analysis and structural analysis programs. These programs communicate with one another via data interfaces.

The structural analysis is usually a two-step operation. In the first step a preliminary analysis is performed. This entails constructing a space-frame model based on the primary characteristics of the platform, whereby the hydrodynamic loads are evaluated and the expected maximum stress and fatigue life are assessed. Figure 14.1 shows a space frame model. The second step consists of performing a detailed structural analysis for pontoons, columns, and critical structural joints. The detailed analysis is more complex and usually

requires a 3-D source-sink distribution hydrodynamic model. Figure 14.2 shows a computer generated source-sink hydrodynamic model for a TLP.

Liu et al. (1980) presented an integrated computational procedure for hydrodynamic loads and structural responses of TLP's. Hydrodynamic loads were generated by using the Morison equation. A flow chart of the integrated method used by Liu et al. (1980) is given in Figure 14.3.

Tein et al. (1981) also presented an integrated motion and structural analysis method for TLP's. In this case they used the potential theory for hydrodynamic load generation. The effect of viscous damping was introduced based on model test data. A flow chart of their approach to the integration of motion and structural analysis programs is shown in Figure 14.4.

## 14.5 Platform Structure Design

### 14.5.1 General

Semisubmersible and TLP platforms must be designed to withstand a number of distinct phases of loading. These phases include fabrication, mating, floatout, installation, operation, survival and platform removal conditions. The primary design consideration is to provide a minimum weight structure which can meet the strength requirements of all phases. In the installed condition, semisubmersible and TLP structures should perform the intended function for the specified time duration. The design of a semisubmersible or TLP is carried out in two stages:

1. Preliminary Design.
2. Final Designs.

A method of overall structural design is summarized in the flow chart presented in Figure 14.5.

In the preliminary design stage an exhaustive investigation of the structure's performance under all possible loading cases is not required. However, a reasonable design and weight estimate of the platform structure may be obtained by considering the following loading conditions.

- o Floatout (damaged and intact condition),
- o Installation,
- o Operation - 1-year storm,
- o Extreme environmental condition - 100-year storm (using maximum and minimum mooring tensions for semisubmersibles and maximum and minimum tendon tensions for TLP's).

In the final design, or production engineering phase, additional conditions, such as deck and hull fabrication, deck loadout, mating and transportation are considered. These conditions induce built-in stresses in the structure which have to be added to the stresses of all other loading conditions when establishing the total stress sum for a structural element.

In the case of onshore mating, the column shell plating and internal framing must be designed to adequately resist high concentration of deck and jacket reaction forces. The shell plating and stiffeners must be checked against interframe buckling, ring stiffener buckling and overall buckling of the hull cylinder as a column.

In either method of connection, the design must consider all the reaction loads of the floatout, installation, operating and extreme operating cases.

#### 14.5.2 Platform Structure Preliminary Design Procedure

A method for the preliminary structural design of a semisubmersible or TLP is given in the flow chart presented in Figure 14.6. The design of the platform structure may be based on the working stress method using applicable industry codes and specifications. Consequently, the recommendations and requirements of the following standards may be used in the design process.

API-RP2A Recommended Practice for Fixed Offshore Platforms

API-RP2P Recommended Practice for the Analysis of Spread Mooring Systems for Floating Drilling Units

ABS American Bureau of Shipping, Draft "Rules for Offshore Installation"

DnV Det norske Veritas, "Rules for Design Construction and Inspection of Offshore Structures"

USGS U.S. Geological Survey, OCS Order No. 8 "Requirements for verifying the Structural Integrity of Outer Continental Shelf Platforms"

USCG U.S. Coast Guard 46 CFR, I "Cargo and Miscellaneous Vessels" 46 CFR IA "Mobil Offshore Drilling Units"

AISC American Institute of Steel Construction, "Manual of Steel Construction"

The AISC specification covers design checks necessary for compressive, flexural and shear resisting members. The methods for the strength evaluation of plate girders and rolled beams are also included in AISC. The stability checks for ring stiffened shells such as hulls, columns, pontoons, and deep plate girders are not



provided for in the AISC rules. Therefore, part of the DnV rules may be used to check the stability of stiffened columns and pontoons. As an additional design tool, Merrison's Rules (1974) may be used to maintain an adequate level of safety and to achieve minimum weight design. The appropriate safety factors consistent with working stress method should be used for the design.

The semisubmersible and TLP hull structures primarily consist of bulkheads, stringers, rings, and stringer-stiffened rectangular or cylindrical shells. The elements in the hull structure must be checked against yielding and buckling for the loading conditions described in Section 14.2.

The API and DnV rules providing considerable guidance for the design of stiffened cylinders may be applied in designing the columns and pontoons. Merrison's Rules provide appropriate methods for the design of stiffened flat plates and are applicable to the pontoons and deck structures. Areas other than shell and plate sections may be designed to conform to the AISC rules. Appropriate safety factors consistent with the working stress method should be used.

#### 14.5.2.1 Deck Design

Two different structural concepts have been considered for the deck. One consists of a plate girder construction, very similar to the approach used in the shipbuilding industry. The other concept is based on the use of a tubular truss as the main deck structure, to be covered by steel plate floors and walls. The latter solution may present the advantage of an increased flexibility of design and operation, since minor modifications needed to accommodate equipment, wiring and piping will not affect the main load-carrying members.

The deck's diaphragms may consist of conventional deck plating and stiffeners. A representative uniformly distributed dead load plus live load over the deck area may be used for sizing the deck

diaphragm. Figure 14.7 shows schematically a deck support structure.

A method of overall deck design procedure is shown in Figure 14.8.

#### 14.5.2.2 Column Design

The columns will be designed for the combined effect of the following loads:

- o Hydrostatic pressure (including astronomical tidal ranges).
- o Additional hydrostatic pressure due to static offset (Setdown).
- o Hydrodynamic pressure and inertia forces obtained from motion analysis.
- o Current loads.
- o Vertical tendon forces transmitted to the stiffened column and horizontal tendon forces transmitted through the cross-load bearing near the keel.
- o Dead weight and buoyancy forces.
- o Boundary forces due to space frame action.

Boat impact loads on the column may be used to design the damage control shell.

The shell plating and stiffeners will be checked for buckling and yielding. API and DnV Rules may be used for this purpose.

Figure 14.9 shows schematically the derivation of hydrodynamic pressure on a column. Figures 14.10 and 14.11 show typical column structural components and a typical column structural arrangement,

respectively, for a TLP.

Figure 14.12 presents an overall column design procedure.

#### 14.5.2.3 Pontoon Design

The objective of pontoon design is the selection of a pontoon structure such that minimum weight will be obtained without compromising the overall structural integrity and stability of the platform. The compartmentation may be based on the requirement for a minimum of two flooded adjacent compartments for damaged stability. Figure 14.13 shows a 3-D view of pontoon framing. Figure 14.14 shows a method for overall design of a TLP pontoon.

A question not yet completely answered is whether a pontoon configuration with a circular cross section would be preferable to one with rectangular cross section. The fabrication of the latter might be easier, but the connection design might be much more difficult.

### 14.6 Structural Analysis

#### 14.6.1 General

Static and dynamic stress analyses of the platform are carried out to obtain internal loads, deflections and stresses associated with the individual members of the structure.

At the first stage of stress analysis (preliminary phase), a space frame model may be used to obtain global forces and stresses in the structure. This model uses beam elements to idealize the pontoons, columns, and a two-level system of beams and truss elements to simulate the deck. This type of model is simple to use but has limitations for large columns and pontoons. However, for preliminary sizing and initial weight estimating the results provide valuable

information and design data.

Suitable programs should be used for static and dynamic analyses. In both types of analysis the appropriate space frame model may be used. The results of these analyses should be combined and used for finalizing the preliminary member sizes in the second phase of the activity.

The second phase of preliminary stress analysis considers the columns and pontoons and the deck plate girders in more detail. In this phase local buckling, yielding and hot spot stresses of major components will be checked, and resizing and design modifications will be implemented. In case of minor design changes, no further stress analysis will be necessary. For critical loading conditions the structure has to be reanalyzed and major components have to be resized to obtain satisfactory results in terms of minimum weight and adequate strength.

#### 14.6.2 Space Frame Model

A beam element space frame model may be used for the platform stress analysis (see Figure 14.1). The beam elements idealize the deck, columns, pontoons and bracings. The space frame provides a simple and effective analysis model to investigate special static and/or quasi-static loading cases. The computer program used for space frame analysis should be able to model shell plating and stiffeners of cylindrical members. Furthermore, the results of these analyses should be checked against appropriate codes. Therefore, as the analysis proceeds for each loading phase, the appropriate member design modification will be carried out. The loads for the space frame model are obtained from preliminary design of the members, from the environmental data, and from the results by other disciplines.

For preliminary design of a semisubmersible the mooring lines may be modeled by linear springs. For each phase of loading the appropriate

environmental conditions and weights must be specified and imposed on the models.

For a TLP, the tendons may be modeled by axial springs at each corner column. Proper ballast should be specified to produce the specified pretension in the tendons.

#### 14.6.3 Static Stress Analysis

The loading conditions which are considered significant for the preliminary phase of the semisubmersible and TLP design and weight estimate are floatout (intact and damaged condition), installation, operating (1-year storm) and extreme storm (100-year storm). The following loads are usually specified in the static analysis.

- o Wind loads which are distributed among the deck beam members and columns above the mean water level. The wind forces may be calculated according to API RP 2A.
- o Current loads are modeled by specifying the current velocity profile and drag coefficients.
- o Buoyancy corresponding to the maximum astronomical tide and maximum static offset (for in-place conditions) may be used in the analysis.
- o The spring stiffness of the tendons (for in-place conditions) can be calculated from the tendon pretension and the position of the TLP at the maximum offset position (See Figure 14.15).
- o The vertical and horizontal components of riser pretensions may be imposed at the well bay area in the form of a constant load.
- o The ballast loads corresponding to the appropriate loading conditions should be specified.

- o The primary dead weights such as structural, drilling and production facilities, tendons, marine growth, anodes, etc. should be tabulated for each condition and properly distributed among the space frame members.
- o The secondary steel work dead weight, which includes stairways, walkways, minor piping, cables, minor supports, wind bracing, etc., must be evaluated on the basis of past experience and properly input into the model.
- o The weight of components which are proposed for the semisubmersible or TLP installation and are to remain permanently on the structure must also be included.

The individual loading cases may be analyzed by suitable computer programs. The members may be checked by suitable computer programs according to API, AISC and DnV rules for yielding and buckling. This type of code check is limited to global frame members and is particularly useful for preliminary resizing of deck trusses or girders. The code check for columns and pontoons is not quite satisfactory and a more detailed investigation is usually required following the static and dynamic analyses. This is discussed in Section 14.6.8.

The results of static stress analyses should provide the following information:

- o Tabulation and summary of loads and load cases
- o Equilibrium check of forces
- o Member global forces and reactions
- o Member stresses and interaction ratios
- o Combination of stresses
- o Code check and tabulation of critical members

The member static force and stress output should be stored and combined with the dynamic analysis results for the detailed analyses.

#### 14.6.4 Dynamic Stress Analysis

In addition to static stress analysis, the dynamic stresses of the semisubmersible and TLP should be determined for the loading conditions described in Section 14.2. In all these analyses a space frame model may be used.

The integrated motion and structural analysis system described is usually used to perform this task.

The results of the dynamic analysis are usually in the form of probabilistic dynamic stresses. The maximum stresses may then be predicted by the superposition of the maximum dynamic stress and static stresses. At any given node on the space frame model, the stresses should be predicted at several circumferential points.

In all the above phases, from floatout through the in-place extreme condition, the combined static and dynamic stresses are obtained and the critical areas of the structure are identified. The members' sizing and details are carefully examined and modified, if necessary, to reduce the level of hot spot stresses. The members are designed to provide strength, ease of fabrication and minimum weight.

#### 14.6.5 Platform Stress Analysis During Floatout of TLP's

The floatout operation is of critical importance to the TLP design. During floatout, the TLP behaves like a compliant floating platform in which the heave, roll, and pitch motions have large amplitudes. These motions may produce significant inertial stresses in the TLP structure at locations which may be quite different from those of a tethered TLP.

During this phase the TLP is to be towed to the installation site from an onshore or near shore location. The platform stress analysis should be performed for a sufficient number of waves, say, ten wave periods at the wave heading considered the most critical for the structure.

The floatout phase should be analyzed for intact and damaged vessel configuration (see Figure 14.16).

#### 14.6.6 Platform Stress Analysis During Installation of TLP's

Platform stress analysis during installation is particularly important for a TLP. During the TLP installation, the structure may experience resonant motions as the tendons are being installed. During the tendon hook-up process the TLP is susceptible to waves with a wide range of periods because of its varying natural period due to the changes in restoring forces and moments.

The platform stress analysis may be performed for the most critical stage of the installation process. Again, the motion characteristics of the TLP will be the criterion for screening. The selected critical wave headings may be determined from the TLP motion characteristics.

#### 14.6.7 Platform Stress Analysis During Operational and Survival Conditions for TLP's

To ensure the operability and survivability of the platform during its entire service life, platform stress analyses may be performed for both the operational and survival conditions. Additional analyses for damaged condition may be required during this phase of the TLP investigation. Figure 14.17 shows schematically a structural analysis of a TLP in damaged condition. Figure 14.18 shows a flow chart describing a method of preliminary structural analysis of a TLP.



#### 14.6.8 Detailed Stress Analysis

A detailed stress analysis should consider all eight phases discussed in Section 14.1. The space frame model will identify the critical phases, loads, wave headings, and the components. These results can be used to limit the number of detailed analyses. The detailed structural analysis may require a 3-D global finite element analysis instead of the space frame model. However, prior to using a detailed 3-D global model, a local finite element analysis of critical components, such as column-pontoon, column-bracing, pontoon-bracing, and deck-column nodes, may be performed to check the adequacy of the connections. The local analyses will reduce the cost of the final 3-D analysis. An example of the column-pontoon finite element model is shown in Figure 14.19.

#### 14.6.9 Local Stress Analysis and Design Modification

The space frame analysis predicts the combined static and dynamic global forces and stresses at a number of points around the beam element cross section at each nodal point. Clearly, this analysis has limitations in that large members such as columns and pontoons are idealized as simple beams. A more representative state of stress is obtained by combining the global stresses with the external pressure. In local analysis, the columns and pontoons are treated as shell structures and the dispersion of forces through the stiffened plates are studied. The stress resultants are used to check the components against yielding and buckling using DnV or other codes. Proper design modifications are made to finalize the design. For major modifications which result in significant changes in the weight, a second stress analysis may be required. However, for minor design and weight changes no new analysis will be needed.

#### 14.6.10 Fatigue Analysis

The result of the 3-D finite element analysis for all the loading conditions are used to calculate the hot spot stresses and the stress concentrations (SCF) at the critical connections. The SCF's are then used to estimate the fatigue life of the joints. A detailed procedure for estimating the fatigue life based on the probabilistic approach is given by Zedan et al. (1981), Tein et al. (1982), and Wallis et al. (1979). The flow chart in Figure 14.20 shows a procedure for fatigue assessment of a TLP.

#### 14.7 Detailed Design

A detailed design of a semisubmersible or TLP structure involves the consideration of all the eight phases discussed in Section 14.1. In this case the structural design of the components will be more stringent. For example, a three dimensional finite element analysis of the nodes, hull and deck structure may be used to obtain proper pressure distribution, stresses and stress concentration factors of the components. The design procedure will basically follow the philosophy outlined before.

#### 14.8 Platform Structure Weight Summary

The main objective of semisubmersible or TLP structural design is to provide a minimum weight structure that satisfies the strength and intended functional requirements. A complete itemized record of the weight of all the structural components must be prepared at the end of the design phase. This information is supplied to the weight control engineer. The weight control engineer, in turn, tabulates all the weights and supplies, and forwards this information to other disciplines such as motion analysis, stability check, drilling, tendon, riser, etc.

## 14.9 Final Structural Configuration

At the completion of preliminary and detailed design changes the design drawings are issued. These drawings should give descriptive information about the major components of the structure. The drawings should show the overall layout and definition of critical items and details of essential items. The minimum number of structural drawings should be composed of the following items:

- o Deck
  - Diaphragm
  - Trusses, girders
  - Well bay truss or plate girder
  
- o Column
  - Shell plating and stiffeners
  - Elevator shaft
  - Tendon tube
  - Bulkheads
  - Trim ballast tank bulkhead
  
- o Pontoon
  - Shell plating and stiffeners
  - Watertight bulkheads
  - Web frame/non-watertight bulkhead
  
- o Bracing
  - Shell plating and stiffeners
  
- o Connection Nodes
  - Column-to-pontoon node
  - Pontoon-bracing node
  - Column-deck connection
  - Column-bracing connection

#### 14.10 Concluding Remarks

In concluding this section it is worthwhile to mention that the design of the Hutton TLP structure posed several new design and configuration problems whose solution gave a huge momentum to this new technology. Most of the ideas presented in the previous sections are inspired by challenges posed by the Hutton TLP. The structural configuration and design features of the Hutton TLP are presented by Ellis et al. (1982). Figure 14.21 shows schematically the analytical procedure used in the Hutton TLP design.

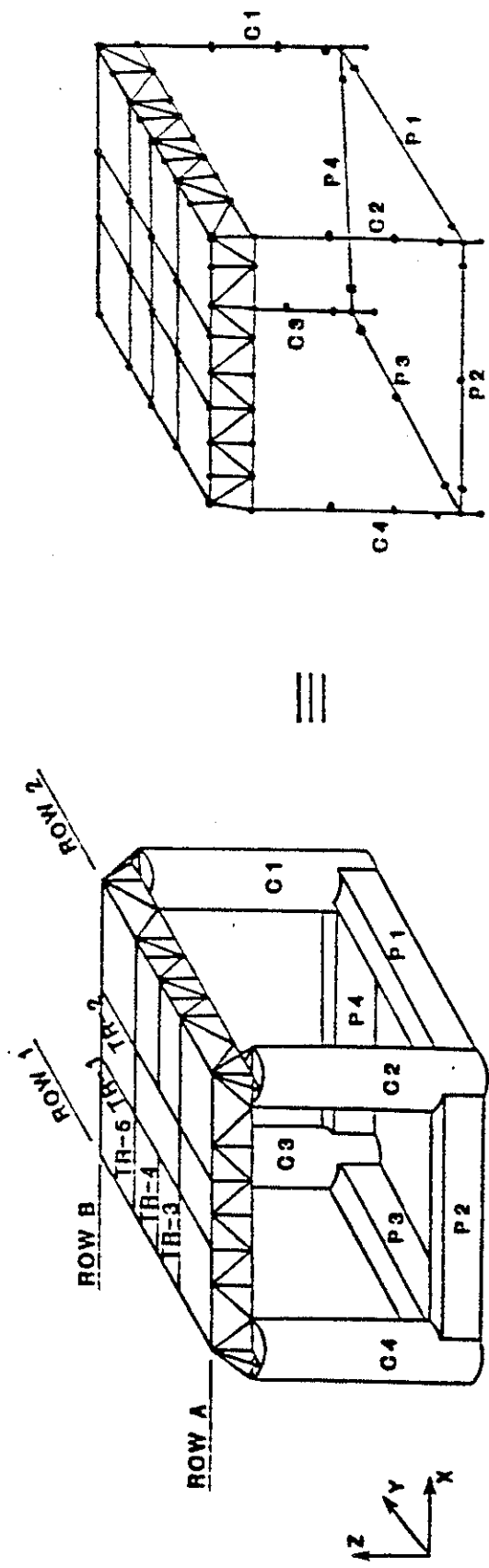
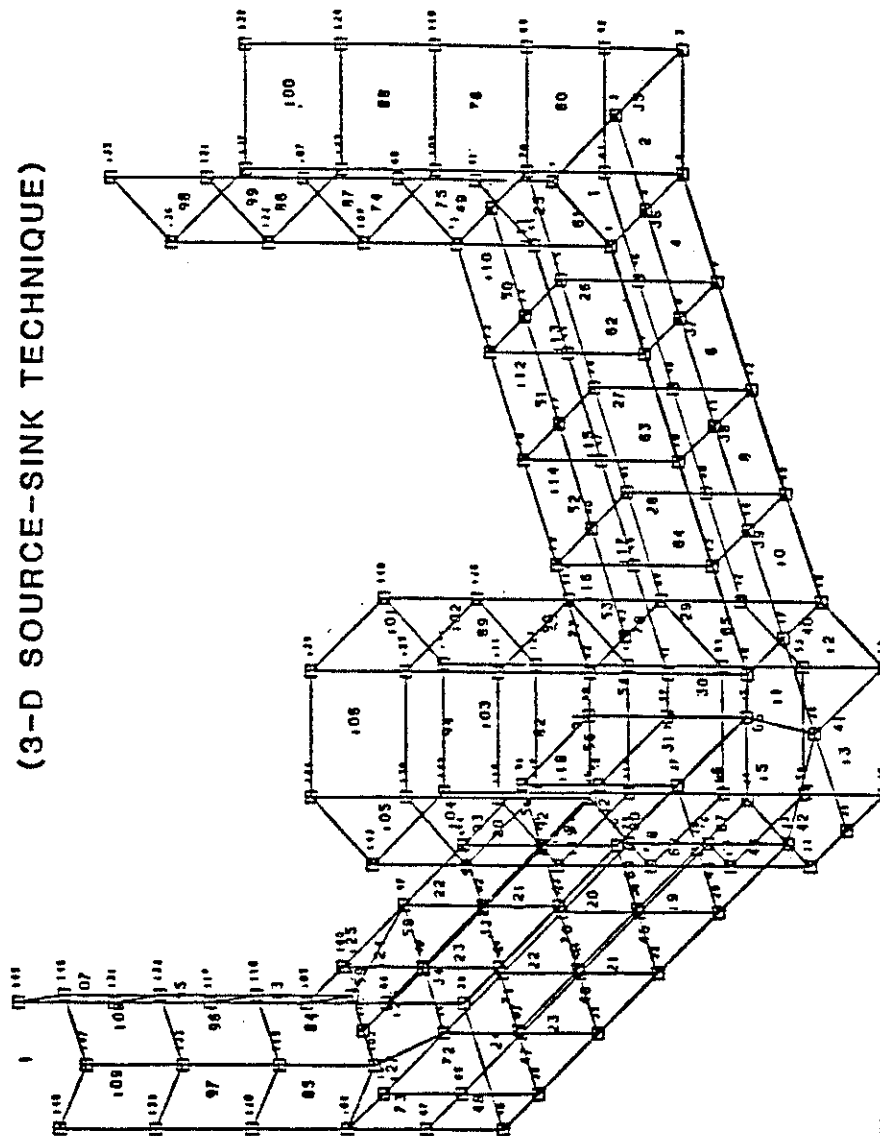


FIGURE 14.1 SPACE FRAME STRUCTURAL MODEL

TLP HYDRODYNAMIC MODEL  
 (3-D SOURCE-SINK TECHNIQUE)



VIEWING ANGLES: ALPHA = 35, BETA = 60.

FIGURE 14.2 COMPUTER GENERATED SOURCE-SINK HYDRODYNAMIC MODEL FOR A TLP

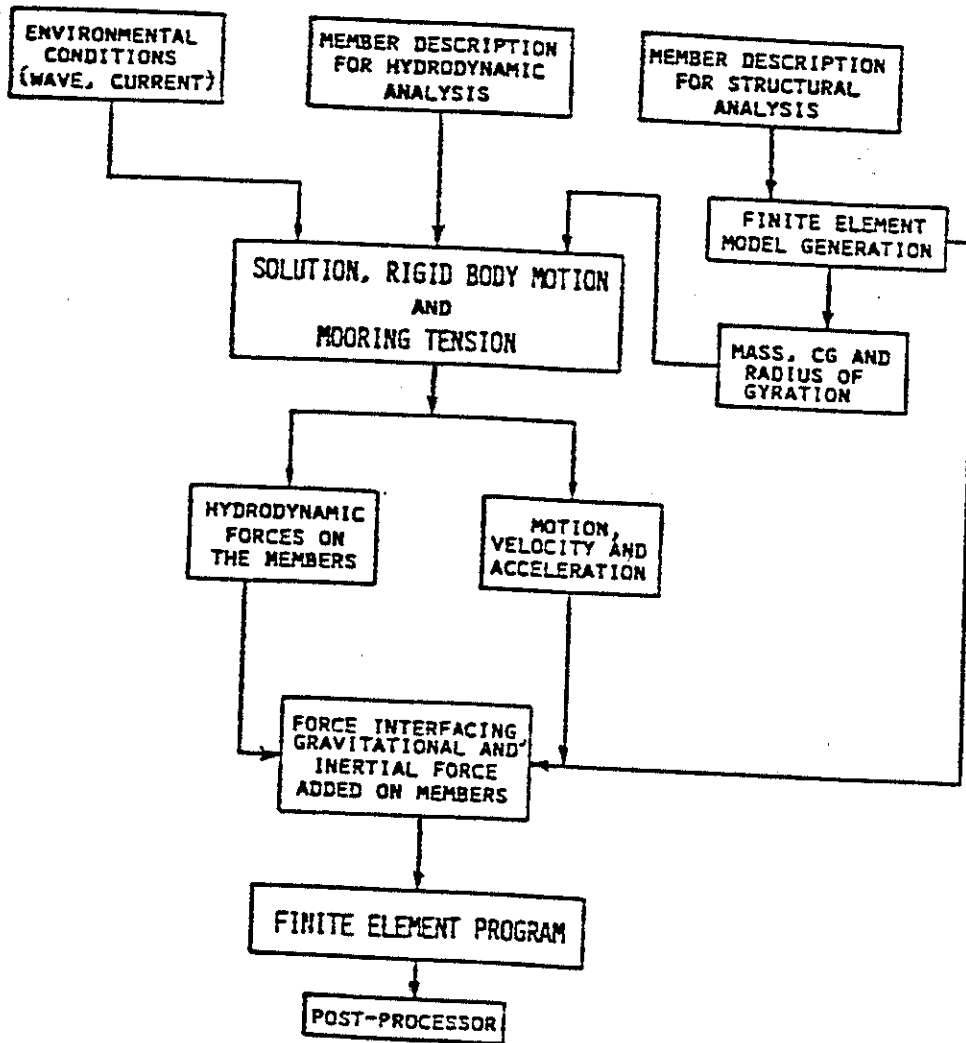


FIGURE 14.3 INTEGRATED MOTION-STRUCTURAL ANALYSIS PROCEDURE FOR TLP (LIU ET AL. 1982)

# INTEGRATED SYSTEM

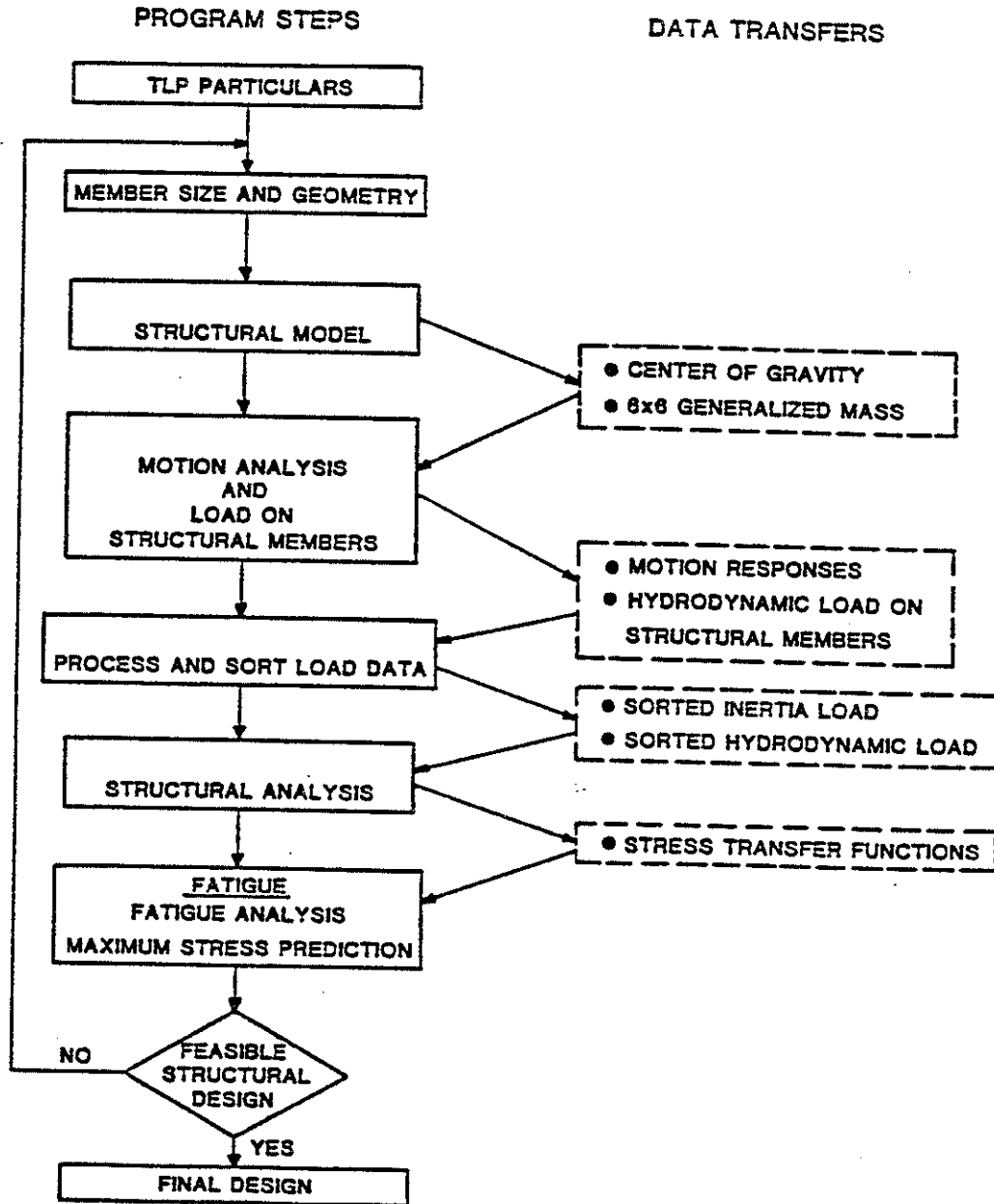


FIGURE 14.4 INTEGRATED MOTION-STRUCTURAL ANALYSIS PROCEDURE FOR TLP (TEIN ET AL. 1982)



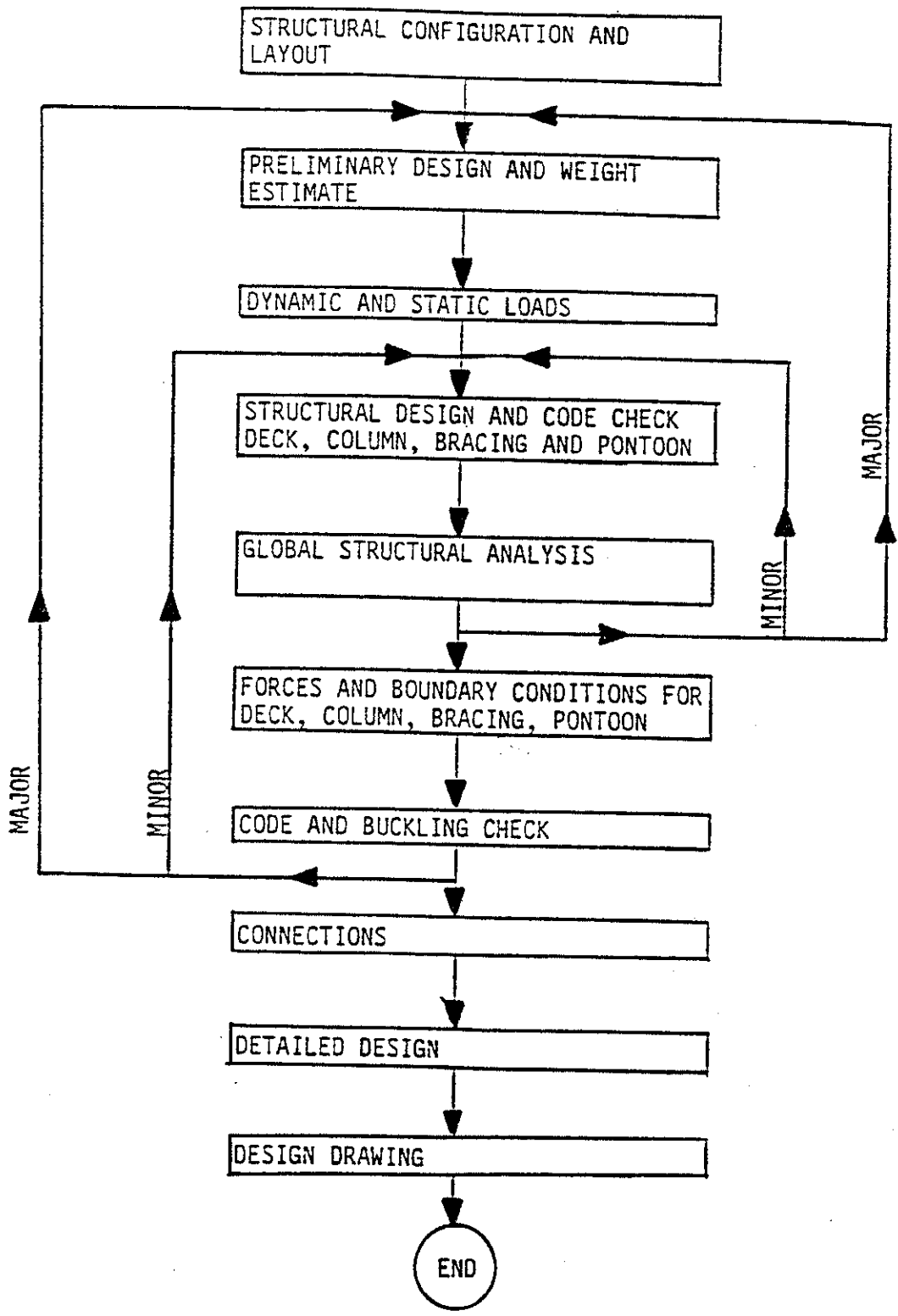


FIGURE 14.5 A METHOD FOR OVERALL STRUCTURAL DESIGN OF A SEMISUBMERSIBLE OR A TLP

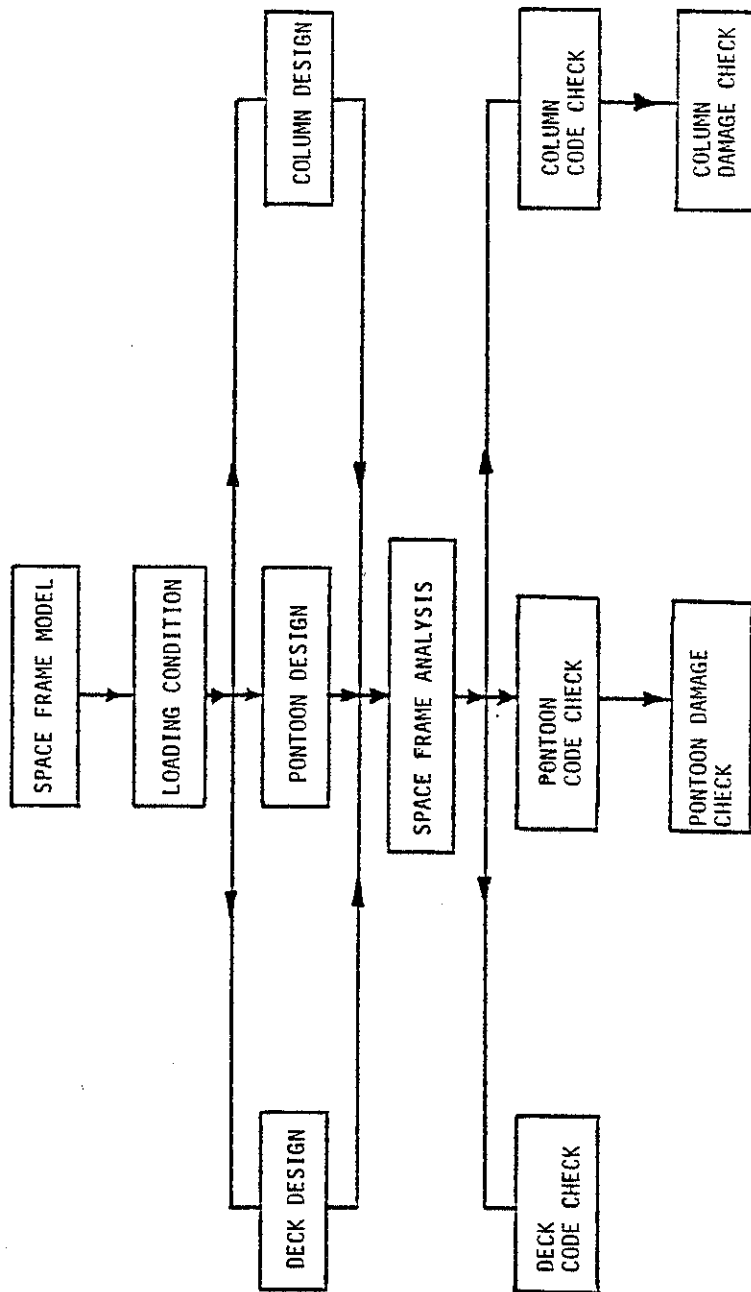


FIGURE 14.6 SEMISUBMERSIBLE OR TLP PRELIMINARY DESIGN PROCESS

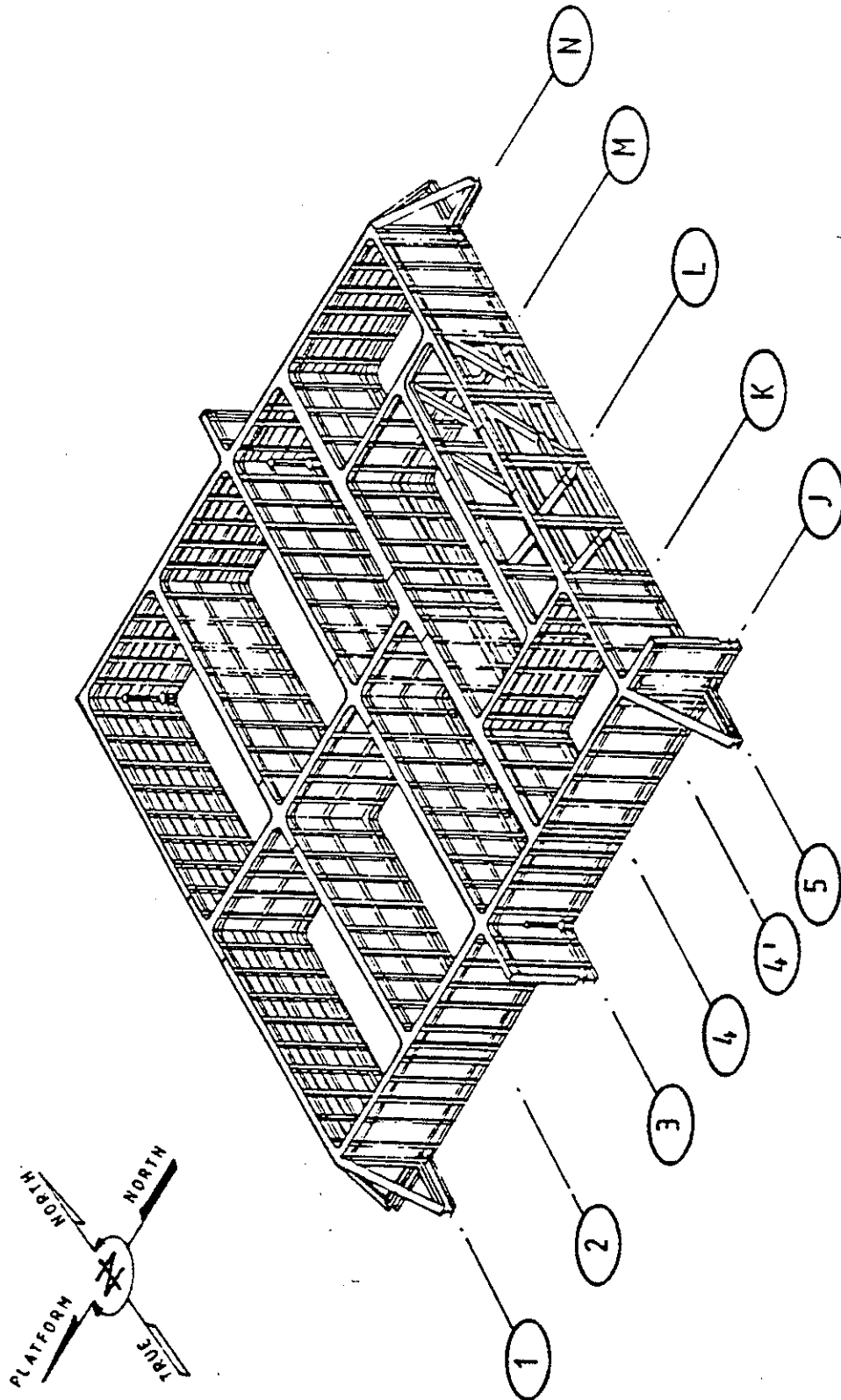


FIGURE 14.7 DECK SUPPORT STRUCTURE

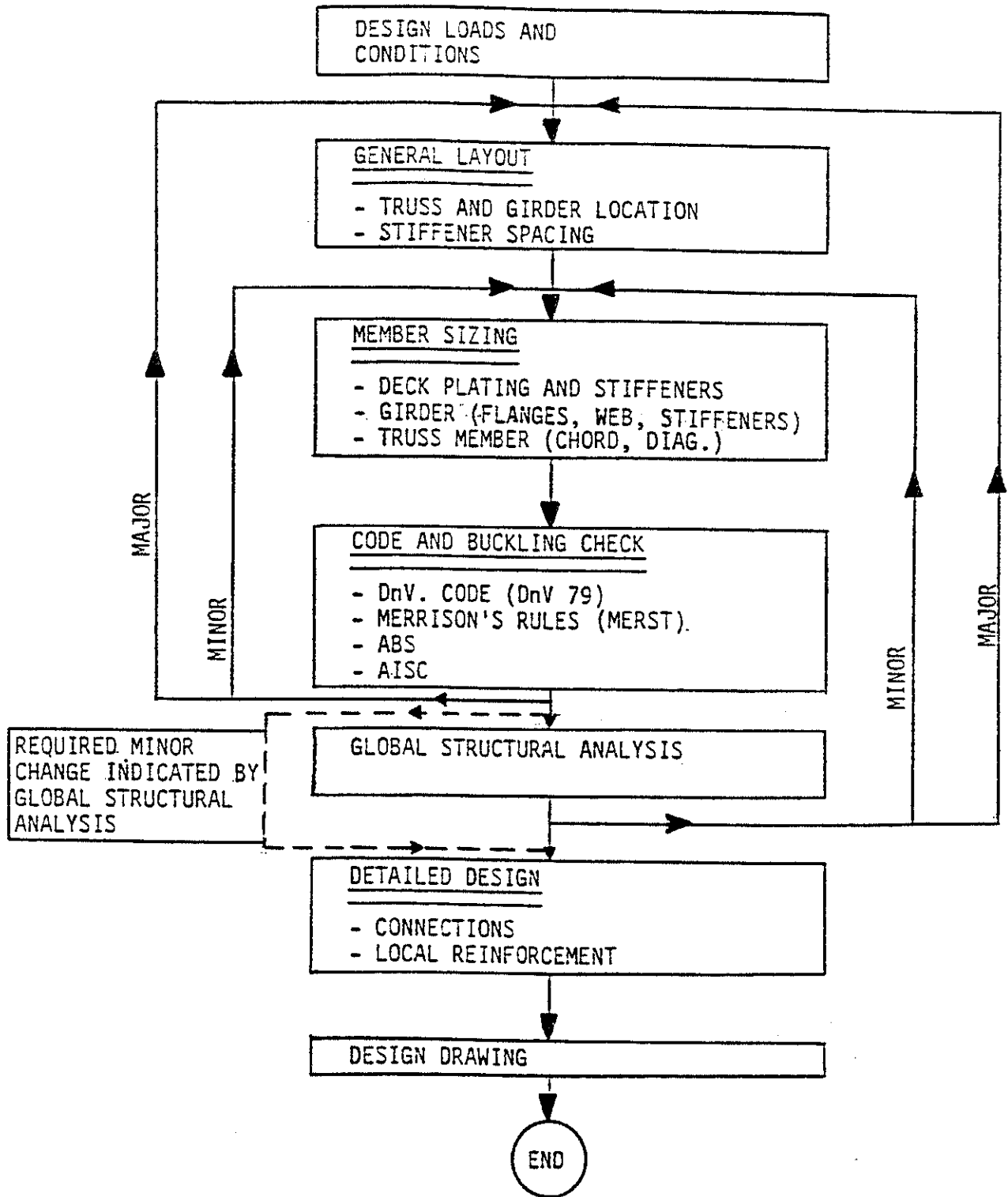


FIGURE 14.8 DECK DESIGN PROCEDURE

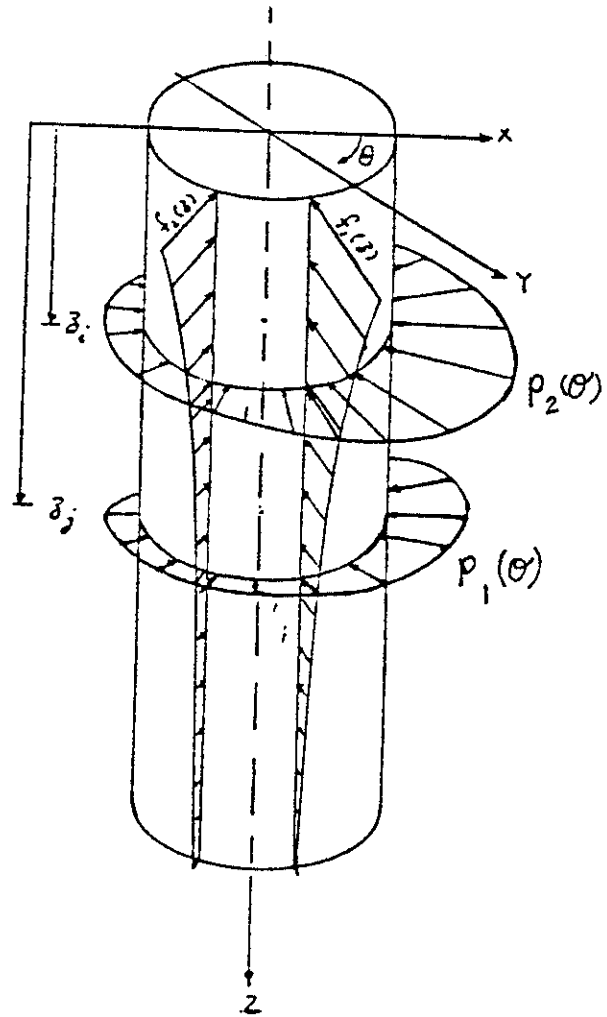


FIGURE 14.9 HYDRODYNAMIC PRESSURE ON A COLUMN

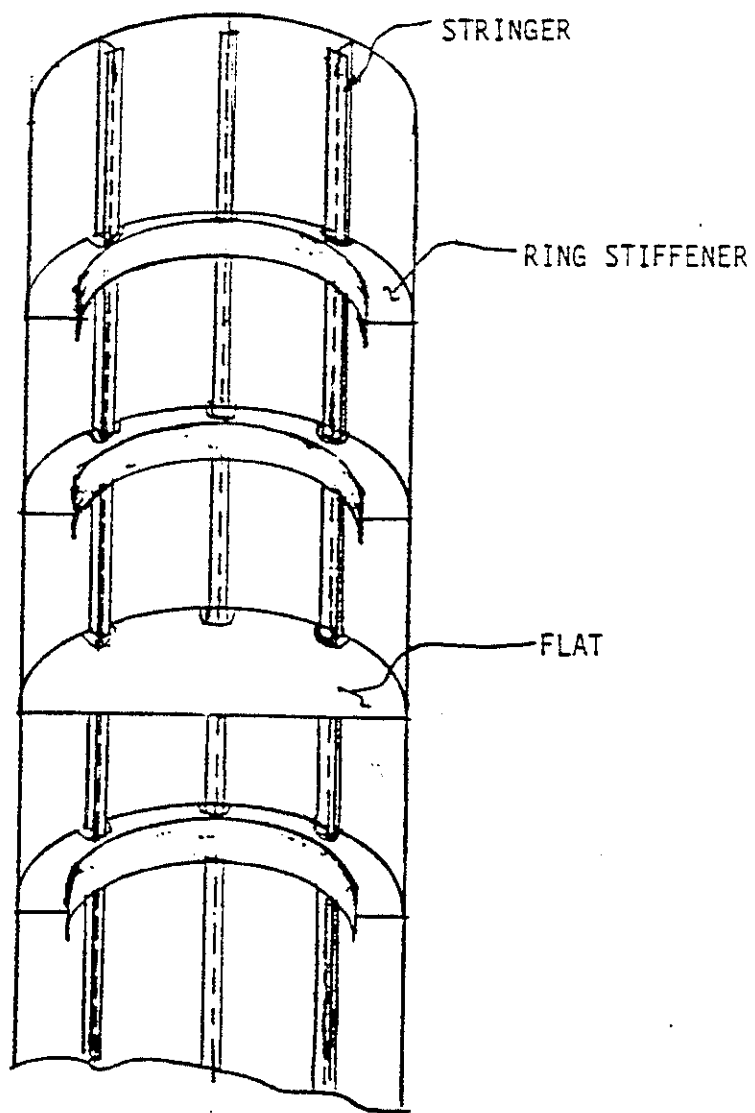


FIGURE 14.10 TLP COLUMN STRUCTURAL COMPONENTS SHOWN IN CUT AWAY VIEW

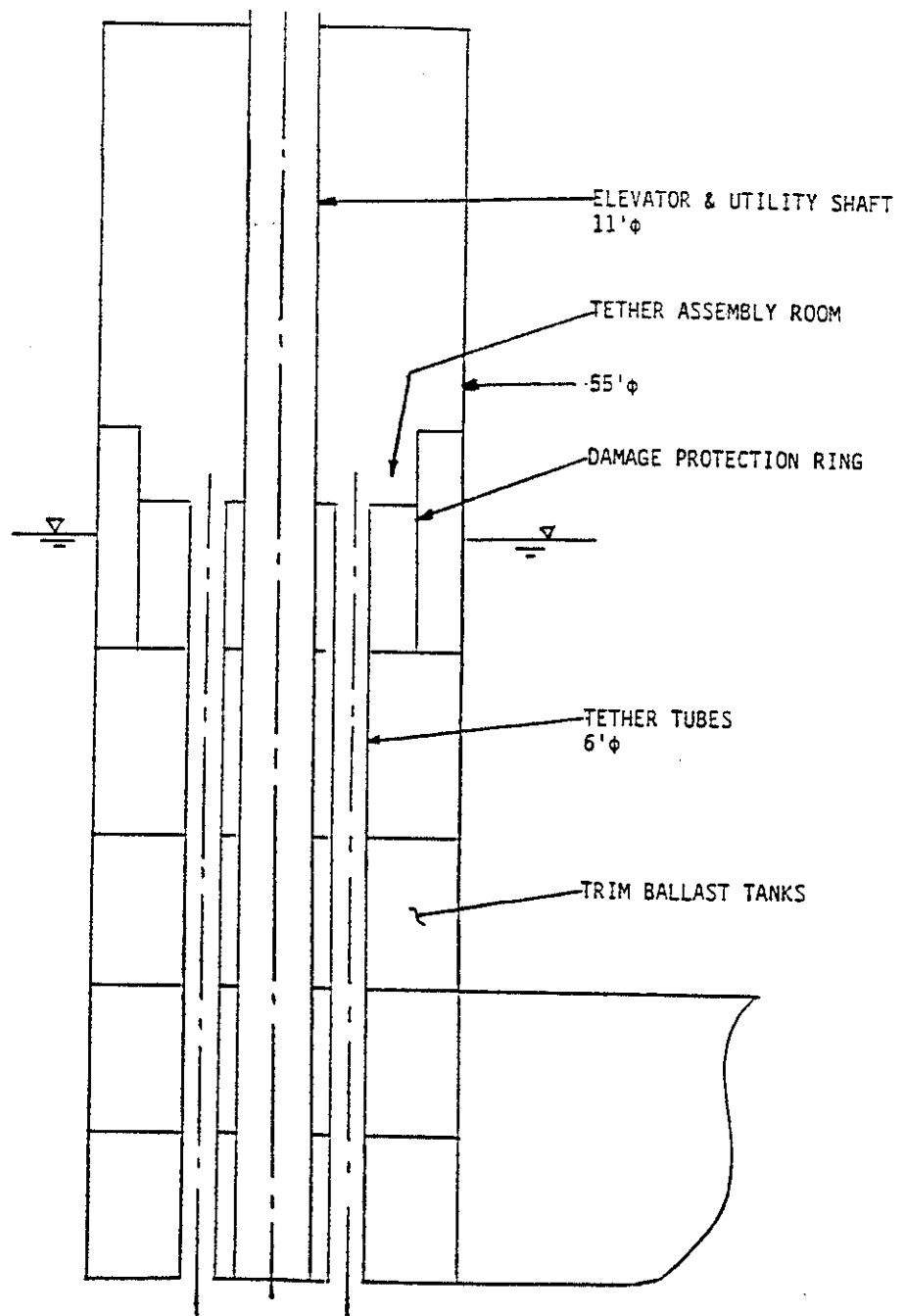


FIGURE 14.11 TLP COLUMN STRUCTURAL ARRANGEMENT

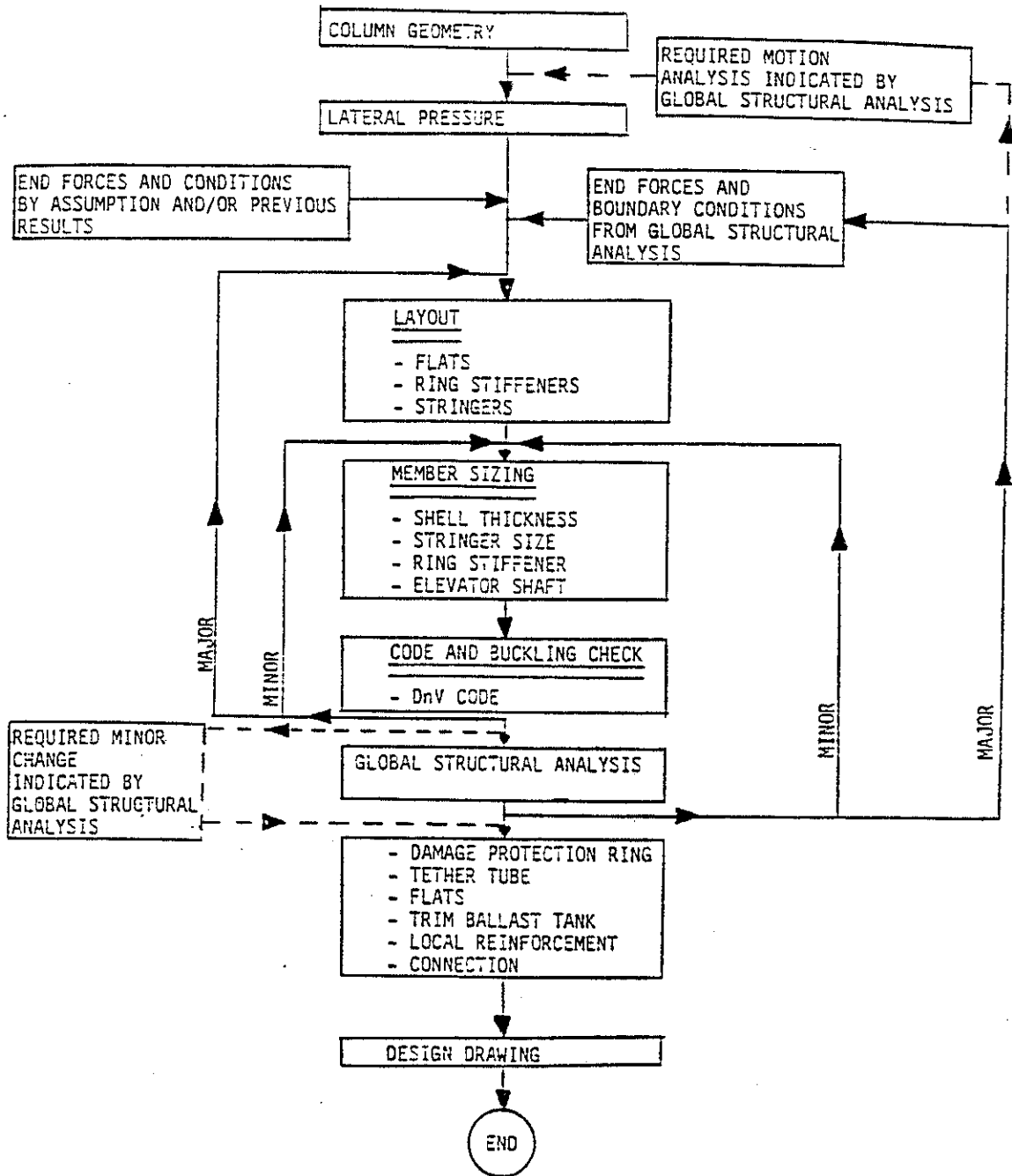


FIGURE 14.12 OVERALL COLUMN DESIGN PROCEDURE



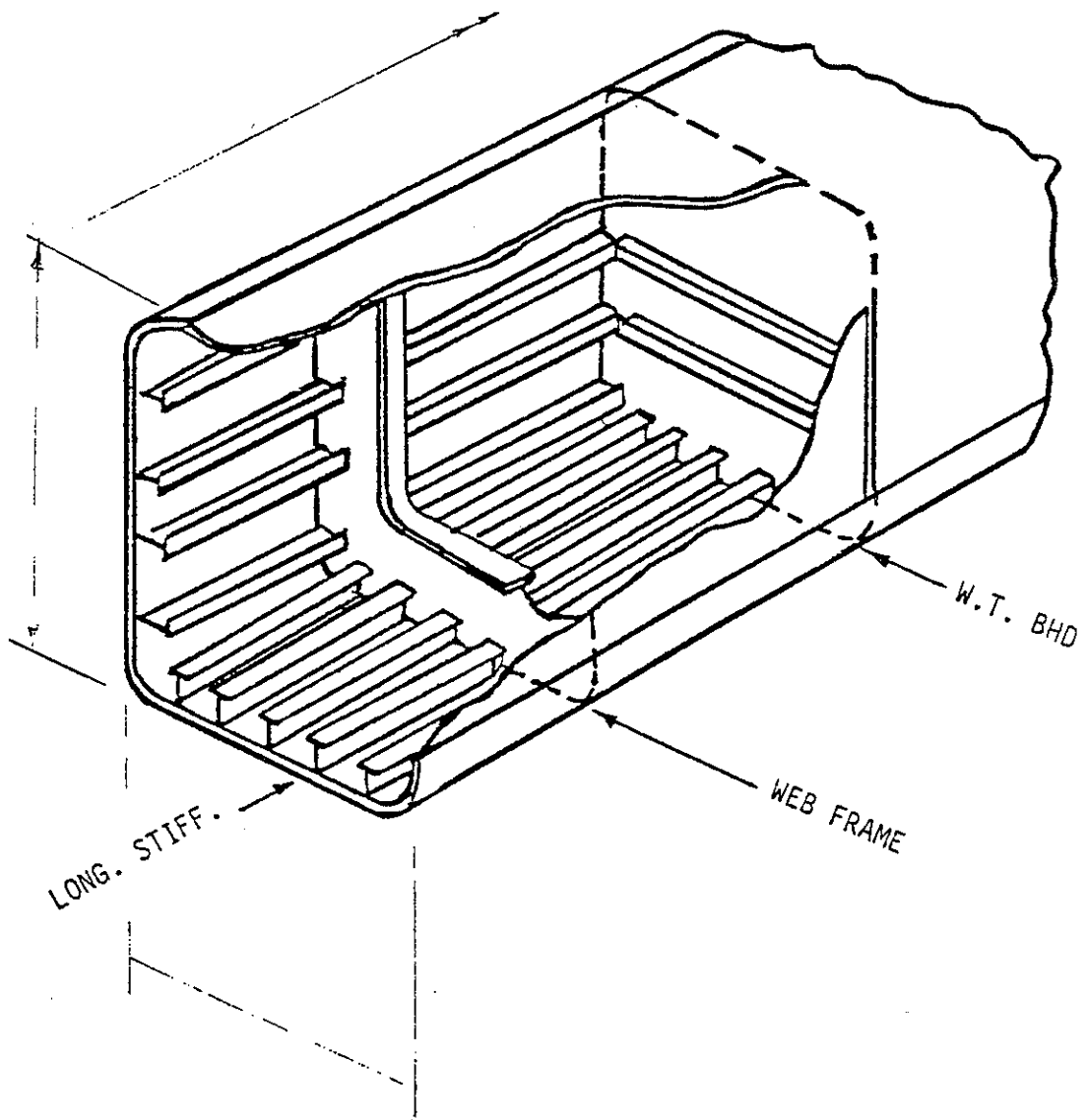


FIGURE 14.13 VIEW OF A PONTOON FRAMING

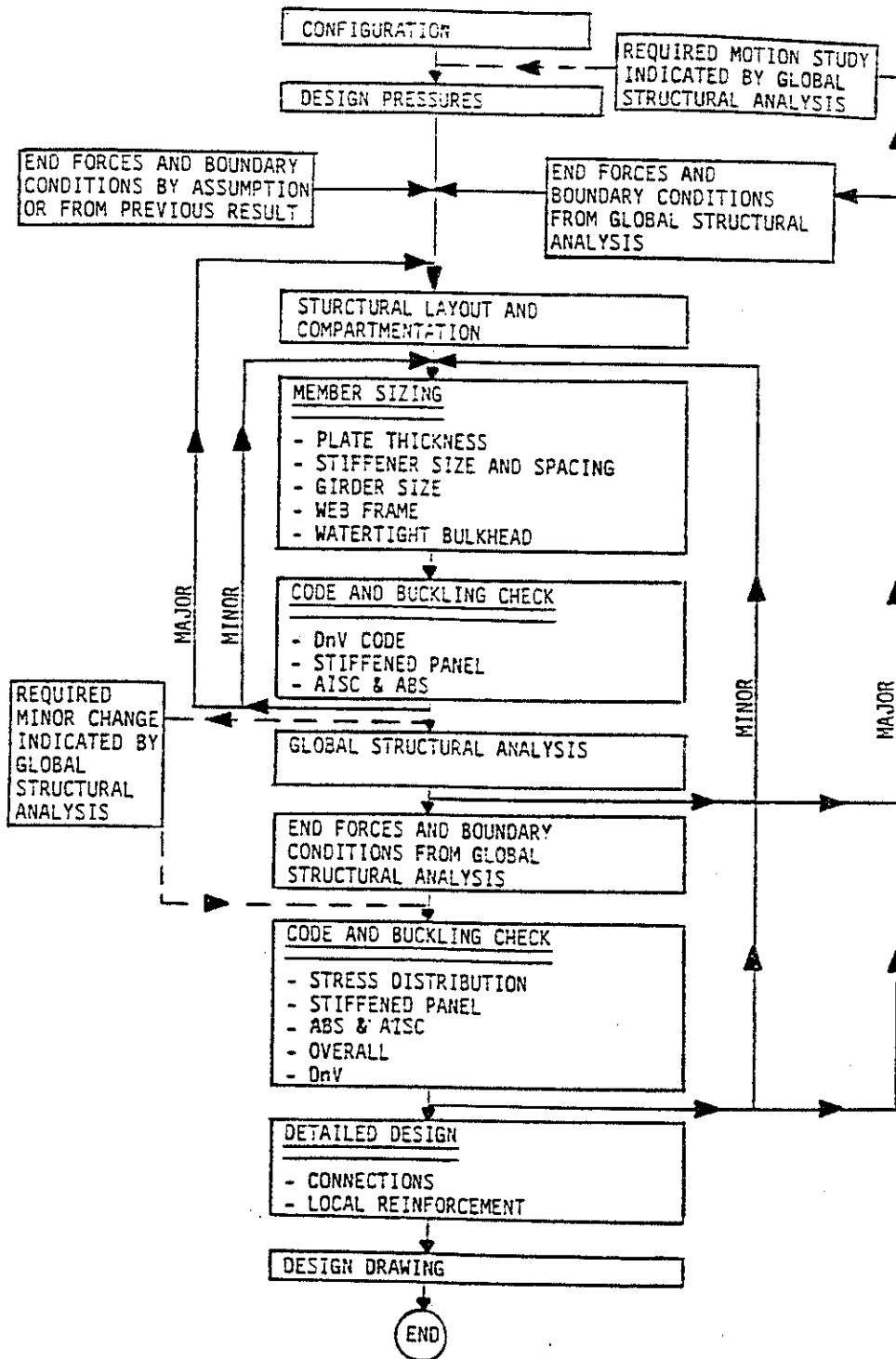


FIGURE 14.14 OVERALL PONTOON DESIGN PROCEDURE

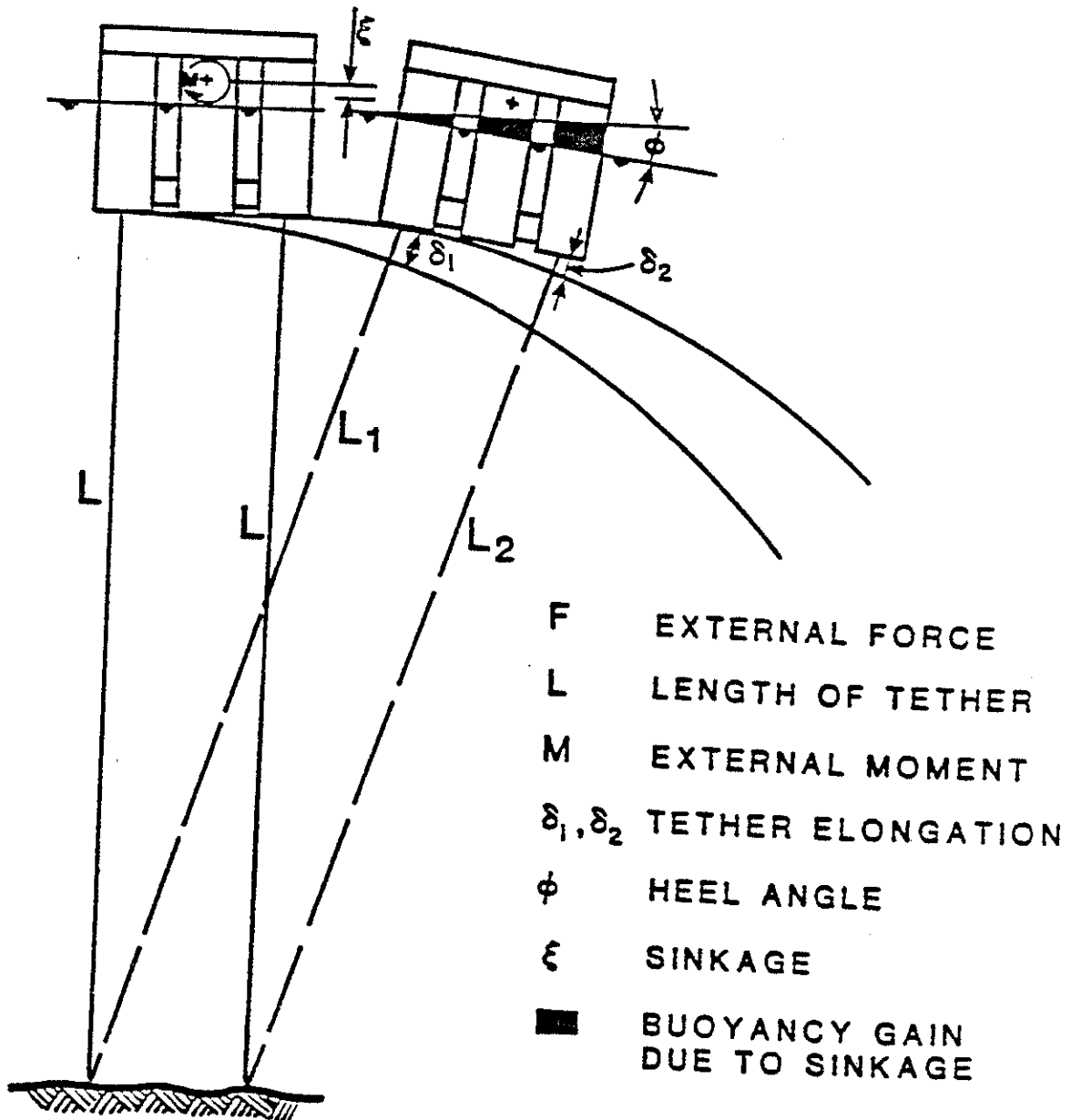
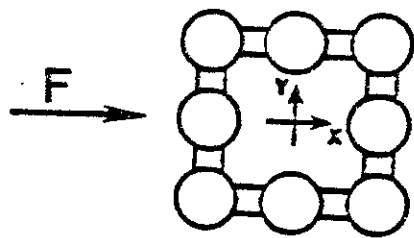


FIGURE 14.15 TLP CONFIGURATION AT MAXIMUM OFFSET

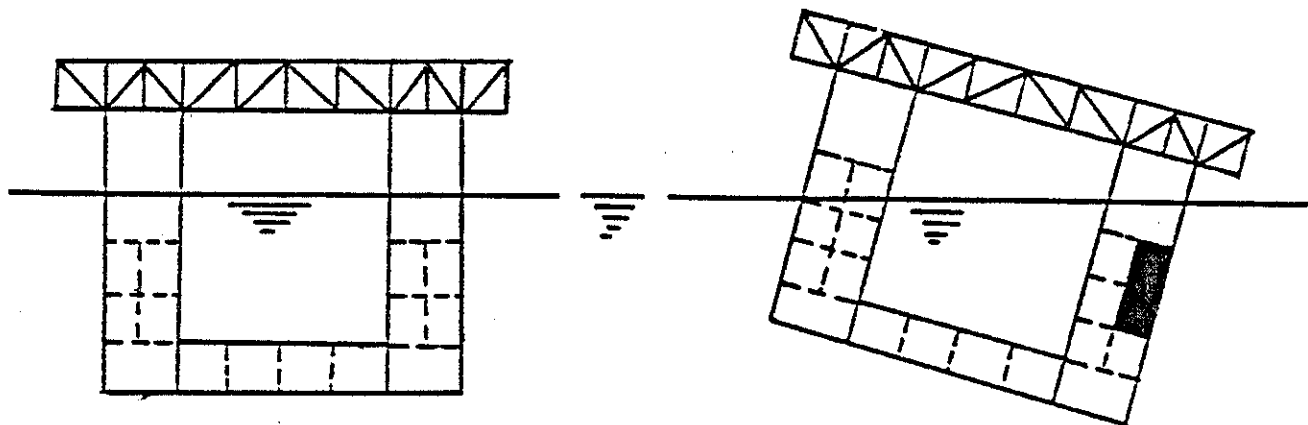
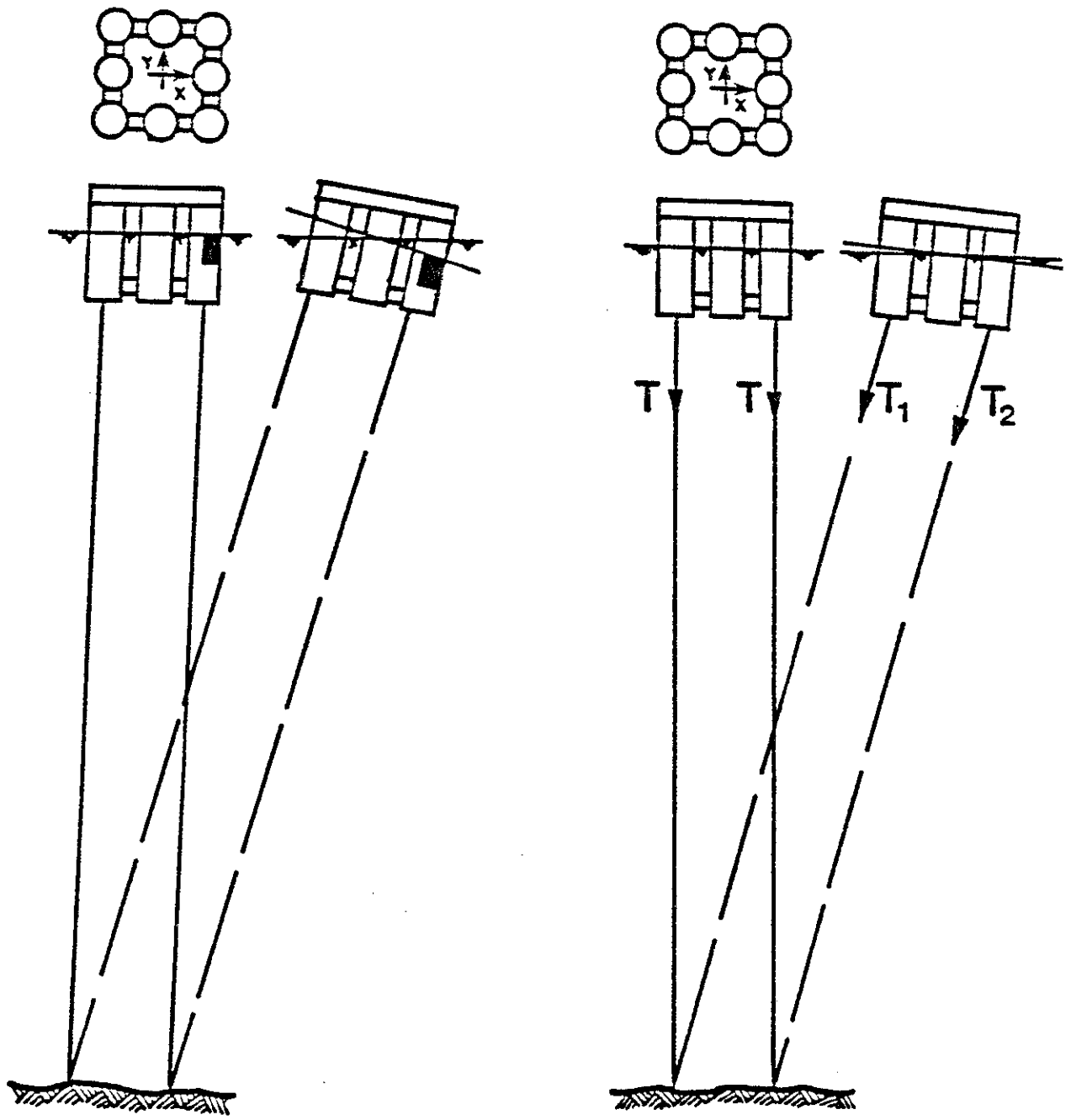


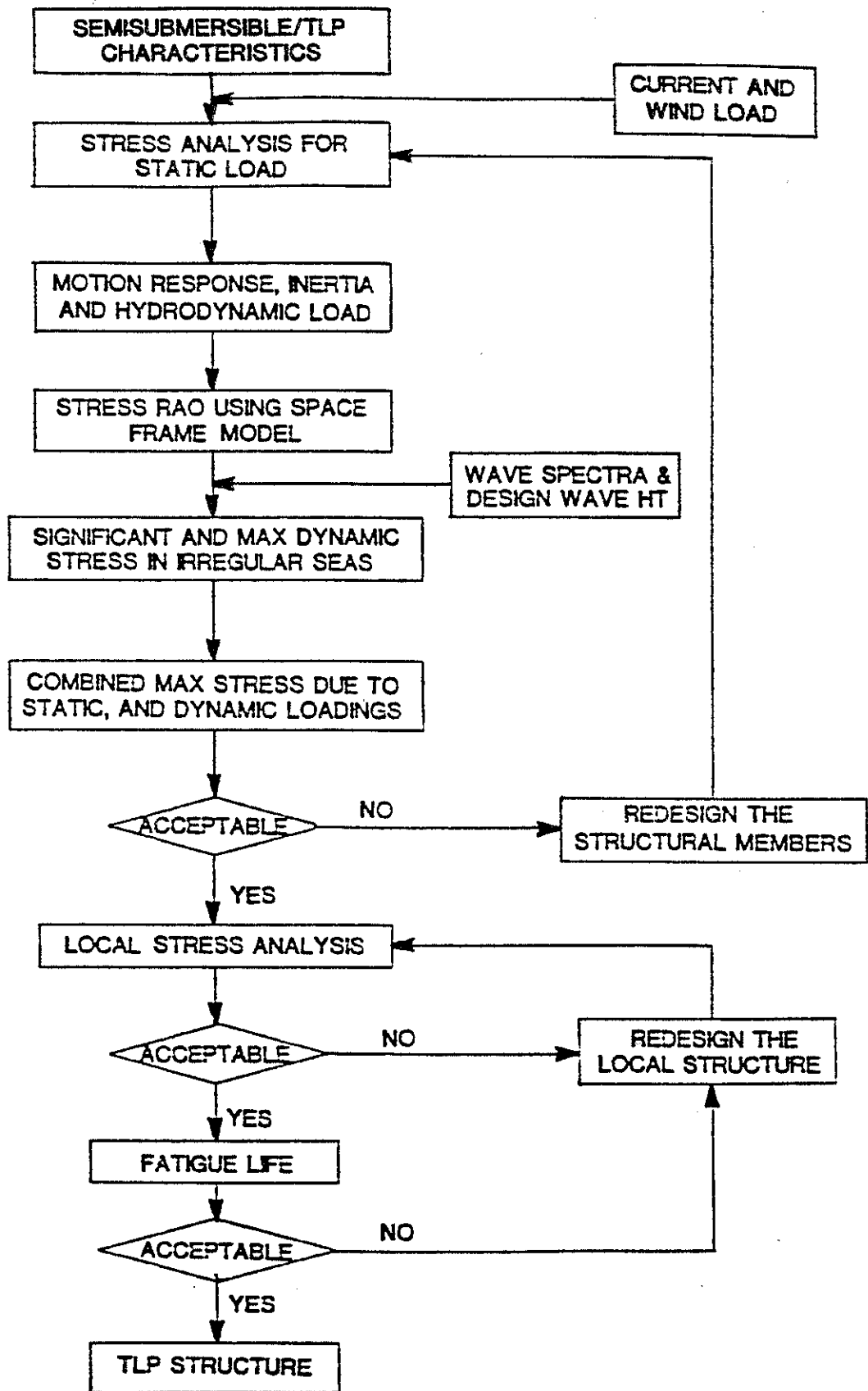
FIGURE 14.16 INTACT AND DAMAGED TLP FLOATOUT



**a) LOSS OF BUOYANCY**

**b) BREAKING OF ONE OR MORE TETHERS**

FIGURE 14.17 IN-PLACE STRUCTURAL ANALYSIS OF TLP FOR DAMAGED CONDITION



METHOD OF SEMISUBMERSIBLE/TLP STRUCTURAL ANALYSIS  
 FIGURE 14.18

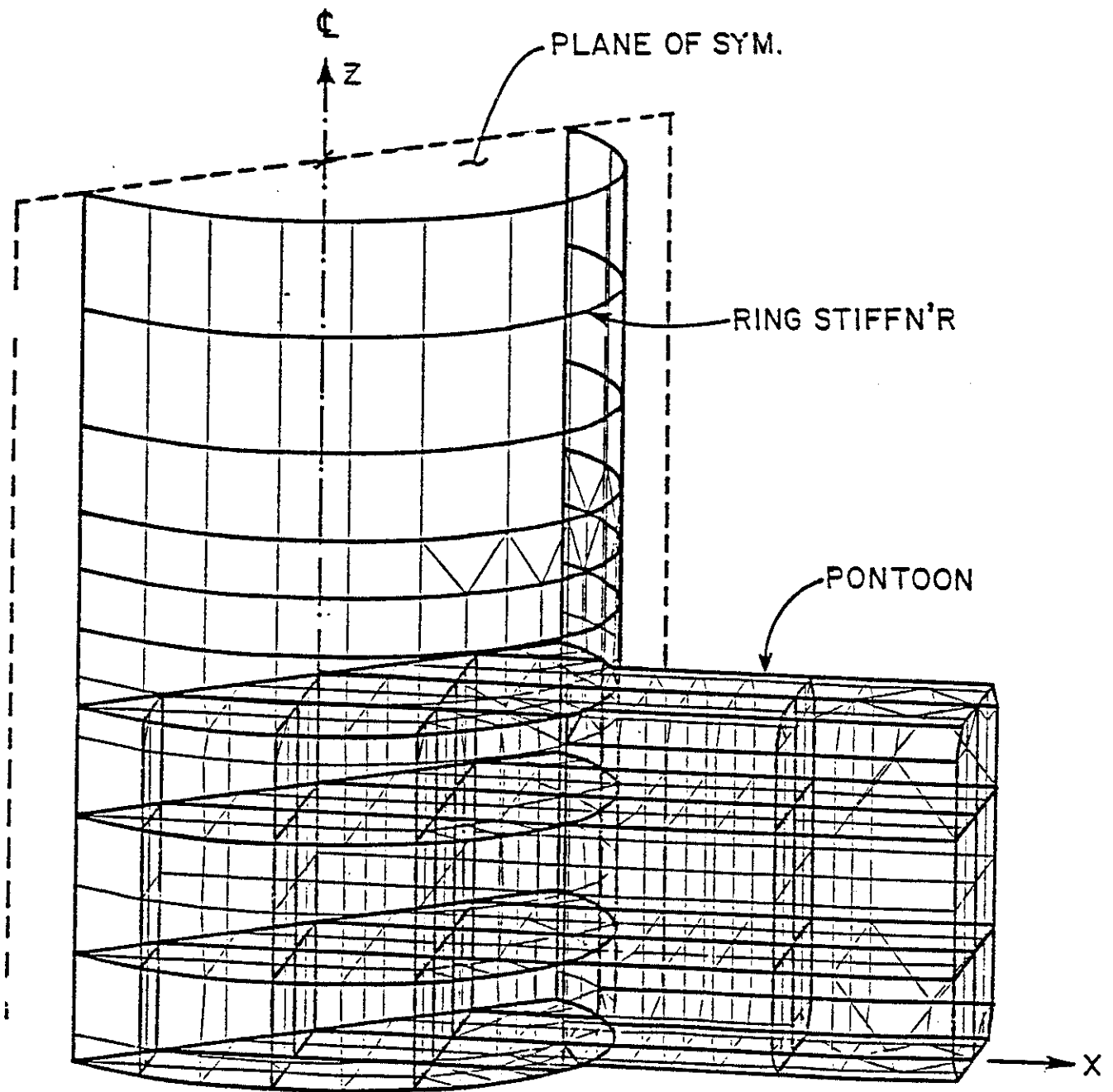
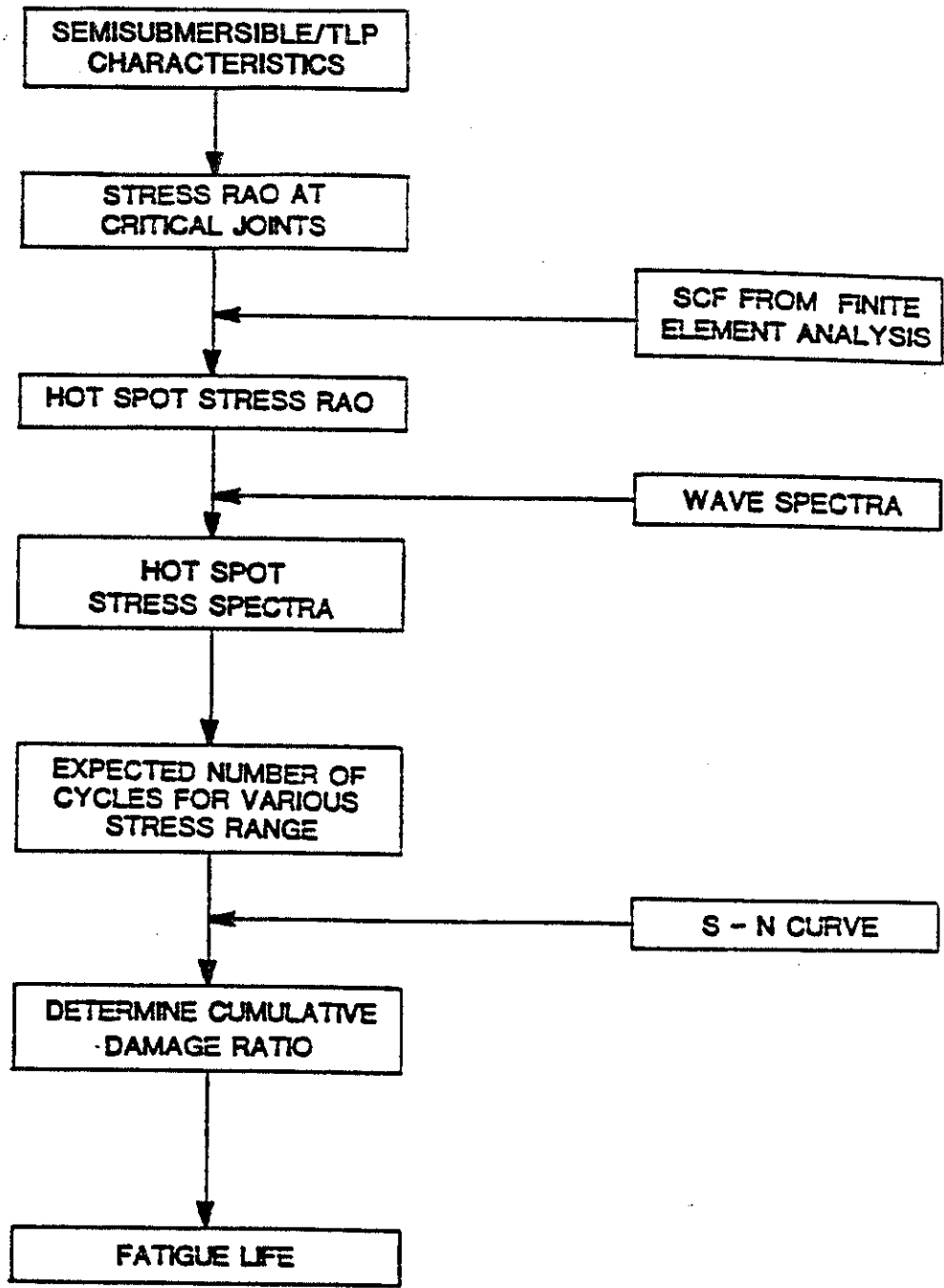


FIGURE 14.19 COLUMN TO PONTOON NODE FINITE ELEMENT ANALYSIS



**FATIGUE LIFE ANALYSIS**

**FATIGUE ANALYSIS PROCEDURE FOR A SEMISUBMERSIBLE/TLP  
FIGURE 14.20**



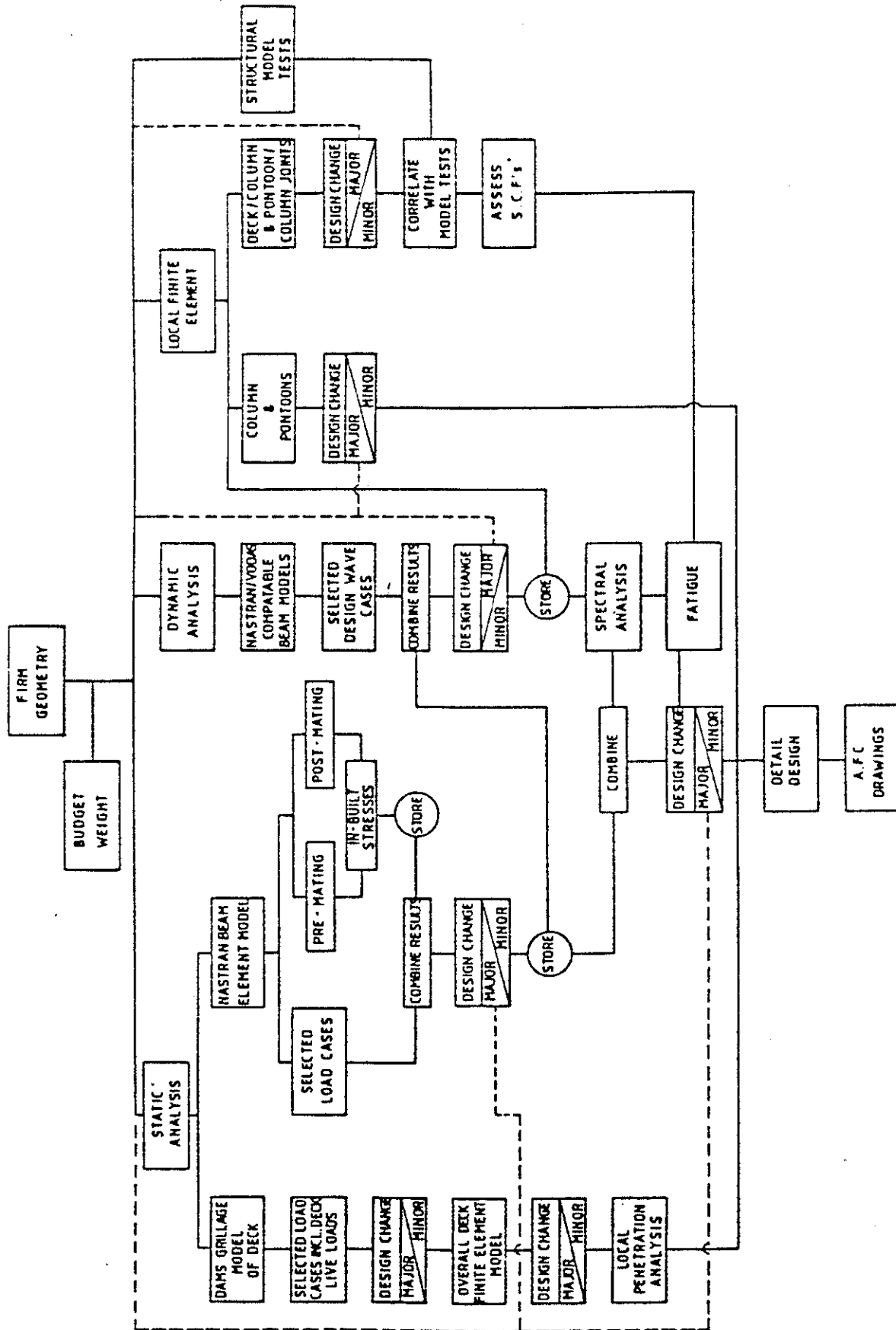


FIGURE 14.21 ANALYTICAL PROCEDURE USED FOR HUTTON TLP STRUCTURAL ANALYSIS. (ELLIS ET AL. 1982)



REFERENCES

- Aagaard, P.M. and Dean, R.G., 1969, "Wave Forces: Data Analysis and Engineering Calculation Method," Offshore Technology Conference, Paper No. OTC 1008, Houston.
- ABS, 1980, "Rules for Building and Classing Offshore Mobile Drilling Units," American Bureau of Shipping, New York.
- Angelides, D.C., Cheng, Y.C. and Stephen, A.W., 1982, "Dynamic Response of Tension Leg Platforms," BOSS Proceedings, Third International Conference, Massachusetts Institute of Technology.
- Angrilli, F. and Cossalter, V., 1981, "Transverse Oscillations of a Vertical Pipe in Waves," Proceedings of the 102nd ASME Winter Annual Meeting [Nov. 1981], Washington, D.C.
- Apelt, C.J. and Macknight, A., 1976, "Wave Action on Large Offshore Structures," Proceedings of 15th Coastal Engineering Conference, ASCE, Chapter 30, pp. 2228-2247.
- API RP 2A, 1982, "Recommended Practice for Planning, Designing and Constructing Fixed Offshore Platforms," 13th Edition, January.
- API RP 2P, 1984, "Recommended Practice for the Analysis of Spread Mooring Systems for Floating Drilling Units," 1st Edition, January.
- Arhan, M.F., Cavanic, A.G. and Ezraty, R.S., 1979, "Determination of the Period Range Associated to the Design Wave," Offshore Technology Conference, Paper No. OTC 3643, Houston.
- Audibert, J.M.E., Dover, A.R., Thompson, G.R. and Hubbard, J.L., 1979, "Geotechnical Engineering for Guyed Tower Offshore Structures," Civil Engineering in the Oceans IV, ASCE, San Francisco, California, September.

Bakmis, C., 1981, "Harmonic Flow About Cylinders," Thesis submitted to the Naval Postgraduate School, Monterey, California.

Batchelor, G.K., 1967, "An Introduction to Fluid Dynamics," Cambridge University Press, Cambridge, Massachusetts.

Bathe, K.J., 1982, "Finite Element Procedures in Engineering Analysis," Prentice-Hall Inc., Englewood Cliffs, New Jersey.

Bathe, K.J. and Wilson, E.L., 1976, "Numerical Methods in Finite Element Analysis," Prentice-Hall Inc., Englewood Cliffs, New Jersey.

Bea, R.G. and Lai, N.W., 1978, "Hydrodynamic Loadings on Offshore Platforms," Offshore Technology Conference, Paper No. OTC 3064, Houston.

Bearman, P.W., 1971, "Wind Loads on Structures in Turbulent Flow," The Modern Design of Wind-Sensitive Structures, Construction Industry Research and Information Association, London, U.K., 1971, pp. 42-48.

Bell, A.O., 1974, "Service Performance of a Drilling Unit," Royal Institution of Naval Architects, Spring Meetings, London.

Berman, M.Y. and Blenkarn, K.A., 1978, "The Vertically Moored Platform for Deepwater Drilling and Production," Offshore Technology Conference, Paper No. OTC 3049, Houston.

Bettess, P., 1977, "Infinite Elements," International Journal of Numerical Methods in Engineering, Volume 11, pp. 53-64.

Beynet, P.A., Berman, M.Y. and Aschwege, von J.T., 1978, "Motion, Fatigue, and the Reliability Characteristics of a Vertically Moored Platform," Offshore Technology Conference, Paper No. OTC 3304, Houston.

Bishop, J.R., 1978, "The Mean Square Value of Wave Force Based on the Morison Equation," National Maritime Institute Report NMI-R-40.

Bishop, J.R., 1979, "R.M.S. Force Coefficients Derived from Christchurch Bay Wave Force Data," National Maritime Institute Report NMI-R-62.

Bishop, J.R., Tickell, R.G. and Gallagher, K.A., 1980, "The U.K. Christchurch Bay Project; a Review of Results," Offshore Technology Conference, Paper No. OTC 3796, Houston.

Bjerregaard, Egon T.D., Velschou, Sven and Clinton, John S., 1978, "Wind Overturning Effect on a Semisubmersible," Offshore Technology Conference, Paper No. OTC 3063, Houston.

Bjerregaard, Egon T.D. and Sorensen, Erik G., 1981, "Wind Overturning Effects Obtained From Wind Tunnel Tests with Various Semisubmersible Models," Offshore Technology Conference, Paper No. OTC 4124, Houston.

Blevins, R.D., 1977, "Flow-Induced Vibrations," Van Nostrand Reinhold, New York.

Blevins, R.D. and Burton, T.E., 1976, "Fluid Forces Induced by Vortex Shedding," Journal of Fluid Engineering, Volume 95, 1976, pp. 19-24.

Bolotin, V.V., 1964, "The Dynamic Stability of Elastic Systems," Holden-Day, Inc., San Francisco, California.

Boreel, L.J., 1975, "Wave Action on Large Offshore Structures," Proceedings of the Conference on Offshore Structures, Institute of Civil Engineers, London, pp. 7-14.

Borgman, L. E., 1958, "Computation of the Ocean-Wave Forces on Inclined Cylinders," Transactions of American Geophysical Union, Volume 39, pp. 885-888.

Borgman, L.E., 1967, "Random Hydrodynamic Forces on Objects," Annual Mathematical Statistics, 38, 37.

Boussinesq, J., 1871, "Theorie de L'intumescence Liquide, Appelee Onde Solitaire ou de Translation se Propageant Dans un Canal Rectangulaire," Comptes Rendus Acad. Sci., Paris, Volume 72, pp. 755-759.

Brebbia, C.A. and Walker, S., 1979, "Dynamic Analysis of Offshore Structures," Newnes-Butterworths, London.

Bretschneider, C.L., 1959, "Wave Variability and Wave Spectra for Wind-Generated Gravity Waves," U.S. Army Corps of Engineers, Beach Erosion Board, Technical Memorandum, No. 118.

Bretschneider, C. L., 1960, "A Theory for Waves of Finite Height," Practices, 7th Conference on Coastal Engineering, The Hague, pp. 146-183.

British Ship Research Association, 1976, "A Critical Evaluation of the Data on Wave Force Coefficients," British Ship Research Association, Wallsend upon Tyne, Contract Report W-278.

Burke, B.G., 1969, "The Analysis of Motions of Semisubmersible Drilling Vessels in Waves," Offshore Technology Conference, Paper No. OTC 1024, Houston.

Burns, C.E., 1981, "Simplified Analysis of a Tension Leg Platform," Proceedings of Deep Offshore Technology Conference.

Burns, C.E., 1983, "Calculating Viscous Drift of a Tension Leg Platform," Proceedings of the Second International Offshore Mechanics and Arctic Engineering Symposium, ETCE, Houston, Texas, January.

Calsen, C.A. and Mathisen, J., 1980, "Hydrodynamic Loading for Structural Analysis of Twin Hull Semisubmersibles," Computational Methods for Offshore Structures, American Society of Mechanical Engineers, AMD Volume 37.

Capanoglu, C., 1979, "Tension Leg Platform, Interaction of Naval Architectural and Structural Considerations," Marine Technology, Volume 16, No. 4, October 1979, pp. 343-352.

Chakrabarti, S.K., 1973, "Wave Forces on Submerged Objects of Symmetry," Journal of Waterways, Harbors and Coastal Engineering Division, ASCE, Volume 99, (WW2), pp. 147-163.

Chakrabarti, S.K., et al., 1975, "Wave Forces on a Randomly Oriented Tube", Offshore Technology Conference, Paper No. OTC 2190, Houston.

Chakrabarti, S.K. and Cotter, D.C., 1983, "Interaction of Waves with a Moored Semisubmersible", Proceedings of the Third International Offshore Mechanics and Arctic Engineering Symposium, New Orleans, Louisiana.

Chan, R.K. and Hirt, C.W., 1974, "Two-Dimensional Calculations of the Motion of Floating Bodies," Proceedings of the 10th Symposium on Naval Hydrodynamics, Cambridge, Massachusetts, pp. 667-683.

Chappelear, J.E., 1961, "Direct Numerical Calculation of Wave Properties," Journal of Geophysical Research, Volume 66, pp. 501-508.

Chappelear, J.E., 1962, "Shallow Water Waves," Journal of Geophysical Research, Volume 67, pp. 4693-4704.

Chen, M.S. and Mei, C.C., 1974, "Oscillations and Wave Forces in a Man-Made Harbor in the Open Sea," Proceedings of the 10th ONR Symposium on Naval Hydrodynamics, Cambridge, Massachusetts, pp. 573-596.

Chenot, J.L., 1975, "Methode Numerique de Calcul du Mouvement d'un Corps Flottant Soumis a l'Influence d'une Houle Peridique en Theorie Lineaire," Rev. Institute Francais du Petrole, Volume 30, pp. 779-802.

Chou, F.S., Ghosh, S. and Huang, E.W., 1983, "Conceptual Design Process of a Tension Leg Platform," Transactions, SNAME, Volume 91,.

CIRIA, 1980, "Review of the Fluid Loading Research Programme for the Offshore Energy Technology Board," Report No. OT-R-8046, CIRIA, September.

Clough, R.W. and Penzien, T., 1975, "Dynamics of Structures," McGraw-Hill Inc., New York.

Comstock, J.P., 1967, "Principles of Naval Architecture," Society of Naval Architects and Marine Engineers.

Crandall, S.H., 1956, "Engineering Analysis," McGraw-Hill Inc., New York.

Cummins, W.E., 1962, "The Impulse Response Function and Ship Motion," D.T.M.B. Report 1661, Washington, D.C.

Currie, I.G., Hartlen, R.T. and Martin, W.W., 1974, "The Response of Circular Cylinders to Vortex Shedding," in Flow-Induced Structural Vibrations, Editor, Naudascher, E., Springer-Verlag, Berlin, pp. 128-142.

Dalrymple, R.A., 1974, "A Finite Amplitude Wave on a Linear Shear Current," Journal of Geophysical Research, Volume 79 (No. 30).

Darbyshire, J., 1952, "The Generation of Waves by Wind," Proceedings of the Royal Society, Serial A, Volume 215, pp. 299-328.



Dalton, C, 1980, "Inertia Coefficients for Riser Configurations," ASME Paper No. 80-Pet-21.

Dalton, C and Helfinstine, R.A., 1971, "Potential Flow Past a Group of Circular Cylinders," Journal of Basic Engineering, ASME, pp. 636-642.

Daring, D.W. and Huang, T., 1979, "Marine Riser Vibration Response by Modal Analysis," Journal of Energy Resource Technology, ASME, 1979, pp. 101, 159.

De, S.C., 1955, "Contribution to the Theory of Stokes Waves," Proceedings of the Cambridge Philosophical Society, Volume 8, pp. 57-74.

Dean, R.G., 1965, "Stream Function Representation of Nonlinear Ocean Waves," Journal of Geophysical Research, Volume 70, pp. 4561-4572.

Dean, R.G., 1970, "Relative Validities of Water Wave Theories," Journal of Waterways, Harbors and Coastal Engineering Division, ASCE, Volume 96, No. WWI, pp. 105-119.

Dean, R.G., 1974, "Evaluation and Development of Water Wave Theories for Engineering Application," Volumes I and II, U.S. Army, Coastal Engineering Research Center, Special Report No. 1, Fort Belvoir, Virginia.

Dean, R.G., 1976, "Methodology for Evaluating Suitability of Waves and Wave Force Data for Determining Drag and Inertia Coefficients," BOSS Proceedings, First International Conference, Trondheim, Norway.

Dean, R. G., 1976, "Methodology for Evaluating Suitability of Wave and Force Data for Determining Drag and Inertia Forces," BOSS '76, Trondheim, Volume 2, pp. 40-64.

Dean, R.G., Lo, J.M. and Johannson, P.I., 1979, "Rare Wave Kinematics vs. Design Practice," Proceedings of the Conference on Civil Engineering in Oceans IV, San Fransisco, ASCE, pp. 1030-1049.

Dean, R.G. and Dalrymple, R.N. 1984, "Water Wave Mechanics for Engineers and Scientists," Prentice-Hall Inc., Englewood Cliffs, New Jersey.

DnV, 1977, "Rules for the Design Construction and Inspection of Offshore Structures," Det norske Veritas, Oslo, Norway.

DnV, 1981, "Rules for Classification of Mobile Offshore Units," Det norske Veritas, Oslo, Norway.

DOE, 1974, "The Offshore Installations (Construction and Survey) Regulations," S.I. No. 289, Department of Energy, U.K.

Donnelly, H.L., Stadter, J.T., Weiss, R.O. and Perez y Perez, L., 1979, "Cold Water Pipe Verification Test," in Proceedings of the 6th Ocean Thermal Energy Conversion Conference, Washington, D.C., June.

Draper, L., 1965, "Wave Spectra Provide Best Basis for Offshore Rig Design," Oil and Gas International, Volume 5, No. 6, pp. 58-60.

Eatock Taylor, R. and Duncan, P.E., 1980, "Fluid-Induced Inertia and Damping in Vibrating Offshore Structures," Applied Ocean Research, Volume 2, pp. 3-12.

Eaton, K.J., (editor), 1974, "Proceedings of the Fourth International Conference of Wind Effects on Buildings and Structures," Cambridge University Press, Cambridge.

Ellis, N., Tetlow, J.H., Anderson, F., Woodhead, A.L., 1982, "Hutton TLP Vessel - Structural Configuration and Design Features," Offshore Technology Conference, Paper OTC No. 4427.

Faltinsen, O., 1969, "A Comparison of Frank Close-fit Method With Some Other Methods Used to Find Two-Dimensional Hydrodynamical Forces and Moments for Bodies Which are Oscillating Harmonically in an Ideal Fluid," Det norske Veritas, Oslo, Norway, Report No. 69-43-S.

Faltinsen, O. and Michelsen, F.C., 1974, "Motions of Large Structures in Waves at Zero Froude Number," Proceedings of the International Symposium on the Dynamics of Marine Vehicles and Structures in Waves, University College, London, pp. 91-106.

Faltinsen, O., Van Hoof, R.W., Fylling, I.J. and Teigen, P.S., 1982, "Theoretical and Experimental Investigations of Tension Leg Platform Behaviour," BOSS Proceedings, Third International Conference, Massachusetts Institute of Technology.

Fenton, J.D., 1978, "Wave Forces on Vertical Bodies of Revolution," Journal of Fluid Mechanics, Volume 85, pp. 241-255.

Fenton, J.D., 1979, "A High-Order Cnoidal Wave Theory", Journal of Fluid Mechanics, Volume 94, pp. 129-161.

Ferretti, C. and Berta, M., 1981, "Viscous Effect Contribution to the Drift Forces on Floating Structures," Proceedings, International Symposium on Ocean Engineering-Ship Handling, Gothenburg, Sweden.

Finn, L.D., 1976, "A New Deepwater Offshore Platform - The Guyed Tower," Proceedings, Offshore Technology Conference, Paper No. OTC 2688, Houston.

Finn, L.D. and Young, K.E., 1978, "Field Test of A Guyed Tower," Proceedings, Offshore Technology Conference, Paper No. OTC 3131, Houston.

Finn, L.D., Wardell, J.B. and Loftin, T.D., 1979, "The Guyed Tower as a Platform for Integrated Drilling and Production Operations," Journal of Petroleum Technology, pp. 1531-1537.

Fischer, F.J., Jones, W.T. and King, R., 1979, "Current Induced Oscillations of Cognac Piles During Installation-Prediction and Measurement," Proceedings of Symposium on Practical Experiences with Flow-Induced Vibrations (Preprint), Karlsruhe, Volume I, 216-228, September.

Forrinstall, G.Z., Ward, E.G., Cardone, V.J. and Borgman, L.E., 1978, "The Theoretical Spectra and Kinematics of Surface Gravity Waves in Tropical Storm Delia," Journal of Physics and Oceanography, Volume 8, pp. 888-909.

Frank, W., 1967, "Oscillation of Cylinders in or Below the Free Surface of Deep Fluids," NSRDC, Washington, D.C., Report 2375.

Garrison, C.J., 1974a, "Hydrodynamics of Large Objects in the Sea, Part I - Hydrodynamic Analysis," Journal of Hydronautics, Volume 8, pp. 5-12.

Garrison, C.J., 1974b, "Dynamic Response of Floating Bodies," Offshore Technology Conference, Paper No. OTC 2067, Houston.

Garrison, C.J., 1975, "Hydrodynamics of Large Objects in the Sea, Part II - Motions of Free-Floating Bodies," Journal of Hydronautics, Volume 9, pp. 58-63.

Garrison, C.J., 1978, "Hydrodynamic Loading of Large Offshore Structures: Three-Dimensional Source Distribution Methods," Numerical Methods in Offshore Engineering, Zienkeiwicz, Lewis, Stagg Editors, John Wiley & Sons.

Garrison, C.J., 1980, "A Review of Drag and Inertia Forces on Circular Cylinders," Offshore Technology Conference, Paper No. OTC 3760, Houston.

Garrison, C.J., 1982, "Forces on Semisubmerged Structures," Ocean Structural Dynamics Symposium 1982 Proceedings, Unbound Paper, Oregon State University, September 1982.

Garrison, C.J. and Rao, V.S., 1971, "Interaction of Waves with Submerged Objects," Journal of Waterways, Harbors and Coastal Engineering Division, ASCE, Volume 97, No. WW2, pp. 259-277.

Garrison, C.J. and Chow, P.Y., 1972, "Wave Forces on Submerged Bodies," Journal of Waterways, Harbors and Coastal Engineering Division, ASCE, Volume 98, No. WW3, pp. 375-392.

Garrison, C.J. and Stacey, R., 1974, "A Comparison of Theory and Experiment," Offshore Technology Conference, Paper No. OTC 2794, Houston.

Garrison, C.J., Torum, A., Iverson, C., Leivseth, S. and Ebbesmeyer, C.C., 1974, "Wave Forces on Large Volume Structures - A Comparison Between Theory and Model Tests," Proceedings, Offshore Technology Conference, Houston, Paper No. OTC 2137, Volume II, pp. 1061-1070.

Garrison, C.J., Gehrman, F.H. and Perkinson, B.T., 1975, "Wave Forces on Bottom-Mounted Large-Diameter Cylinder," Journal of Waterways, Harbors and Coastal Engineering Division, ASCE, Volume 101 (WW4), pp. 343-356.

Garrison, C.J., Field, J.B. and May, M.D., 1977, "Drag and Inertia Forces on a Cylinder in Periodic Flow," Journal of Waterways, Ports, Coastal, and Ocean Division, ASCE, Volume 103 (WWZ), pp. 193-204.

Garrison, C.J. and Stacey, R., 1977, "Wave Loads on North Sea Gravity Platforms: A Comparison of Theory and Experiment," Offshore Technology Conference, Paper No. OTC 2794, Houston.

Garzke, W.H., Petrie, G.L., McClure, A.C., Fink, C. and Giannotti, J., 1978, "Design of a Reflector Buoy for AWACS Radar: Engineering Report on Design and Computer Analysis," NOAA Data Buoy Office, NSTL Station, Mississippi, July.

Gelb, A. and Vander Velde, W.E., 1968, "Multiple-Input Describing Functions and Nonlinear System Design," McGraw-Hill, N.Y.

Gerstner, F., 1802, "Theorie Der Wellen, Abhandlungen der Koniglichin Bohimshen Gesellschaft der Wissenschaften, Prague," (see Also Gilbert, Annalen der Physik, Volume 32, pp. 412-425.

Ghosh, S., Chou, F.S. and Huang, E.W., 1979, "A Rational Approach to the Design of a Pipelay/Derrick Semisubmersible Barge," Transactions, SNAME, Volume 87.

Ghosh, S., Chou, F.S. and Huang, E.W., 1980, "Design Consideration of a Tension Leg Platform," Society of Petroleum Engineers, SPE 10753.

Gibson, R.J and Wang, H., 1977, "Added Mass of Pile Group," Journal of Waterways, Harbors and Coastal Engineering Division, ASCE, (WW2), pp. 215-223.

Glasscock, M.S. and Finn, L.D., 1984, "Design of a Guyed Tower for 1000 Feet of Water," Journal of Structural Engineering, Volume 110, No. 5, ASCE, May.

Goda, Y., 1964, "Wave Forces on a Vertical Circular Cylinder and a Proposed Method of Wave Force Computation", Report of Port and Harbor Technical Research Institute, No. 8, pp. 1-74.

Goldberg, L.L. and Tucker, R.G., 1974, "Current Status of U.S. Navy Stability and Buoyancy Criteria for Advanced Marine Vehicles," AIAA/SNAME Advanced Marine Vehicle Conference.

Griffin, O.M., 1980, "OTEC Cold Water Pipe Design for Problems Caused by Vortex Excited Oscillations," NRL Memorandum Report No. 4157, Naval Reserch Laboratory (March), Washington, D.C.

Griffin, O.M., 1982, "The Response of Marine Tubulars and Risers to Current-Induced Hydrodynamic Loading," Proceedings of the 37th ASME Petroleum Mechanical Engineering Workshop and Conference (September 1981), Dallas, Texas. Also updated in ASME Transactions, Journal of Energy Resources Technology, Volume 104.

Griffin, O.M. and Ramberg, S.E., 1975, "On Vortex Strength and Drag in Bluff Body Wakes," Journal of Fluid Mechanics, Volume 69, pp. 721-728.

Griffin, O.M. and Ramberg, S.E., 1976, "Vortex Shedding From a Cylinder Vibrating in Line with an Incident Uniform Flow," Journal of Fluid Mechanics, Volume 75, pp. 257-271

Gudmestad, O.T. and Connor, J.J., 1983, "Linearization Methods and Influence of Current on the Nonlinear Hydrodynamic Drag Force," Applied Ocean Research, Volume 5, No. 4.

Hallam, M.G., Heaf, N.J. and Wootton, L.R., 1978, "Dynamics of Marine Structures: Methods of Calculating the Dynamic Response of Fixed Structures Subject to Waves and Current Action," Report UR8, 2nd Edition, CIRIA, Underwater Engineering Group, UK, October.

Hanna, S.Y., Mangiavacchi, A. and Suhendra, R., 1981, "Nonlinear Dynamic Analysis of Guyed Tower Platforms," ASME Paper No. 81-WA/OCE-9, ASME Winter Annual Meeting, Washington, D.C., November.

Hara, H., Zienkiewicz, O.C. and Bettess, P., 1979, "Application of Finite Elements to Determination of Wave Effects on Offshore Structures," Proceedings of the 2nd International Conference on the Behaviour of Offshore Structures, BOSS '79, London, Volume I, pp. 383-390.

Hartlen, R.T. and Currie, I.G., 1970, "Lift-Oscillator Model of Vortex-Induced Vibration," Journal of the Engineering Mechanics Division of ASCE, Volume 96, EM5, pp. 557-591.

Hasselmann, K., et al., 1973, "Measurements of Wind - Wave Growth and Swell Decay During the Joint North Sea Wave Project," Deut. Hydrogr. Z., Reihe A, No. 112.

Havelock, T.H., 1940, "The Pressure of Water Waves Upon a Fixed Obstacle," Proceedings of the Royal Society, London, Serial A, Volume 963, pp. 175-190.

Heideman, J.C., Olsen, O.A. and Johansson, P.I., 1979, "Local Wave Force Coefficients," Civil Engineering in the Oceans IV, ASCE, pp. 684-699.

Hoerner, S.F., 1965, "Fluid-Dynamic Drag," 2nd Edition Book published by the author, New Jersey.

Hogben, N., Osborne, J. and Standing, R.G., 1974, "Wave Loading on Offshore Structures - Theory and Experiment," Proceedings of the Symposium on Ocean Engineering, National Physical Laboratory, London, RINA, pp. 19-36.

Hogben, N. and Standing, R.G., 1974, "Wave Loads on Large Bodies," Proceedings of the Symposium on Dynamics of Marine Vehicles and Structures in Waves, Institute of Mechanical Engineers, London, pp. 258-277.



Hogben, N. and Standing, R.G., 1975, "Experience in Computing Wave Loads on Large Bodies," Offshore Technology Conference, Paper No. OTC 2189, Houston.

Hogben, N., Miller, B.L., Searle, J.W. and Ward, G., 1977, "Estimation of Fluid Loading on Offshore Structures," Proceedings, Institution of Civil Engineers, Volume 63, Part 2, pp. 515-562.

Hogben, N. and Rowe, S.J., 1979, "Theoretical and Experimental Paramater Study of the Deep-Section Concept of Tethered Buoyant Platform," National Maritime Institute Report No. NMI R59, Feltham, 15p.

Hoof, J.P., 1971, "A Mathematical Method of Determining Hydrodynamically Induced Forces on a Semisubmersible," Proceedings of SNAME Annual Meeting, New York, November.

Horikawa, K., 1978, "Coastal Engineering, An Introduction to Ocean Engineering," Wiley, New York.

Horton, E., 1975, "Tension Leg Platform Prototype Completes Pacific Coast Test," Ocean Industry, September.

Horton, T.E., Feifarek, M.J. and Rish, J.W., III, 1982, "Formulation of the One-Dimensional Wave Force Algorithm Using the Inertial Pressure Concept," Proceedings of the First Offshore Mechanics/Arctic Engineering/Deepsea Systems Symposium, ASME, Volume I, 1982, pp. 59-60.

Howe, R.J., 1967, "Development of Offshore Drilling and Production Technology," ASME Underwater Technology Division Conference, April 30 - May 3.

Hudspeth, R.T., 1983, "Environmental Forces on Ocean Platforms," NCEL Technical Note TN No. N-1681, Naval Civil Engineering Laboratory, Port Hueneme, California, November.

Huntington, S.M. and Thompson, D.M., 1976, "Forces on a Large Vertical Cylinder in Multi-Directional Random Waves," Offshore Technology Conference, Paper No. OTC 2539, Houston.

Hutchison, B.L., Bringloe, J.T., 1978, "Application of Seakeeping Analysis," Marine Technology, Volume 15, No. 4, October.

Hwang, L.S. and Tuck, E.O., 1970, "On the Oscillations of Harbors of Arbitrary Shape," Journal of Fluid Mechanics, Volume 42, pp. 447-464.

Hydraulic Research Station, 1981, "Dynamic Instabilities of Tethered Buoyant Platforms," Department of Energy Offshore Energy Technology Board, Report OT-R-8138, Wallingford, England, May 1981.

Inglis, R.B. and Price, W.G., 1980, "Comparison of Calculated Responses for Arbitrary Shaped Bodies Using Two and Three-Dimensional Theories," International Shipbuilding Progress, Volume 27, No. 308, pp. 86-95.

Ippen, A.T., ed. 1966, "Estuary and Coastline Hydrodynamics," McGraw-Hill, New York.

Isaacson, M., 1979a, "Nonlinear Inertia Forces on Bodies," Journal of Waterways, etc. Division, ASCE, No. WW3, pp. 213-227.

Isaacson, M., 1979b, "Wave Induced Forces in the Diffraction Regime," In Mechanics of Wave-Induced Forces on Cylinders, ed. T.L. Shaw, Pitman, London, pp. 68-89.

Isaacson, M., 1981, "Steep Wave Forces on Large Offshore Structures," Offshore Technology Conference, Paper No. OTC 3955, Houston.

Isaacson, M. and Maul, D.J., 1976, "Transverse Forces on Vertical Cylinders in Waves," Journal of Waterways, Harbors, and Coastal Engineering Division, ASCE, Volume 102, No. WW1, February, pp. 49-60.

ISSC Spectrum, 1964, "Environmental Conditions," Committee No. 1, Proceedings of Second International Ship Structures Congress, Delft, Netherlands.

Iwagaki, Y. and Sakai, T., 1969, "Experiment on Horizontal Water Particle Velocity of Finite Amplitudes Waves," (In Japanese) Proceedings, 16th Conference on Coastal Engineering in Japan, pp. 15-21. Also, Horizontal Water Particle Velocity of Finite Amplitude Waves. Proceedings, 12th Coastal Engineering Conference, Washington, D.C., pp. 309-326.

Iwan, W.D., 1974, "The Vortex Induced Oscillation of Elastic Structural Elements," Journal of Engineering for Industry, Volume 97, pp.1378-1382.

Iwan, W.D. and Blevins, R.D., 1974, "A Model for Vortex-Induced Oscillation of Structures," Journal of Applied Mechanics, Volume 41.

John, F., 1950, "On the Motion of Floating Bodies," Parts I and II; Communication on Pure Applied Mathematics Volume 2, pp. 13-57, and Volume 3, pp. 45-101.

Johns Hopkins University, Applied Physics Laboratory, 1980, "Verification Test for Cold Water Pipe Analysis, Part A: Test Description Results and Model Comparisons," JHU/APL SR 80-2A, October.

Karsan, D.I. and Mangiavacchi, A., 1982, "Tension Leg Platforms: State of the Art and Future Research and Development Requirements," Proceedings, Ocean Structural Dynamics Symposium, Oregon State University, Corvallis, Oregon.

Keulegan, G.H. and Patterson, G.W., 1940, "Mathematical Theory of Irrotational Translation Waves," Journal of Research, National Bureau of Standards, Volume 24, pp. 47-101.

Keulegan, G.H. and Carpenter, L.H., 1956, "Forces on Cylinders and Plates in an Oscillating Fluid," National Bureau of Standards, Report No. 4821.

Keulegan, G.H. and Carpenter, L.H., 1958, "Forces on Cylinders and Plates in an Oscillating Fluid," Journal of Research of the National Bureau of Standards, Volume 60, No. 5.

Keuning, J.A. and Beukelman, W., 1979, "Hydrodynamic Coefficients of Rectangular Barges in Shallow Water," Proceedings of the 2nd Conference on the Behaviour of Offshore Structures (BOSS '79), London, Volume 2, pp. 105-124.

King, R., 1977, "A Review of Vortex Shedding Research and Its Application," Ocean Engineering, Volume 4, pp. 141-171.

Kinsman, B., 1965, "Wind Waves: Their Generation and Propagation on the Ocean Surface," Prentice-Hall Inc., Englewood Cliffs, New Jersey.

Kokkinowrachos, K., 1978, "Hydrodynamic Analysis of Large Offshore Structures," Proceedings, 5th Ocean Development Conference, Tokyo.

Korteweg, D.J. and De Vries, G. 1895, "On the Change of Form of Long Waves Advancing in a Rectangular Canal, and on a New Type of Long Stationary Waves," Philosophical Magazine, 5th Series, Volume 39, pp. 422-443.

Korvin-Kroukovsky, B.V., 1961, "Theory of Seakeeping," Society of Naval Architects and Marine Engineers, New York, 360 pp.

Krolikowski, L.P. and Gay, T.A., 1980, "An Improved Linearization Technique for Frequency Domain Riser Analysis," Offshore Technology Conference, Paper No. OTC 3777, Houston.

Krylov, N. and Bogoliubov, N., 1943, "Introduction to Nonlinear Mechanics," Princeton University Press, New Jersey.

Laitone, E.V., 1961, "The Second Approximation to Cnoidal and Solitary Waves," Journal of Fluid Mechanics, Volume 9, pp. 430-444.

Lamb, H., 1945, "Hydrodynamics," 6th Edition, Dover, New York, also Cambridge University Press, 1932.

Lambrakos, K.F. and Brannon, H.R., 1974, "Wave Force Calculations for Stokes and Non-Stokes Waves," Proceedings of Offshore Technology Conference, Paper No. OTC 2039, Houston.

Le Mehaute, B., 1976, "An Introduction to Hydrodynamics and Water Waves," Springer-Verlag, Dusseldorf.

Le Mehaute, B., Diboky, D. and Lin, A., 1968, "Shallow Water Waves: A Comparison of Theories and Experiments," Proceedings, 11th Coastal Engineering Conference, London, pp. 87-107.

LeBlanc, L.A., 1983, "Exxon Installs First Guyed Tower," Offshore, August.

LeBlond, P.H. and Mysak, L.A., 1978, "Waves in the Ocean," Elsevier, Amsterdam.

Lebreton, J.C. and Margnac, A., 1968, "Calcul des Mouvements d'un Navire ou d'une Plateforme Amarrées dans la Houle; La Houille Blanche," Volume 23, pp. 379-389.

Lebreton, J.C. and Cormault, P., 1969, "Wave Action on Slightly Immersed Structures, Some Theoretical and Experimental Considerations," Proceedings, Symposium on Research on Wave Action, Delft.

Lewis, F.M., 1929, "The Inertia of Water Surrounding a Vibrating Ship," Transactions, Society of Naval Architects and Marine Engineers, New York, Volume 27, pp. 1-20.

Lienhard, J.H., 1966, "Synopsis of Lift, Drag, and Vortex Frequency Data for Rigid Circular Cylinders," Washington State University, College of Engineering, Research Division, Bulletin 300.

Lighthill, M.J., 1979, "Waves and Wave Loading," Proceedings, 2nd Conference on Behavior of Offshore Structure (Boss 79), London, Volume 1, pp. 1-40.

Liu, O., Chen, Y.N., Shin, Y.S. and Chen, P.C., 1980, "Integrated Procedure for Hydrodynamic Loads and Structural Response of a Tension Leg Platform," Computational Methods for Offshore Structures, ASME Winter Annual Meeting, AMO - Volume 37.

Longuet-Higgins, M.S., 1956, "The Refraction of Sea Waves in Shallow Water," Journal of Fluid Mechanics, Volume I, pp. 163-176.

Longuet-Higgins, M.S. and Stewart, R.W., 1964, "Radiation Stresses in Water Waves: A Physical Discussion with Applications," Deep Sea Research, Volume 11, pp. 529-562.

Lundgren, H., Sand, S.E. and Kirkegaard, J., 1982, "Drift Forces and Damping in Natural Sea States: A Critical Review of the Hydrodynamics of Floating Structures", BOSS Proceedings, Third International Conference, Volume 2, Massachusetts Institute of Technology.

Macy, R.H., 1966, "Towing, Motions and Stability Characteristics of Ocean Platforms," Sixth Symposium on Naval Hydrodynamics, Washington.

Macy, R.H., 1969, "Drilling Rigs," Chapter XVI of "Ship Design and Construction," A.M. D'Archangelo, Editor, SNAME.

Malaeb, D.A., 1982, "Dynamic Analysis of Tension Leg Platforms," Ph.D. Thesis, Texas A&M University, December.

Malhotra, A.K. and Penzien, J., 1970, "Nondeterministic Analysis of Offshore Tower Structures," Journal of Engineering Mechanics Division, ASCE, Volume 96, No. EM6, pp. 985-1003, (see also Volume 97, EM3, 1971, pp. 1028-1029).

Mangiavacchi, A., Abbott, P.A., Hanna, S.Y. and Suhendra, R., 1980, "Design Criteria of a Pile Founded Guyed Tower," Proceedings, Offshore Technology Conference, Paper No. OTC 3882, Houston.

Marine Construction, Offshore Magazine, January 1983.

Marks, W., 1963, "The Application of Spectral Analysis and Statistics to Seakeeping," ANAME T&R Bulletin, No. 1-24.

MacCamy, R.C. and Fuchs, R.A., 1954, "Wave Forces on Piles: A Diffraction Theory," U.S. Army Corps of Engineers, Beach Erosion Board, Technical Memo No. 69, Washington.

McClure, A.C., 1965, "Development of the Project Mohole Drilling Platform," Transactions, SNAME, Volume 73, 1965, pp. 50-99.

McClure, A.C. and Kirschner P.N., 1983, "Semi-Submersible Buoy for Stormy Seas", Unpublished Document.

McCowan, J., 1891, "On the Solitary Wave," Philosophical Magazine, Volume 32, pp. 45-58.

MD, 1973, "Regulations for Mobile Drilling Platforms with Installations and Equipment Used for Drilling for Petroleum in Norwegian Internal Waters, in Norwegian Territorial Waters, and in That Part of the Continental Shelf Which is Under Norwegian Sovereignty," Norwegian Maritime Directorate, issued September 1973.

Mei, C.C., 1978, "Numerical Methods in Water-Wave Diffraction and Radiation," Annual Review of Fluid Mechanics, Volume 10, pp. 393-416.

Mercier, J. A., 1973, "Large Amplitude Oscillations of a Circular Cylinder in a Low-Speed Stream," Ph.D. Dissertation submitted to the Stevens Institute of Technology.

Mercier, J.A., Goldsmith, R.G. and Curtis, L.B., 1982, "The Hutton TLP: A Preliminary Design," Journal of Petroleum Technology, January, pp. 208-216.

Merrison Committee, 1974, "Interim Design and Workmanship Rules for the Design of Box Girder Bridges," HMSO, London.

Mes, M.J., 1978, "New Studies Improve Wave Force Spectral Calculations," The Oil and Gas Journal, April.

Michel, W.H., 1967, "How to Calculate Wave Forces and Their Effects," Ocean Industry, June.

Michel, W.H., 1968, "Sea Spectra Simplified," Marine Technology, January.

Migliore, H.J. and Palo, P.A., 1979, "Prediction of Ocean Platform Response," NCEL Technical Memorandum, M-44-79-4, Port Hueneme, California, January.



Miller, B.L., 1976, "The Hydrodynamics Drag of Roughened Circular Cylinders," Journal, Royal Institute of Naval Architects, RINA Spring Meeting.

Milne-Thompson, L.M., 1968, "Theoretical Hydrodynamics," 5th Edition, MacMillan, New York.

Miner, E.W., Griffin, O.M., Ramberg, S.E. and Fritts, M.J., 1979, "Numerical Calculation of Wave Effects on Structures," Proceedings, Civil Engineering in the Oceans IV, ASCE, San Francisco, Volume I, pp. 17-27.

Mobile Rig Construction, 1983, "Joint Effort to Create Climatized Semi," Offshore Magazine, January.

Mobile Rig Construction, 1983, "New RS 35 Semis Designed for North Sea," Offshore Magazine, January.

Mobile Rig Construction, 1983, "Odeco Super Semi Built for Arctic Work," Offshore Magazine, January.

Morison, J.R., O'Brien, M.P., Johnson, J. W. and Schaaf, S. A., 1950, "The Forces Exerted by Surface Waves on Piles," Petroleum Transactions, AIME, Volume 189, pp. 149-157.

Motora, S. and Koyama, T., 1959, "On Wave Excitationless Ship Forms," Journal of Society of Naval Architects of Japan, 3.

Muga, B.J. and Wilson, J.F., 1970, "Dynamic Analysis of Ocean Structures," Phenum Press, New York.

Munk, W.H., 1951, "Origin and Generation of Waves," Proceedings, 1st Conference on Coastal Engineering, pp. 1-4.

Munk, W.H., Tucker, M.J., Snodgrass, F.E., 1956, "Remarks on the Ocean Wave Spectrum," Proceedings, Naval Hydrodynamics, September, Washington, D.C., Publication 515, National Academy.

Nath, J.H., 1980, "Marine Growth on Offshore Platforms," Interim Report for National Science Foundation, November.

Nath, J.H., 1981, "Hydrodynamic Coefficients for Cylinders with Pronounced Marine Growths," Final Report to API, API PRAC Project 80-31, October.

Nath, J.H., 1982, "Heavily Roughened Horizontal Cylinders in Waves," BOSS Proceedings, Third International Conference, Massachusetts Institute of Technology.

Nath, J.H., 1983a, "Vertical vs. Horizontal Cylinders in Waves," ASCE Specialty Conference on Pipelines in Adverse Environments, San Diego, California, November.

Nath, J.H., 1983b, "Hydrodynamic Coefficients for Cylinders with Pronounced Marine Growths," Final Report to API, API PRAC Project 80-31-13, Vertical Cylinder, January.

Nath, J.H., 1983c, "Hydrodynamic Coefficients for Cylinders Roughened by Marine Growths From the Gulf of Mexico," Final Report to API, API PRAC Project 82-31, January.

Nath, J.H., 1983d, "Hydrodynamic Roughness of Marine Growths on Cylinders," Final Report to National Science Foundation, Civil and Environmental Engineering Division, December.

Nath, J.H., 1984, "Hydrodynamic Coefficients for Cylinders Covered with Soft Organisms, Particularly Sea Anemones," Final Report to API, API PRAC Project 83-31, June.

Nath, J.H. and Wankmuller, R.N., 1982, "Wave Forces on Kelp Covered Horizontal Cylinders," Ocean Structural Dynamics Symposium, Oregon State University, Corvallis, Oregon, September.

Nath, J.H., Hsu, M.K., Hudspeth, R.T. and Dummer, J., 1984, "Laboratory Wave Forces on Vertical Cylinders," to be presented at Ocean Structural Dynamics Symposium, Oregon State University, Corvallis, Oregon, September.

Natvig, B.J. and Pendered, J.W., 1979, "Motion Response of Floating Structures to Regular Waves," Offshore Structures Engineering, Volume 2, Proceedings, International Symposium on Offshore Engineering, Rio de Janeiro, Brazil, 1981. Houston, Texas: Gulf Publishing Company.

Naudascher, E., 1974, (editor), "Flow-Induced Structural Vibrations," Springer-Verlag, Berlin.

Neumann, G., 1953, "On Ocean Wave Spectra and a New Method of Forecasting Wind-Generated Sea," U.S. Army Corps of Engineers, Beach Erosion Board, Technical Memo, No. 43.

Newman, J.N., 1961, "The Damping of an Oscillating Ellipsoid Near a Free Surface," Journal of Ship Research 5, (3), 44-54.

Newman, J.N., 1962, "The Exciting Forces on Fixed Bodies in Waves," Journal of Ship Research, Volume 6, pp. 10-17.

Norton, D.J., Heideman, J.C. and Mallard, W.W., 1981, "Wind Tunnel of Inclined Circular Cylinders", Offshore Technology Conference, Paper No. OTC 4122, Houston.

Numata, E. and Michel, W.H., 1974, "Experimental Study of Stability Limits for Semi-Submersible Drilling Platforms," Offshore Technology Conference, Paper No. OTC 2032, Houston.

Numata, E., Michel, W.H. and McClure, A.C., 1976, "Assessment of Stability Requirements for Semisubmersible Units," Transactions, SNAME, Volume 84.

Ochi, M.K. and Hubble, E.N., 1976, "Six-Parameter Wave Spectra," Proceedings, 15th Coastal Engineering Conference, Honolulu, Volume, I, pp. 301-328.

Ochi, M.K. and Wang, S., 1976, "Prediction of Extreme Wave-Induced Loads on Ocean Structures," BOSS Proceedings, First International Conference, Trondheim, Norway.

Ogilvie, T.F., 1964, "Recent Progress Towards the Understanding and Prediction of Ship Motions," Proceedings, 5th ONR Symposium on Naval Hydrodynamics, Bergen, pp. 3-97.

Ogilvie, T.F. and Shin, Y.S., 1978, "Integral-Equation Solutions for Time-Dependent Free-Surface Problems," Naval Architecture and Ocean Engineering, Society of Naval Architects, Japan, Volume 16, pp. 86-96.

Ohkusu, M., 1974, "Hydrodynamic Forces on Multiple Cylinders in Waves," Proceedings, Symposium on Dynamics of Marine Vehicles and Structures in Waves, Institute of Mechanical Engineers, London, pp. 107-112.

Olsen, O.A., 1974, "Investigation of Drag Coefficients Based on Published Data," Report A74-2-S, Det norske Veritas.

Omer, G.C. and Hall, H.H., 1949, "The Scattering of Tsunami by a Cylindrical Island," Journal of Seismological Society of America, Volume 39, No. 4, pp. 257-260.

Oran, C., 1983, "Overall Dynamic Characteristics of Tension Leg Platforms," Proceedings, 15th Offshore Technology Conference, Paper No. OTC 4640, Houston, Texas.

Parkinson G.V., 1974, "Mathematical Models of Flow-Induced Vibrations of Bluff Bodies," in Flow-Induced Structural Vibrations, Edited, Naudascher, E., Springer-Verlag, Berlin, pp. 81-127.

Paruzzolo, A., 1981, "Tecnomore Creates Its Own TLP," Offshore, November.

Patel, M.H. and Lynch, E.J., 1983, "The Coupled Dynamics of Tensioned Buoyant Platforms and Mooring Tethers," Journal of Engineering Structures, to be published.

Patel, M.H. and Lynch, E.J., 1983, "A Calculation Method for the Wave Induced Motion Response of a Tensioned Buoyant Platform Including the Effects of Mooring Tether Dynamics," Program Manual for UCLTBP; Version 2, Mechanical Engineering Department, University College, London.

Paulling, J.R. 1970, "Wave Induced Forces and Motions of Tubular Structures," Eighth Symposium on Naval Hydrodynamics, Office of Naval Research, Pasadena, Calif.

Paulling, J.R., 1975, "Elastic Response of Stable Platform Structures to Wave Loading," Proceedings of the International Symposium on Dynamics of Marine Vehicles and Structures in Waves, The Institute of Mechanical Engineers, London, England.

Paulling, J.R., 1977, "Time Domain Simulation of Semisubmersible Platform Motion with Application to the Tension Leg Platform," SNAME Spring Meeting/STAR Symposium, San Francisco.

Paulling, J.R., 1981, "The Sensitivity of Predicted Loads and Responses of Floating Platforms to Computational Methods," Proceedings, Conference on Integrity of Offshore Structures, Glasgow.

Paulling, J.R., 1982, "Mathieu Instabilities in TLP Response," Ocean Structural Dynamics Symposium '82 Proceedings, Oregon State University, September 8-10.

Paulling, J.R. and Horton, E.E., 1970, "Analysis of the Tension Leg Stable Platform," Offshore Technology Conference, Paper No. OTC 1263, Houston.

Paulling, J.R. and Horton, E.E., 1971, "Analysis of the Tension Leg Platform," Society of Petroleum Engineers Journal, September, pp. 285-294.

Pearcey, H.H., 1979a, "Some Observations on Fundamental Features of Wave-Induced Viscous Flows Past Cylinders," Mechanics of Wave-Induced Forces of Cylinders (ed. T. L. Shaw), Pitman, London, pp. 1-54.

Pearcey, H.H., 1979b, "The Effect of Surface Roughness on the Wave Loading for Cylindrical Members of Circular Cross Section," National Marine Institute Report No. NMI R651, Feltham, 18 p.

Pearcey, H.H. and Bishop, J.R., 1979, "Wave Loading in the Drag and Drag-Inertia Regimes; Routes to Design Data," BOSS, London, Paper No. 23.

Peregrine, D.H., 1972, "Equations for Water Waves and the Approximations Behind Them," In Waves on Beaches and Resulting Sediment Transport, Editor R.E. Meyer, Academic Press, New York, pp. 95-121.

Perrett, G.R., Webb, R.M. 1980, "Tethered Buoyant Platform Production System," Offshore Technology Conference, Paper No. OTC 3881, Houston.

Phillips, O.M., 1977, "The Dynamics of the Upper Ocean," 2nd Edition, Cambridge University Press.

Pierson, W.J., Newmann, G. and James, R.W., 1955, "Practical Methods for Observing and Forecasting Ocean Waves," U.S. Navy Hydrographic Office Publication, No. 603.

Pierson, W.J. and Moskowitz, L., 1964, "A Proposed Spectral Form for Fully Developed Wind Seas Based on the Similarity Theory of S.A. Kitaigorodskii," Journal of Geophysical Research, Volume 69, pp. 5181-5190.

Pinkster, J.A., 1981, "Mean and Low Frequency Wave Forces on Semisubmersibles", Offshore Technology Conference, Paper No. OTC 3951, Houston.

Pinkster, J.A. and Van Oortmerssen, G., 1976, "Computation of the First and Second Order Wave Forces on Bodies Oscillating in Regular Waves," Proceedings, 2nd Conference on Numerical Ship Hydrodynamics, Berkeley, pp. 136-156.

Porter, W.R., 1960, "Pressure Distributions, Added Mass and Damping Coefficients for Cylinders Oscillating in a Free Surface," University of California, Berkeley, Institute of Engineering Research Series 82, Issue 16, 181p.

Prandtl, L., 1904, "Uber Flussigkeitsbewegung bei sehr kleiner Reibung," Proceedings 3rd Internation Math. Congr., Heidelberg.

Price, W.G. and Bishop, R.E.D., 1974, "Probabilistic Theory of Ship Dynamics," John Wiley and Sons, N.Y.

Raichlen, F. and Naheer, E., 1976, "Wave Induced Oscillations of Harbors with Variable Depth," Proceedings, 15th Coastal Engineering Conference, Honolulu, Volume IV, pp. 3536-3556.

Raines, T. S., 1981, "Harmonic Flow About Smooth and Rough Cylinders," Thesis submitted to the Naval Postgraduate School, Monterey, Calif.

Rainey, R.C.T., 1977, "The Dynamics of Tethered Platforms," Transactions, Royal Institution of Naval Architects, Volume 120, London.

Rajabi, F., 1979, "Hydroelastic Oscillations of Smooth and Rough Cylinders in Harmonic Flow," Ph.D Thesis, Naval Postgraduate School, Monterey, California (December).

Rajabi, F., Zedan, M.F. and Mangiavacchi, A., 1983, "Vortex Induced Dynamic Response of Marine Risers," Proceedings of 2nd Offshore Mechanics and Arctic Engineering Symposium ETCE, Houston, Texas, Jan.

Rajabi, F. and Mangiavacchi, A., 1984, "Guyed Tower Model Test Joint Industry Project, Correlation Studies," Report to 13 oil companies on guyed tower model test results, 3 volumes, Houston.

Ramberg, S.E. and Niedzwecki, J.M., 1979, "Some Uncertainties and Errors in Wave Force Computations," Offshore Technology Conference, Paper No. OTC 3597, Houston.

Rance, P.J., 1969, "Wave Forces on Cylindrical Members of Structures," Hydraulics Research, Hydraulic Research Station, Wallingford, pp. 14-17.

Remery, G.F.M. and Hermans, A.J., 1971, "The Slow Drift Oscillations of a Moored Object in Random Seas", Offshore Technology Conference, Paper No. OTC 1500, Houston.

Richardson, J.R., 1979, "Mathieu Instabilities and Response of Compliant Offshore Structures," National Maritime Institute, Report 49, February.



Ried, R.O., 1958, "Correlation of Water Level Variations with Wave Forces on a Vertical Pile for Nonperiodic Waves," Proceedings of Sixth Conference on Coastal Engineering, Miami Beach, Florida.

Robertson, J.M., 1965, "Hydrodynamics in Theory and Application," Prentice-Hall Inc., Englewood Cliffs, New Jersey.

Rodnight, T.V., 1983, "New Generation of Semis Improves Offshore Drilling Operations," Petroleum Engineer International, October.

Rowe, S.J. and G.E. Jackson, 1980, "An Experimental Investigation of Mathieu Instabilities on Tethered Buoyant Platform Models," National Maritime Institute, Report 73, January.

Russel, J.S., 1844, "Report on Waves," 14th Meeting, British Association of Advanced Science, pp. 311-390.

Salvesen, N., Tuck, E.O., Faltinsen, O., 1970, "Ship Motions and Sea Loads," Transactions, SNAME, Volume 78, pp. 250-287.

Salvesen, N., Von Kerczek, C.H., Yue, D.K. and Stern, F., 1982, "Computation of Nonlinear Surge Motion of Tension Leg Platforms," Offshore Technology Conference, Paper No. OTC 4394, Houston.

Sarchin, T.H. and Goldberg, L.L., 1962, "Stability and Buoyancy Criteria for U.S. Naval Surface Ships," Transactions, SNAME.

Sarpkaya, T., 1976a, "Vortex Shedding and Resistance in Harmonic Flow about Smooth and Rough Cylinders at High Reynolds Numbers," Naval Postgraduate School, Technical Report No. NPS-59SL76021, (February).

Sarpkaya, T., 1976b, "In-Line and Transverse Forces on Smooth and Sand-Roughened Cylinders in Oscillatory Flow at High Reynolds Numbers," Naval Postgraduate School, Technical Report No. NPS-69SL76062, Monterey, California.

Sarpkaya, T., 1977, "Unidirectional Periodic Flow About Bluff Bodies," Report No. NPS-69SL77051, Naval Postgraduate School, Monterey, California.

Sarpkaya, T., 1978, "The Hydrodynamic Resistance of Roughened Cylinders in Harmonic Flow," Transactions, Royal Institution of Naval Architects, London, Volume 120, pp. 41-58.

Sarpkaya, T., 1980, "Assessment of the Morison Equation," CR 80-022, Naval Civil Engineering Laboratory, Naval Construction Battalion Center, Port Hueneme, California.

Sarpkaya, T., 1981a, "A Critical Assessment of Morison's Equation," Proceedings of Hydrodynamics in Ocean Engineering, August, The Norwegian Institute of Technology, Trondheim, Norway.

Sarpkaya, T., 1981b, "Morison's Equation and the Wave Forces on Offshore Structures," CR 82-008, Naval Civil Engineering Laboratory, Naval Construction Battalion Center, Port Hueneme, California.

Sarpkaya, T., 1981c, "On Hydrodynamic Response of Risers to Waves and Currents," Proceedings of the 37th ASME Petroleum Mechanical Engineering Workshop and Conference (September), Dallas, Texas.

Sarpkaya, T. and Collins N.J., 1978, "Discussions on Reference 31," Journal of Waterways, Port, Coastal and Ocean Division, ASCE, Volume 104 (WWI).

Sarpkaya, T. and Rajabi, F., 1979, "Dynamic Response of Piles to Vortex Shedding in Oscillating Flow," Offshore Technology Conference, Paper No. OTC 3647, Houston.

Sarpkaya, T. and Isaacson, M., 1981, "Mechanics of Wave Forces on Offshore Structures," Van Nostrand Reinhold, New York.

Sarpkaya, T., Rajabi, F., Zedan, M.F. and Fisher, F.J., 1981, "Hydroelastic Response of Cylinders in Harmonic and Wave Flow," Offshore Technology Conference, Paper No. OTC 3992, Houston.

Schlichting, H., 1968, "Boundary-Layer Theory," McGraw-Hill Book Co., New York, 6th ed.

Schwartz, L.W. , 1974, "Computer Extension and Analytic Continuation of Stokes' Expansion for Gravity Waves," Journal of Fluid Mechanics, Volume 62, pp. 553-578.

Scott, J.R., 1965, "A Sea Spectrum for Model Tests and Long-Term Ship Protection," Journal of Ship Research, Volume 9, pp. 145-152.

Shen, S.F., 1977, "Finite Element Methods in Fluid Mechanics," Annual of Revised Fluid Mechanics, Volume 9, pp. 421-445.

Shields, D.R., Maris, A.T. and Vega, L.A., 1983, "Long Term Sensor Platforms," Proceedings of the 1983 Symposium on Buoy Technology, Marine Technology Society, New Orleans, Louisiana, April.

Shields, D.R. and Zueck, R.F., 1984, "Deepwater Semisubmersible Motion Simulation," Proceedings Oceans 84, Marine Technology Society, Washington, D.C., September.

Shoaf, R.L., 1978, "A Discrete Vortex Analysis of Flow about Stationary and Transversely Oscillating Circular Cylinders," Ph.D. Thesis, Naval Postgraduate School, Monterey, California (December).

Shore Protection Manual, 1977, U.S. Army Coastal Engineering Research Center, in 3 volumes.

Sigbjomsen, R., Bell, K. and Holland, I., 1978, "Dynamic Response of Framed and Gravity Structures to Waves," Numerical Methods in Offshore Engineering, Zienkewicz, Lewis, Stagg Editors, John Wiley & Sons.

Silvester, R., 1974, "Coastal Engineering, I," Elsevier, Amsterdam.

Simiu, E. and Leigh, D.S., 1984, "Turbulent Wind and Tension Leg Platform Surge," Journal of Structural Engineering, ASCE, Volume 110, No. 4, April, pp. 785-802.

Skjelbreia, L., 1958, "Gravity Waves, Stokes Third Order Approximation Tables of Functions, June 11.

Skjelbreia, L. and Hendrickson, J.A., 1960, "Fifth Order Gravity Wave Theory," Practices, 7th Coastal Engineering Conference, The Hague, pp. 184-196.

Skop, R.A. and Giffin, O.M., 1973, "A Model for the Vortex-Excited Resonant Response of Bluff Cylinders," Journal of Sound and Vibration, Volume 27, pp. 225-233.

Smith, E., 1978, "On Nonlinear Random Vibration," Ph.D. Thesis, Division of Structural Mechanics, The Norwegian Institute of Technology, Trondheim, Norway.

Sorensen, R.M., 1978, "Basic Coastal Engineering," Wiley, New York.

Spring, B.H. and Monkmeyer, P.L., 1974, "Interaction of Plane Waves with Vertical Cylinders," Proceedings of the 14th Coastal Engineering Conference, ASCE, Volume III, pp. 1828-1847.

St. Denis, M. 1975, "On the Motions of Oceanic Platforms," Proceedings, Symposium Dynamics of Marine Vehicles and Structures in Waves, Institute of Mechanical Engineers, London, pp. 113-134.

St. Denis, M. and Pierson, W.J., 1953, "On the Motion of Ships in Confused Seas," Transactions, SNAME, Volume 61, pp. 280-357.

St. Denis, M. and Almendinger, E., 1971, "Problems of Ocean Platforms," Spring Meeting SNAME, Honolulu, Hawaii, May 25-28.

Standing, R.G., 1978, "Application of Wave Diffraction Theory," International Journal of Numerical Methods in Engineering, Volume 13, pp. 49-72.

Standing, R.G., 1979, "Use of Potential Flow Theory in Evaluating Wave Forces on Offshore Structures," Proceedings, Conference on Power from Sea Waves, Institute of Mathematical Applications, Edinburgh.

Standing, R.G., 1980, "Wave-by-Wave Analysis of Data from Christchurch Bay Wave Force Experiment," NMI Report No. R-86.

Standing, R.G., 1981, "Wave Loading on Offshore Structures: A Review," NMI, R102, OT-R-8113.

Stoker, J.J., 1957, "Water Waves," Interscience, New York.

Stokes, G. G., 1847, "On the Theory of Oscillatory Waves", Transactions of Cambridge Philosophical Society, Volume 8, pp. 441-455, Also "Mathematical Physics Papers," Volume 1, Cambridge University Press, 1880.

Strouhal, V., 1878, "Uber eine besondere Art der Tonerregung," Annual Phys. und Chemie, New Series Volume 5, 1878, pp. 216-251

Tasai, F., 1960, "On the Damping Force and Added Mass of Ships Heaving and Pitching," Translation Issued at University of California, Berkeley, Institute of Engineering Research Series 82, Issue 15, 24p.

Tein, Y., Chianis, J., Teymourian, J., Chou, F., 1981, "An Integrated Motion and Structural Analysis for Tension Leg Platforms," Offshore Technology Conference, Paper No. OTC 4072, Houston.

Tein, Y., Chianis, J., Teymourian, J. and Chou, F., 1982, "An Integrated Motion and Structural Analysis for Tension Leg Platforms," Offshore Technology Conference, Paper No. OTC 4072, Houston.

Thompson, W.T., 1972, "Theory of Vibration with Applications," Prentice-Hall, Englewood Cliffs, New Jersey.

Tickell, R.G., 1979, "The Probabilistic Approach to Wave Loading on Marine Structures," Mechanics of Wave-Induced Forces on Cylinders, ed. T.L. Shaw, Pitman, London, pp. 152-178.

Torum, A.M. and Reed, K., 1982, "On the Spanwise Correlation of Wave Forces on Slender Structures," Offshore Technology Conference, Paper No. OTC 4226, Houston.

Tung, C.C. and Huang, N.E., 1973, "Combined Effects of Current and Waves on Fluid Force," Ocean Engineering, 2, 183.

Unknown Author, 1980, "Gulf TLP to Feature In-leg Wells," Offshore, April, pp. 136-138.

Ursell, F., 1949, "On the Heaving Motion of a Circular Cylinder on the Surface of a Fluid," Quarterly Journal of Mechanics and Applied Mathematics, Volume 2, pp. 218-231.

Van Oortmerssen, G., 1972, "Some Aspects of Very Large Offshore Structures," Proceedings, 9th ONR Symposium on Naval Hydrodynamics, Paris, pp. 975-1001.

Van Oortmerssen, G., 1976a, "The Motions of a Ship in Shallow Water," Ocean Engineering, Volume 3, pp. 221-255.

Van Oortmerssen, G., 1976b, "The Motion of a Moored Ship in Waves," N.S.M.B. Publication No. 510.

Van Opstal, G.H.C., Hans, D., Salmons, J.W. and Vander Viles, J.A., 1974, "MOSAS: A Motion Strength Analysis System for Semisubmersible Units and Floating Structures," Proceedings, Offshore Technology Conference, Paper No. OTC 2105, Houston.

Van Sluijs, M.F. and Minkenberg, H.L., 1977, "A Review of Studies of Ocean Platform Motions," Ocean Engineering Volume 4, pp. 75-90, Pergamon Press. Printed in Great Britain.

Verley, R.L.P. and Moe, G., 1979, "The Forces on a Cylinder Oscillating in a Current," River and Harbour Laboratory, The Norwegian Institute of Technology, Report No. STF60 A79061.

Von Schwind, J.J. and Reid, R.O., 1972, "Characteristics of Gravity Waves of Permanent Form," Journal of Geophysics Research, Volume 77, pp. 420-433.

Vugts, J.H., 1968, "The Hydrodynamic Coefficients for Swaying, Heaving and Rolling Cylinders in a Free Surface," International Shipbuilding Progress, Volume 15, pp. 251-276.

Vugts, J.H., 1970, "The Hydrodynamic Forces and Ship Motions in Waves," Ph.D. Thesis, Delft Technological University, 113 pp.

Wade, B.G. and Dwyer, M., 1976, "On the Application of Morison's Equation to Fixed Offshore Platforms", Offshore Technology Conference, Paper No. OTC 2723, Houston.

Wallis, J.R., Bayazitoglu, Y.O., Chapman, F.M. and Mangiavacchi, A., 1979, "Fatigue Analysis of Offshore Structures," Offshore Technology Conference, Paper No. OTC 3379, Houston.

Wehausen, J.V. and Laitone, E.V., 1960, "Surface Waves," in Handbuch der Physik, ed. S. Flugge, Springer-Verlag, Berlin, Volume IX, pp. 446-778.

Wheeler, J.D., 1970, "Method for Calculating Forces Produced by Irregular Waves," Journal of Petroleum Technology, March.

Whitham, G.B., 1974, "Linear and Nonlinear Waves," Wiley, New York.

Wiegel, R.L., 1960, "A Presentation of Cnoidal Wave Theory for Practical Application," Journal of Fluid Mechanics, Volume 7, pp. 273-286.

Wiegel, R.L., 1964, "Oceanographical Engineering," Prentice-Hall Inc., New Jersey.

Wiegel, R.L., 1975, "Design of Offshore Structures Using Wave Spectra," Oceanography International Conference, March, pp. 233-243.

Wu, S.C. and Tung, C.C., 1975, "Random Response of Offshore Structures to Wave and Current Forces," Sea Grant Publication UNC-SG-75-22, North Carolina State University, Raleigh, N.C.

Yamamoto, T., 1976, "Hydrodynamic Forces on Multiple Circular Cylinders," Journal of Hydrodynamic Division, ASCE, Volume 102, No. HY9, pp. 1193-1210.

Yamamoto, T. and Nath, J.H., 1976, "Forces on Many Cylinders Near a Plane Boundary," ASCE National Water Resources and Ocean Engineering Convention, Preprint No. 2633.

Yue, D.K., Chen, H.S. and Mei, C.C., 1976, "Three-Dimensional Calculations of Wave Forces by a Hybrid Element Method," Proceedings, 11th Symposium of Naval Hydrodynamics, Office of Naval Research.



Zdravkovich, M.M., 1977, "Review of Flow Interference Between Two Circular Cylinders in Various Arrangements," Journal of Fluid Engineering, Transactions, ASME, Volume 99, Serial 1, No. 4, pp. 618-633.

Zedan, M.F., Young, J., Salane, H. and Fischer, F.J., 1980, "Dynamic Response of a Cantilever Pile to Vortex Shedding in Regular Waves," ASME Transactions, Journal of Energy Resources Technology, Volume 103, pp. 32-40. Also Proceedings of the Offshore Technology Conference, Paper No. OTC 3799, Houston.

Zedan, M.F., Bayazitoglu, Y.O., Chianis, J. and Tein, Y., 1981, "A Quasi-Static Approach for Transportation Analysis of Offshore Platforms," Offshore Technology Conference, Paper No. OTC 4161, Houston.

Zedan, M.F. and Rajabi, F., 1981, "Lift Forces on Cylinders Undergoing Hydroelastic Oscillations in Waves and Two-Dimensional Harmonic Flow," Proceedings of Hydrodynamics in Ocean Engineering, August, The Norwegian Institute of Technology, Trondheim, Norway.

Zienkiewicz, O.C., 1977, "The Finite Element Method," 3rd Edition, McGraw-Hill, London.

Zienkiewicz, O.C., Bettess, P. and Kelly, D.W., 1978, "The Finite Element Method for Determining Fluid Loadings on Rigid Structures Two- and Three-Dimensional Formulations," In Numerical Methods in Offshore Engineering, eds. O.C. Zienkiewicz, P. Lewis, and K.G. Stagg, John Wiley, Chichester, England, pp. 141-183.



## 16.0 BIBLIOGRAPHY

1. Abkowitz, M.N., Stability and Motion Control of Ocean Vehicles, M.I.T. Press, Cambridge MA, 1972.
2. American Bureau of Shipping, Rules for Building and Classing: Mobile Offshore Drilling Units, American Bureau of Shipping, New York, NY, 1980.
3. American Bureau of Shipping, Rules for Building and Classing: Steel Vessels, American Bureau of Shipping, New York, NY, 1982.
4. Batchelor, G.K., An Introduction to Fluid Dynamics, Cambridge University Press, Cambridge, MA, 1967.
5. Bathe, K.J., Finite Element Procedures in Engineering Analysis, Prentice-Hall, Inc., Englewood Cliffs, NJ, 1982.
6. Bendat, J.S. and Piersol, A.G., Random Data: Analysis and Measurement Procedures, John Wiley and Sons, Inc., New York, NY, 1971.
7. Bendat, J.S. and Piersol, A.G., Engineering Applications of Correlation and Spectral Analysis, John Wiley and Sons, Inc., New York, NY 1980.
8. Bhattacharyya, R., Dynamics of Marine Vehicles, John Wiley and Sons, New York, NY, 1978.
9. Blevins, R.D., Flow-Induced Vibrations, Van Nostrand Reinhold Co., New York, NY, 1977.
10. Carnahan, B., Luther, H.A. and Wilkes, J.O., Applied Numerical Methods, John Wiley and Sons, Inc., New York, NY, 1969.
11. Clough, R.W. and Penzien, J., Dynamics of Structures, McGraw-Hill Inc., New York, NY, 1975.
12. Comstock, J.P., Principles of Naval Architecture, The Society of Naval Architects and Marine Engineers, New York, NY, 1967.
13. Dawson, T.H., Offshore Structural Engineering, Prentice-Hall, Englewood Cliffs, NY, 1983.
14. Dean, R.G., and Dalrymple, R.N., Water Wave Mechanics for Engineers and Scientists, Prentice-Hall, Inc., Englewood Cliffs, NJ, 1984.
15. Dean, R.G., Evaluations and Development of Water Wave Theories for Engineering Application, Vol I, II (SR-1), U.S. Army Coastal Engineering Research Center, Fort Belvoir, VA, Nov 1974.
16. Gerald, C.F., Applied Numerical Analysis, 2nd edition, Addison-Wesley, Reading, MA, 1978.
17. Gillmer, T.C. and Johnson, B., Introduction to Naval Architecture, Naval Institute Press, Annapolis, MD, 1982.

18. Hallam, B.G., Heaf, N.J. and Wootton, L.R., Dynamics of Marine Structures: Methods of Calculating the Dynamic Response of Fixed Structures Subject to Wave and Current Action, 2nd edition, Report UR8, CIRIA Underwater Engineering Group, 6 Storey's Gate, London, Oct 1978.
19. Hooft, J.P., Advanced Dynamics of Marine Structures, John Wiley and Sons, Inc., New York, NY, 1982.
20. Kinsman, B., Wind Waves: Their Generation and Propagation on the Ocean Surface, Prentice-Hall, Inc., Englewood Cliffs, NJ, 1965.
21. Lamb, H., Hydrodynamics, Dover Publications, New York, NY, 1945.
22. Le Mehaute, Introduction to Hydrodynamics and Water Waves, Springer-Verlag, Berlin, Germany, 1975.
23. Mei, C.C., The Applied Dynamics of Ocean Surface Waves, John Wiley and Sons, Inc., New York, NY, 1983.
24. Meirovitch, L., Methods of Analytical Dynamics, McGraw-Hill, Inc., New York, NY, 1970.
25. Milne-Thomson, L.M., Theoretical Hydrodynamics, 4th edition, MacMillan Co., New York, NY, 1960.
26. Muga, B.J. and Wilson, J.F., Dynamic Analysis of Ocean Structures, Plenum Press, New York, NY, 1970.
27. Newman, J.N., Marine Hydrodynamics, MIT Press, Cambridge, MA, 1977.
28. Price, W.G. and Bishop, R.E.D., Hydroelasticity of Ships, Cambridge University Press, New York, NY, 1979.
29. Price, W.G. and Bishop, R.E.D., Probabilistic Theory of Ship Dynamics, John Wiley and Sons, Inc., New York, NY, 1974.
30. Sarpakaya, T. and Isaacson, M., Mechanics of Wave Forces on Offshore Structures, Van Nostrand Reinhold Co., New York, NY, 1981.
31. Taggart, R., Ship Design and Construction, The Society of Naval Architects and Marine Engineers, New York, NY, 1980.
32. Thomson, W.T., Theory of Vibration with Applications, 2nd Edition, Prentice-Hall, Inc., Englewood Cliffs, NJ, 1981.
33. U.S. Coastal Engineering Research Center, Shore Protection Manual, 3rd edition, Vol. I-III, U.S. Coastal Engineering Research Center, Fort Belvoir, VA, 1977.
34. Vallentine, H.R., Applied Hydrodynamics, SI edition, Butterworth and Co., London, England, 1969.

